STRUCTURAL AND METAMORPHIC STUDIES IN THE SNOW LAKE AREA, TRANS-HUDSON OROGEN, MANITOBA, CENTRAL CANADA

by

Jürgen Kraus

M.Sc., Georg-August-Universität, Göttingen, 1991

A Thesis submitted in Partial Fulfilment of
the Requirements for the Degree of

Doctor of Philosophy

in the Academic Unit of Geology

Supervisor: Dr. Paul F. Williams, Ph.D., M.Sc., B.Sc., Department of Geology

Examining Board: Dr. J.T. Dunn, Department of Geology
Dr. J. Rickards, Department of Forestry and Environmental Management
Dr. G. Villemure, Department of Chemistry

External Examiner: Dr. K.E. Ashton, Saskatchewan Energy and Mines

THE UNIVERSITY OF NEW BRUNSWICK

December, 1998

0-612-46294-3

ABSTRACT

The Snow Lake Allochthon is a zone of tectonic interleaving of sedimentary rocks of the inverted Kisseynew marginal basin (Kisseynew Domain) with island arc and oceanic rocks in the southeastern part of the internal Trans-Hudson Orogen in Manitoba, Canada. The allochthon formed, was deformed, and was metamorphosed up to high grade at low to medium pressure during the Hudsonian orogeny as a result of the collision of the Archean Rae–Hearne and Superior cratons ~1.84–1.77 Ga ago. A combined structural and metamorphic study in the central part of the allochthon around Snow Lake has shown that four generations of folds (F_1–F_4) formed in at least three distinct kinematic frames over a period of more than 30 m.y. Tight to transposed $F_{1/2}$ structures with a southerly vergence are refolded by large open F_3 folds and, locally, by tight to open F_4 folds. The axes of the early $F_{1/2}$ folds are parallel, or near-parallel, to the axes of late F_3 folds, owing to progressive reorientation of the $F_{1/2}$ axes during southerly $F_{1/2}$ tectonic transport, followed by F_3 refolding around the previous linear anisotropy. The research has revealed complex relationships between cleavage development, porphyroblast growth, and large-scale folding in the well-bedded Burntwood group metaturbidites exposed in the staurolite zone. A domainal cleavage (S_2), which is axial planar to F_2 folds, is the only regionally pervasive fabric, and it is locally overprinted by F_3 crenulations. It is demonstrated: (a) that cleavage in anisotropic pelitic rock develops when microfolding is possible and that initiation of the cleavage, which is pervasive on the scale of a fold, commonly predates folding, (b) how a new axial planar fabric can develop on one fold limb of a symmetrical fold and not on the

other, and (c) how two cleavages of different generations can be present in adjacent beds. The observed porphyroblast–matrix relationships are used to show that rigid porphyroblasts that grew before or during folding and concurrent cleavage development, do generally rotate with respect to the geographical reference frame, even if the straining is non-coaxial—although it has been claimed otherwise. The allochthon is characterised by a "Barrovian" type metamorphic zonation with an increase in metamorphic grade towards the Kisseynew Domain from a chlorite zone to a migmatite zone at a consistent pressure of 4–6 kbar. Pressure and temperature estimates calculated on representative samples from a temperature window of 500–700°C (staurolite and sillimanite zones) yield evidence for two successive thermal regimes that varied in time and intensity from south to north. F_1 was the major burial event, which may have been followed by thermal relaxation between F_1 and F_2. In the staurolite zone and at lower grade, growth of the peak metamorphic mineral assemblage coincided with early F_2 folding, and cooling commenced by the time of F_3. In the sillimanite zone, however, metamorphism was related to a thermal event in the Kisseynew Domain. Here, peak conditions continued until after F_3 (a duration of more than 10 m.y.), on the basis of isograds/isotherms crosscutting large F_3 structures. It is suggested that low- to medium-pressure, high-temperature metamorphism in the Kisseynew Domain resulted from heat associated with ~1.815 Ga peraluminous granitoids. A possible cause for the formation of granitic magma in the lower crust of the Kisseynew Domain was high basal heat-flow resulting from convective thinning of the mantle lithosphere during crustal thickening.

CONTENTS

LIST OF FIGURES

LIST OF TABLES

Everywhere I go I am asked if I think the university stifles writers.
My opinion is that they don't stifle enough of them.
Flannery O'Connor

ACKNOWLEDGEMENTS

I thank my supervisor Dr. Paul Frederick Williams for his support throughout the thesis project. His enthusiasm, inspiration through many long discussions, advice, suggestions, criticisms, encouragement, and granting me the academic freedom to write this thesis as a series of papers, are greatly appreciated. I further thank him and Pam Williams for their generous hospitality on countless occasions. I am grateful to my co-supervisor Dr. Stephen B. Lucas for many stimulating discussions, for providing logistical field support, and for funding my travels to LITHOPROBE workshops. My other co-supervisor, Dr. John G. Spray, is thanked for discussion, practical advice, and encouragement. I am thankful to Drs. Al Bailes and Al Galley, who introduced me to the geology of the Snow Lake area. Al Bailes' interest and support throughout the project is gratefully acknowledged. It was an extreme pleasure to have been around Dr. Tony Norman; I am much indebted to him for getting me kickstarted in the early days of this project. Drs. Todd Dunn and Thomas Menard much refined my skills in metamorphic petrology. I am also thankful to Dr. Dunn for his outstanding support in his function as Director of Graduate Studies. Dr. Menard is further thanked for coauthoring the published version of Chapter 4. Dr. Dazhi Jiang contributed much to my structural database by informing me with his cutting edge structural geology in many long discussions. Dr. Peter Stringer carefully read major parts of this thesis and he greatly improved my written command of the English language. I thoroughly enjoyed discussions with him, particularly on the geology of Scotland. Dr. Bruce Broster is thanked specifically for his advice in questions of style and professional appearance. Drs. Tom Al, Ken Burke, Jim Noble, Adrian Park, Wouter van de Poll, Ron Pickerill, Nick Susak, and Joe White are thanked for their encouragement, criticisms, and for countless discussions. Joe White's unconventional logistical help "after hours" is gratefully acknowledged. I am thankful to Mrs. Nina Chrzanoswski for her great support, her inspiration, and for acting as a mediating link between faculty and graduate students. Dick Grant's dynamic company is also appreciated.

I extend my gratitude to many generations of fellow students for discussion, companionship, and friendship. This accounts in particular for my Trans-Hudson partner-in-crime, Jim Ryan, but also for Ali Ahmadi, Jeff Allaby, Chris Beaumont Smith and his wife Petra, David Copeland, Plinliang Dong, Lindsay Dunn, Cynthia Dyck, Gord Clarke, Heather Gibson, Rowenna Gilbertson, Bill Gray, Chris Hawkes, Falk Hüttmann, Dave Huntley, Dennis Johnston and his wife Gretchen, Dave Keighley, Martin de Keijzer, Yvette Kuiper, Shoufa Lin, Julia Linke, Dave MacDougall, Paul McNeill, John O'Connor, Ron Scott, Cuneyt Sen, Bob Spark, Chris Stanley, Andrew Stumpf, Lucy Thompson, James Whitehead, and Chris Wood.

Dr. Douglas Hall is thanked for assisting in the operation of the microprobe. Dr. Rob Berman re-calculated the P–T data listed in table 4.5 using his TWQ 1.02 database. The assistance of Mr. David Pirie, Mr. Ancel Murphy, Mr. Calvin Nash, who produced grade A thin sections, of Mr. Angel Gomez, who helped with some of the line drawings and digital photoplates, and of Mr. Bob McCulloch, who developed all printed photographs, is gratefully acknowledged. Drafts of some of the figures in Chapter 1 were provided by the Geological Survey of Canada and the Manitoba Energy and Mines department. I am grateful for help by Mrs. Merrill Beatty, Christine Lodge, Pam Racette, Diane Tabor, and Sherri Townsend.

This thesis also directly and indirectly benefited from comments and contributions by people who are not involved with UNB's Geology department: Mark Fedikow, Edgar Froese, Frank Fueten, Bill Fyson, Paul Gilbert, Terry Gordon, Mariette and the late Jack Henderson, Paul Hoffman, Peter Hudleston, Jerry Kitzler, Matt Kohn, Maarten Krabbendam, Richard Lisle, Dave McRitchie, Michiko Nishijima, Gerhard Oertel, John Percival, Jürgen Reinhardt, Ed Sawyer, Frank Spear, Cees van Staal, Mel Stauffer, John Tarney, Eva Zaleski, Dan Ziehlke, and Herman Zwanzig.

Logistical field support was provided by the Geological Survey of Canada, the Manitoba Energy and Mines department, and Hudson Bay Mining and Smelting Co. Ltd. The field work could not have been completed without the help of numerous people in Snow Lake, who granted additional logistical support: I am particularly indebted to my "adoptive parents" Mike and Sylvia Botten, and their son Michael. A scholarship "for studies abroad" by the Deutscher Akademischer Austauschdienst, awarded in the final stages of this project, is highly appreciated.

I thank my brother Michael and his wife Christine for their encouragement, as well as Colin Bulger and Claudia Lorenz in Hull (U.K.) for their hospitality during my traditional first European stop on my annual Christmas trips back to Germany. I cordially thank Kazuko Saruwatari for her moral support, in particular during the last months of this thesis project. Furthermore, I am grateful to my previous teachers at the universities of Würzburg, Hull (U.K.), and Göttingen for providing me with the background that qualified me to pursue a Ph.D. project.

Last but most importantly I thank my parents, Mrs. Annelore Kraus and the late Mr. Alfons Kraus, for supporting my study of geology.

The beginning is the most important part of the work.
Plato, The Republic, Book II. 377B

Chapter 1

Introduction

INTRODUCTION

The mining town of Snow Lake (geographical coordinates: 54°53' N; 100°01' W) is located in northern Manitoba, 685 km north of Winnipeg, at the northern termination of Provincial Road #392, between Thompson, one of the world's large Ni producers 250 km to the northeast, and the city of Flin Flon 200 km to the west (Fig. 1.1). Since the discovery of gold in 1914 (Stockwell, 1937), the area around Snow Lake has attracted the attention of geologists, prospectors and the mining industry. Staked in 1927, the Nor–Acme mine north of Snow Lake has been producing (with interruptions) gold or base metals since 1949.

Following the early gold rush, major base metal deposits (Chisel, Ghost, Stall, Osbourne) were discovered by the Hudson Bay Mining and Smelting Co. Ltd in 1956. Further finds included Anderson in 1963, North Chisel in 1987, and Photo Lake in 1993. Today, the Snow Lake area hosts eleven operating and past operating Cu-rich, Zn-rich and Cu–Zn–Au volcanic-hosted massive sulphide (VHMS) deposits of the Noranda type (Morton and Franklin, 1987; Galley *et al.*, 1993, Bailes and Galley, 1996). Exploration is continuing and looks very promising.

Figure 1.1 Simplified tectonic map of the Trans-Hudson Orogen showing the locations of LITHOPROBE seismic lines (numbered) and the NATMAP Shield Margin Project area. AC, Amisk collage; FF, Flin Flon; GD, Glennie Domain; HLB, Hanson Lake Block; KD, Kisseynew Domain; LLD, Lynn Lake Domain; LRD, La Ronge Domain; RD, Rottenstone Domain; RLD, Rusty Lake Domain; SID, Southern Indian Domain; SL, Snow Lake; SLA, Snow Lake Allochthon; TB, Thompson Belt; Th, Thompson; WB, Wathaman batholith; WD, Wollaston Domain; W, Archean basement windows; *NFSZ*, Needle Falls shear zone; *SW*, Sturgeon–Weir shear zone; *TF*, Tabbernor fault zone.

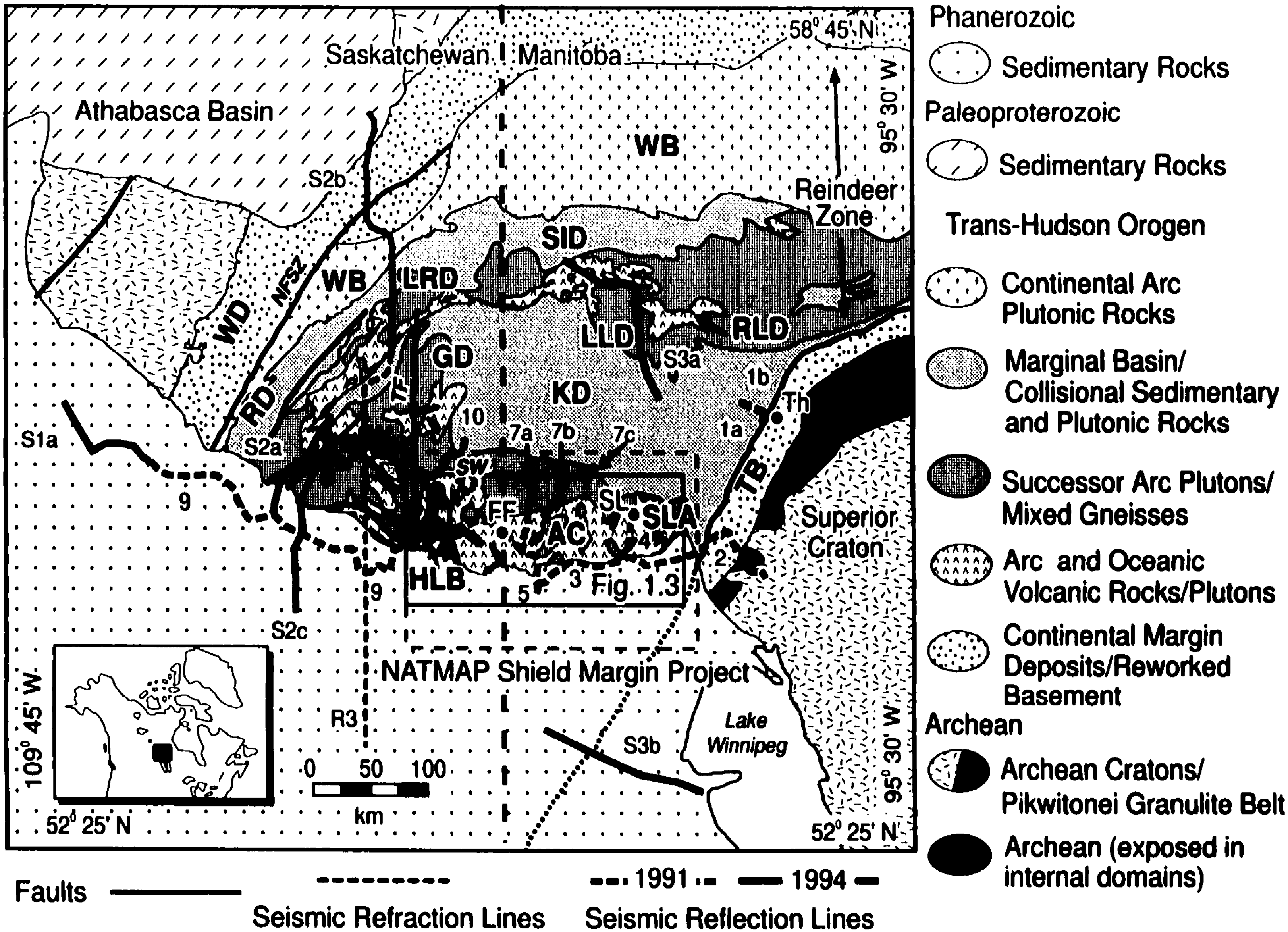
Saskatchewan
Manitoba
Athabasca Basin
58° 45' N
95° 30' W
WB
S2b
Reindeer Zone
SID
WB
LRD
NFSZ
WD
LLD
RLD
GD
S3a
1b
KD
Th
RD
TF
10
7a
7b
7c
1a
S1a
S2a
SW
TB
9
FF
SL
SLA
Superior Craton
AC
4
2
HLB
5
3
Fig. 1.3
9
S2c
NATMAP Shield Margin Project
R3
Lake Winnipeg
S3b
109° 45' W
0
50
100
km
95° 30' W
52° 25' N
52° 25' N
Faults
Seismic Refraction Lines
1991
1994
Seismic Reflection Lines
Phanerozoic
Sedimentary Rocks
Paleoproterozoic
Sedimentary Rocks
Trans-Hudson Orogen
Continental Arc Plutonic Rocks
Marginal Basin/ Collisional Sedimentary and Plutonic Rocks
Successor Arc Plutons/ Mixed Gneisses
Arc and Oceanic Volcanic Rocks/Plutons
Continental Margin Deposits/Reworked Basement
Archean
Archean Cratons/ Pikwitonei Granulite Belt
Archean (exposed in internal domains)

Mapping in the area was performed by Bruce (1917), Alcock (1920), Armstrong (1941), Harrison (1949), Russell (1957), Froese and Moore (1980) and Bailes and Galley (1994). Most recently, this part of the internal Trans-Hudson Orogen area has been one of the foci of the NATMAP Shield Margin Project[1] and the LITHOPROBE[2] Trans-Hudson Orogen Transect, two collaborative and multidisciplinary efforts involving lithological and structural mapping, metamorphic petrology, geochronology, geochemistry and geophysics. Contributors are the Geological Survey of Canada, the Manitoba and Saskatchewan Energy and Mines departments, and several Canadian and U.S. universities.

OUTLINE AND SCOPE OF THE THESIS

This thesis is divided into three regional and two complementary thematic parts. In

---

[1]The NATMAP (National Mapping) Shield Margin Project (1991–1996) was a major geoscience initiative, aimed at increasing knowledge of the early Paleoproterozoic Flin Flon–Glennie Complex, the Snow Lake Allochthon, their sub-Paleozoic continuation, and the southern flank of the Kisseynew Domain. The project area extends 270 km east–west and 150 km north–south (Fig. 1.1).

[2]LITHOPROBE (1984–2003) is Canada's national, collaborative, multi-disciplinary earth science research project, established to develop a comprehensive understanding of the evolution of the North American lithosphere. This is achieved by determining the present 3D-structure and the past geotectonic processes which have been active in forming that structure. LITHOPROBE's principal scientific and operational components are built around a series of ten transects or study areas. The LITHOPROBE Trans-Hudson Orogen transect (1990–1998) involved the acquisition of more than 1100 km of vertical vibroseis seismic reflection data in 1991 and 1994, and 750 km refraction lines in 1993 (Fig. 1.1).

the regional studies (Chapters 4 and 5), the tectonometamorphic history of the Snow Lake Allochthon is reconstructed, and the findings are extrapolated to adjacent domains. In addition to the regional geology, the general validity of the relationships between, cleavage development, large-scale folding and the growth sequence of porphyroblasts as observed in the Burntwood group metaturbidites (the stratigraphic names of the units in the Snow Lake area have never been formally defined so that the descriptor "group" is not capitalised in this thesis) is examined (Chapter 2). Based on this example and published work, a solution to the contentious question is presented, whether rigid porphyroblasts rotate or not with respect to geographical coordinates (Chapter 3). A synthesis is presented in Chapter 6. Chapters 2, 4 and 5, were published in, or have been submitted for publication to, international, refereed journals. For that reason, some repetition has been incorporated throughout the thesis. During this investigation, several government reports and conference abstracts were published (Kraus and Williams, 1993a, b, c, 1994a, b, c, 1995a, b; Kraus and Menard, 1995, 1996; Kraus *et al.*, 1996).

METHODS

This study involved three summers of structural field mapping (scale 1:5000) between 1992 and 1994 covering over 1000 outcrops in an area of about 100 km^2. The petrography, and structural and metamorphic textures of the exposed rocks were examined microscopically using 700–800 thin sections. Microprobe analyses were performed on thirteen representative samples and the results were used for calculating metamorphic pressures and temperatures. Using the acquired data and the results of other published studies (geochronology, geochemistry, crustal heat flow studies, melting experiments etc.), an attempt was made to draw on many separate lines of evidence to synthesize a coherent tectonic interpretation. This interpretion is placed within the framework of competing processes regarding low- to medium-pressure metamorphism during continent–continent collision (Chapter 4).

Laurentia's first gigayear resembles a symphony in four movements: 2.0–1.8 Ga (allegro), 1.8–1.6 Ga (andante), 1.6–1.3 Ga (adagio), and 1.3–1.0 Ga (allegro).

P.F. Hoffman (1989a)

GEOLOGICAL SETTING

Lithotectonic elements of the Trans-Hudson Orogen

The Trans-Hudson Orogen (Hoffman, 1981) is part of a network of Paleoproterozoic[3] belts in North America, Greenland, Scotland and Scandinavia, that represent former continental collision zones between Archean microcontinents, contributing to the assembling of the Laurentia–Baltica protocraton between 2.0 and 1.8 Ga (Fig. 1.2) (Gibb and Wallcott, 1971; Dewey and Burke, 1973; Gibb, 1975; Hoffman, 1988, 1989b, 1990).

Paleoproterozoic collisional orogens between seven former Archean microcontinents

---

[3]2.5–1.6 Ga (Cowie and Basset, 1989; Cowie *et al.*, 1989)

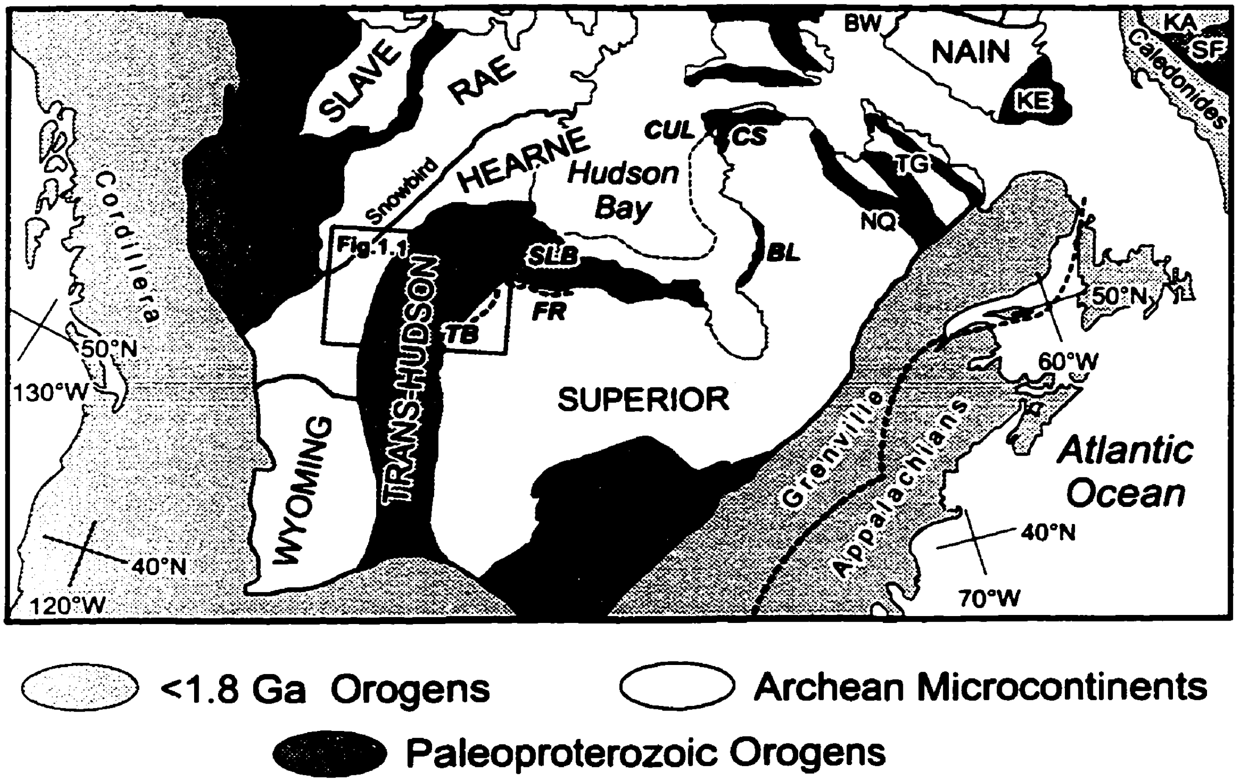

Figure 1.2 Simplied map of the Precambrian tectonic elements of Laurentia–Baltica (pre-Iapetus reconstruction). *BL*, Belcher Belt; *CS*, Cape Smith Belt; *FR*, Fox River Belt; *SLB*, Split Lake Block; *CUL*, Circum-Ungava Line; *TB*, Thompson Belt; BW, Burwell Craton; KA, Karelian; KE, Ketilidian; NQ, New Quebec; SF, Svecofennian; TG, Torngat. After Hoffman (1988).

(Superior, Wyoming, Slave, Nain, Hearne, Rae and Burwell) have been recognised in North America (Hoffman, 1988, 1989b). These microcontinents may be the fragments of a Late Archean supercontinent (Aspler and Chiarenzelli, 1997, 1998; Heaman, 1997); however, only the Trans-Hudson Orogen, which welds the Wyoming and Hearne microcontinents to the larger Superior microcontinent, preserves a significant volume of juvenile Proterozoic crust (Hoffman, 1989b). Today, the Trans-Hudson Orogen is ~500 km wide, extends for some 5000 km from South Dakota through Hudson Bay to Greenland (Fig. 1.2) (Green *et al.*, 1979, 1985; Hoffman, 1981, 1988, 1990; Sharpton *et al.*, 1987; Klasner and King, 1990; Lewry and Collerson, 1990; Nelson *et al.*, 1993), and has a possible continuation in the Belomorides of the Baltic Shield (cf. Gower, 1985; Hoffman, 1988; Park, 1991; Friend *et al.*, 1997). The orogen is divided into the Manitoba–Saskatchewan and Dakota segments in the southwest, and the Hudson Bay and Ungava segments in the northeast (Hoffman, 1988, 1989b). The exposed part of the Trans-Hudson Orogen (approximately north of the 55th parallel) is further subdivided into an external zone, which comprises the deformed eastern and northern margin of the Superior plate to the east (Thompson, Split Lake, Fox River, Belcher and Cape Smith belts), and the Wollaston and Seal River fold belts to the west, and an internal zone (La Ronge, Lynn Lake, Rusty Lake, Glennie Lake, Hanson Lake, Flin Flon (Amisk collage), Rottenstone–Southern Indian and Kisseynew domains), which contains the accreted terranes between the Superior zone and the Wathaman batholith (Fig. 1.1) (Lewry, 1981; Lewry *et al.*, 1981, 1987, 1990; Stauffer, 1984; Hoffman, 1988, 1989b, 1990). A frequently used term "Reindeer zone" refers to the internal Trans-Hudson orogen plus the Wathaman batholith (Fig. 1.1) (Stauffer, 1984; Lewry and Collerson, 1990). The external belts are interpreted as a major circum-Superior suture zone, characterised by distinct positive gravity anomalies (Gibb and Walcott, 1971; Dewey and Burke, 1973; Gibb, 1975, 1983; Mukhopadhyay and Gibb, 1981).

Like other Paleoproterozoic collisional orogens resulting from subduction of oceanic lithosphere, the Trans-Hudson Orogen is asymmetrical in terms of sedimentation, structure, metamorphism and magmatism (Hoffman, 1988, 1989b). To the east, a sedimentary prism is thrust onto the Superior foreland, and to the north and west a continental magmatic arc (Wathaman batholith) formed during northwest-directed subduction toward the reactivated Ray–Hearne hinterland (Fig. 1.1) (Hoffman, 1988, 1989b; Bleeker, 1990a; Meyer *et al.*, 1992).

External zone of the Trans-Hudson Orogen

The external zone of the Trans-Hudson Orogen (Figs 1.1 and 1.2), which represents the tectonically modified remnants of a Paleoproterozoic continental Superior margin that formed in response to the breakup of a late Archean supercontinent, shows >200 m.y. of convergent and divergent plate margin activity (Hoffman, 1988, 1989b, 1990; Bleeker, 1990a; St-Onge *et al.*, 1992; St-Onge and Lucas, 1993; Aspler and Chiarenzelli, 1997, 1998; Heaman, 1997). Lithologies include continental rift to oceanic sequences, granitoid intrusions, and reworked Archean basement, but little juvenile magmatic additions (Hoffman, 1988, 1989b, 1990; Bleeker, 1990a; Bleeker *et al.*, 1995). All external belts show evidence of thrusting onto the Superior Plate during final collision (Hoffman, 1985, 1988, 1989b, 1990; Lucas, 1989, 1990; Bleeker, 1990a, b; Weber, 1990; St-Onge *et al.*, 1992; St-Onge and Lucas, 1993).

Manitoba–Saskatchewan segment: Thompson Belt, Split Lake Block and Fox River Belt

The northwest-trending Thompson Belt (or Thompson Nickel Belt; Fig. 1.2) is an early collision zone formed due to north–south or northwest–southeast oblique convergence between the Superior plate and the internal Trans-Hudson Orogen (e.g. Baragar and Scoates, 1981; Lewry, 1981; Hoffman, 1988, 1989b, 1990; Bleeker, 1990a, b). Geophysical data reveal a southeasterly sub-Phanerozoic extension as far as south Dakota (Fig. 1.2) (Green *et al.*, 1979, 1985; Thomas *et al.*, 1987; Klasner and King, 1990). To the northwest, the Thompson Belt is bounded by the Kisseynew Domain of the internal Trans-Hudson Orogen along the Setting Lake fault zone (e.g. Bleeker, 1990b). To the southeast, the Hudsonian front, that is the boundary between unreworked Archean crust (low- to medium-grade granite–greenstone terranes and the high-grade Pikwitonei gneisses, respectively) and the Thompson Belt, is tentatively assumed to be defined by an abrupt trend change of aeromagnetic fabrics from boundary-parallel northeast–southwest to east–west (Kornik and MacLaren, 1966; for discussion see Bleeker, 1990a, fig.2).

The Thompson Belt hosts variably reworked and retrogressed Archean basement gneisses that are overlain by a Paleoproterozoic rift sequence (Ospwagan group) along the western margin (e.g. Bleeker, 1990a). The age of the Ospwagan group is poorly constrained between 2.1 and 1.88 Ga (Brooks and Theyer, 1981; cf. Ansdell and Bleeker, 1997). A metadiorite intrusion dated at 1836 +5/-3 Ga is the oldest calc-alkaline pluton in the Thompson Belt, and is similar in age to post-accretion calc-alkaline magmatism in the adjacent Kisseynew Domain (Gordon, 1989; Gordon *et al.*, 1990; Bleeker *et al.*, 1995). Intrusion of the Molson dykes at ~1.88 Ga (Heaman *et al.*, 1986), initially regarded as being related to rifting along the Superior margin (e.g. Green *et al.*, 1985), clearly postdates early compressional deformation (Bleeker, 1990a, b; Hoffman, 1990). Rifting is more likely correlatable with a ~2.1 Ga dyke swarm (Zhai and Halls, 1994; Heaman and Corkery, 1996), and the 2025 +/- 25 Ma cement in sediments of the Richmond Gulf group at the northern Hudson Bay coast (Chandler and Parrish, 1989). During F_1/F_2 ductile deformation, retrogressed basement and Proterozoic cover were thrust westerly onto the Superior foreland (Hoffman, 1988, 1989b; Bleeker, 1990a, b; Lucas *et al.*, 1996b). F_3 upright folding with associated mylonitisation and pegmatites at ~1.79 Ga marked the onset of west-vergent thrusting of the Superior plate margin over the internal Trans-Hudson Orogen leading to rapid uplift of the Thompson Belt (Bleeker and Macek, 1996).

The metamorphic history of the Thompson Belt is characterised by an inferred clockwise P–T–t loop (Bleeker, 1990a, b). Peak metamorphic conditions up to upper medium grade outlasted F_2. The peak metamorphism is bracketed by a post-F_1, pre-F_3 granite at ~1.82 Ga, and the intrusion of ~1.79–1.77 Ga pegmatites coeval with F_3 folding and retrograde metamorphism (Machado *et al.*, 1987; Bleeker, 1990a, b). The metamorphic peak was thus broadly coeval in the Thompson Belt and in the internal juvenile domains. The granitic magmatism in the Thompson Belt was interpreted as resulting from thermal relaxation following crustal thickening (Bleeker, 1990a, b).

The east-trending Split Lake Block and Fox River Belt (Fig. 1.2) are northeasterly extensions of the Thompson Belt (Baragar and Scoates, 1981; Scoates, 1981; Hoffman, 1988, 1989b, 1990; Bleeker, 1990a; Weber, 1990). The Split Lake Block, like the Thompson Belt, comprises variably reworked basement gneisses intruded by Paleoproterozoic dyke swarms, but lacks rift sediments (ibid.). The Fox River Belt, on the other hand, comprises a north-dipping thrust stack of very low-grade supracrustal rocks that are correlated with the Ospwagan group and related intrusive rocks (Baragar and Scoates, 1981; Hoffman, 1988, 1989b, 1990; Bleeker, 1990; Weber, 1990). The Fox River Belt is structurally sandwiched between medium-grade metaturbidites of the Kisseynew Domain and retrogressed medium-grade to pristine high-grade Pikwitonei gneisses in the hanging wall and footwall, respectively (Weber and Scoates, 1978; Weber, 1990).

Hudson Bay segment: Belcher and Cape Smith belts

The Belcher Belt in eastern Hudson Bay (Fig. 1.2) comprises a rift to trans-oceanic sequence including a rift-valley prism, post-rift shelf carbonates, plateau basalts, and foredeep deposits, all metamorphosed at very low grade (Ricketts and Donaldson, 1981; Hoffman, 1988, 1989b). The sequence was juxtaposed with medium-grade Archean gneisses of the Superior craton during east-directed thrusting. U–Pb ages for basalt flows in the rift-related rocks are between 1.96 and 1.81 Ga, and were interpreted as maximum ages for the sedimentation (Todt *et al.*, 1984). The east–west-trending Cape Smith Belt (Fig. 1.2) at the northern tip of the Ungava peninsula is a klippe of an infolded south-vergent fold and thrust belt (Hoffman, 1985, 1988, 1990; Lucas, 1989, 1990; Lucas and St-Onge, 1992; St-Onge and Lucas, 1993). The exposed volcanic and sedimentary rocks record the evolution of the rifted northern margin of the Superior plate. Continental rift facies rocks yielded ages between ~204 and ~1.92 Ga (Parrish, 1989; Machado *et al.*, 1993). The ~2.00 Ga Watts group is the only clearly identified ophiolite in the Trans-Hudson Orogen. As in the Thompson Belt, thrusting over the Superior foreland began prior to 1.87 Ga, and thermotectonism persisted until ~1.8 Ga (Parrish, 1989; Lucas and St-Onge, 1992; St-Onge *et al.*, 1992; St-Onge and Lucas, 1991, 1993). The peak of metamorphism up to kyanite grade has not been dated in the Cape Smith Belt; in the Archean hinterland it is dated at ~1.83–1.82 Ga (Parrish, 1989; St-Onge and Lucas, 1991; cf. Scott and St-Onge, 1995; St-Onge and Lucas, 1995).

Internal zone of the Trans-Hudson Orogen

The internal zone of the Trans-Hudson Orogen (Fig. 1.1) contains a collage of deformed and metamorphosed, juvenile 1.92–1.84 Ga volcanic arc, oceanic and sedimentary rocks (e.g. Baldwin *et al.*, 1987; Lewry, 1981; Lewry *et al.*, 1981, 1987; van Schmus *et al.*, 1987; Watters and Pearce, 1987; Hoffman, 1988, 1989b, 1990; Bickford *et al.*, 1990; Gordon *et al.*, 1990; Thom *et al.*, 1990; Lucas *et al.*, 1994, 1996a; Stern *al.*, 1995a, b).

Wathaman batholith and Rottenstone–Southern Indian Domain

The Wathaman batholith (1.865–1.850 Ga; Fig. 1.1), located at the western and northwestern margin of the Trans-Hudson Orogen, is a ~900 km long and up to 100 km wide Andean type magmatic arc built at least in part on Archean crust, against which the domains of the internal Trans-Hudson Orogen were accreted (Lewry *et al.*, 1981; Fumerton *et al.*, 1984; Halden *et al.*, 1990; Meyer *et al.*, 1992). The arc is separated from the Archean Rae–Hearne hinterland in the northwest by the steep northwesterly dipping Needle Falls shear zone (Fig. 1.1), which is interpreted as a late collisional structure (Stauffer and Lewry, 1993; Lewry *et al.*, 1994). The orogen-parallel-trending Rottenstone–Southern Indian Domain (Fig. 1.1) consists of migmatised supracrustal rocks and related intrusive suites (e.g. Lewry, 1981; Lewry *et al.*, 1987; van Schmus *et al.*, 1987). To the southeast, the La Ronge Domain and the similar Lynn Lake and Rusty Lake domains (Fig. 1.1) represent stacks of northwest- to north-dipping tectonostratigraphic volcanic packages, most of which are bound by high strain zones (Lewry *et al.*, 1990, 1994). The geochemical signatures of these rocks suggest formation in an island arc setting (Watters and Pearce, 1987; Syme, 1990). U–Pb zircon dating has established that the earliest island arc volcanism occurred at ~1.91 Ga in the Lynn Lake Domain, approximately coeval with the Amisk collage (Baldwin *et al.*, 1987; Stern *et al.*, 1995a, b).

Flin Flon–Glennie Complex

The Flin Flon–Glennie Complex or Flin Flon Belt (Figs 1.1 and 1.3) is the middle element of a crustal-scale tectonic stack sandwiched between the Kissynew Domain and Archean rocks in the hanging wall and footwall, respectively (Lucas *et al.*, 1997). Three

Figure 1.3 Geological map approximately coinciding with the NATMAP Field Margin Project area, comprising the Hanson Lake Block (HLB), the Amisk collage (AC), the southern flank of the Kisseynew Domain (SFKD), part of the central Kisseynew Domain (KD), and the Snow Lake Allochthon (within dashed border). PD, Pelican décollement zone.

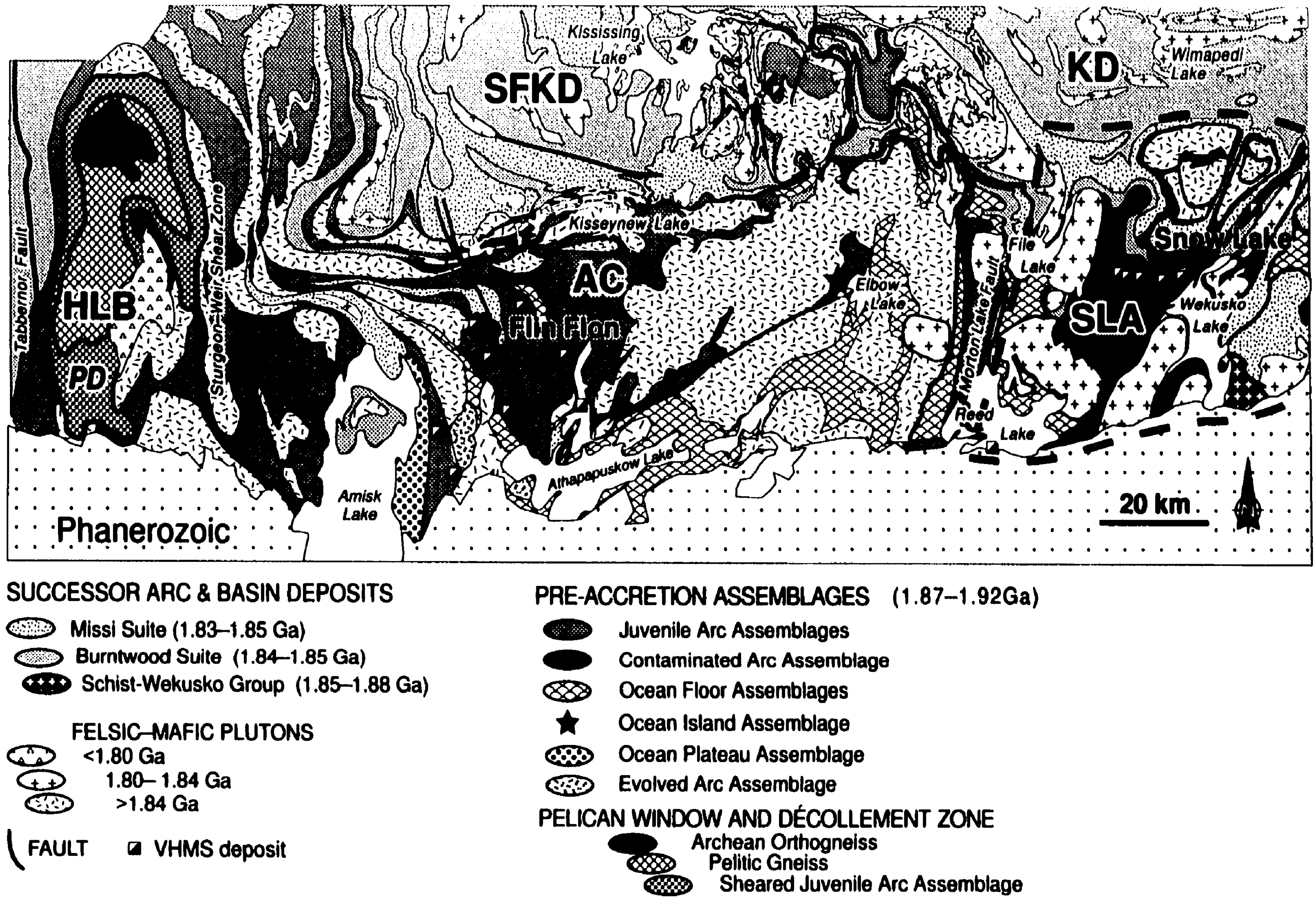
Kississing Lake
SFKD
KD
Wimapedi Lake
Kisseynew Lake
AC
Flin Flon
HLB
PD
Tabbernor Fault
Sturgeon-Weir Shear Zone
Amisk Lake
Athapapuskow Lake
Elbow Lake
Morton Lake Fault
File Lake
Reed Lake
Snow Lake
SLA
Wekusko Lake
Phanerozoic
20 km
SUCCESSOR ARC & BASIN DEPOSITS
Missi Suite (1.83–1.85 Ga)
Burntwood Suite (1.84–1.85 Ga)
Schist-Wekusko Group (1.85–1.88 Ga)
FELSIC–MAFIC PLUTONS
<1.80 Ga
1.80–1.84 Ga
>1.84 Ga
FAULT
VHMS deposit
PRE-ACCRETION ASSEMBLAGES (1.87–1.92Ga)
Juvenile Arc Assemblages
Contaminated Arc Assemblage
Ocean Floor Assemblages
Ocean Island Assemblage
Ocean Plateau Assemblage
Evolved Arc Assemblage
PELICAN WINDOW AND DÉCOLLEMENT ZONE
Archean Orthogneiss
Pelitic Gneiss
Sheared Juvenile Arc Assemblage

major lithotectonic elements distinguished (from west to east) are the Glennie Domain, the Hanson Lake Block (including the Attitti Block), and the Amisk collage (previously referred to as "Flin Flon Domain"). They are separated by the steep Tabbernor fault and the Sturgeon–Weir shear zone, respectively (Figs 1.1 and 1.3) (Lewry and Sibbald, 1977; Lewry, 1981; Stauffer, 1984; Ashton *et al.*, 1987; Lewry *et al.*, 1990; Elliott, 1995, 1996b; Syme *et al.*, 1995; Lucas *et al.*, 1996a, 1997). Some workers include the Snow Lake Allochthon as the most easterly segment of the Flin Flon–Glennie Complex (e.g. Lucas *et al.*, 1996a). I, however, regard the Snow Lake Allochthon as its own lithotectonic domain for reasons given below.

The Glennie Domain (Fig. 1.1) hosts mainly volcanic and plutonic packages with minor supracrustal rocks in narrow arcuate belts, accreted to the La Ronge arc (Lewry, 1981). The adjacent Hanson Lake Block (Figs 1.1 and 1.3) comprises a refolded ductile nappe complex of mainly low- to medium-grade plutonic and juvenile volcanic rocks (Lewry, 1981; Lewry *et al.*, 1990).

The well-understood Amisk collage (Fig. 1.3) is a former intra-oceanic accretionary complex that was assembled prior to sedimentation in the Kisseynew marginal basin, and prior to the terminal collision of the Wyoming–Hearne plate with the Superior plate (Hudsonian orogeny; see below) (Lucas *et al.*, 1996a, 1997). It consists of an amalgamation of distinct tectonostratigraphic assemblages (Amisk collage), which is segmented by major shear zones with protracted, up to 100 m.y., histories (Ryan and Williams, 1995, 1996a, in press; Stern *et al.*, 1995a, b; Lucas *et al.*, 1996a). Four main assemblages have been distinguished (Syme, 1990; Syme and Bailes, 1993; Watters *et al.*, 1994; Stern *et al.*, 1995a, b): (1) isotopically juvenile oceanic arc (1.90–1.88 Ga); (2) ocean floor (~1.9 Ga); (3) oceanic plateau/ocean island (1.92–1.9 Ga); and (4) isotopically-evolved arc (1.92–1.9 Ga). Initial ϵ_{Nd} values (typically between +3.1 to +4.8) indicate derivation dominantly from depleted mantle sources (Stern *et al.*, 1995a).

The tectonometamorphic history of the Amisk collage can be divided into three stages: (1) convergent margin (oceanic) tectonism and magmatism (1.92–1.84 Ga); (2) consumption of oceanic basins and intracontinental deformation associated with the terminal stages of continental collision (1.84–1.80 Ga), and (3) post-collisional intracontinental deformation (~1.8–1.77 Ga) (Bickford *et al.*, 1990; Gordon *et al.*, 1990; Ashton *et al.*, 1992; Ansdell and Norman, 1995; Fedorowich *et al.*, 1995; David *et al.*, 1996; Hajnal *et al.*, 1996; Lucas *et al.*, 1996a; Ryan and Williams, in press). The first stage involved amalgamation of the 1.92–1.88 Ga assemblages along thrusts and/or shear zones during 1.88–1.87 intra-oceanic collision tectonism to form an accretionary complex (Amisk collage) (Lucas *et al.*, 1996a; Ansdell and Ryan, 1997). Continental crust was produced by intrusion of felsic to mafic calc-alkaline plutons into the tectonostratigraphic assemblages (1.87–1.84 Ga), and by deposition of sedimentary and volcanic rocks in successor arc basins (1.86–1.84 Ga) during ongoing intra-arc (shear zone) deformation; some of these packages are also preserved in younger basins (< 1.83 Ga) (Lucas *et al.*, 1996a). Crustal growth and syntectonic uplift established the Flin Flon microcontinent (1.85–1.84 Ga), which is similar to the Japan and Philippine microcontintents, and the former was subsequently dismembered during intracontinental deformation (Bickford *et al.*, 1990; Lewry *et al.*, 1990; Stern *et al.*, 1995a, b; Lucas *et al.*, 1996a). The microcontinent is interpreted as having been juxtaposed with structurally overlying metasediments of the Kisseynew Domain and underlying Archean basement during southwest-directed thrusting related to the terminal collision of Archean microcontinents at ~1.84–1.81 Ga. During this period, the deformation in the Amisk collage continued to be accommodated along steep shear zones (Bickford *et al.*, 1990; Zwanzig, 1990; Lucas *et al.*, 1994, 1996a; Lewry *et al.*, 1994; Norman *et al.*, 1995; Ryan and Williams, in press).

Basement rocks in the Flin Flon–Glennie Complex

Rare Archean basement gneisses constitute the deepest structural levels of the Flin Flon–Glennie Complex. They are interpreted as structural windows of the buried "Saskatchewan" craton (Lewry, 1981; Green *et al.*, 1985; van Schmus *et al.*, 1987; Chiarenzelli and Lewry, 1988; Lewry *et al.*, 1990, 1994; Lucas *et al.*, 1993, 1994, 1996a; Ansdell *et al.*, 1995, in press; Chiarenzelli *et al.*, 1996, 1998; Aspler and Chiarenzelli, 1997, 1998; Ashton *et al.*, in press). The Saskatchewan craton is interpreted to be regionally extensive beneath the domains of the internal Trans-Hudson Orogen, including the Kisseynew Domain, and appears to have a considerable lateral extent to the south, sandwiched between the sub-Paleozoic continuations of the Rottenstone Domain and the Amisk Collage. The craton may represent a fragment of the Archean supercontinent that broke apart between ~2.1 and 1.9 Ga (Lewry, 1981; Green *et al.*, 1985; Lucas *et al.*, 1993, 1994; Lewry *et al.*, 1994; Ansdell *et al.* 1995; Chiarenzelli *et al.*, 1996, 1998; Heaman, 1997, Ashton *et al.*, in press; Aspler and Chiarenzelli, 1998).

The most prominent of the Archean inliers, the Sahli charnockitic granite, occupies an anticlinal core (Pelican window) within a large dome and basin interference structure in the Hanson Lake Block (Fig. 1.3) (Lewry, 1981; van Schmus *et al.*, 1987; Lewry *et al.*, 1990, 1994; Ashton *et al.*, in press). The Pelican window is rimmed by a 3–7 km wide mylonite zone (Pelican décollement; Fig. 1.3), which is interpreted as the root zone related to the ~1.84–1.81 Ga southwest-directed thrusting that predated and/or coincided with the peak of metamorphism in the internal Trans-Hudson Orogen (Lewry *et al.*, 1996; Ashton *et al.*, in press). Considering that Archean crust is generally cold and depleted in radioactive elements (Tarney, 1976, pers. comm. 1997), the proposed extent of underthrust basement is in apparent contrast with the metamorphic history for the Kisseynew Domain delineated in this thesis (Chapter 4). This problem is discussed further in the concluding chapter.

Kisseynew Domain

The Kisseynew Domain (Fig. 1.1) constitutes a former marginal basin, which was inverted and metamorphosed under high-grade conditions during continental convergence between 1.84 and 1.81 Ga (Bailes and McRitchie, 1978; Bailes, 1980b; Gordon, 1989; Gordon *et al.*, 1990; Zwanzig, 1990; Norman *et al.*, 1995; Ansdell *et al.*, 1995; David *et al.*, 1996). The distribution of tectonostratigraphic packages in the Kisseynew Domain is symmetrical along a north–south profile (Zwanzig, 1990). The tectonostratigraphic packages comprise: (1) ~1.86–1.84 Ga turbidites of the Burntwood group, now uniform garnet–cordierite and K-feldspar–sillimanite migmatitic paragneisses, which are exposed throughout the central Kisseynew Domain. The Kisseynew Domain is thus the highest-grade metamorphic portion of the Trans-Hudson Orogen (lower granulite grade); the paragneisses are intruded by (2) a ~1.84–1.83 Ga calc-alkaline suite (tonalite and enderbites) and (3) ~1.815 Ga peraluminous granites, likely derived from partial melting at the base of the basin (Chapter 3); (4) at the southern, southeastern and northern margins of the Kisseynew Domain, fluvial–alluvial sedimentary rocks of the Missi group overlie Burntwood group and rocks of the adjacent previously deformed domains (Harrison, 1951; Bailes, 1980a, b, 1985; Gordon, 1989; Gordon *et al.*, 1990; Stauffer, 1990; Zwanzig, 1990; Machado and Zwanzig, 1995; David *et al.*, 1996). Initial ϵ_{Nd} values indicate that, in contrast to the juvenile volcanic domains, the Burntwood group and granitoids contain a minor Archean component (Chauvel *et al.*, 1987; Thom *et al.*, 1987). This is supported by U–Pb ages of detrital zircons from the Burntwood and Missi groups, which cluster around 2.45–2.0 Ga and 1.9–1.84 Ga (Ansdell, 1993; Machado and Zwanzig, 1995; David *et al.*, 1996; Machado *et al.*, 1996), suggesting distinct Archean and Proterozoic source rocks.

The structural trend of the Kisseynew Domain is west-northwest, and thus at a high angle to the orogen-parallel trends of the juvenile volcanic to oceanic terranes (see Zwanzig, 1990, fig. 14). These differences in structural grain arise from the fact that the primary layering of the juvenile intra-oceanic domains had already been steepened during early deformation prior to basin sedimentation (see Lucas *et al.*, 1996a; Ryan and Williams, 1996a). In contrast to metamorphism and tectonostratigraphy, the structure across the Kisseynew Domain is markedly asymmetrical; the Kisseynew gneisses were thrust in a southerly direction onto the Flin Flon–Glennie Complex, and were coevally overthrust by the Lynn Lake Domain from the north at ~1.84–1.81 Ga (Zwanzig, 1990; Kraus and Williams, 1994b; Norman *et al.*, 1995; White *et al.*, 1996). After a period of broadly east–west shortening at ~1.8 Ga, which produced northerly-trending upright open folds, renewed southerly transport resulted in local westerly trending late structures (Bailes, 1975; Zwanzig, 1990; David *et al.*, 1996; Chapter 5).

Snow Lake Allochthon

The term Snow Lake Allochthon is introduced herein to delimit the zone of tectonic interleaving of the Burntwood and Missi groups, the Snow Lake assemblage, and the ocean floor assemblages on northeast Reed Lake and east of Wekusko Lake (Fig. 1.3) (Syme *et al.*, 1995). The Snow Lake Allochthon terminates against the Amisk collage to the west along the Morton Lake fault zone (Fig. 1.3) (Stern *et al.*, 1995a, 1995b; Lucas *et al.*, 1996a). To the northwest of the Morton Lake fault zone, it continues as the southern flank of the Kisseynew Domain in the structural hanging wall of the Amisk collage, the Hanson Lake Block, and the Glennie Domain (Zwanzig, 1990; Ansdell and Norman, 1995; Norman *et al.*, 1995; Machado *et al.*, 1996). The southern flank of the Kisseynew Domain is a broad transitional zone of tectonic interleaving of rocks of the Kisseynew Domain and of the Flin Flon–Glennie Complex.

The Snow Lake (arc) assemblage (Fig. 1.4) is similar to the arc assemblages of the Amisk collage, but the former displays more extensive hydrothermal alteration (Fig. 1.5) and a higher metamorphic grade (Harrison, 1949; Menard and Gordon, 1995; Bailes and Galley,

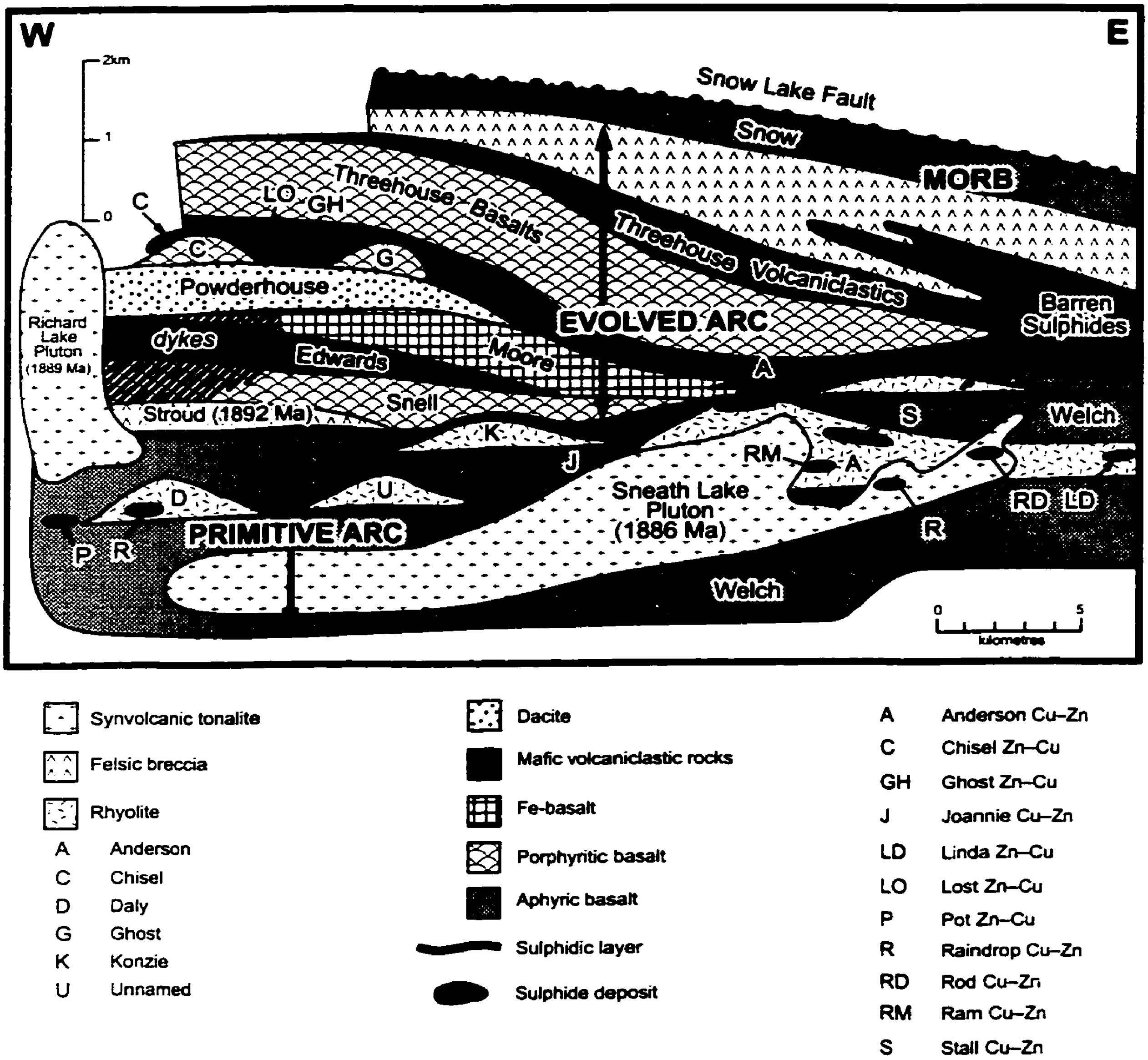

Figure 1.4 Schematic geological cross section of the Snow Lake assemblage. From Bailes and Galley (1996).

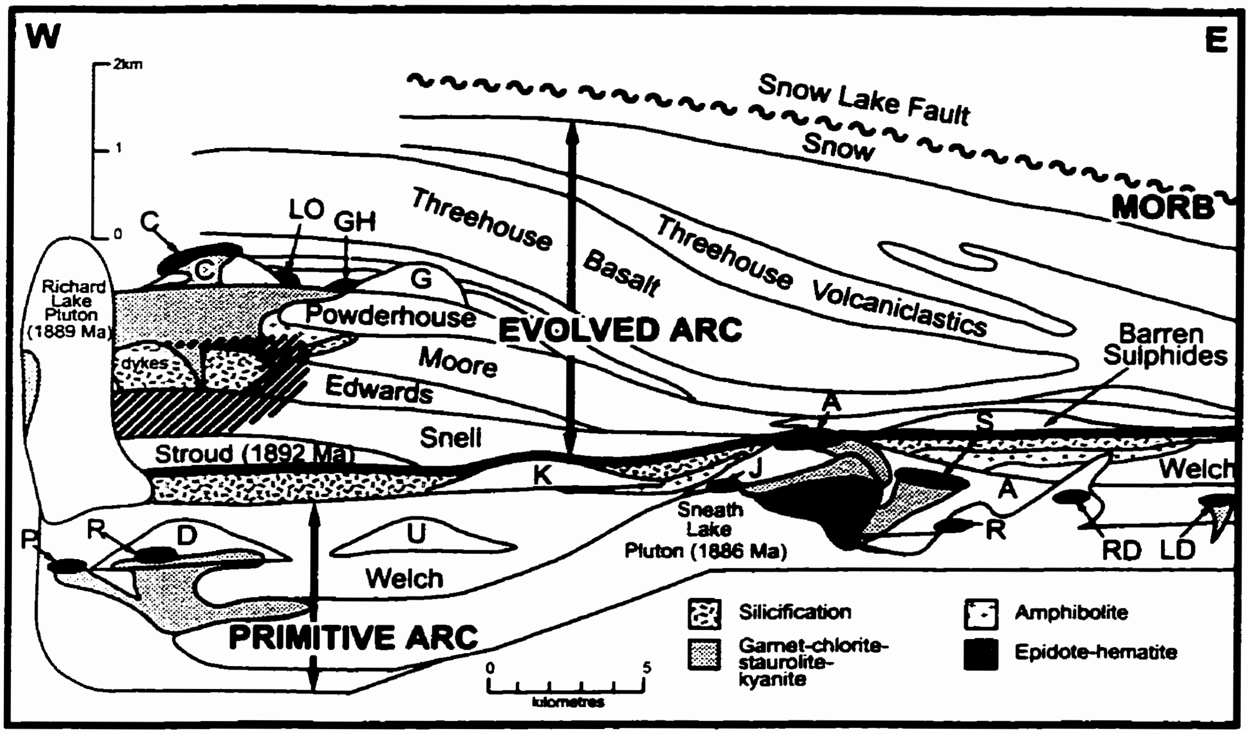

Figure 1.5 Distribution of hydrothermally altered rocks in the Snow Lake assemblage. For explanation of abbreviations, see Figure 1.4. From Bailes and Galley (1996).

1996). The most significant differences are that, compared to the Amisk collage, the Snow Lake assemblage has lower initial ϵ_{Nd} values (-0.4 to + 3.1) (Stern *et al.*, 1995a) and inherited Archean zircons in rhyolite and synvolcanic intrusions (David *et al.*, 1996). These data indicate contamination by Archean crust, possibly related to sediment subduction and/or building of the Snow Lake arc on a rifted continental fragment (Stern *et al.*, 1995a; Chapter 5). The Snow Lake assemblage was intruded by the pervasive 1.84–1.83 Ga calc-alkaline suite (see above), but not affected by the 1.87–1.845 Ga successor arc plutonism that was widespread in the Amisk collage (Gordon *et al*, 1990; Stern *et al.*, 1995a; David *et al.*, 1996; Lucas *et al.*, 1996a). Until recently, the Burntwood group, Snow Lake arc assemblage and the assemblages constituting the Amisk collage were uniformly referred to as the "Amisk group" as defined by Bruce (1918); however, the results of new geochemical, geochronological and structural work cited above require the present distinction (Lucas *et al.*, 1996a, 1997).

Bailes and Galley (1996) established a > 6 km thick stratigraphic succession (Figs 1.4 and 1.5), which shows upward maturing (and thus a temporal evolution) from primitive arc to evolved arc lithologies, and is locally overlain by a thin sliver of ocean floor basalt. Arc volcanic rocks were mainly deposited subaqueously, but minor shallow marine to subaerial pyroclastic rocks are also present (Bailes and Galley, 1996). The bimodal, primitive arc sequences include Welch basalt/basaltic andesite, rhyolite, and the synvolcanic ~ 1.9 Ga Sneath Lake tonalite. The > 3km thick Welch complex was interpreted as having formed in a forearc setting (Stern *et al.*, 1995a). Cu-rich VHMS deposits are contained in rhyolite, with the Sneath Lake tonalite as the driving heat source for the hydrothermal system

(Walford and Franklin, 1982). The bimodal, evolved arc sequence contains a series of mafic flows (e.g. the Snell, Moore, Vent, and Threehouse flows), felsic flows (Powderhouse dacite, and the Chisel, Ghost, and Photo rhyolites), and intrusions (~ 1.9 Ga Richard Lake tonalite), which, in comparison with the underlying primitive arc sequence, are thinner and laterally less continuous. As in the primitive arc, Zn-rich VHMS deposits are stratigraphically related to felsic flows, whereas Cu–Au–Zn-rich deposits are of uncertain affinity.

In summary, the Snow Lake Allochthon is distinct from the Amisk collage of the Flin Flon–Glennie Complex, so that I consider it as its own lithotectonic domain. In contrast to the neighbouring Amisk collage, the Snow Lake Allochthon has a structural grain and records a structural and magmatic history similar to that of the Kisseynew Domain and its southern flank, with no clearly identified pre-Missi (accretionary) structures in the volcanic assemblages. The arc assemblages of the Amisk collage and the Snow Lake Allochthon are of different origin. The allochthon contains large volumes of Kisseynew Domain rocks.

Syntectonic igneous rocks in the Trans-Hudson Orogen

Along the southern flank of the Kisseynew Domain, the Missi group contains early tectonic 1.84–1.83 Ga metagabbros and metatonalites (Ansdell and Norman, 1995; Norman *et al.*, 1995), that correlate well in age with enderbite and tonalite intrusions in the La Ronge, Glennie and central Kisseynew Domains (Bailes, 1985; Lewry *et al.*, 1987; Gordon, 1989; Bickford *et al.*, 1990; Gordon *et al.*, 1990). The Missi group of the Snow Lake Allochthon east of Wekusko Lake (Fig. 1.3) contains a bimodal volcanic suite of broadly the same age as the igneous rocks above (Ansdell *et al.*, 1995, in press). Ansdell *et al.* (1995) related the East Wekusko volcanic suite to southward subduction of Kisseynew crust. Alternatively, the magmas were derived directly from the mantle, and obtained their geochemical signatures by assimilation.

Manikewan ocean closure, the Hudsonian Orogeny, and post-Hudsonian events

Paleomagnetic data suggest that Paleoproterozoic continental accretion tectonism involved the consumption of ~5000 km of ocean floor during the closure of the Manikewan ocean, which commenced at ~1.92 Ga, initiating active-margin arc magmatism (Stauffer, 1984; Baldwin *et al.*, 1987; Symons *et al.*, 1995, 1996; Stern *et al.*, 1995a, b; Lucas *et al.*, 1996a). At ~1.85 Ga, most of the shrinking Manikewan ocean was located between the Wathaman batholith and the Rottenstone Domain, at tropical paleolatitudes comparable to present northern South America (Dunsmore and Symons, 1990; Symons, 1991, 1994; Symons *et al.*, 1995, 1996). The ocean closed by ~1.84 Ga, coeval with cessation of arc magmatism and flysch sedimentation (Kisseynew basin), and the local development of a regolith and fluvial-alluvial fans on the Flin Flon–Glennie microcontinent (e.g. Holland *et al.*, 1989; Gordon *et al.*, 1990; Stauffer, 1990; Ansdell, 1993; Ansdell *et al.*, 1995; David *et al.*, 1996; Lucas *et al.*, 1996a).

Stockwell (1961) suggested the term "Hudsonian orogeny" for the "last period of folding, metamorphism, and intrusion" in the Churchill Province [4], constrained by 1.85 to 1.55 Ga K/Ar ages from granitic or high-grade metamorphic rocks. In the presently used terminology, "Hudsonian orogeny" refers to the ~1.84–1.77 Ga *intracontinental*, nappe-forming thermotectonism during terminal continent–continent collision (Machado *et al.*, 1987; Bickford *et al.*, 1990; Bleeker, 1990a; Gordon *et al.*, 1990; Ansdell *et al.*, 1995; Norman *et al.*, 1995; Lucas *et al.*, 1996a; Ryan and Williams, in press). After ~1.8–1.77 Ga, the bulk of deformation was accommodated by oblique-slip movements along steep, orogen-parallel faults (Lewry *et al.*, 1990, 1994; Elliott, 1995, 1996a; Hajnal *et al.*, 1996). Following the onset of uplift at ~1.79 Ga, hornblende and biotite cooled through the closure temperature of the Ar–Ar and K–Ar system between ~1.77 and 1.70 Ga (closure temperature for hornblende: 450–525°C, biotite: 260–350°C; Spear, 1993), broadly coeval with the age of the brittle–ductile transition (Stockwell, 1961; Gordon, 1989; Bickford *et al.*, 1990; Bleeker, 1990a; Gordon *et al.*, 1990; Hunt and Roddick, 1992, 1993; Fedorowich *et al.*, 1995; Ryan and Williams, 1995; Marshall *et al.*, 1997). After a long phase of thermotectonic quiescence, the Trans-Hudson Orogen was affected by the 1.265 Ga Mackenzie igneous event; LITHOPROBE lines 2b (Fig. 1.1) showed shallow reflectors from the northwestern hinterland to the Glennie Domain interpreted as horizontal mafic to ultramafic intrusions (Mandler and Clowes, 1997). This post-Hudsonian event was attributed to either Middle Paleozoic compressional tectonics preceding the Grenville orogeny, or to moderate extension

---

[4]Churchill Province (Stockwell, 1961) is an abandoned term for the tectonic hinterland, welded by Paleoproterozoic collision zones to the Archean Superior, Nain, Slave and Wyoming microcontinents. It is now subdivided into the Archean Rae, Hearne and Burwell micro-continents, and the internal Trans-Hudson Orogen (Hoffman, 1988, 1990).

(Mandler and Clowes, 1997). Post-Ordovician movements along the Tabbernor fault and parallel structures precluded tectonic activity in the cratonised Trans-Hudson Orogen (Figs 1.1 and 1.3) (Elliott 1995, 1996a).

RESULTS OF PREVIOUS STUDIES

Structure

Following early economic studies (e.g. Bruce, 1917; Alcock, 1920; Stockwell, 1937), a first structural analysis of the Snow Lake area as part of an extensive regional mapping project was attempted by Harrison (1949) of the Geological Survey of Canada. Harrison distinguished "at least two periods of folding and faulting", and noted a northerly trend of folded structures with northerly or southerly plunges (depending on location). He further recognised and named the large-scale folds and shear zones (his terminology is used in this thesis); however, he did not establish their relative ages and overprinting. In particular, Harrison discovered the faulted nature of the contacts between "staurolite schists" (Burntwood group) and the "Amisk group volcanic rocks" (Snow Lake assemblage). Based on the orientations of "slickensides", he interpreted normal movements with downthrow to the northeast (contrary to the present interpretation; Chapter 5). In a subsequent study, Russell (1957) presented the three-dimensional geometry by means of numerous cross sections drawn along lines of an arbitrary coordinate system. He did not add anything to the fold generations established by Harrison (1949), but distinguished three major fault trends (northeast, west-northwest and north); he did not notice that the northeast and west-northwest trends were generated by open refolding of structures which predate northerly trending structures (Chapter 5). Russell also found evidence of southward overthrusting. Moore and Froese (1972), Bailes and McRitchie (1978), Froese and Moore (1980) and Galley *et al.* (1988) distinguished isoclinal folds (F_1) that are overprinted by large-scale open folds (F_2). In addition, Froese and Moore (1980) speculated about a third generation of structures producing a dome and basin interference pattern mapped in the gneiss domes north of Snow Lake (Fig. 1.3).

Metamorphism

Froese and Gasparrini (1975) established metamorphic zones *sensu* Barrow (1912) separated by metamorphic reaction isograds as described by Carmichael (1970). Although based on mineral assemblages in the Burntwood group, the zonal pattern was extrapolated through the Snow Lake assemblage and the Missi group. Froese and Gasparrini (1975) noted a northward increase of metamorphic grade from low grade at Wekusko Lake to high grade in the vicinity of the prominent gneiss domes (Fig. 1.3). Bailes (1975) recorded a metamorphic culmination resulting in migmatisation and granitoid formation in the southern central Kisseynew Domain around Wimapedi Lake (Fig. 1.3), immediately north of Froese and Gasparrini's study area. A preliminary summary of the metamorphism of the Snow Lake area was given by Froese and Moore (1980).

In studies subsequent to Froese and Gasparrini (1975), the metamorphic zones were extrapolated westward to the File Lake area, eastward to the east of Wekusko Lake, and northward through the Kisseynew Domain and adjacent granite–greenstone domains; the large-scale distribution of metamorphic isograds yielded, analogous to the distribution of tectonostratigraphic packages, a bilaterally symmetrical pattern from north to south with the entire Kisseynew Domain forming the locus of a thermal anomaly (Bailes and McRitchie, 1978; Bailes, 1980a, 1985; Gordon, 1981, 1989; Gordon and Gall, 1982; Perkins, 1991; Briggs and Foster, 1992; Gordon *et al.*, 1993, 1994a, b).

With the genesis of VHMS deposits in mind, recent work has focussed mainly on the metamorphism of fluid-altered arc volcanic rocks (Jackson, 1983; Trembath, 1986; Skirrow, 1987; Bristol and Froese, 1989; Zaleski, 1989; Zaleski *et al.*, 1991; Menard and Gordon, 1995, 1997). Zaleski *et al.* (1991) established that the metamorphic assemblages in the altered volcanic rocks around the Linda deposit west of Wekusko Lake (Fig. 1.3), which are now, after alteration, of semi-pelitic composition, are not diagnostic of metamorphic grade. For example, they demonstrated that the assemblage kyanite + biotite + chlorite formed at a lower grade than in typical pelites as a result of reversed Fe–Mg partitioning between biotite and chlorite, and of elevated Zn and F contents in the system. Menard and Gordon (1995) established that whole rock compositional alteration was not, as previously believed, exclusively synvolcanic (Walford and Franklin, 1982), but also occurred in response to fluid flow during syntectonic metamorphism.

Prior to this investigation, temperature and/or pressure estimates were calculated by Bristol (1974), Scott (1976), Hutcheon (1978, 1979), Aggarwal and Nesbitt (1987), Bryndzia and Scott (1987), and Zaleski *et al.* (1991), using samples from the Snow Lake assemblage in the vicinity of the VHMS deposits (Linda deposit and Anderson/Stall mines, which are at a tectonostratigraphic level that corresponds to the staurolite zone of the Burntwood group). Sphalerite barometry yielded pressure estimates of 4–10 kbar (Bristol, 1974; Scott, 1976; Hutcheon, 1978; Bryndzia and Scott, 1987; Zaleski *et al.*, 1991). Sulfide–oxide–silicate equilibria calculations (Hutcheon 1979) yielded temperatures of ~620° and ~625°C for the Anderson and Stall mines, respectively. Calculated temperatures for the Anderson mine area (Aggarwal and Nesbitt, 1987) ranged from 530 °C to 680°C at associated pressures of 5–6 kbar, using the garnet–biotite thermometer and silica equilibria, respectively. The relatively large scatter of P–T data and the notable difference from results in this investigation (Chapter 4) arise from both the inaccuracy of the sphalerite barometer (Bristol, 1974; Scott, 1976; Hutcheon, 1978; Bryndzia and Scott, 1987; Zaleski *et al.*, 1991), and from the use of garnets, which are compositionally outside the calibration range for thermometers based on Fe–Mg exchange (Aggarwal and Nesbitt, 1987). More conservative estimates, based on mineral assemblages and reactions, suggest temperatures of 450–500°C in the chlorite+biotite zone, and ~750–800°C in the central Kisseynew Domain, at associated pressures of 3.5–6 kbar (Froese and Gasparrini, 1975; Bailes and McRitchie, 1978; Gordon, 1989). The most accurate pressure and temperature estimates, and P–T paths calculated recently (Menard and Gordon, 1995, 1997; Kraus and Menard, 1995) are discussed in detail in Chapter 4.

You can pretend to be serious; you can't pretend to be witty.
Sacha Guitry

Chapter 2[1]

Relationships between foliation development, porphyroblast growth and large-scale folding in a metaturbidite suite, Snow Lake, Canada

Abstract: Complex relationships exist between cleavage development, metamorphism and large-scale folding in the well-bedded, polydeformed, staurolite-grade metaturbidites of the Burntwood group, internal Paleoproterozoic Trans-Hudson Orogen at Snow Lake, Manitoba, Canada. It is demonstrated (a) that cleavage in anisotropic pelitic rock develops when microfolding is possible and, that commonly, initiation of a cleavage, which is pervasive on the scale of a fold, predates folding, (b) how a new axial planar fabric can develop on one fold limb of a symmetrical fold and not on the other, and (c) how two cleavages of different generations can be present in adjacent beds. It is further shown that porphyroblasts rotate with respect to geographical coordinates during folding. Finally, dissolution of cleavage septa is suggested here as an alternative mechanism for the generation of schistosity. The Burntwood group is exposed on the dismembered limb of a macroscopic, isoclinal F_2

---

[1]An earlier version of this chapter was published in the Journal of Structural Geology, volume 20, Kraus, J. and Williams, P.F. "Relationships between foliation development, porphyroblast growth and large-scale folding in a metaturbidite suite, Snow Lake, Canada", pages 61–76 (1998). Reproduction here is with kind permission from Elsevier Science Ltd., The Boulevard, Langford Lane, Kidlington OX5 1GB, U.K.

structure and preserves a domainal cleavage (S_2), which locally grades into a schistosity. S_2 developed from crenulation of a generally bedding-parallel S_1 cleavage that is axial planar to F_1 isoclinal folds formed at 1.84 Ga. Porphyroblast growth coincided with crenulation of S_1 early during F_2 folding at 1.820–1.805 Ga. Early stages of S_2 development are recorded by inclusion trails (S_i) in the porphyroblasts. During F_2 flexural-flow folding, variations in magnitude of bedding-parallel shear in lithologies of different competency resulted in a strong S_2 refraction and thus heterogeneous strains between beds. Independent of shear magnitude and resulting S_0/S_2 angle, S_i and S_2 remained sub-orthogonal everywhere, and thus porphyroblasts and the enveloping S_2 rotated by equal amounts with respect to S_0. As the different magnitudes of porphyroblast rotation in different beds could not be exactly balanced by the counteracting rotation of the fold limbs (same magnitude for all beds) during fold tightening, most porphyroblasts also rotated with respect to geographical coordinates. S_2 was crenulated prior to F_3 large-scale folding, where favourably oriented. F_3 crenulations were tightened on the eastern F_3 limb and unfolded by sinistral layer-parallel shear on the western limb, where, respectively, F_2 and F_3 layer-parallel shears were of opposite and the same sense. As a result, the initial developmental stages of an S_3 are developed only on the eastern F_3 limb and there only in incompetent layers, whereas S_2 is preserved in the competent layers. On the western limb, S_2 is preserved and appears axial planar to the F_3 structure. The S_2 domainal fabric was locally transformed into a schistosity by dissolution of the septa during widespread fluid activity, which endured until syn- or post-F_3.

INTRODUCTION

Cleavage formation in strongly anisotropic micaceous pelitic rocks is regarded essentially as a crenulation process (e.g. Williams, 1972, 1977, 1979, 1990; Weber, 1976, 1981; Knipe and White, 1977). Microfolding of a sedimentary or tectonic foliation leads to a crenulation fabric. Crenulation is believed to initiate prior to or during the initial stages of large-scale folding. Thus, if the earlier fabric was approximately bedding-parallel, the crenulations form with their axial planes at a high angle to bedding (e.g. Kienow, 1942; Williams, 1972, 1979; Knipe and White, 1977; Nickelsen, 1979; Weber, 1981; Williams and Schoneveld, 1981; Henderson *et al.*, 1986; Wright and Henderson, 1992).

During cleavage development, one or more of three competing metamorphic processes are generally operative to varying degrees: (1) solution transfer, (2) recrystallisation, and (3) neocrystallisation (e.g. Rickard, 1961; Williams, 1972, 1977, 1990; Marlow and Etheridge, 1977; Knipe, 1981). As a result, the final fabric might be a domainal fabric, such as a differentiated crenulation cleavage, differentiated layering (e.g. Williams, 1972, 1990), domainal slaty cleavage (e.g. Hoeppener, 1956; Hobbs *et al.*, 1976, p. 222), or a penetrative fabric, such as a penetrative slaty cleavage (e.g. Williams, 1972, 1977; Hobbs *et al.*, 1976, p. 222), or a schistosity (e.g. Williams, 1977, 1985). Undifferentiated crenulation cleavages (not to be confused with crenulation that has not developed into a true cleavage) appear to be the exception.

Cleavage-forming mechanisms and the relationship between fabric development and folding are commonly studied in low-grade rocks, where the phyllosilicates do not experience coarsening. Low-grade rocks, unfortunately, generally lack porphyroblasts, which are useful for establishing the relative timing of deformation and metamorphism. Particularly useful are synkinematic porphyroblasts, which preserve stages of fabric development as inclusion trails (S_i). The relationship between S_i and the foliation external to the porphyroblast (S_e) is in some cases ambiguous, especially where S_i and S_e are discontinuous. This relationship has therefore been the subject of extensive discussion (e.g. Zwart, 1960, 1962; Spry, 1969; Vernon, 1977, 1978, 1988, 1989; Bell, 1985; Williams, 1985; Bell *et al.*, 1986, 1992c; Passchier *et al.*, 1992; Johnson and Vernon, 1995). Since the early 1980s, many of the microfabric studies in medium-grade pelitic rocks have focussed on porphyroblast–matrix relationships *per se* in order to correlate metamorphic events with stages of foliation formation, and the question of whether porphyroblasts rotate or not with respect to the enveloping fabric and/or geographical coordinates (e.g. Bell, 1985; Vernon, 1988; Bell *et al.*, 1992a, b, c; Passchier *et al.*, 1992; Johnson and Vernon, 1995). In most of these studies the porphyroblast–cleavage relationships were not considered in the context of associated mesoscopic and macroscopic structures. However, such relationships are important tools for the delineation of the tectonometamorphic history of an area. Evaluating porphyroblast–matrix relationships around a fold can also help eliminate at least some S_i/S_e ambiguities, as demonstrated by Williams (1985).

In this chapter I establish complex relationships between the development and overprinting of the regional S_2 cleavage, porphyroblast growth and two phases of large-scale folding (F_2 and F_3) in a well-bedded metaturbidite sequence at Snow Lake, Canada. In order to extract the maximum information from the rock, the porphyroblast–matrix relationships

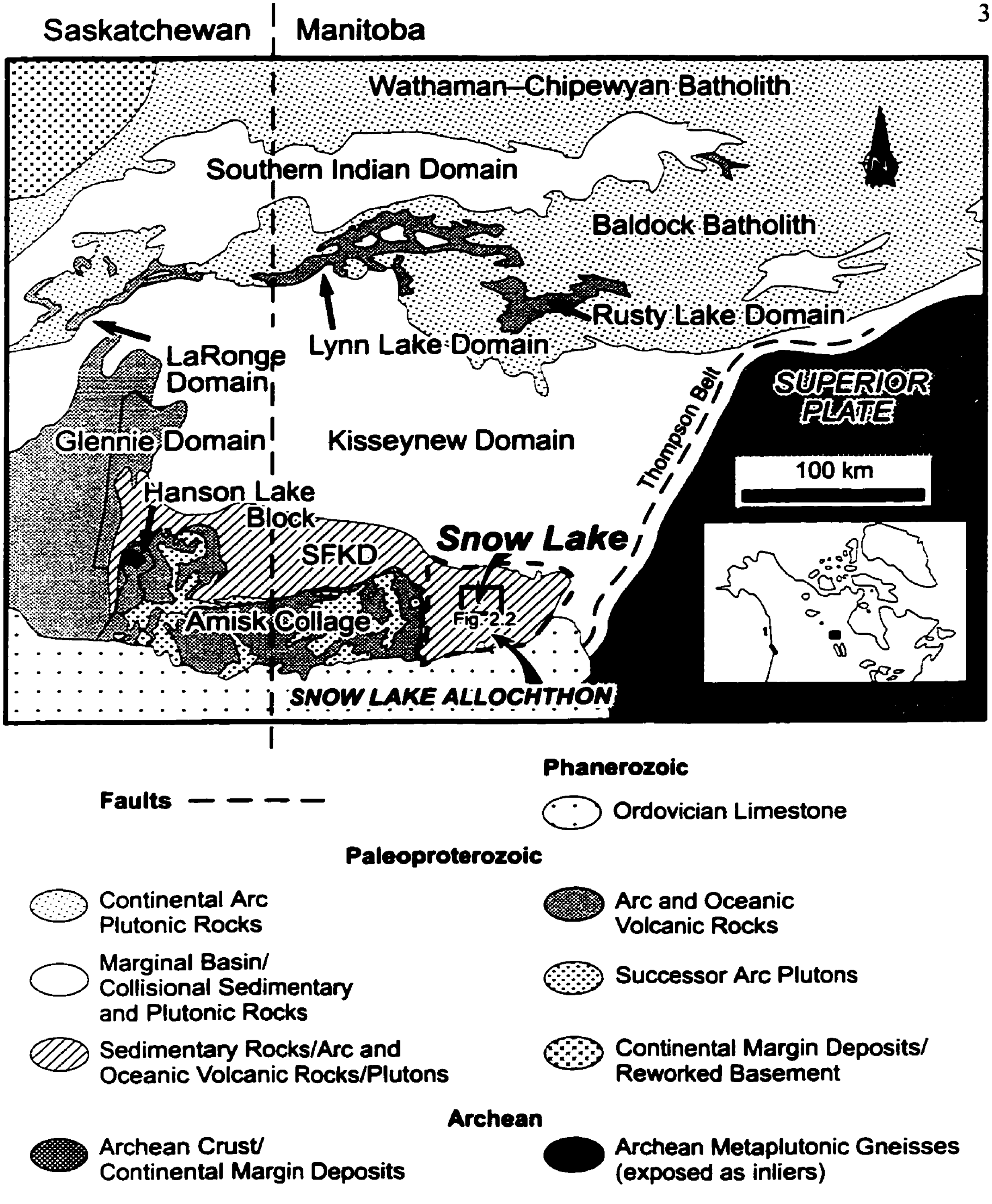

Figure 2.1 Lithotectonic domains of the internal Trans-Hudson Orogen (after Hoffman, 1988). SFKD = southern flank of Kisseynew Domain.

were studied across a portion of heterogeneously deformed layering, which shows strong cleavage refraction. Selective overprinting of the cleavage, where favourably oriented, by subsequent F_3 crenulation, is helpful in eliminating ambiguous porphyroblast–matrix relationships and gives evidence of cleavage initiation during layer-parallel shortening prior to, or in the early stages of, F_2 folding. It is further shown how an axial planar cleavage may develop on one fold limb only and how different generations of cleavage may be present in adjacent beds. Moreover, it can be demonstrated that dissolution of S_2 cleavage septa, defined by muscovite, during widespread fluid activity on the retrograde metamorphic path, is responsible for the local transition of a domainal cleavage into a schistosity.

GEOLOGICAL SETTING

The Snow Lake area is situated in a transitional zone in the Paleoproterozoic Trans-Hudson Orogen (Lewry and Stauffer, 1990) of Manitoba, Canada (Fig. 2.1), in which the Snow Lake assemblage and the Kisseynew Domain, a former marginal basin, were interleaved during the Hudsonian orogeny (Fig. 2.2) (Kraus and Williams, 1994b; Connors, 1996). This zone of interleaving is referred to as the Snow Lake Allochthon (Chapter 4). The Snow Lake assemblage comprises rocks of island arc affinity that formed at ~1.9 Ga (Stern *et al.*, 1995a; Lucas *et. al*, 1996a; David *et al.*, 1996). The Kisseynew Domain consists of metamorphosed metaturbidites (Burntwood group), which are intercalated with their terrestrial facies correlative (Missi group) (Bailes, 1980b; Stauffer, 1990; Zwanzig,

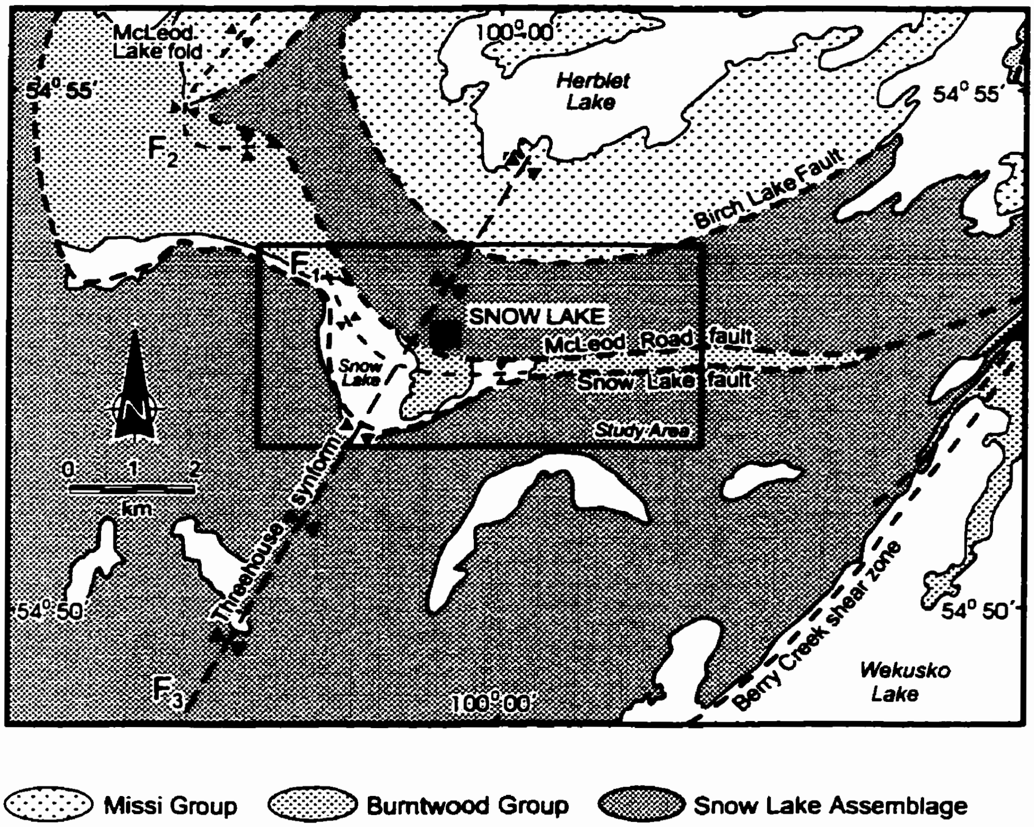

Figure 2.2 Simplified geological map of the Threehouse synform at Snow Lake.

1990). U–Pb geochronology of detrital zircons has yielded a sedimentation age younger than ~1.859 Ga for the Burntwood group (David *et al.*, 1996) and ~1.845 Ga for the Missi group (Ansdell, 1993). Southwest movement of the Kisseynew sedimentary basin over the Snow Lake arc (e.g. Kraus and Williams, 1994b; Connors, 1996) resulted in two generations of isoclinal folds, F_1 and F_2, and related thrusting, which led to multiple repetition of the contact between the two domains (Kraus and Williams, 1994c; Connors, 1996). F_1 folds are truncated by 1.84–1.83 Ga granitoid plutons (Kraus and Williams, 1995c; Connors, 1996; David *et al.*, 1996).

Peak thermal conditions were reached at 1.820–1.805 Ga (Gordon *et al.* 1990; Parent *et al.*, 1995; David *et al.*, 1996) coeval with F_2 in the study area (Menard and Gordon, 1997; Chapter 4). Post 1.8 Ga sinistral-oblique collision of the Superior Province with the Trans-Hudson Orogen along the Thompson Nickel Belt (Hoffman, 1988; Bleeker, 1990a) generated north-northeast trending open F_3 folds of the tectonostratigraphic sequence (Kraus and Williams, 1994c). The large, symmetrical F_3 Threehouse synform largely controls the map-scale pattern in the Snow Lake area (Fig. 2.2).

The rocks discussed here form a slice of Burntwood group metaturbidites (previously referred to as File Lake Formation by Bailes, 1980b) that are exposed around the town of Snow Lake (Fig. 2.2). The northerly to easterly dipping slice (Fig. 2.3a) varies in thickness from several hundred metres to 4–5 kilometers. It is in structural contact above and below with rocks of the arc assemblage. The bounding faults are the Snow Lake fault below and the McLeod Road fault above (Fig. 2.2), which are of F_1 and F_2 age, respectively (Kraus and Williams, 1994b; Connors, 1996). Detailed structural mapping has revealed that the slice

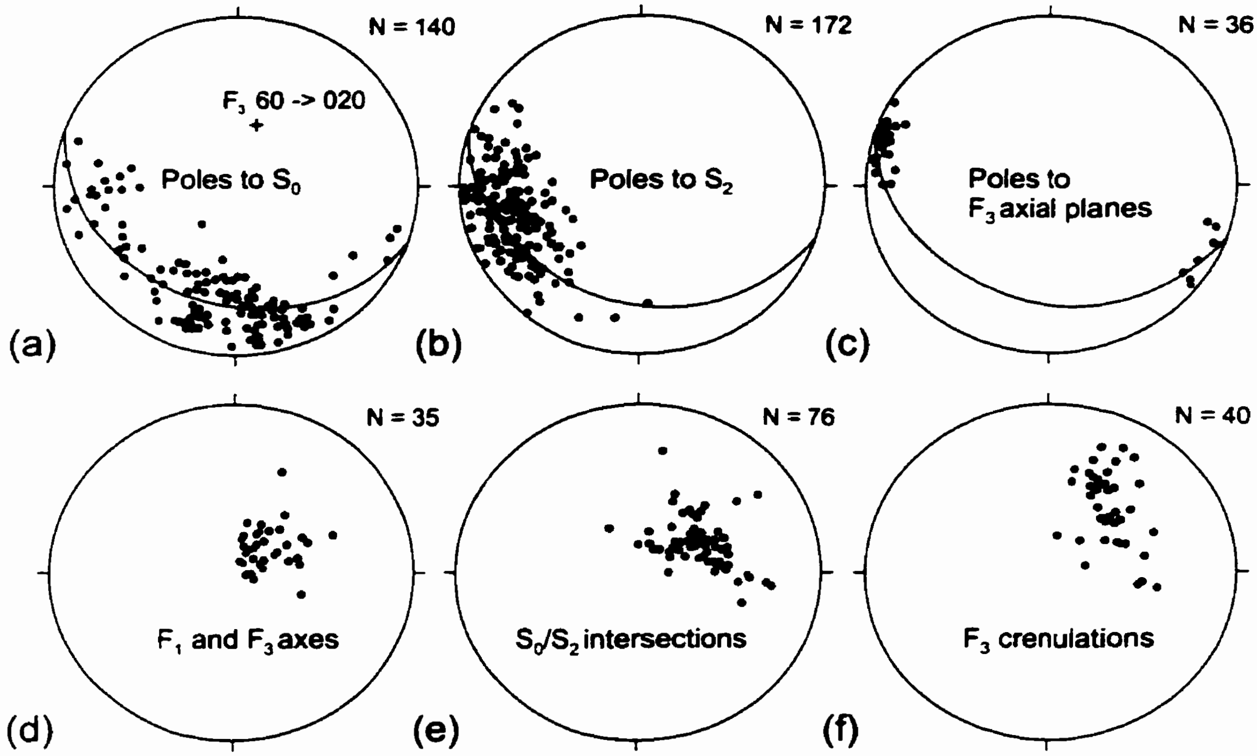

Figure 2.3 Equal area projections (lower hemisphere, Schmidt net) of structural data. (a)–(c) Foliations. (a) Poles to bedding. (b) Poles to S_2. (c) Poles to axial planes of F_3 crenulations. (d)–(f) Linear features. (d) Fold axes. (e) S_0/S_2 intersection lineations (calculated). (f) F_3 crenulation axes on S_2.

is the dismembered lower limb of a macroscopic F_2 fold (McLeod Lake fold), which was truncated along a normal fault, the McLeod Road fault, in the tightening stages of F_2 folding (Fig. 2.2; see also Fig. 2.6c) (Kraus and Williams, 1994b). The F_2 structure overprints macroscopic F_1 folds and, together with the reverse faults, is openly refolded by the symmetrical F_3 Threehouse synform (Fig. 2.2). In the core of the F_3 Threehouse synform at Snow Lake, all linear features are broadly coaxial, plunging moderately to steeply to the northeast (Fig. 2.3) (Kraus and Williams, 1994c). On the eastern and western limbs, bedding dips moderately to steeply in northerly and easterly directions, respectively (Fig. 2.3).

Metamorphism

In the Snow Lake area, the metamorphic grade increases to the north, towards the upper tectonostratigraphic levels, from chlorite-grade at Wekusko Lake to partial melting at the southern margin of the Kisseynew Domain (Figs 2.1 and 2.2) (e.g. Froese and Gasparrini, 1975; Bailes and McRitchie, 1978; Menard and Gordon, 1997; Chapter 4). Around the F_3 Threehouse synform at Snow Lake, the turbidites are metamorphosed at staurolite-grade, containing the assemblage staurolite + biotite + garnet + muscovite + plagioclase + graphite ± chlorite, with minor ilmenite, rutile, pyrrhotite, tourmaline, magnetite, zircon and monazite. Chlorite is abundant only as inclusions in porphyroblasts and as a retrograde phase partially replacing biotite, and rims on garnet and staurolite. Temperatures of 560–570 °C at an associated pressure of 4–4.5 kbar were calculated on representative samples (Chapter 4) using the following methods: the TWQ 1.02 program (Berman, 1991) with thermodynamic data from Berman (1988, 1990), Fuhrman and Lindsley (1988), Berman and Koziol (1991), McMullin *et al.* (1991), and Mäder *et al.* (1994); the garnet-biotite thermometer (Kleemann and Reinhardt, 1994); and the garnet-biotite-muscovite-plagioclase barometer (Hodges and Crowley, 1985; Powell and Holland, 1988; Hoisch, 1990). These results were interpreted as representing peak metamorphic conditions (Chapter 4).

The Burntwood group metaturbidites

The metaturbidite sequence is composed of greywacke beds, up to 1 m thick, alternating with mudstones and siltstones. The greywacke beds have preserved grading and other primary features such as scours, rip-up clasts, calcareous concretions and rare flame structures. Locally, the Burntwood group appears as a pelitic schist up to several metres thick. The compositional change within graded greywacke beds is reflected in reversed grading (due to the coarser grain size of metamorphic minerals in the more pelitic parts). At the base of the beds, biotite (up to 2 mm) is the dominant porphyroblast phase. With increasing Al-content towards the top, euhedral to subhedral pinhead garnet (1–3 mm in diameter), and large staurolite (up to 14 cm long) become abundant.

CLEAVAGE DESCRIPTION

In the sequence, there is only one discrete cleavage, S_2, which appears as a small-cale differentiated layering (domainal cleavage) or a penetrative schistosity that is strongly refracted across lithological layering (Fig. 2.4a). In hand specimen, S_2 is defined by trails of dimensionally and crystallographically well-aligned, lensoid to angular biotite of variable aspect ratio (Fig. 2.4a). The biotite grains are locally enveloped by thin films of muscovite. S_2 streamlines around garnet and staurolite. Locally, staurolite is also aligned parallel to the cleavage, but it is commonly a magnitude larger than the cleavage domains. Many biotite and staurolite porphyroblasts are pulled apart and extended in S_2, the stretching direction being at a high angle to the S_0/S_2 intersection (Fig. 2.4a; see also Fig. 2.8a). There is no cleavage in mica-poor portions of the greywackes. In thin section (*all thin sections described in this chapter are cut perpendicular to the S_0/S_2 intersection*), S_2 shows a variety of microstructures. The domainal character of the cleavage indicates its origin as a crenulation cleavage (Fig. 2.4) (cf. Williams, 1972, 1990). Garnet and biotite are confined to quartz-rich domains, which constitute the microlithons (Fig. 2.4; see also Fig. 2.7). An earlier fabric (S_1) is preserved as S_i in the porphyroblasts, the significance of which is discussed below. S_2 is accentuated by a quartz shape fabric in the quartz-rich domains, where, in rare cases, the matrix quartz is not annealed. Thin muscovite films, which constitute the S_2 septa, anastomose around the porphyroblasts (Fig. 2.4b–d). The basal planes of the muscovite grains are parallel to S_2 in both the films and quartz-rich domains (Fig. 2.4b–d). Locally, closely spaced porphyroblastic biotite fish are separated by thin

Figure 2.4 (a)–(d) Bedding–cleavage–porphyroblast relationships on the Threehouse synform east limb (Fig. 2.2). (a) Refraction of domainal fabric (S_2) across layer interface (S_0). Upper bed: S_2 and pressure-shadows of biotites (fine white strings) are refolded into Z-asymmetrical open F_3crenulations. Lower bed: The high-angle S_2 is undeformed. Geometrical relationships are as in Fig. 2.6d. (b) – (d) Photomicrographs of (a). S_0 is parallel to bases of photomicrographs. (b) Lower bed: S_2 domainal schistosity at high angle to S_0. Biotite fish contain planar S_i (=S_1) of elongate quartz grains. Width is 1.7 mm. (c) Upper bed: The biotite blast overgrew S-asymmetrical F_2 crenulations of S_1. Note the graphitic residue (double arrow) and the depleted muscovite films. Opaque phase is ilmenite. Width is 1.1 mm. (d) Upper bed, same thin section as (c): Varying degrees of matrix homogenisation. Graphite-enriched S_2 septa are preserved locally. Quartz pressure-shadows of biotite are recrystallised. Width is 4.2 mm. (e) Relict S-asymmetrical F_3 crenulations, Threehouse synform west limb.

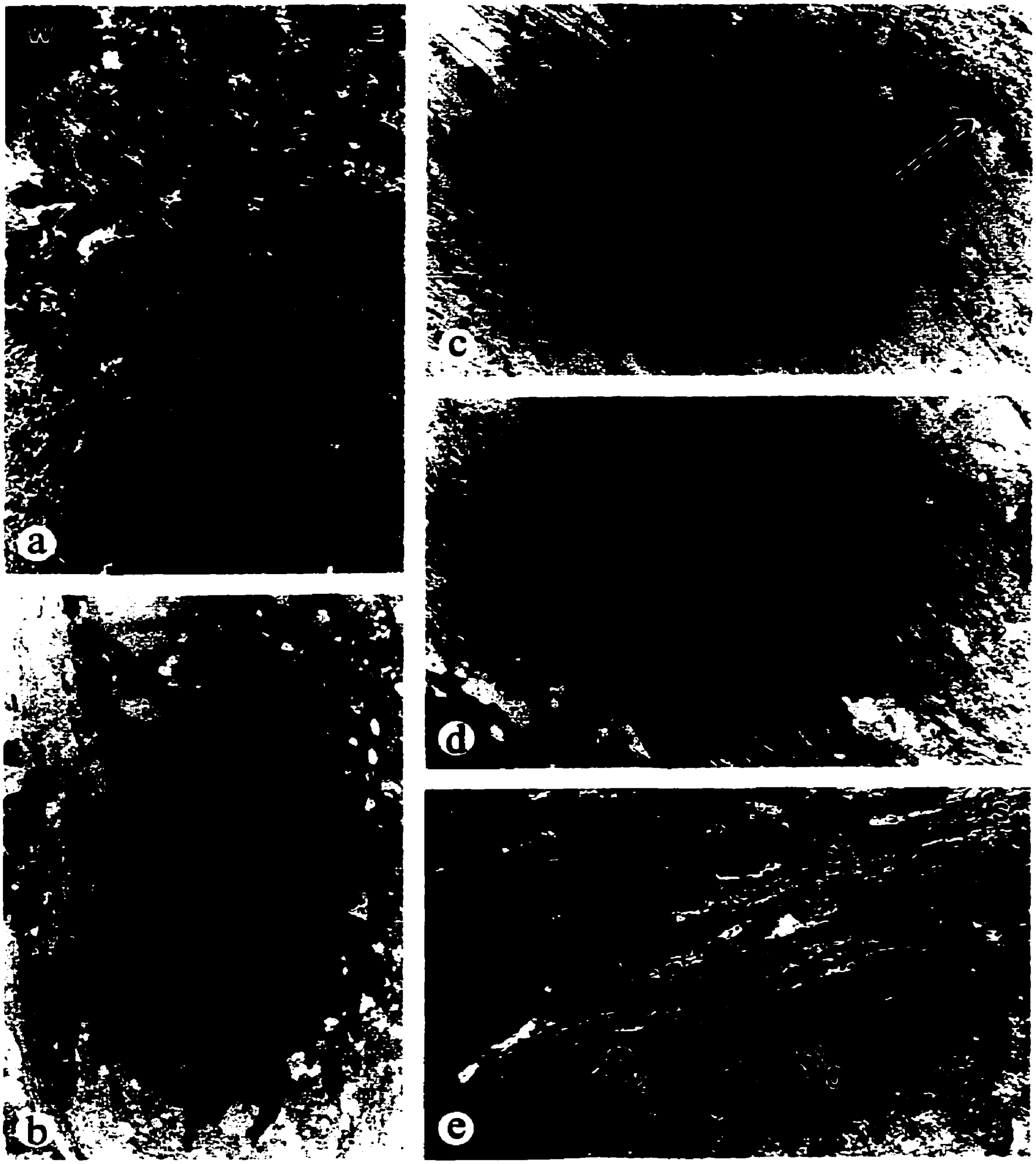
W
E
a
b
c
d
e

anastomosing muscovite films and the overall cleavage morphology resembles that of a domainal schistosity (Figs 2.4b and 2.5) (cf. Hobbs *et al.*, 1976, p. 227). The films are commonly accentuated by graphite trails, which probably resulted from passive concentration by the dissolution of quartz from the developing septa (Fig. 2.4c & d). At the scale of a thin section, these muscovite films are preserved in some domains of a microbed, but they may have been dissolved to varying degrees in others so that the domainal character of the fabric locally gives way to a more homogeneous distribution of aligned muscovite in the matrix (Fig. 2.4d). In domains strongly affected by muscovite dissolution, the overall appearance of the fabric approaches one of a penetrative schistosity (Fig. 2.5). Here, the former septa are locally tracked by trails of the less soluble graphite. The removal of muscovite is discussed in more detail below. Toward the base of the greywacke beds, which were initially poor in muscovite, the rare muscovite is randomly oriented or less orderly crenulated.

CLEAVAGE–FOLD RELATIONSHIPS

Distribution and overprinting of cleavage in the Threehouse synform

The deformation sequence in the study area was previously considered to comprise two phases of folding (Russell, 1957; Froese and Moore, 1980; Galley *et al.*, 1988). A first generation of isoclinal folds (F_1) was believed to have been refolded by the open Threehouse

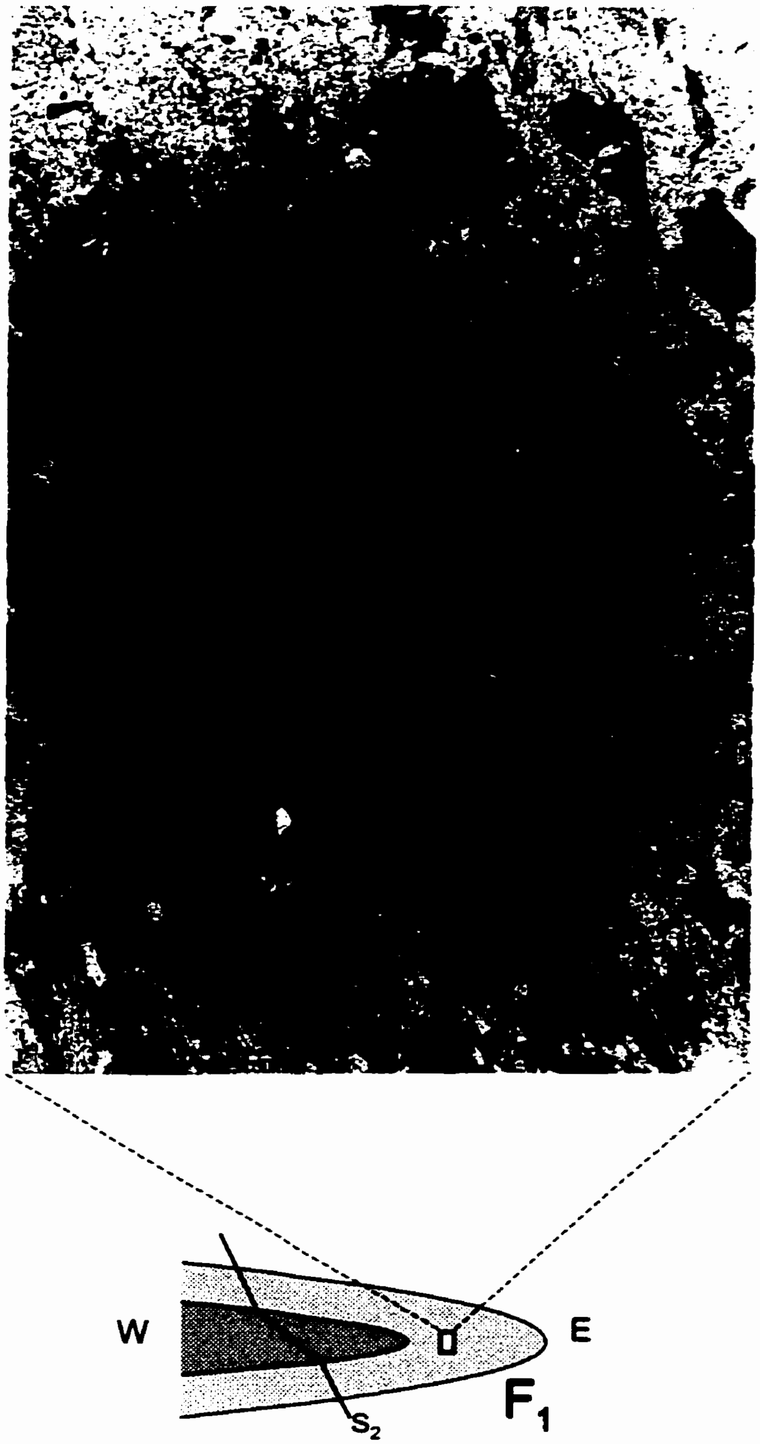

Figure 2.5 Photomicrograph of porphyroblast–matrix relationships in hinge of minor F_1 fold on the Threehouse synform east limb. Refracted S_2 cuts the F_1 axial plane at intermediate to high angles. Straight S_i (=S_1) in garnet and biotite are suborthogonal to S_2. Quartz as inclusions in garnet are elongate and smaller than in the matrix. Left-hand side of photomicrograph: S_2 is developed as a domainal cleavage. Right-hand side: S_2 septa are not preserved. Width is 4.2 mm.

synform (F_2; *ibid.*). The prominent regional S_2 was considered to be axial planar to the Threehouse synform (*ibid.*). My detailed structural mapping showed that the regional S_2 cuts mesoscopic and macroscopic F_1 folds, is axial planar to a second generation of macroscopic isoclinal folds (F_2) (Kraus and Williams, 1994b), and is deformed by the F_3 Threehouse synform (Fig. 2.2). Mesoscopic F_2 folds are very rare. Further evidence for this deformation sequence is given by the constant sinistral asymmetry of S_2 and S_0 on the exposed limb of the F_2 McLeod Lake fold around the F_3 Threehouse synform *(Note: all asymmetries and shear senses given in this chapter refer to the F_2 profile plane looking down the northeast plunging S_0/S_2 intersection; the asymmetry is sinistral, if the clockwise intersection angle between S_0 and S_2 is < 90 °; it is dextral, when the dihedral angle is > 90 °)* .

On both F_3 limbs, S_0/S_2 dihedral angles vary significantly in adjacent beds from close to 90° in competent greywackes to 10° in some incompetent mudstones. On the east limb, wherever S_0/S_2 angles are small, S_2 is refolded by Z-asymmetrical tight to open F_3 crenulations or, in micaceous portions, by kinks, whose wavelengths exceed the spacing of S_2 domains considerably (Fig. 2.4a; see also Fig. 2.8a). These crenulations, which do not constitute a true cleavage, were not noted by previous writers. The axial surfaces of the crenulations are approximately axial planar to the Threehouse synform, dip steeply east-southeast, and containing the F_3 fold axis. S_2 is undeformed, where it is at a high angle to S_0.

On the Threehouse west limb, S_0/S_2 dihedral angles are generally smaller than in comparable lithologies on the east limb. Here, S_2 is not overprinted except at three localities, where tight to gentle, S-asymmetrical F_3 crenulations are developed (Fig. 2.4e).

Interpretation

The reconstruction of the cleavage and folding history during F_2 and F_3 based on the geometrical relationships reported above is shown in Fig. 2.6. It is assumed that S_2 formed originally at a high angle to S_0 during F_2 layer-parallel shortening (Fig. 2.6a). This assumption is discussed below. S_2 refraction occurred due to differential sinistral layer-parallel shear on the exposed lower limb of the F_2 McLeod Lake fold during F_2 fold development (Fig. 2.6b). The mudstones and incompetent portions of the graded beds maximised F_2 layer-parallel shear or shear-induced vorticity (Lister and Williams, 1983); the competent portions maximised F_2 spin (Lister and Williams, 1983). The large-scale F_2 fold was subsequently dismembered along the McLeod Road fault (Fig. 2.6c). The constant sinistral S_0/S_2 asymmetry across the Threehouse synform indicates that the turbidite sliver represents the southern limb of the easterly closing F_2 McLeod Lake fold (Fig. 2.6c). During F_3 folding, layer-parallel shear was of opposite sense on the opposite limbs of the Threehouse synform (Fig. 2.6d). Continued sinistral layer-parallel shearing on the west limb resulted in a further decrease in S_0/S_2 dihedral angles. Here, S_2 appears to be axial planar to the Threehouse synform, because the exposed limb of the F_2 structure has the same asymmetry as the western limb of the F_3 synform and thus the F_2 asymmetry of S_0 and S_2 is preserved. It is important to note that F_2 and F_3 must be approximately coaxial or S_2 would not appear to be axial planar to F_3. This coaxiality is indicated by the poles to S_0, S_2 and the axial planes of F_3 crenulations plotting on approximately the same great circle (Fig. 2.3a–c).

On the Threehouse synform east limb, the shear sense reversed from F_2-related

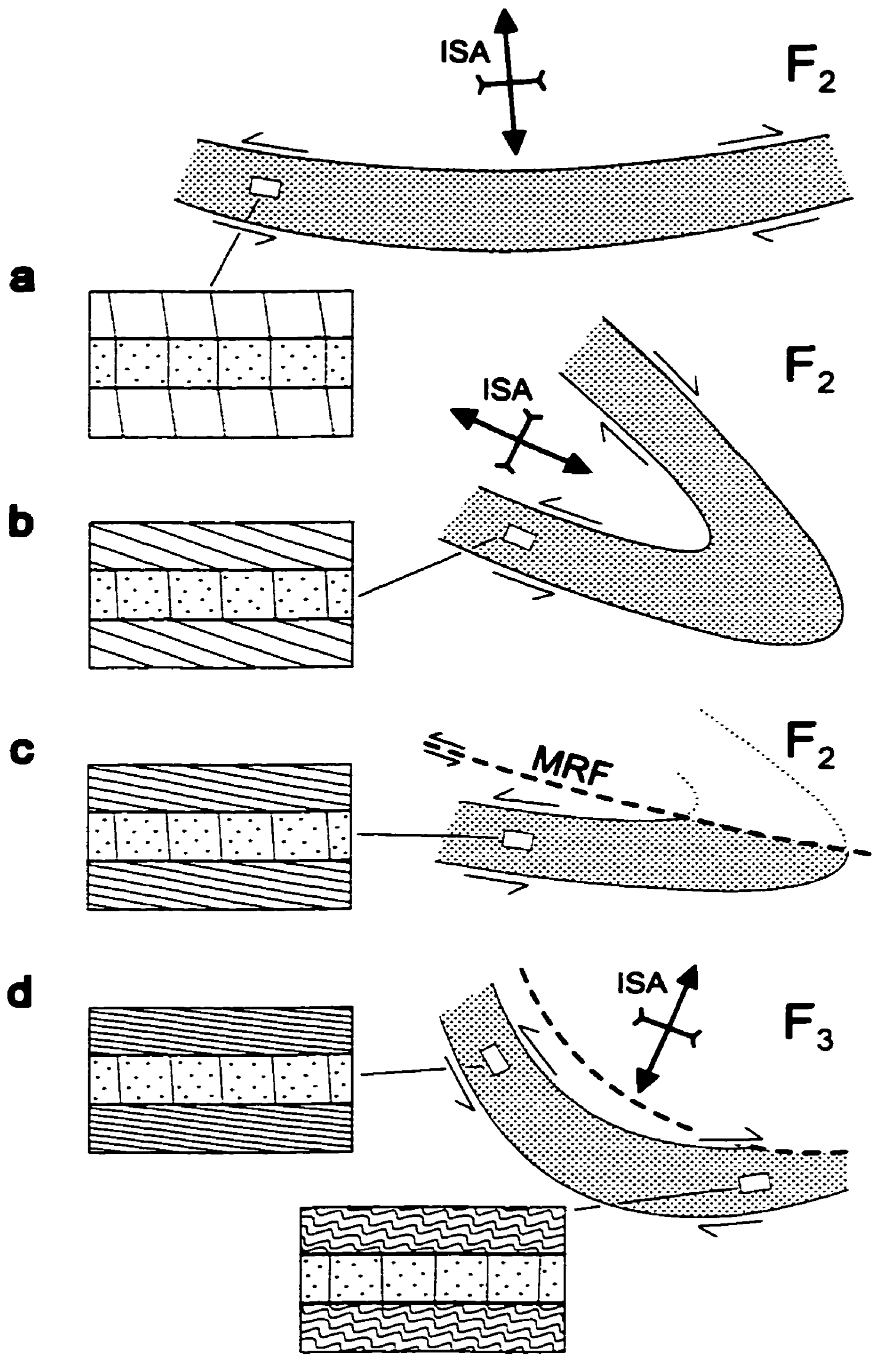

Figure 2.6 Sequential development of folding and cleavage during F_2 and F_3. (a) S_2 initiation during F_2 layer-parallel shortening and early buckling. (b) Subsequent S_2 refraction during fold amplification. (c) The F_2 structure becomes dismembered by the McLeod Road fault. (d) The relict lower F_2 limb is refolded by the F_3 Threehouse synform. During (d) the low-angle S_2 experiences differential overprinting on both F_3 limbs. ISA = instantaneous stretching axes of the bulk flow.

sinistral shear to F_3-related dextral shear following initial layer-parallel shortening (Fig. 2.6d). S_2 was in the shortening sector of the instantaneous F_3-related shear strain and, where it was at a shallow angle to S_0, the finite strain was sufficient to result in well developed open to tight crenulations. As shearing continued the crenulations were constrained to become Z-asymmetrical. Where S_2 was at a high angle to S_0 it started in the shortening field, but after accumulating only a small amount of shear strain it was rotated into the extensional sector. Any crenulation developed in response to the initial shortening would be unfolded. Thus the net effect is that where S_2 was inclined to S_0 at an angle approaching 90° it was not folded by F_3 shear.

Timing of crenulation initiation with respect to folding

In the discussion above, it has been assumed that crenulations form early in the folding history, with axial planes at a high angle to the earlier fabric when this earlier fabric was parallel to or at a low angle to bedding (cf. Kienow, 1942; Williams, 1972, 1979; Knipe and White, 1977; Nickelsen, 1979; Weber, 1981; Henderson *et al.*, 1986; Wright and Henderson, 1992). This assumption fits the experiments and models of fold development in multilayer systems (Ramberg, 1963, 1964; Biot, 1964; see also Williams and Schoneveld, 1981), in which small-scale folds develop in fine layering prior to larger-scale buckling. It has been indirectly verified in the field with the help of strain markers such as sand volcanoes or organic borings parallel to the new cleavage (Nickelsen, 1979; Henderson *et al.*, 1986; Wright and Henderson, 1992).

Further evidence for the initiation of cleavage early during folding is presented based on the local overprinting of a low-angle S_2 by tight to gentle, S-asymmetrical F_3 crenulations on the western Threehouse synform limb (Fig. 2.4e). During sinistral layer-parallel F_2 and F_3 shearing, S_2 was always in the instantaneous extensional field (Fig. 2.6d), and thus no crenulations could develop in response to layer-parallel shear. However, as pointed out above, crenulations do occur locally on the western limb. I believe that this crenulation of low-angle S_2 could only have resulted from F_3 layer-parallel shortening prior to major F_3 folding. During subsequent large-scale buckling, when layer-parallel shear became effective in the incompetent layers, F_3 crenulations were tightened and forced to become asymmetrical on the eastern limb, and crenulations on the western limb were mostly unfolded (cf. Williams and Schoneveld, 1981, p. 329). The unfolded S_2 continued rotation towards parallelism with lithological layering. I regard this timing of crenulation formation as generally applicable in anisotropic rocks with a penetrative cleavage on the scale of a macroscopic fold, including the initiation of S_2 in the Snow Lake area.

For the following determination of the timing of metamorphism with respect to deformation, only samples and locations from the eastern Threehouse synform limb are considered, since this is the only place where F_2 and F_3 strains can be distinguished.

SEQUENCE OF PORPHYROBLAST GROWTH—EVIDENCE FROM INCLUSION TRAILS

In the Burntwood group, the presence of S_i in the porphyroblasts makes it possible to establish the sequence of porphyroblast growth and also to examine early increments of S_2 development. Generally, there are two independent lines of evidence for the order of porphyroblast growth: (1) variations in S_i morphologies in different porphyroblast phases adjacent to each other, and (2) metamorphic textures, such as inclusions of one index mineral in another, dissolution of grain boundaries by metamorphic reactions, and pseudomorphic relationships. Based on metamorphic textures, the following reaction sequence for the Burntwood group at Snow Lake during heating was inferred (Froese and Gasparrini, 1975; Kraus and Menard, 1995):

$$\text{Chl} + \text{Bt} + \text{Pl} + \text{Gr} = \text{Grt} + \text{Ms} + \text{Fluid} \quad (1)$$

$$\text{Chl} + \text{Ms} + \text{Grt} = \text{St} + \text{Bt} + \text{Qtz} + \text{Fluid} \quad (2)$$

$$\text{Chl} + \text{Ms} = \text{St} + \text{Bt} + \text{Qtz} + \text{Fluid} \quad (3)$$

(mineral abbreviations after Kretz, 1983). This order of porphyroblast growth was tested on the S_i geometries. S_i is defined by graphite and/or deformed quartz and is generally sub-parallel in neighbouring porphyroblast phases (Figs 2.4b–d, 2.5 and 2.7b & c). Quartz inclusions have a shape fabric and are smaller than matrix quartz (Fig. 2.7b). Locally, S_i appears parallel to bedding; however, it is inclined at high angles to S_0 in the hinges of minor

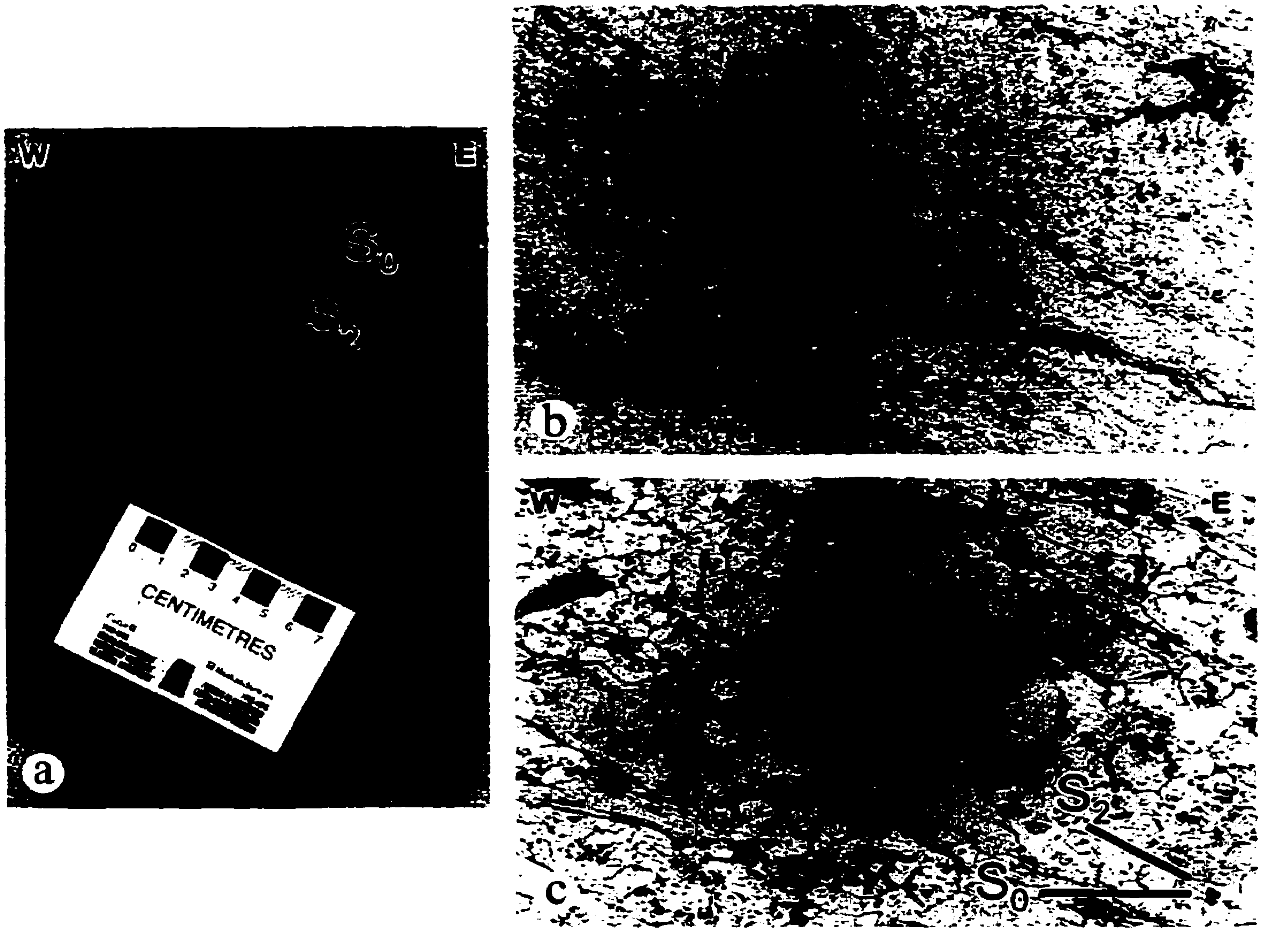

Figure 2.7 Bedding–cleavage–porphyroblast relationships on the Threehouse synform east limb. (a) Domainal fabric (S_2) in garnetiferous siltstone, only weakly affected by F_3 crenulation. (b) Photomicrograph of (a). Garnet contains planar S_i (=S_1). S_2 septa are partly dissolved. Width is 1 cm. (c) Crystallographically aligned biotite grains form a low-angle S_2 schistosity. Enveloping muscovite films are not preserved. S_0 is parallel to base of photomicrograph. Width is 1.7 mm. The context of a low S_0/S_2 dihedral angle and planar S_i at a high angle to S_2 in (b) and (c) indicates rotation of S_2 and porphyroblasts with respect to S_0. For further explanation see text.

F_1 folds (Fig. 2.5). Therefore, S_i is a tectonic fabric (S_1), which appears to have been axial planar to F_1 structures. Euhedral to subhedral garnet lacks graphite as inclusions and as concentrations around the rims suggesting that graphite was a reactant in reaction (1). In most garnets, the quartz-S_i is planar (Figs 2.5 and 2.7b). The generally undeformed biotite grains contain a straight to smoothly curved S_i mainly composed of graphite (Figs 2.4c & d, 2.5 and 2.7c). In the quartz-rich, competent beds, where S_2 is sub-orthogonal to S_0, biotite dimensions and wavelengths of included crenulations are generally larger than in incompetent beds (Fig. 2.4a). Idioblastic to strongly corroded staurolite varies from highly poikiloblastic to inclusion-free depending on the matrix it overgrew. Due to the large staurolite dimensions, S_i, where present, describes several crenulations within each grain. The S_i in staurolite is identical in wavelength and composition to the S_i in the neighbouring biotite suggesting simultaneous growth of both phases by reactions (2) and (3).

The different stages of F_2 crenulation development recorded by S_i in the different porphyroblast phases are in accord with the above inferred sequence of metamorphic growth and imply that the porphyroblasts grew synkinematically. The constant curvatures of the included crenulations from core to rim further suggest that the porphyroblasts grew rapidly with respect to strain rates. The asymmetry of S_i in some but not all porphyroblasts indicates that growth occurred when the crenulations in some incompetent beds were constrained to become asymmetrical. Such stages of the S_2 development coincided with F_2 bulk layer-parallel shortening preceding folding and/or during the earlier stages of large-scale fold amplification.

Growth of the porphyroblasts during early F_2 can be confirmed by the timing of their

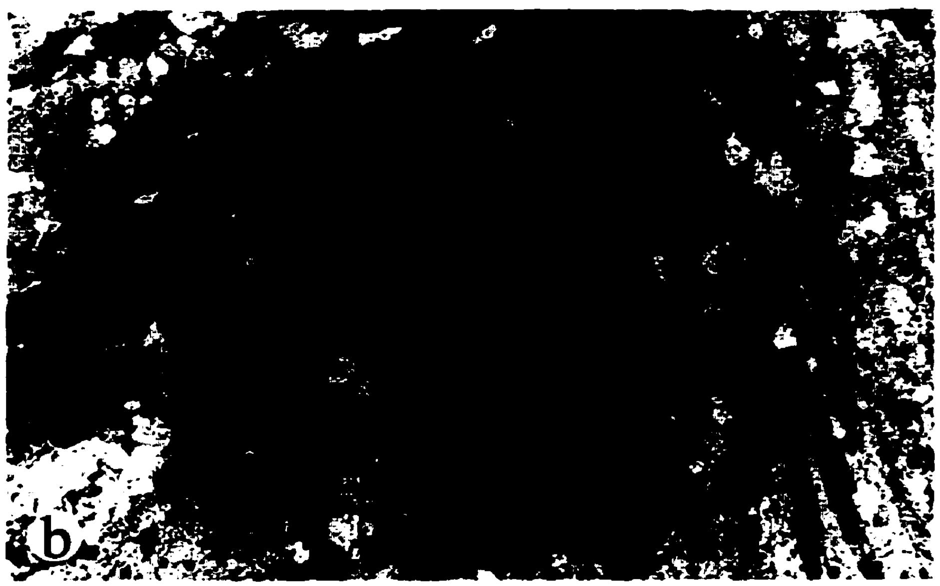

Figure 2.8 Selective overprinting of F_2 on the east limb of the Threehouse synform. (a) Lower bed: Staurolite aligned and pulled apart parallel to S_2. Note the pressure shadows along S_2 being refracted across the layer boundary. Middle bed: Z-asymmetrical F_3 crenulations deforming quartz pressure shadows of staurolite grains. Upper bed: Strongly poikiloblastic staurolite at base of greywacke bed. For further explanation see text. (b) Photomicrograph of F_3 crenulation hinge from (a). High-angle S_1/S_2 relationships are preserved after crenulation. S_2 septa are missing. Note the relict stylolitic residue tracking the former septa. Width is 4.2 mm.

overprinting with respect to folding, which gives an upper limit for porphyroblast growth. This is illustrated in Fig. 2.8a. In the lower bed, quartz pressure-shadows of some staurolites which are located close to the layer boundary across which cleavage refraction occurs, extend into the adjacent bed, continue tracking the low-angle S_2, and are crenulated by F_3. This deflection across lithological boundaries indicates that pressure shadow developed prior to significant S_2 refraction and therefore early during F_2.

INCLUSION TRAIL–CLEAVAGE RELATIONSHIPS—PORPHYROBLAST NON-ROTATION WITH RESPECT TO GEOGRAPHICAL COORDINATES?

Independent of S_0/S_2 dihedral angles, S_2 and S_i in garnet and biotite are discontinuous and at a high angle to each other everywhere in the Burntwood group around Snow Lake (Figs 2.4b–d, 2.5 and 2.7b & c). This suggests that garnet and biotite porphyroblasts did not rotate, or rotated very little, with respect to S_2 during F_2 and F_3. Such lack of relative rotation between porphyroblast and enveloping cleavage has been interpreted by some workers as indicative of porphyroblast non-rotation with respect to geographical coordinates (e.g. Bell, 1985, 1986; Bell *et al.*, 1992a, b, c). Nonetheless, in this case, most porphyroblasts rotated in space during folding, because (a) they rotated with respect to S_0 by the same amount as S_2 wherever cleavage refraction occurred in response to F_2 layer-parallel shear, and (b) S_0 itself rotated with respect to geographical coordinates. Thus, different amounts of S_2 refraction in different layers resulted in variable S_i orientations relative to S_0 across layering.

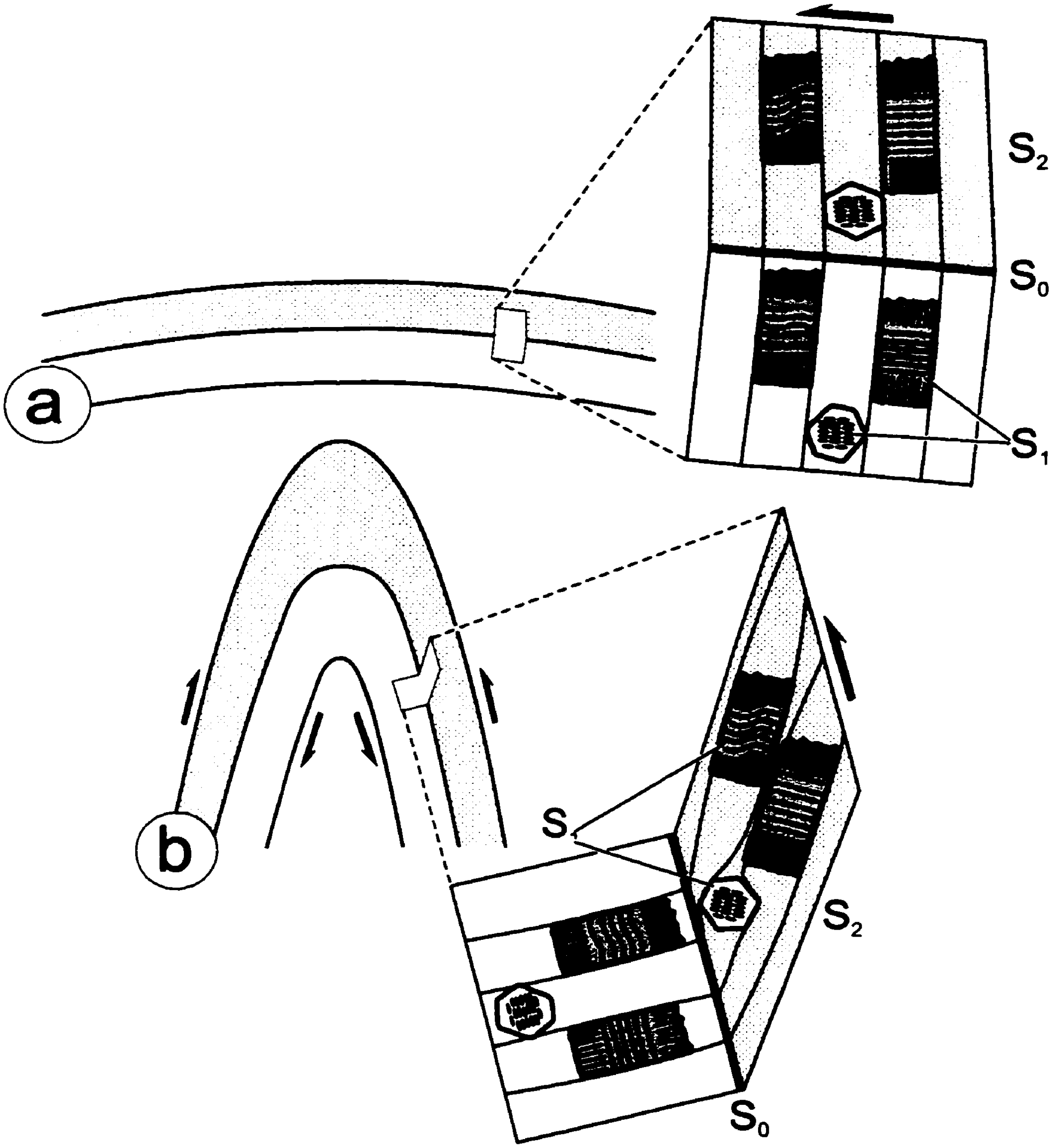

Figure 2.9 Schematic summary of bedding–porphyroblast–cleavage relationships during F_2 folding. (a) Garnet and biotite porphyroblasts overgrew an S_0-parallel S_1 during early F_2 and thus contain straight to smoothly curved S_i. (b) During fold amplification and S_2 refraction, the porphyroblasts did not rotate with respect to S_2 in the incompetent beds (stippled). In the competent greywacke (white), S_2 and the porphyroblasts did not rotate with respect to S_0.

On a small-scale, however, S_i in neighbouring porphyroblasts remained more or less parallel (Figs 2.5, 2.7 and 2.9). It may be argued that the garnet and biotite overgrew S_2 after folding and therefore did not rotate with respect to any reference frame. This possibility can be ruled out, because the planar geometry of S_i in many beds, which show small S_0/S_2 dihedral angles, indicates that locally no significant shortening of S_1 had occurred prior to porphyroblast growth (Fig. 2.7b & c). Whether staurolite rotated relative to S_0 and S_e cannot be determined with certainty, as most of the specimens do not contain an S_i. In places, where S_2 was subsequently crenulated by F_3, S_i remained sub-orthogonal to the enveloping S_2-septa everywhere in the crenulations (Fig. 2.8b). Non-rotation of porphyroblasts with respect to their enveloping cleavage can therefore not be an argument for non-rotation with respect to geographical coordinates.

VEIN–FOLD RELATIONSHIPS

Quartz veins (sub-)parallel to S_2 are ubiquitous throughout the layered sequence. They cut through staurolite porphyroblasts and are locally folded by F_3 crenulations. Depending on the S_0/S_2 angles and thus on lithology, these veins are stubby in the quartzose beds and are rather spindly and locally boudinaged in the mudstones (Fig. 2.10). In the light of the above observations, I attribute these veins to layer-parallel extension in the advanced stages of F_2 folding (Fig. 2.10c). Layer-parallel extension was controlled by the S_2 anisotropy and thus was accommodated differently in different lithologies. Rigid competent

Figure 2.10 Late-F_2 quartz veins parallel to S_2. (a) Spindly, boudinaged veins on the Threehouse synform west limb record continual sinistral F_2 and F_3 layer-parallel shear. Anticlockwise rotation of veins is indicated by S-folds in the competent calcsilicate layer at their base. Note stubby vein within the competent layer at the left hand side. (b) Stubby veins with S_0 tightened around them, Threehouse synform east limb. (c) Sketch showing vein development during F_2 folding.

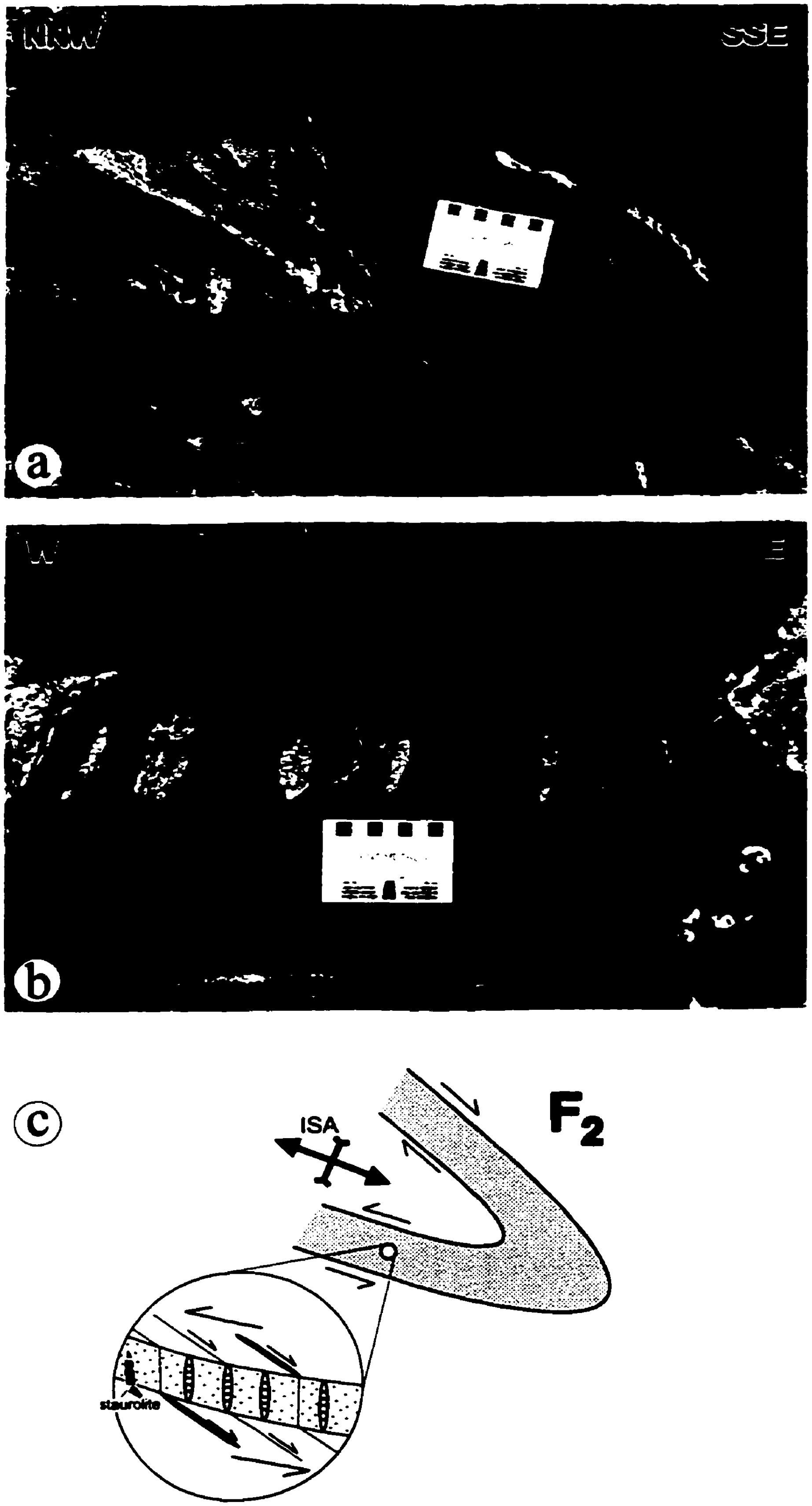
NNW
SSE
a
W
E
b
c
ISA
F_2
staurolite

layers were simply torn apart along the high-angle S_2, whereas pelitic layers were extended by slip along S_2 septa. The large thickness of the stubby veins is a consequence of the relatively low ductility of the competent beds.

DEVELOPMENT OF SCHISTOSITY FROM DIFFERENTIATED LAYERING—AN ALTERNATIVE MODEL

As mentioned above, the S_2 morphologies in the metaturbidites record gradations from differentiated layering to a coarse schistosity defined by aligned biotite. This aspect requires further discussion. Schistosity in metamorphosed micaceous pelitic rocks has been reported to develop in several ways. For example, a schistosity which is defined by coarse-grained micas is assumed to have developed during growth of these minerals (Voll, 1960; Tobisch *et al.*, 1970; Dallmeyer *et al.*, 1983). If the bulk of the mica growth predates the cleavage forming event, as in the Burntwood group, other mechanisms must account for schistosity formation. Mathematical theories of rigid body rotation of randomly distributed single grains have been proposed by Jefferey (1922) and March (1932). However, their models cannot explain the locally domainal fabric. Alternatively, schistosity may grow from a coarsening crenulation cleavage (e.g. Williams, 1977, 1985) or involve kinking of an earlier foliation (Williams, 1977; Williams *et al.*, 1977; Williams and Compagnoni, 1983), but the continuous S_i in biotite (see above) also rules out these possibilities (Figs 2.4b–d and 7c).

Microfabrics, metamorphic textures, and metamorphic reactions suggest that the schistosity in the Burntwood group developed from the destruction of the domainal cleavage by preferential muscovite removal from cleavage septa. Loss of muscovite is indicated by the different preservation states of adjacent cleavage septa in the same microbed on the scale of a thin section. Locally, septa (adjacent to well-preserved septa) may have been completely destroyed so that porphyroblasts 'float' freely in a quartz matrix that shows no anisotropy (Fig. 2.5; see also Figs 2.7c and 2.8b). In such domains now devoid of muscovite, the graphite-S_i in biotite porphyroblasts is identical in shape and geometry to S_i in biotite in adjacent domains where the septa are preserved (Fig. 2.5) suggesting that a layered anisotropy existed in both domains during porphyroblast growth. Here, the schistosity is defined by trains of well-aligned biotite, which are the loci of the former microlithons, in a coarsened quartz matrix (Figs 2.4a, 2.5 and 2.7c). The local demise of the S_2 septa indicates that schistosity developed after S_2 differentiation and after growth of the prograde metamorphic assemblage. Muscovite dissolution endured until syn- or post-F_3 as recorded by skeletal F_3 crenulations, in which only the aligned biotite porphyroblasts are preserved (Fig. 2.8b). I believe that muscovite was dissolved by fluids and was flushed out of the system. During fluid infiltration, S_2 septa possibly acted as channels of enhanced fluid flow in a way described by Williams (1990). Evidence of fluid activity is given by the deficiency of matrix muscovite in many samples and by the local corrosion of biotite and staurolite rims in the absence of a higher grade aluminosilicate-forming reaction. Chlorite and muscovite participated in reactions (2) and (3) and muscovite must have been left over when the reactions stopped. The presence of these phyllosilicates prior to reactions (2) and

(3) is also indicated by their inclusion in porphyroblasts. Although Al, as contained in the muscovite, is considered to be relatively immobile (Carmichael, 1969), it is suggested that Al was flushed out of the system by high-pH and/or low-pH fluids (Kraus and Menard, 1995; see also Glen, 1979 and Mancktelow, 1994). This interpretation correlates with a widespread fluid activity in the adjacent Snow Lake assemblage during F_2 and F_3 causing syntectonic alteration of volcanic-hosted massive sulphide deposits (Menard and Gordon, 1995, 1997).

SYNTHESIS AND CONCLUSIONS

In the Burntwood group metaturbidites at Snow Lake a single penetrative cleavage, S_2, is ubiquitously developed as a domainal fabric, which shows all gradations into a schistosity. The fabric developed from crenulation of a bedding-parallel S_1, which formed during F_1 isoclinal folding at 1.84 Ga. Such crenulations are included as S_i in porphyroblasts of staurolite and biotite. These porphyroblasts grew between 1.820 and 1.805 Ga, when F_2 crenulations were constrained in some incompetent layers to become asymmetrical prior to F_2 fold tightening during a very small deformation increment. Associated peak conditions of metamorphism were 560–570 °C and 4–4.5 kbar. Local transformation of the differentiated layering into a schistosity by muscovite dissolution endured until syn- or post-F_3 after 1.8 Ga. In incompetent beds, S_2 and porphyroblasts rotated with respect to S_0 during F_2 tightening on the presently exposed limb of the F_2 McLeod Lake fold. However, they did not rotate relative to one another (in micro-beds on the scale of a thin section) and remained more or less stationary with respect to S_0 in competent beds. Layer-parallel extension during the later stages of F_2 was accommodated by separation along S in the competent beds, resulting in quartz-vein formation. S_2 and porphyroblast pressure-shadows, where favourably oriented, were crenulated prior to F_3 large-scale folding. F_3 crenulations were accentuated by dextral layer-parallel shear on the eastern limb of the Threehouse synform and unfolded by continued sinistral layer-parallel shear on the western limb. As a result, the initial developmental stages of an S_3 are preserved on the eastern F_3 limb only. On the other limb, S_2 was largely unaltered, and after rotation associated with F_3 appears axial planar to the F_3 structure.

This work supports the hypothesis that in areas of polydeformed anisotropic micaceous pelitic rocks, cleavage may start to develop prior to folding. In general, domainal cleavage develops when microfolding is possible. Whether and when microfolding takes place during large-scale folding strongly depends on the orientation of the anisotropy to be crenulated with respect to layering. In special circumstances, a cleavage may develop late. For example, in a setting such as the west limb of the Threehouse synform, where a pervasive new cleavage does not form because of the orientation of the old cleavage, a local cleavage may form late during folding in the hinges of minor folds. The Threehouse synform example also shows that a domainal cleavage may develop locally, for example on one fold limb only, and there only in selected layers depending on the orientation of the previous fabric. As crenulation and differentiation involve the destruction of the previous fabric (e.g. Tobisch and Paterson, 1988; this study) the only foliations present in alternating lithologies may be of different generations. This has implications for other areas, for example: the Slave Province, Canada, where, in the Yellowknife Supergroup metaturbidite sequence, two subsequent, morphologically similar fabrics alternate in adjacent beds, displaying a chevron pattern (Fyson, 1982, 1984; Henderson, 1997). This pattern possibly formed by the same mechanisms operating in the Threehouse synform area with the difference that, in the Yellowknife Supergroup, the later fabric experienced complete differentiation.

I no naka no kawazu taikai wo shirazu
(the frog in the well doesn't know the ocean).
Japanese proverb

Chapter 3

Rotating porphyroblasts during folding: real or unreal?

Abstract: It has been claimed that rigid porphyroblasts that grow before or during folding and concurrent cleavage development do not rotate with respect to a geographical reference frame (GRF), even if the straining is non-coaxial (Bell, 1985; Bell and Johnson, 1990). The explanation offered is based on strain partitioning. It is argued that the initial orientations of early fabrics included as internal foliations (S_i) in the porphyroblasts have been preserved after polyphase deformation, and even after successive orogenies. According to the strain partitioning model, the porphyroblasts are fixed in domains of coaxial straining (microlithons) and are isolated from the non-coaxial straining associated with the enveloping septa (S_e). This hypothesis, and its discussions both pro and contra, suffer from insufficient attention to reference frames. I attempt to demonstrate: (a) the need for rigorous treatment of reference frames in geological interpretations; (b) that grains in coaxial domains generally rotate with respect to the GRF; and (c) that the non-rotation hypothesis is in conflict with heterogeneous deformation (cleavage refraction). Finally, I question the validity of the evidence in studies by Ramsay (1962) and Fyson (1980), cited in support of non-rotation with respect to the GRF during folding. In detail, I show that rotations with respect to

different reference frames are not kinematically equal, because any two reference frames are mutually incongruent. Consequently, the strain partitioning model *does not* preclude porphyroblast rotation with respect to the GRF, unless S_e is fixed with respect to the GRF throughout folding. The latter condition demands rare folding mechanisms (slip fold model, or a special case of the flexural-flow fold model). Fyson (1980) reported orientations of S_i that are constant, after folding, over a large area; this scenario is a product of selective data acquisition. Ramsay's (1962) model requires a special folding mechanism, which does not appear to be generally applicable in natural rocks. In summary, my investigation shows that non-rotation of porphyroblasts with respect to a GRF during folding, while possible, is not universal. The development of microstructures (e.g. curved S_i) is only related to the local deformation path, the characterisation of which does not rely on the GRF.

INTRODUCTION

The analysis of textures in porphyroblasts has proven very useful in elucidating the tectonometamorphic evolution of various areas, particularly in rocks in which matrix fabrics have been transposed into composite foliations during multiple deformation and/or obscured by coarsening or dissolution. In such rocks, internal foliations (S_i) in porphyroblasts are commonly the only evidence of earlier fabrics. Sigmoidal S_i may provide information on certain developmental stages of an external fabric (S_e), for example a crenulation cleavage, and variations of S_i geometries in different porphyroblast phases may permit the correlation of the growth sequence of metamorphic assemblages with the corresponding increments of small-scale deformation (e.g. Zwart, 1960, 1962; Spry, 1969; Vernon, 1977, 1978; Bell and Rubenach, 1983). Criteria for the interpretation of porphyroblast–matrix relationships have been established (e.g. Zwart, 1960, 1962; Spry, 1969; Vernon, 1977, 1978). Ambiguities, however, can remain inherent where S_i and S_e are discontinuous (e.g. Ferguson and Harte, 1975; Williams, 1985; Visser and Mancktelow, 1992; Johnson and Vernon, 1995; Bell *et al.*, 1997).

Based on a graphical strain field diagram and a strain partitioning model (Bell, 1981, 1985, fig. 1, 1986) (Fig. 3.1), it has been argued that porphyroblasts never rotate with respect to a geographical reference frame (GRF) during non-coaxial heterogeneous ductile deformation (e.g. Bell, 1985, 1986; Steinhardt, 1989; Bell and Johnson, 1989, 1990, 1992; Johnson, 1990; Hayward, 1990, 1992; Bell *et al.*, 1992c; Aerden, 1994, 1995; Bell and Forde, 1995). If this non-rotation hypothesis were correct, then oriented hand specimens

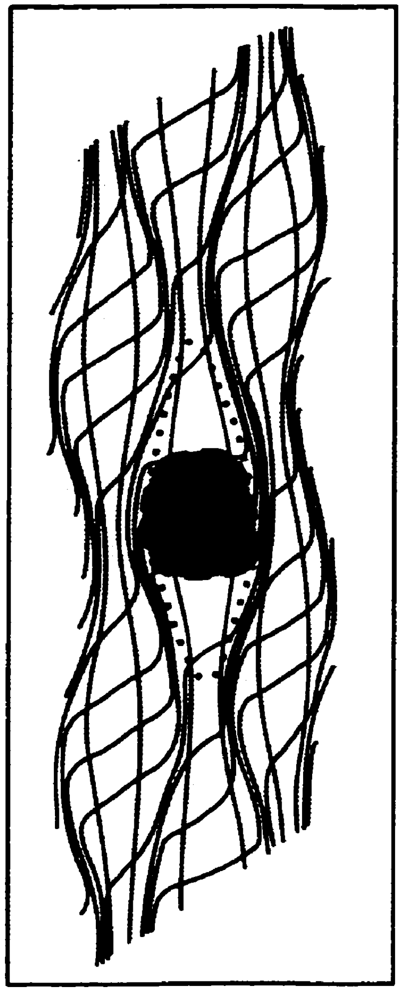

Figure 3.1 The strain field diagram of Bell (1985, 1986), redrawn from Johnson (1990).

would be sufficient for deciphering the sequence of tectonometamorphic events in a spatial context (Bell *et al.*, 1995, 1997). Hence, complex S_i would permit the reconstruction of the original orientation of fold axes, and even of orogenic events and plate movements (Bell and Johnson, 1989; Hayward, 1990; Bell *et al.*, 1995).

In my opinion, there are major defects in the non-rotation hypothesis of Bell (1985, 1986), which have not been conclusively refuted by previous writers, who argued in favour of porphyroblast rotation (with respect to the GRF) (Passchier *et al.*, 1992; Wallis, 1992; Lister, 1993; Henderson, 1997). Therefore, in this paper I rigorously investigate the roots of the problem inherent in the non-rotation hypothesis and adherent to the discussion of porphyroblast–matrix relationships in general; I discuss ambiguous data presentation and inconsistent use of reference frames. Although it has long been known that rotation is relative and hence reference-frame dependent, this axiom, as noted by Means (1994), is all too often neglected. The fact that such oversight flaws structural interpretations and models, makes the present discussion necessary. In detail, I demonstrate both in theory and in a natural example that rotation of rigid objects with respect to the GRF during non-coaxial heterogeneous ductile deformation *does* exist and is *independent* of the strain partitioning model of Bell (1985, 1986). I also question the interpretations by others of the studies of Ramsay (1962) and Fyson (1980), which have been cited in support of general porphyroblast non-rotation with respect to the GRF.

STRUCTURAL SETTINGS CONSIDERED

Generally, S_i/S_e relationships are discussed for two different structural environments, shear zones and folds, in which the porphyroblasts grew either pre- or synkinematically. In a shear zone, the c–planes, which are (sub-)parallel to the shear zone boundaries are referred to as S_e, relative to which porphyroblasts rotate. In a fold environment, a domainal axial-plane foliation is commonly referred to as S_e (unless no axial-plane cleavage develops, in which case bedding or a bedding-parallel fabric is taken as S_e). The amount of strain, and hence the magnitude of slip on S_e and the resulting rotation with respect to S_e, are expected to be much larger in the shear zone than in a fold. Consequently, genuine spiralling of S_i *sensu* Bailey (1923), Rosenfeld (1970) and Schoneveld (1977, 1979) (i.e. angles greater than 90°) occurs only in a shear zone. In a fold, smoothly curved (sigmoidal) S_i (i.e. angles smaller than 90°) in synkinematic porphyroblasts may constitute former matrix crenulations and thus preserve increments of axial-plane cleavage (S_e) development. In most reported shear zone cases, S_i represents the same foliation as S_e, but transposed, whereas in folds S_i and S_e represent two distinct generations of fabric (S_e = axial-plane cleavage). Another marked difference is that, in so far as S_e is fixed in orientation with respect to the shear zone boundary, S_e is also fixed with respect to the GRF during shear zone deformation, because, generally, a shear zone as a whole does not rotate with respect to the GRF. In contrast, on fold limbs the axial-plane cleavage is commonly rotated with respect to S_0 during fold amplification, so that the cleavage is refracted from layer to layer (e.g. Hobbs *et al.*, 1976, p. 216; Williams, 1979; Henderson *et al.*, 1986; Chapter 2). It is therefore necessary, when discussing porphyroblast–matrix relationships, to distinguish between the environments *a priori* and the basis for the distinction must be given. In many published accounts this distinction is missing and consequently the reader cannot evaluate the interpretation (e.g. Vernon, 1989, fig. 1; Wallis, 1992, fig. 1a; Passchier and Trouw, 1996, fig. 7.32).

In this chapter, I consider folds with straight to sigmoidal S_i in porphyroblasts. The porphyroblasts grew early in the history of a folding event, while a domainal axial-plane cleavage (S_c) gradually developed, so that S_i predated S_c. These are the relationships found in most published examples discussing non-rotation of porphyroblasts with respect to the GRF (e.g. Fyson, 1975, 1980; Bell, 1985, 1986; Vernon 1988; Reinhardt and Rubenach, 1989; Steinhardt, 1989; Johnson, 1990; Bell and Forde; 1995; Henderson, 1997). Further, in all but one of my examples, S_i and S_e have not rotated relative to each other (Fig. 3.2). This, however, is far from true in general (for a detailed discussion of the relative rotation of S_i and S_e, see Williams and Schoneveld, 1981, and references therein).

ROTATION AND REFERENCE FRAMES—GENERAL REMARKS

Rotation is here taken to be a finite change of orientation from an earlier configuration in the context of an arbitrary, but specified, reference frame (e.g. Sander, 1930; Hobbs *et al.*, 1976, pp. 31–32; Passchier, 1987; Means, 1994; Passchier and Trouw, 1996, p. 176). The choice of reference frames is subjective (Means, 1994). Failure to specify a reference frame, and to refer to it consistently, has been recognised as a major problem in the

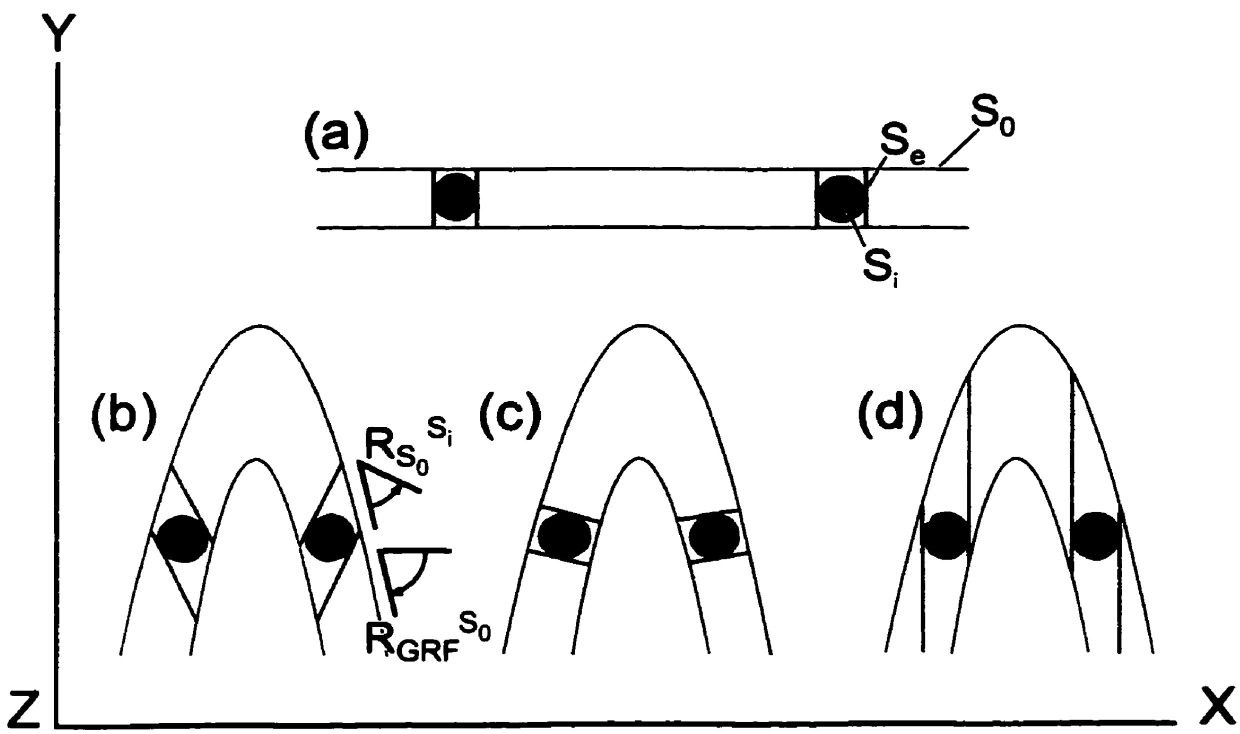

Figure 3.2 Theoretical bedding–cleavage–porphyroblast relationships during folding without relative rotation between S_i and S_e. Reference frame is pinned to geographical coordinates (X, Y, Z). Fold shapes are schematic. (a) Porphyroblasts overgrow a bedding-parallel fabric (S_0); an enveloping cleavage (S_e) is initiated during the layer-parallel shortening that precedes folding. Three distinct further developments: (b) Either, porphyroblasts rotate with respect to the GRF and with respect to S_0. (c) Or porphyroblasts rotate with respect to the GRF, but remain fixed with respect to S_0. (d) Or, porphyroblasts rotate with respect to S_0, but not with respect to the GRF.

argument about porphyroblast rotation (Visser and Mancktelow, 1992; Wallis, 1992; Mancktelow and Visser, 1993; Lister, 1993; Means, 1994; Kraus and Williams, 1995b). Many writers do not specify a reference frame and may imply rotation with respect to the GRF, while others do not distinguish between rotations occurring with respect to different reference frames.

In folding, rotation is commonly referred to one or more of five distinct reference frames. One of them (GRF) can be regarded for our purposes as fixed on earth. The other four reference frames, attached to S_0, S_e, S_i in neighbouring porphyroblasts, and to the directions of maximum and minimum stretching *at any instant* (instantaneous stretching axes), are local and may be *non-fixed* (i.e. they may, over a time interval, have rotated) with respect to (a) each other, and (b) the GRF.

A porphyroblast containing an S_i may have rotated on a fold limb with respect to the enveloping axial-plane cleavage (S_e) by $R_{Se}{}^{Si}$ (R denotes the magnitude of rotation; the subscript and superscript denote the reference frame and the rotating object, respectively). If S_e has also rotated with respect to layering (S_0), then the magnitude of rotation of S_i with respect to S_0 is:

$$R_{S0}{}^{Si} = -R_{Si}{}^{S0} = R_{Se}{}^{Si} + R_{S0}{}^{Se} \qquad (1)$$

As the fold limb (S_0) itself rotates with respect to the GRF, the rotation of S_i with respect to the GRF can be written:

$$R_{GRF}{}^{Si} = R_{Se}{}^{Si} + R_{S0}{}^{Se} + R_{GRF}{}^{S0} \qquad (2)$$

Equations (1) and (2) are valid for both rotation rates (angular velocities) and finite rotations in three dimensions. If the sum of the relative rotations is zero, $R_{GRF}{}^{Si} = 0$. Obviously, any two reference frames are *mutually incongruent* so that the different relative rotations are not kinematically equivalent. Further, rotation is independent of scale as long as a reference frame is specified.

AN EXAMPLE OF PORPHYROBLAST ROTATION WITH RESPECT TO THE GRF— THE IMPLICATIONS OF CLEAVAGE REFRACTION

Owing to the fact that rocks preserve finite strains, it is impossible to unambiguously reconstruct the orientations of primary layering and rigid porphyroblasts prior to a given folding event. The first folds (F_1) constitute an exception, because they generally deform originally horizontal layers. I am, however, not aware of a reported case in which the first folding affected rocks at medium-grade regional metamorphism that allowed porphyroblast growth. Although it may be impossible to reconstruct spatial strain and rotation paths, it can sometimes be unambiguously shown that at least some porphyroblasts have rotated with respect to the GRF during a folding event subsequent to F_1. Such a case is given when S_i in neighbouring porphyroblasts were parallel prior to folding, and the porphyroblasts have rotated relative to each other during folding. On the other hand, parallelism of S_i in adjacent porphyroblasts prior and after folding does not eliminate the possibility that these porphyroblasts have rotated with respect to the GRF.

My example is from a well-bedded metamorphosed greywacke–mudstone turbidite sequence in the internal Trans-Hudson Orogen at Snow Lake, Manitoba, Canada (for details, see Chapter 2). Turbidites form a large refolded F_2 fold limb and they contain an S_2 domainal cleavage that is strongly refracted in heterogeneously deformed beds. Garnet and biotite occupy the microlithons and enclose straight to openly curved (sigmoidal) S_i ($=S_1$) that is, independent of S_0/S_2 dihedral angles, at a high angle to the enveloping S_2 septa ($=S_e$). Hence, S_i everywhere varies in orientation from layer to layer, but is consistent with the orientation in neighbouring grains (Fig. 3.3). The porphyroblasts overgrew a bedding-parallel S_1 before S_2 existed and during the early stages the formation in the F_2 fold. S_2 was originally at a high angle to $S_0 = S_i$ (Fig. 3.2a). During folding, the bulk deformation was partitioned so that, depending on layer competency, S_2 rotated differentially with respect to S_0 between $0°$ and $80°$ (Figs 3.2b & c and 3.3). Thus, at the thin-section scale, neighbouring garnet and biotite grains in the same fine layer did not rotate noticeably, either relative to one another or with respect to S_2. Locally, where S_2 was subsequently crenulated by F_3, S_i remained sub-orthogonal to the enveloping S_2 septa around the crenulations. As expected, most of these porphyroblasts have therefore rotated with respect to the GRF during F_2 and F_3. Nonetheless, the magnitude of rotation of the individual porphyroblasts with respect to the GRF cannot be quantified, because the geographical orientation of bedding prior to F_2 folding cannot be reconstructed. Hence, the GRF is of limited use for micro-scale kinematic analysis in folds, unless the porphyroblast did not rotate with respect to the GRF.

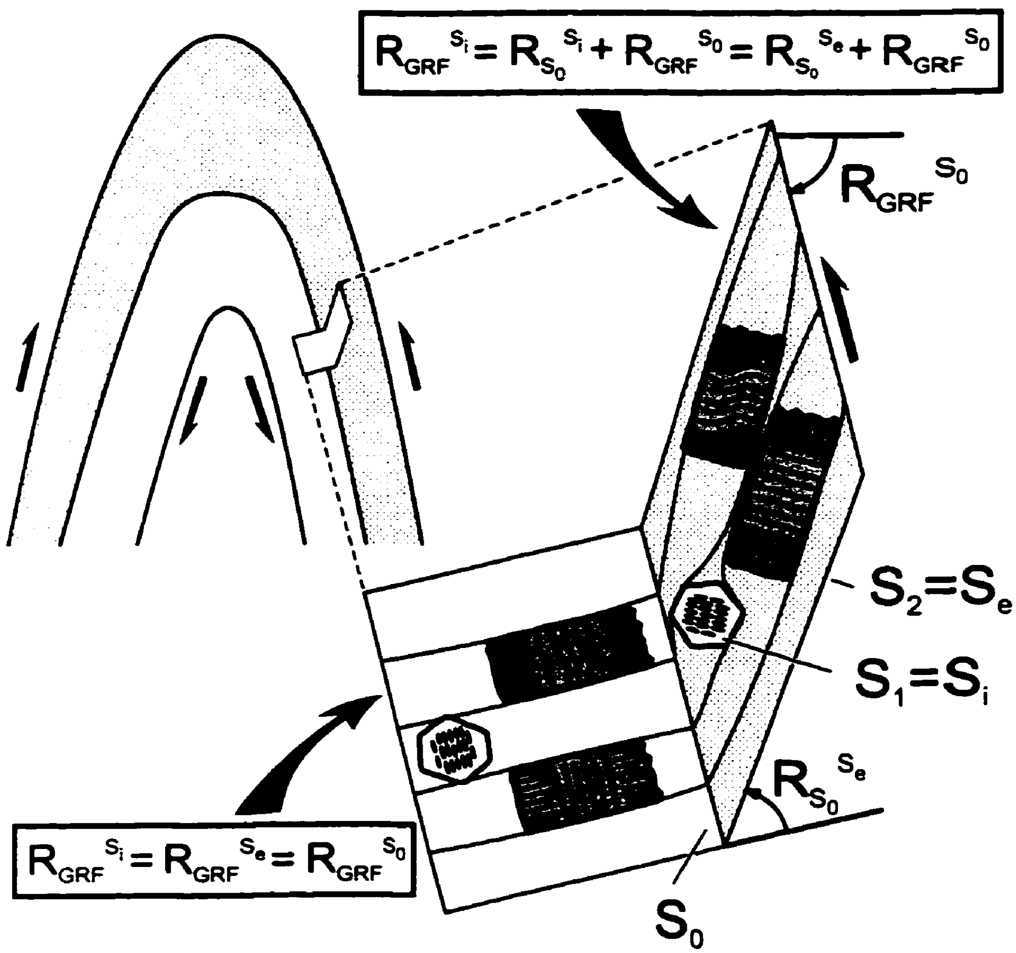

Figure 3.3 Schematic bedding–porphyroblast–cleavage relationships during F_2 folding in metaturbidites at Snow Lake, Manitoba, Canada. Garnet and biotite porphyroblasts overgrew an S_0-parallel S_1 early and thus contain straight to smoothly sigmoidal S_i. During fold amplification, the porphyroblasts retained their orientation relative to S_e (= S_2), but, depending on layer competency, rotated through different angles with respect to the GRF; in incompetent mudstone (stippled), the porphyroblasts have rotated with respect to S_0, but not in competent greywacke (white). Within an individual bed, at thin-section scale, S_i in neighbouring porphyroblasts has similar orientations.

THE NON-ROTATION HYPOTHESIS OF BELL

Bell (1985, 1986) and some subsequent writers (e.g. Bell and Johnson, 1989, 1990; Johnson, 1990; Bell *et al.*, 1992a, b, c; Bell and Forde, 1995) have claimed that non-deformable, synkinematic porphyroblasts never rotate with respect to either the GRF or S_e (enveloping cleavage septa) during bulk non-coaxial heterogeneous ductile deformation, associated with the development of a domainal cleavage (Fig. 3.2a & d). According to Bell (1985, fig. 1), non-rotation of porphyroblasts with respect to cleavage septa arises from deformation partitioning; cleavage septa (S_e) alone accommodate the non-coaxial part of deformation, whereas the microlithons are domains of coaxial deformation (Fig. 3.1) (see also Williams and Schoneveld, 1981, p. 312). Non-rotation with respect to S_e is indicated by the parallelism of the axial planes of curved S_i with S_e and by the parallelism of S_i in neighbouring porphyroblasts of the same phase (cf. Bell, 1985, fig. 3b). From this it has been concluded that porphyroblasts never rotate with respect to the GRF and they thus preserve orientations of earlier foliations (e.g. Bell, 1985, p. 115, 1986; Bell and Johnson, 1989, 1990; Hayward, 1990; Bell *et al.*, 1992a, b, c, 1995). This conclusion, however, is based on the assumption that the axial-plane cleavage (S_e) does not rotate relative to the GRF during folding. Implicit in this conclusion is the assumption that folds form according to the slip fold model (Schmidt, 1932; de Sitter, 1956, p. 168; Turner and Weiss, 1963, p. 480) (Fig. 3.4) or according to a special case of the flexural-flow fold model (Turner and Weiss, 1963; Donath and Parker, 1964) (Fig. 3.5) that requires exact balancing of the relative rotations ($R_{S0}{}^{Si} = R_{S0}{}^{Se} = -R_{GRF}{}^{S0}$) (Steinhardt, 1989, fig. 10; Johnson, 1990; Bell and Johnson,

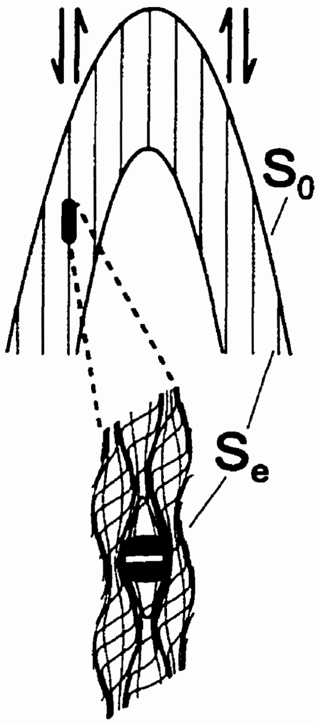

Figure 3.4 Shearing along an axial-plane cleavage as a hypothetical folding mechanism (slip fold model) that allows porphyroblasts not to rotate with respect to the GRF ($S_0 = S_i$ remains horizontal). Note that this model requires opposite shear sense along the strictly parallel S_e-planes on the two fold limbs. Schematic after Steinhardt (1989).

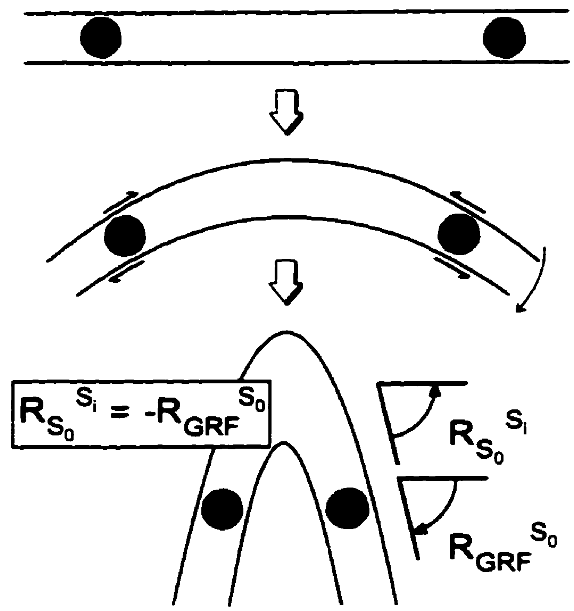

Figure 3.5 Hypothetical exact balancing of bed rotation (with respect to the GRF) and the relative rotation between porphyroblast and bedding in a flexural-flow fold. The porphyroblasts enclose a bedding-parallel fabric as S_i. Modified from Bell and Forde (1995).

1992, fig. 13; Hayward, 1992, fig.16; Bell and Forde, 1995, fig. 1). The slip fold model has been questioned on mechanical grounds (Hobbs *et al.*, 1976, pp. 193–195). However, even if the model were applicable, the near-ubiquity of cleavage refraction, albeit small in some cases, indicates that slip folds are rare. The only reasonable way that I am aware of, for porphyroblasts not to rotate with respect to the GRF, is for rotation to occur in response to S_0-parallel shear during folding. Such a situation is given where folding approximates the flexural-flow fold model and shear is homogeneously distributed throughout the fold limb, $R_{S0}{}^{Si} = -R_{GRF}{}^{S0}$ (Williams and Schoneveld, 1981; Johnson, 1990), and therefore $R_{GRF}^{Si} = 0$ (Fig. 3.5). This, however, is a special case incompatible with cleavage refraction, which proves heterogeneity of any S_0-parallel shear. Thus, even if the Bell model were correct, porphyroblasts should still, in general, and in the Snow Lake example described here, rotate with respect to the GRF (Figs 3.3 and 3.6).

To avoid this logical problem, proponents of non-rotation with respect to the GRF generally consider the porphyroblasts out of context. Commonly, their discussion concentrates upon a particular thin section or hand specimen, and only the relationship of the porphyroblast to the cleavage is taken into account, not that of the cleavage to the fold, except perhaps by a statement or implication that the cleavage parallels the fold's axial plane (e.g. Bell, 1985, 1986; Bell and Johnson, 1989, 1990, 1992; Johnson, 1990; Bell *et al.*, 1992a, b; Hayward, 1992; Aerden, 1995; Bell and Forde, 1995).

Two papers, one by Ramsay (1962) and one by Fyson (1980), are commonly quoted as examples of porphyroblasts that have not rotated relative to the GRF. But, are these valid examples, and if so, are they only special cases?

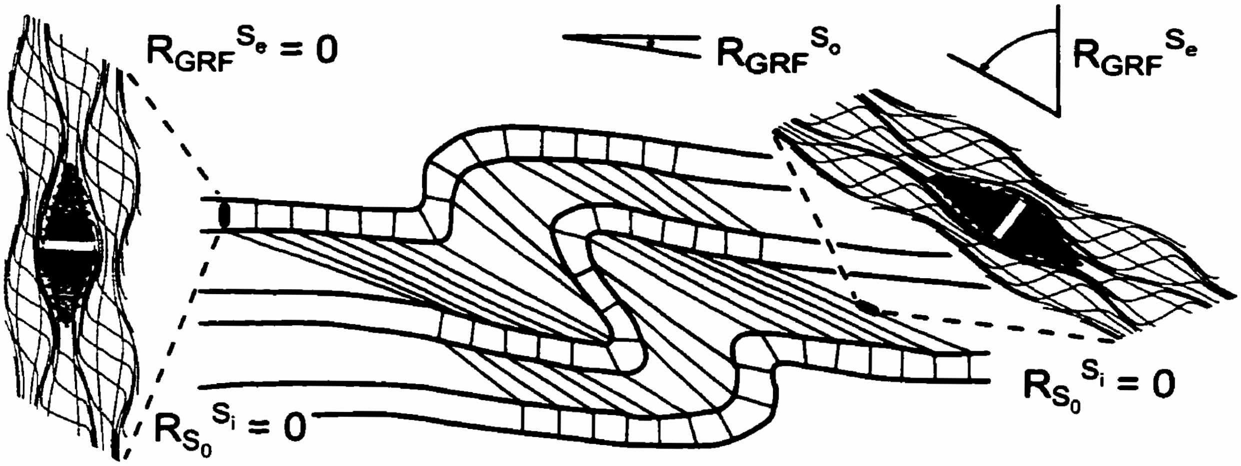

Figure 3.6 Strain field diagrams as in Bell (1985, 1986), but drawn for an asymmetrical fold with axial-plane cleavage, showing that R_{Se}^{Si} and R_{GRF}^{Si} are unrelated. Bedding ($S_0 = S_i$) assumed to have been horizontal prior to folding.

FYSON'S INCLUSION TRAIL FORM SURFACE LINES—AN ARGUMENT FOR PORPHYROBLAST NON-ROTATION WITH RESPECT TO THE GRF?

Fyson (1980) described S_i orientations in biotite in a greywacke–mudstone sequence from the Northwest Territories, Canada, and they appear to be consistent over large areas. At Cleft Lake, he connected S_i between grains and plotted these as "form lines" on a map; these form lines trend apparently east–west, for some 20 km in a 5 km wide corridor, across the axial plane of a large-scale subvertical, symmetrical F_3 fold (Fig. 3.7). Cleavage morphologies and refraction patterns, dimensional and crystallographic preferred orientation of biotite parallel to the cleavage, sub-orthogonal S_i/S_e relationships, and the relative timing between cleavage development and porphyroblast growth are identical to the relationships at Snow Lake. The biotite porphyroblasts overgrew a straight to slightly curved S_2 during the early stages of an S_3 crenulation cleavage development and thus developed early during large-scale F_3 folding (cf. Hobbs *et al.*, 1976; Williams, 1979; Chapter 2). At thin-section scale, S_i is approximately parallel from one biotite to the next. Fyson (1980) concluded that the porphyroblasts did not rotate noticeably relative to one another and that S_i records the fossil orientation of an S_2.

Fyson's form lines of S_i have been regarded as either an example of, or a general proof of, porphyroblast non-rotation with respect to the GRF (e.g. Jamieson and Vernon, 1987; Vernon, 1988, 1989; Reinhardt and Rubenach, 1989; Bell and Johnson, 1990; Gibson, 1992; Hayward, 1992; Phillips and Key, 1992; Williams, 1994; Bell and Forde, 1995; Stewart, 1997). I, however, disagree with these interpretations for the following reasons: (1)

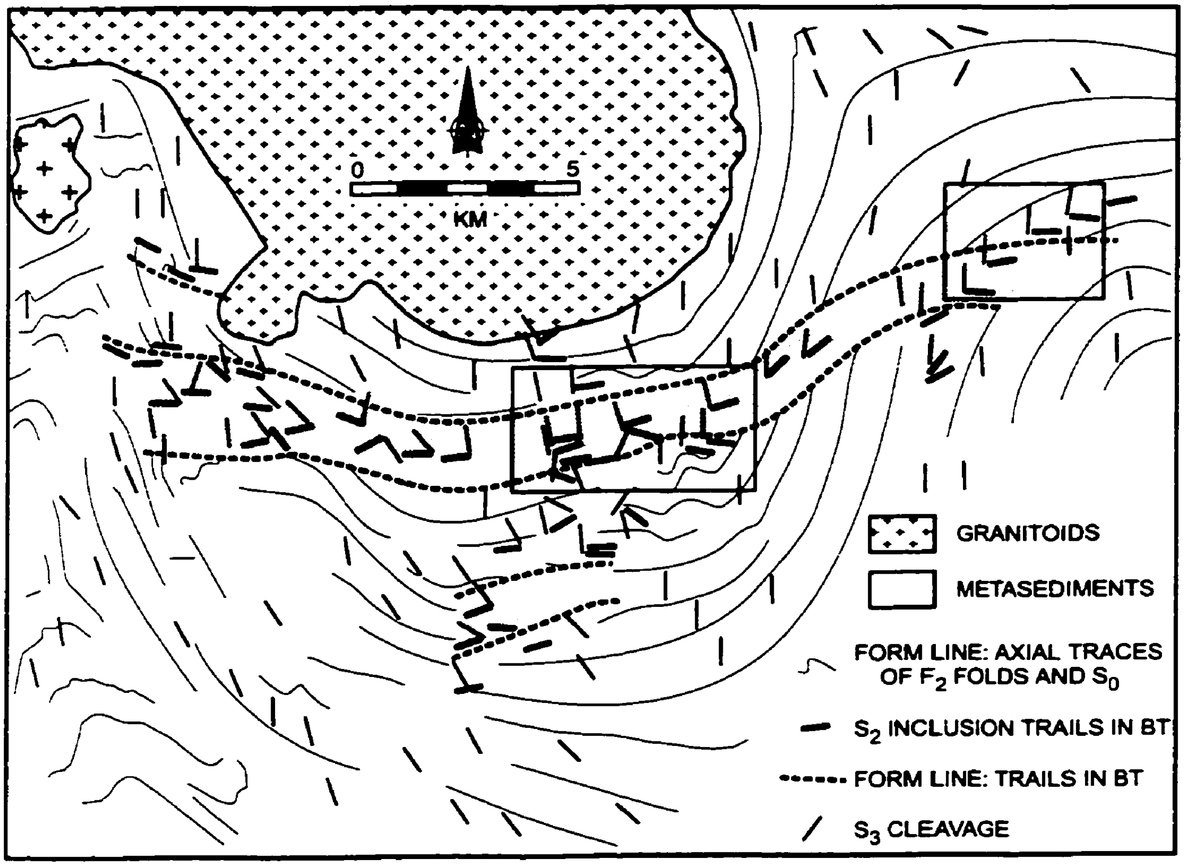

Figure 3.7 Form surface map, Cleft Lake area, Northwest Territories, Canada, illustrating the relationships of the regional S_2 foliation, S_3 cleavage, and trend of S_i in biotites. Note S_i/S_e relationships. Shaded areas highlight zones of relatively high sample density, and boxes emphasise high angle S_i/S_e relationships. Modified from Fyson (1980).

S_i in biotite is not always parallel across the fold at Cleft Lake, but locally varies in orientation by up to 90° (Fig. 3.7) (see Passchier *et al.*, 1992; Visser and Mancktelow, 1992), and (2) the shape of the form lines results from selective data.

Visser and Mancktelow (1992) recognised a consistent pattern of S_i across Fyson's F_3 fold (cf. Fig. 3.8), which corresponds to the pattern in garnets across a minor fold at Lukmanier pass, Central Alps (Visser and Mancktelow, 1992, fig. 7). In both cases, S_i form lines are not straight but describe 'folds' which are more open than the related major fold. Visser and Mancktelow (1992) believed that these patterns arose from counteracting relative rotations. It is apparent that the opening angle of a 'form line fold' systematically decreases with increasing $R_{S0}{}^{Si}$ as a function of shear strain on the fold limbs and the form lines theoretically become straight, if the counteracting relative rotations balance (Fig. 3.8). Therefore, high layer-parallel shear strains (and subsequent fold flattening) may give rise to little porphyroblast net-rotation with respect to the GRF.

Fyson's (1980) openly curved form lines are not objective, because sampling was restricted to pelitic beds (Fyson, personal communication 1997), where, on the fold limbs, non-coaxial deformation, and therefore $R_{S0}{}^{Se}$, was maximised (cf. Figs 3.3 and 3.6). Fyson (1980), however, reported a strong cleavage refraction between greywacke and mudstone layers. Two situations are possible in the less strained competent layers. (1) Most likely, and in analogy to the incompetent beds, $R_{Se}{}^{Si} = 0$ *sensu* Bell, and thus $R_{GRF}{}^{Si} \neq 0$ (as in Fig. 3.2b). Under these circumstances, the form lines would display more complex geometries (Fig. 3.8). (2) $R_{GRF}{}^{Si} = 0$, and hence, taking into account cleavage refraction, $R_{Se}{}^{Si} \neq 0$. This second possibility could justify Fyson's form lines (if $R_{Se}{}^{Si} + R_{S0}{}^{Se} \approx R_{GRF}{}^{S0}$), it would,

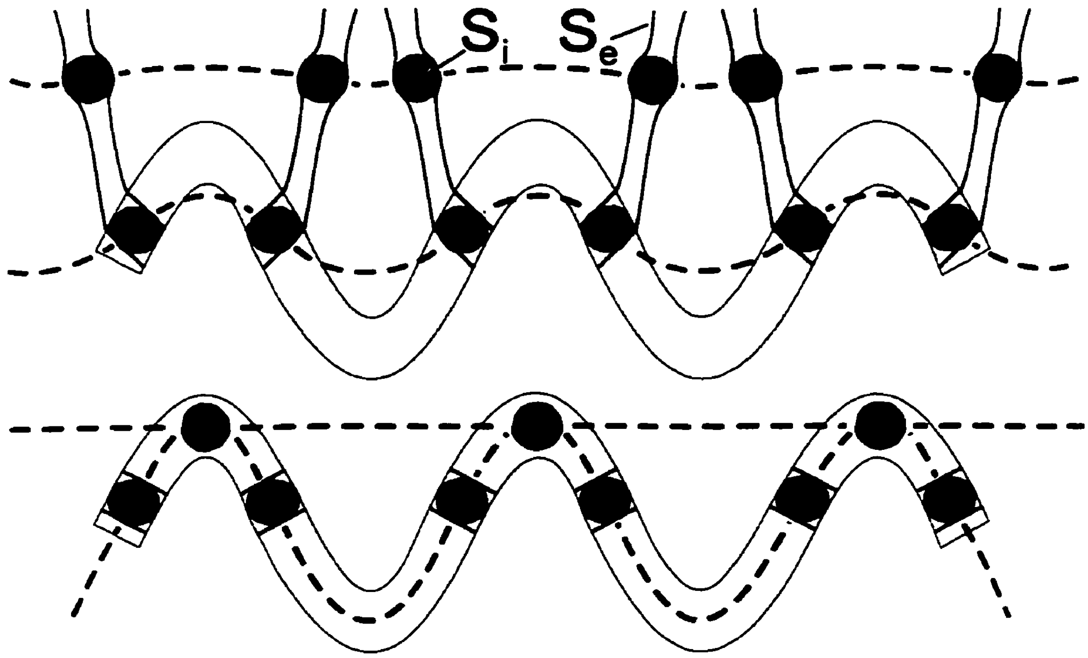

Figure 3.8 Two-layer model demonstrating that the geometries of inclusion trail from lines (dashed) are a function of the layers' rheology. It is inferred that the porphyroblasts overgrew a bedding-parallel fabric prior to folding and no relative rotation of S_i and S_e has occurred. On the fold limbs the more competent beds (shaded) record lower non-coaxial strain and thus smaller magnitudes of porphyroblast rotation with respect to S_0 than the more competent beds (unshaded). Form lines become straighter with decreasing rock competency.

however, invalidate Bell's strain partitioning model and hence the whole non-rotation argument. In order to obviate this problem and use Fyson's observations in support of their argument, Bell and Johnson (1990; fig. 1) incorrectly reproduced Fyson's fold as a slip fold with a cleavage truly parallel to the axial plane (as in Fig. 3.4).

Recently, Dr. W.K. Fyson has informed me (personal communication 1997) of a new interpretation of the S_i form lines at Cleft Lake. Based on reconnaissance work (Fyson, 1982; Fyson and Helmstaedt, 1988), he concludes that S_3 and the porphyroblasts postdate the F_3 folding. Although such static overgrowth would explain biotite non-rotation with respect to the GRF, the recorded structural features such as cleavage refraction, rule out this proposed relative timing of folding and cleavage development (cf. Hobbs *et al.*, 1976; Williams, 1979; Chapter 2)

In summary, Fyson's (1980) form lines and interpretations are not valid evidence of porphyroblast non-rotation with respect to the GRF, either in his particular or in the general case.

RAMSAY'S NON-ROTATED PORPHYROBLASTS WITH RESPECT TO THE GRF—A GENERALLY VALID MODEL?

Ramsay (1962) has discussed synkinematic porphyroblasts that he believes have remained in their original orientation during the development of similar folds. The folding mechanism was assumed to be uniform flattening. S_i and S_e are foliations of the same generation that predated the folding, and no new axial-plane cleavage developed during folding. Parallelism of straight S_i in adjacent grains at the scale of a hand specimen was interpreted as signifying rotation of S_e with respect to S_i, whereby the undeformable porphyroblasts merely changed position relative to each other during the folding (Fig. 3.9).

This example can provide no argument for the general non-rotation of porphyroblasts with respect to a GRF during folding (and was never claimed to by Ramsay). It requires a special deformation mechanism in a sequence of materials that are mechanically homogeneous and isotropic and for them to remain so during deformation; therefore, S_e has to be a purely passive marker. This is obviously not realistic as a general mechanism for folding although it may be appropriate in some rocks.

CONCLUSIONS

In geological interpretations, reference frames must be treated rigorously: (1) Rotation is always relative to, and dependent on, reference frames; thus, any statement that a porphyroblast has either 'rotated' or 'not' is pointless without specifying the reference frame. (2) Any different reference frames are mutually incongruent, so that rotation (or not) with respect to one frame does not imply rotation (or none) with respect to another; hence, the proposal by Bell and coworkers is invalid: that porphyroblasts never rotate with respect to the geographical reference frame during deformation and that S_i can therefore be used for the spatial reconstruction of polyphase orogenic events. (3) Information from oriented hand

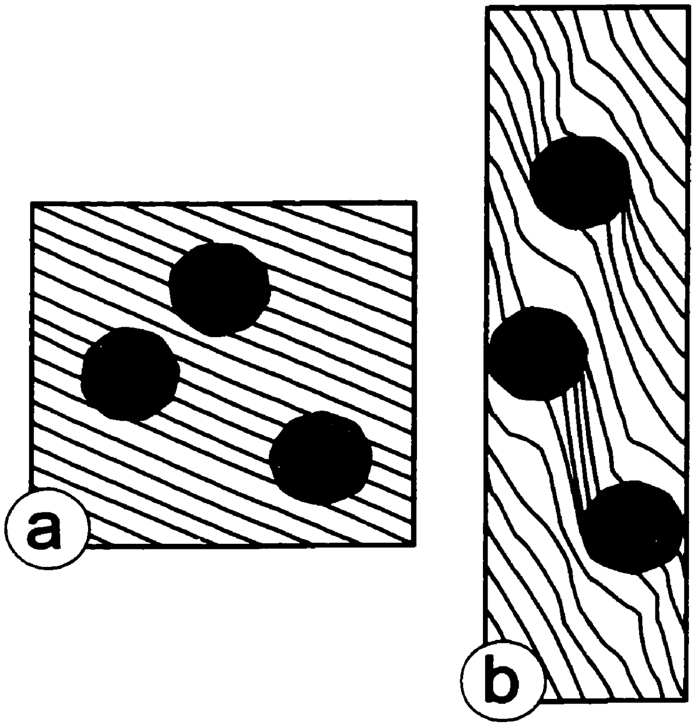

Figure 3.9 Rotation of a passive marker foliation with respect to geographically fixed porphyroblasts during uniform flattening. (a) Porphyroblasts have overgrown a fully developed fabric prior to folding ($S_i = S_e$). No new cleavage develops. (b) Deformation is coaxial throughout folding. Therefore, S_e rather than the porphyroblasts rotates relative to the edges of the box. Redrawn from Ramsay (1962).

specimens and thin section alone, without their structural context, is insufficient for such a reconstruction.

A study by Fyson (1980) was re-examined, according to which S_i appears to be approximately constant in orientation over a large area after folding, because rotation of the fold limbs with respect to the GRF was approximately equal and opposite to rotation of the porphyroblasts with respect to bedding (i.e. $R_{GRF}^{S0} = -R_{S0}^{Si}$). Fyson's S_i-form lines, however, are not representative of the whole sequence, because S_i was only considered in incompetent rock units.

Ramsay's (1962) case of poprhyroblasts that have not rotated with respect to a GRF requires a special folding mechanism in isotropic materials, which is probably rare in nature. These studies do therefore not support general non-rotation of porphyroblasts with respect to a GRF.

Few workers were concerned with geographical coordinates as a reference frame before Bell wrote his papers in 1985 and 1986. This is important for the present discussion, because Bell and coworkers claim that original S_i orientations are preserved throughout several orogenic events. Yet, rigid objects generally change their orientation with respect to the geographical reference frame during deformation, but by amounts that in most cases cannot be determined. The development of microstructures is only related to the local deformation path, the characterisation of which does not rely on the geographical reference frame.

Never express yourself more clearly than you think.
Niels Bohr

Chapter 4[1]

A thermal gradient at constant pressure: implications for low- to medium-pressure metamorphism in a compressional tectonic setting, Snow Lake Allochthon and Kisseynew Domain, Trans-Tudson Orogen, Central Canada

Abstract: The Kisseynew Domain, a major tectonostratigraphic domain in the internal Trans-Hudson Orogen, Canada, originated as a sedimentary basin filled with the Burntwood group turbidites at 1.86–1.84 Ga. Rocks of the Kisseynew Domain were thrust southwestward over, and structurally interleaved with, both the 1.9 Ga Snow Lake island arc assemblage and ocean floor assemblages during convergence of the Trans-Hudson Orogen and the Archean Superior craton at ~ 1.84–1.81 Ga. At Snow Lake, the zone of tectonic interleaving records polyphase deformation (F_1–F_4) and is characterised by a northerly increase in metamorphic peak temperatures at 4–6 kbar pressure. The central Kisseynew Domain was metamorphosed at a uniform high grade of 750 ± 50°C and 5–6 kbar. Pressure

---

[1]An earlier version of this chapter was published in the Canadian Mineralogist, volume 35, Tectonometamorphic Studies in the Canadian Shield (part I), ed. R.G. Berman and R.M. Easton, Kraus, J. and Menard. T. "A thermal gradient at constant pressure: implications for low- to medium-pressure metamorphism in a compressional tectonic setting, Flin Flon and Kisseynew Domains, Trans-Hudson Orogen, Central Canada", pp. 1117–1136 (1997).

and temperature calculations on thirteen representative samples from the Snow Lake area in a critical temperature window of 500–700°C (staurolite and sillimanite zones) yield evidence for two successive thermal regimes that varied in time and intensity from south to north. F_1 (1.842–1.835 Ga) was the major burial event, which may have been followed by thermal relaxation in a 15–35 m.y. time interval between F_1 and F_2. Garnet commenced growing during early F_2 (1.82–1.805 Ga) at ~500°C and ~ 4 kbar throughout the study area. During F_2, temperature and pressure in the staurolite zone increased by ~50°C and 1–1.5 kbar to peak conditions. In the staurolite zone, cooling had commenced by the time of F_3, as indicated by chlorite-grade F_3 assemblages. In the sillimanite zone, however, metamorphism was related to a thermal event in the Kisseynew Domain. Here, peak conditions continued until after F_3 (duration of more than 10 m.y.), on the basis of isograds/isotherms crosscutting large F_3 structures. I suggest that low- to medium-pressure, high-temperature metamorphism in the Kisseynew Domain resulted from heat advected by sheets of ~1.815 Ga peraluminous granitoids. The solidi of the granitoids buffered the temperatures of metamorphism. A possible cause for the formation of granitic magma in the lower crust of the Kisseynew Domain was high basal heat-flow resulting from convective thinning of the lithosphere during crustal thickening.

INTRODUCTION

Low-pressure, high-temperature metamorphism is characteristic of extensional tectonic settings, such as the Pyrenean massifs in France (Zwart, 1962, 1967, 1969; Wickham and Oxburgh, 1985, 1987), but it also occurs in compressional regimes, for example in the Slave province, Canada (Thompson, 1989), and in some Proterozoic inliers in Australia (e.g. Wyborn *et al.*, 1988; Sandiford and Powell, 1991; Reinhardt, 1992). High-temperature metamorphism in middle to upper crustal levels results from heat advection by intruding magmas (Wells, 1980; Lux *et al.*, 1986; Warren and Ellis, 1986; Bohlen, 1987; Barton and Hanson, 1989; De Yoreo *et al.*, 1989a, b, 1991; Harley, 1989; Loosveld, 1989; Sandiford and Powell, 1991). The generation of magmas in the lower crust requires anomalously high basal heat-flow, which is commonly manifested in rift settings by condensed isograds caused by lithospheric thinning (McKenzie, 1978; Thompson, 1981). In compressional settings, anomalously high basal heat-flux can be produced by a variety of tectonic processes including crust–mantle delamination, convective removal of the lithospheric mantle root, and simultaneous thickening of the crust and thinning of the lithosphere (Bird, 1979; Houseman *et al.*, 1981; Loosveld and Etheridge, 1990; Platt and England, 1993).

The Paleoproterozoic Kisseynew Domain, a 300 x 150 km lithotectonic domain in the interior Trans-Hudson Orogen of Manitoba and Saskatchewan, Canada (Fig. 4.1), was metamorphosed at low- to medium-pressure, high-temperature conditions during compressional deformation (Gordon, 1989; Gordon *et al.*, 1990, 1993). Peak metamorphic

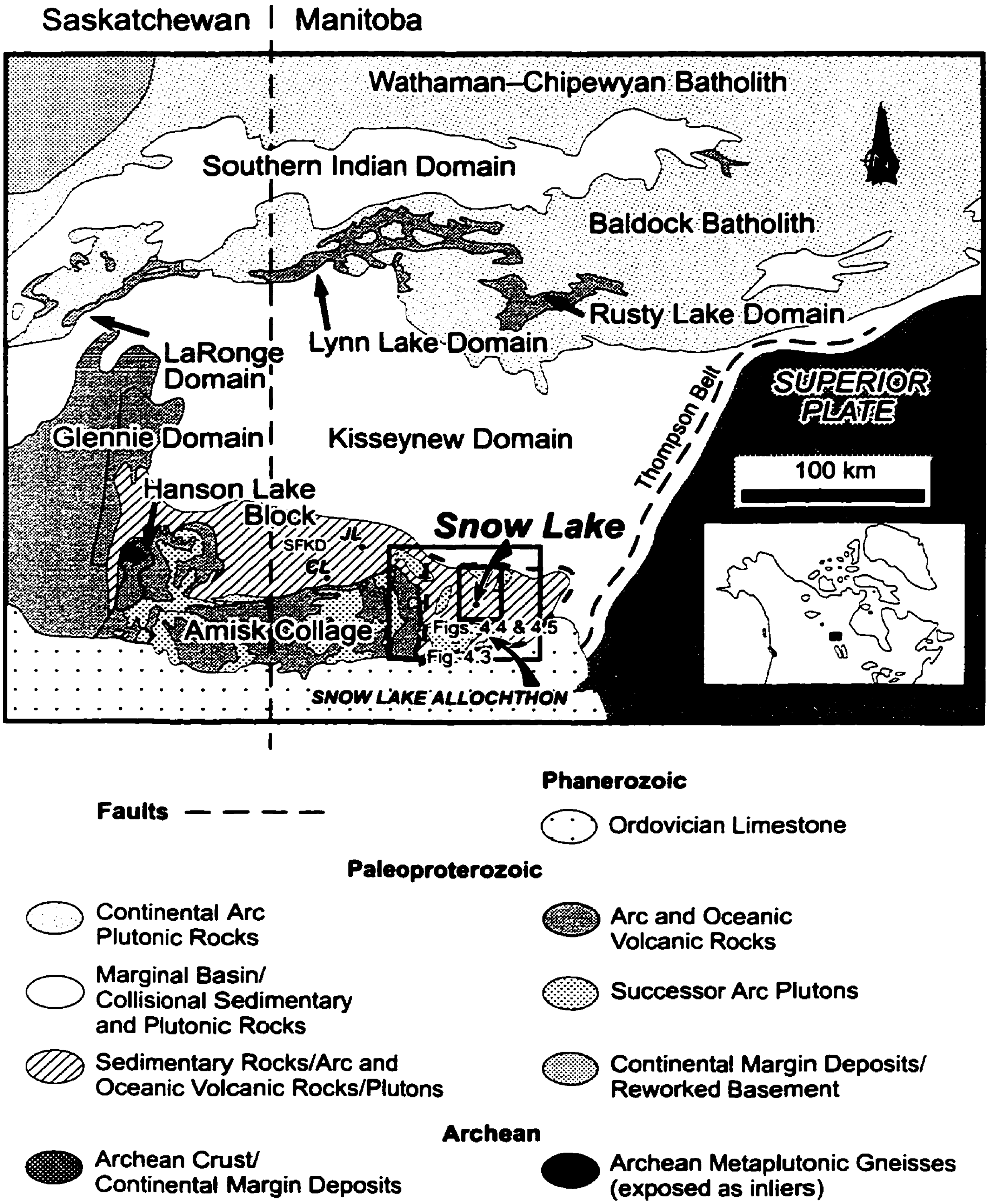

Figure 4.1 Lithotectonic domains of the Trans-Hudson Orogen, and location of the Snow Lake Allochthon (within dashed border). After Hoffman (1988). *CL*, Cleunion Lake; *JL*, Jungle Lake; SFKD, southern flank of Kisseynew Domain.

grade was uniformly high in the central Kisseynew Domain, but was much lower at the north and south flanks (Fig. 4.2) (Bailes and McRitchie, 1978; Froese and Moore, 1980; Gordon, 1989 and references therein; Perkins, 1991; Briggs and Foster, 1992; Gordon *et al.*, 1993, 1994a, b).

This study has concentrated on the southern boundary zone of the Kisseynew Domain (Fig. 4.1). Detailed structural work is presented in Chapters 2 and 5. Microstructural studies and geothermobarometry are used in this study to interpret the tectonometamorphic history of the area. A companion study by Menard and Gordon (1997) presents detailed metamorphic P–T–t paths calculated from hydrothermally altered volcanic rocks of the Snow Lake assemblage (see below).

GEOLOGICAL SETTING

The Snow Lake area hosts three distinct tectonostratigraphic assemblages. The first comprises Fe-rich, Al-poor distal metaturbidites of the Burntwood group, which were deposited on oceanic crust in the marginal Kisseynew basin at 1.86–1.84 Ga, probably during rifting (Fig. 4.3) (Bailes, 1980b; Zwanzig, 1990; Ansdell and Norman, 1995; Machado and Zwanzig, 1995; David *et al.*, 1996). The second is the correlative fluvial-deltaic Missi group (e.g. Stauffer, 1990; Ansdell, 1993; Ansdell and Norman, 1995; Ansdell *et al.*, 1995). The third is the Snow Lake assemblage, comprising ~ 1.9 Ga island arc rocks and synvolcanic intrusions, which are coeval with the amalgamated island arc and oceanic assemblages of the

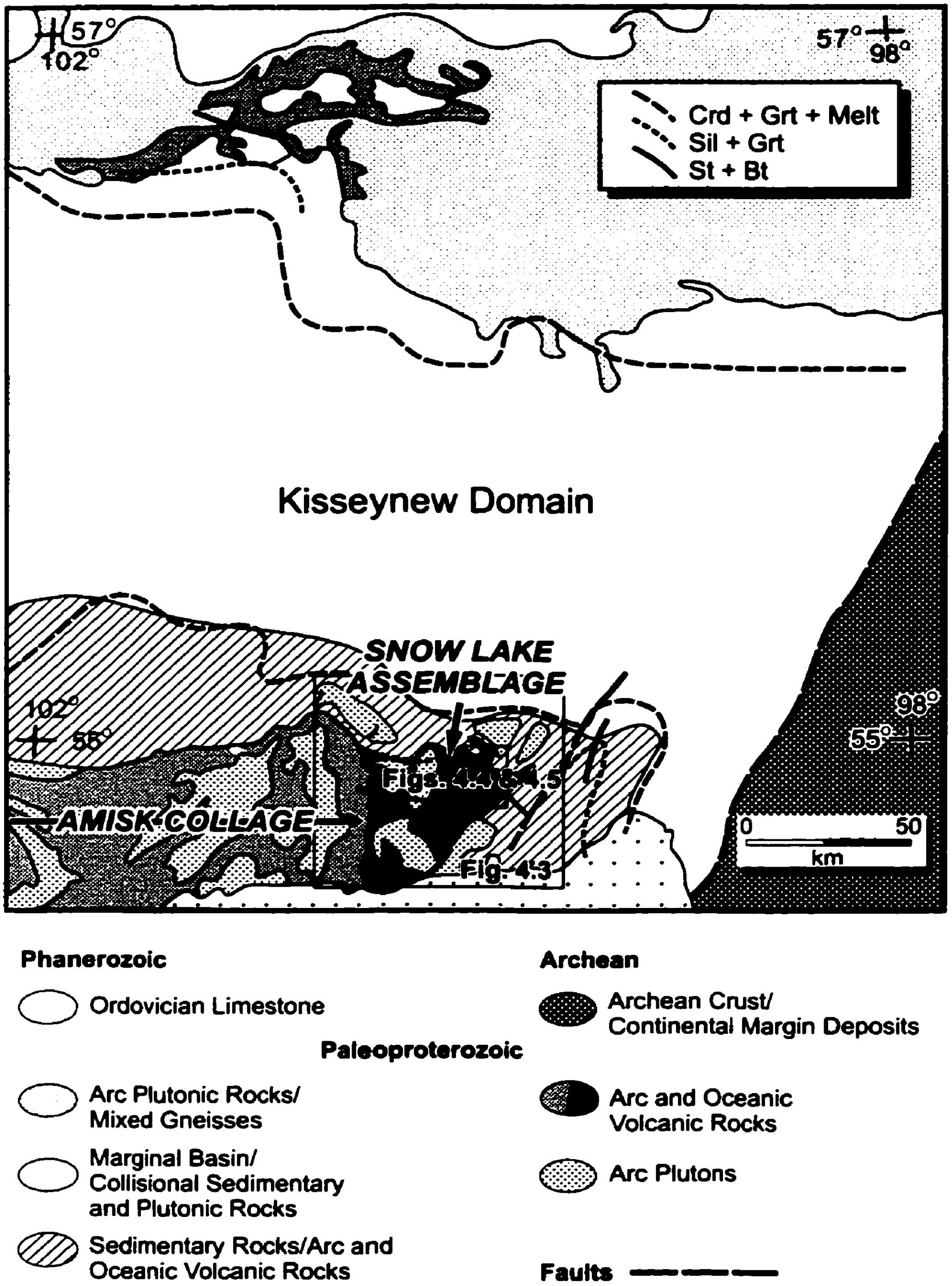

Figure 4.2 Metamorphic isograds of the southeastern Trans-Hudson Orogen, after Gordon (1989). Mineral symbols after Kretz (1983).

Amisk collage to the west, although the Snow Lake assemblage and the Amisk collage are chemically and structurally distinct (Stern *et al.*, 1995a, b; Lucas *et al.*, 1996a; David *et al.*, 1996; Ryan and Williams, 1996b). Sandstones of the Missi group may have unconformably overlain the Kisseynew basin margin. They now sit unconformably on the Snow Lake assemblage rocks east of Wekusko Lake (K.A. Connors and K.M. Ansdell., pers. comm., 1996). The southern boundary zone of the Kisseynew Domain around Snow Lake constitutes a series of folded tectonic slices of sedimentary and volcanic rocks (Fig. 4.3). I define this zone of tectonic interleaving, which also includes ocean floor assemblages at the northeast side of Reed Lake and east of Wekusko Lake (Fig. 4.3) (Syme *et al.*, 1995), as the Snow Lake Allochthon. The Snow Lake Allochthon terminates to the west against the Amisk collage along the Morton Lake fault (Fig. 4.3) (Stern *et al.*, 1995a, b; Syme *et al.*, 1995; Lucas *et al.*, 1996a). To the northwest of the Morton Lake fault, the continuation of the Snow Lake Allochthon comprises interleaved rocks of the Kisseynew Domain and the Amisk collage, and is called the south flank of the Kisseynew Domain (Zwanzig, 1990; Ansdell and Norman, 1995; Norman *et al.*, 1995). The Amisk collage and the Snow Lake Allochthon constitute the former central and eastern segments of the "Flin Flon Belt", respectively.

Tectonic interleaving, that occurred during two phases of folding (F_1–F_2), obscured the precise location of the southern boundary of the Kisseynew Domain and structurally underlying assemblages (Chapter 2; Connors, 1996; David *et al.*, 1996; E. Froese, pers. comm., 1996). Kisseynew sedimentary rocks were transported generally to the southwest during north–south convergence of the forming Trans-Hudson Orogen and the Superior

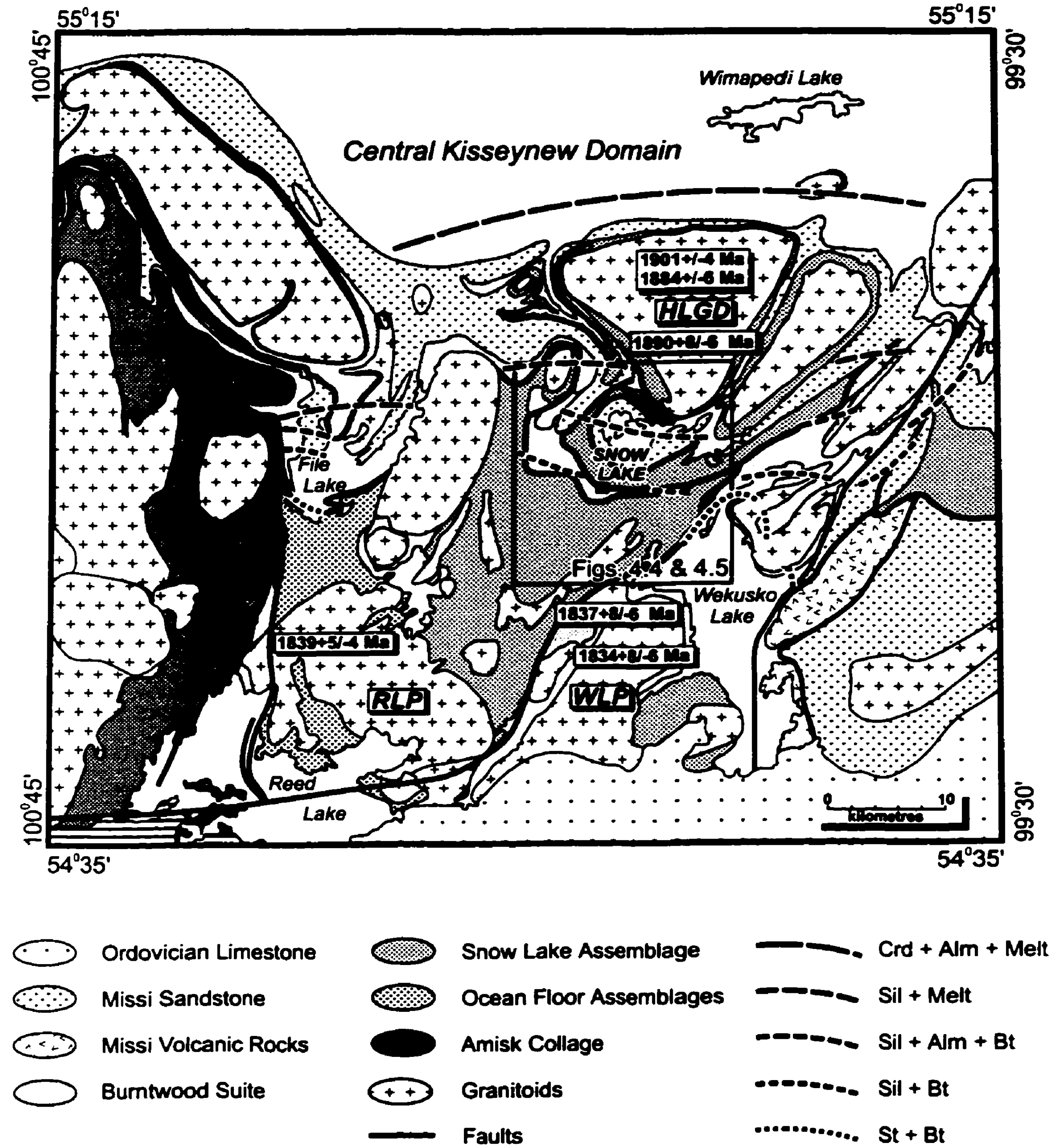

Figure 4.3 Snow Lake–File Lake–Wekusko Lake map, including isograds of Froese and Gasparrini (1975), Bailes and McRitchie (1978), Gordon (1981), Gordon and Gall (1982), and Zaleski and Gordon (1990). *HLGD*, Herblet Lake gneiss dome; *RLP*, Reed Lake pluton; *WLP*, Wekusko Lake pluton. Geochronological data refer to the ages of emplacement of granitic rocks, as cited in text.

craton at 1.84–1.81 Ga (Zwanzig, 1990; Zwanzig and Schledewitz, 1992; Norman *et al.*, 1995; Ansdell *et al.*, 1995; Lucas *et al.*, 1996a; David *et al.*, 1996; Chapter 2).

In the Snow Lake Allochthon, F_1 produced transposed and dismembered isoclinal ductile folds at all scales (Fig. 4.3). Large-scale F_1 structures were truncated by late F_1 movements on the Snow Lake and Berry Creek faults. F_1 may have spanned a narrow time interval, which is bracketed by the ages of the youngest detrital zircons from Burntwood group samples (1845 ± 2 Ma and 1842 ± 2 Ma; Machado and Zwanzig, 1995), and the age of the post-F_1 Wekusko Lake granite (1841 ± 5 Ma, 1837 +8/-6 Ma, and 1834 +8/-6 Ma; Gordon *et al.*, 1990; David *et al.*, 1996) (Fig. 4.3).

During F_2 at 1.820–1.805 Ga (Gordon *et al.*, 1990; Ansdell and Norman, 1995; Parent *et al.*, 1995; David *et al.*, 1996), the tectonostratigraphic sequence was folded into southwest-verging, tight to isoclinal curvilinear structures, such as the McLeod Lake fold (Fig. 4.4) with moderately to steeply dipping axial planes, producing a regionally pervasive axial plane S_2 fabric (Chapter 2). F_2 structures were dismembered by late F_2 reverse faults, such as the McLeod Road and Birch Lake faults (Fig. 4.4), that had southwest-directed transport (Chapter 2).

F_3 produced the large-scale, open, upright, north-northeast trending Threehouse synform (Fig. 4.4) (Chapter 2) during broadly east–west shortening at ~ 1.81 Ga (Ansdell and Norman, 1995; Connors, 1996). Folding was associated with sinistral oblique collision of the Trans-Hudson Orogen with the Superior province (Hoffman, 1988; Bleeker, 1990a Connors, 1996; Chapter 2).

East–west-trending F_4 cross folds north of Snow Lake overprint favourably oriented,

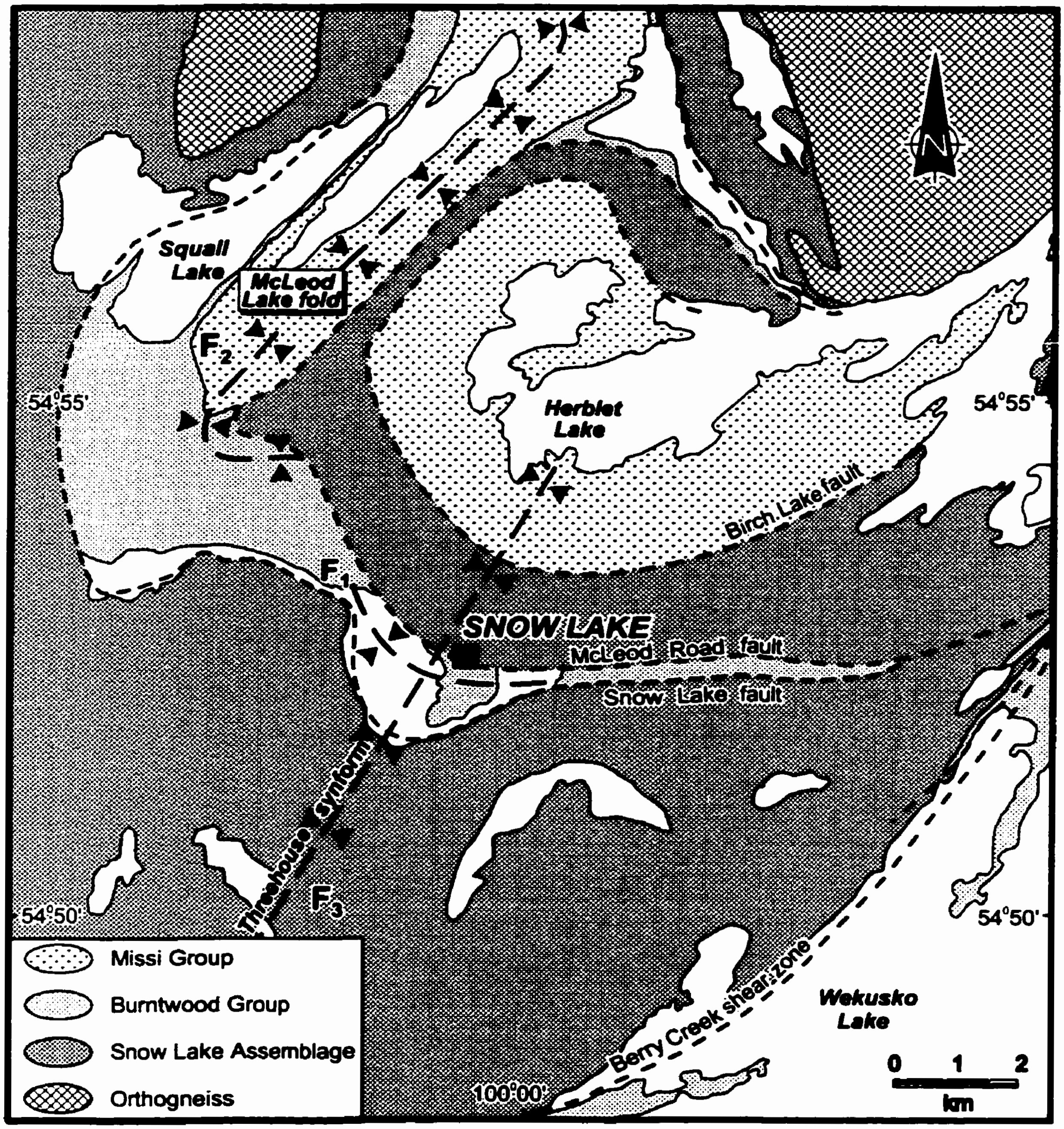

Figure 4.4 Simplified structural map of the Snow Lake area.

large-scale F_3 folds, yielding dome-and-basin to mushroom-shaped interference patterns (Fig. 4.3). These domes are cored by synvolcanic intrusions, which are now orthogneisses (Bailes, 1975; Gordon *et al.*, 1990; David *et al.*, 1996). I interpret the F_4 folds to result from renewed north–south convergence.

Metamorphic grade increases to the north, from sub-biotite grade at Wekusko Lake to lower granulite grade in the central Kisseynew Domain (Figs 4.2, 4.3 and 4.5). Metamorphic zones in the Snow Lake Allochthon extend ~70 km eastward from File Lake to east of Wekusko Lake (Figs 4.2 and 4.3) (Harrison, 1949; Froese and Gasparrini, 1975; Bailes and McRitchie, 1978; Gordon, 1981; Gordon and Gall, 1982; Bailes, 1985; Zaleski and Gordon, 1990; Briggs and Foster, 1992).

North of the study area, sillimanite-bearing migmatites in the vicinity of the Herblet Lake gneiss dome (Fig. 4.3) were produced by partial melting (Bailes, 1975; Bailes and McRitchie, 1978). The entire central Kisseynew Domain, north of the Snow Lake gneiss domes, is characterised by the widespread occurrence of quartz + plagioclase + biotite + garnet + cordierite + sillimanite + graphite assemblages, which suggest uniform peak conditions of metamorphism at temperatures of $750 \pm 50°C$ and pressures $< 5.5 \pm 1$ kbar (Figs 4.2 and 4.3) (Bailes and McRitchie, 1978; Gordon, 1989; W.D. McRitchie, pers. comm., 1996). Two suites of voluminous granitoids are present. An older calc-alkaline suite dated at 1.84–1.83 Ga (e.g. the Wekusko Lake pluton; Fig. 4.3), which also intruded the Amisk collage and the Snow Lake Allochthon, and a younger peraluminous suite, which is restricted to the central Kisseynew Domain (Gordon, 1989; Gordon *et al.*, 1990). The younger suite occurs as sheets of granitoids, which have been interpreted as the products of

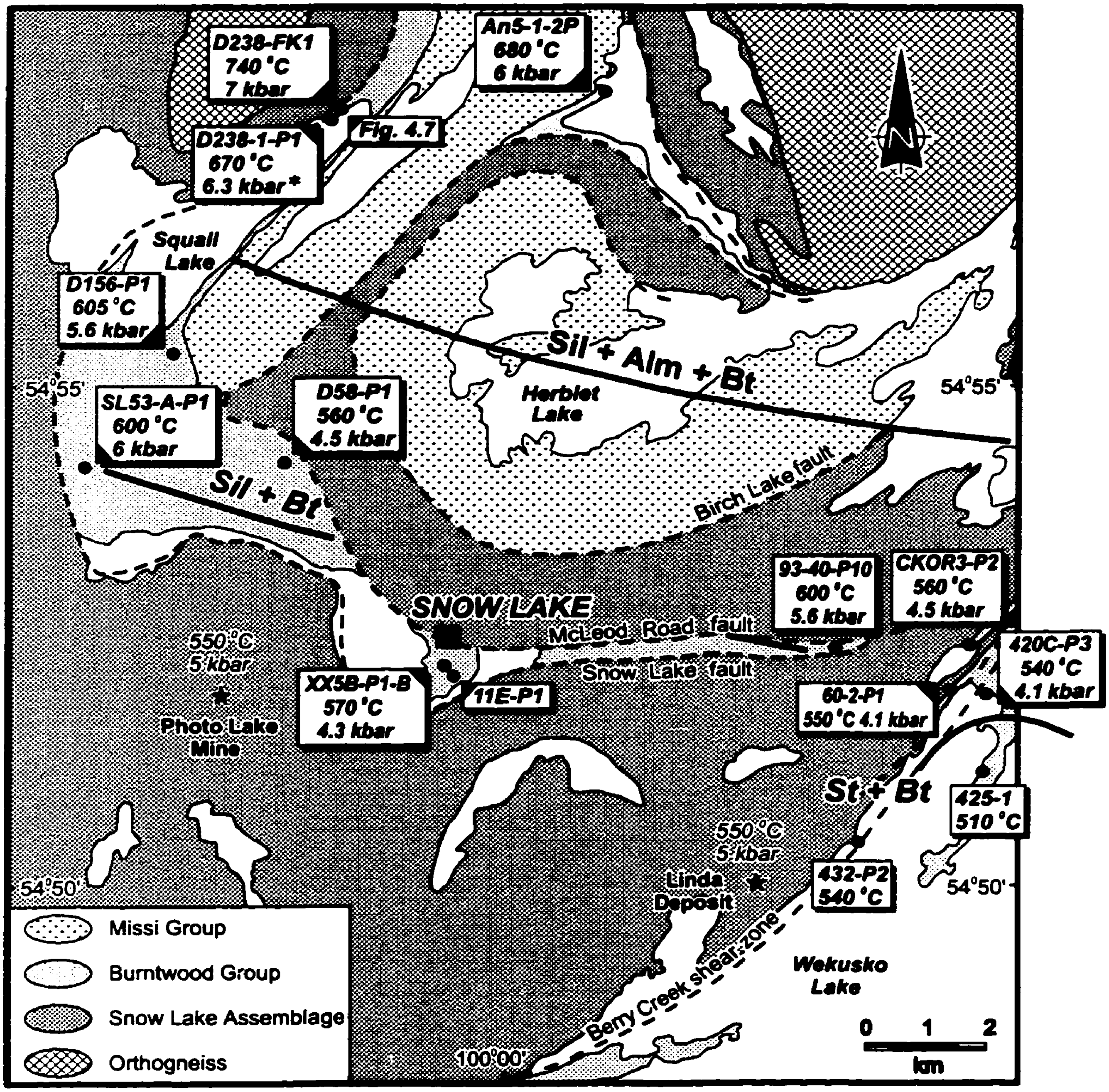

Figure 4.5 P–T data [calculated with TWQ 1.02, except * calculated with the database of Hoisch (1990); see Table 4.5] and isograds of the Snow Lake area. For comparison, P–T estimates calculated with conventional thermobarometers are given in Table 4.5.

in situ anatexis during low- to medium-pressure, high-temperature metamorphism (Bailes, 1975; Bailes and McRitchie, 1978; Gordon, 1989; Zwanzig, 1990; Gordon *et al.*, 1993). These granitoids have yielded ages of 1816 +23/-12 and 1814 +17/-11 Ma (Gordon, 1989; Gordon *et al.*, 1990), which are generally regarded as the age of the thermal peak of metamorphism in the Kisseynew Domain.

Regional metamorphism began during F_1 and has been interpreted as having peaked during the early stages of F_2, at 1.820–1.805 Ga, along the southern flank of the Kisseynew Domain (Zwanzig and Schledewitz, 1992; Ansdell and Norman, 1995; Norman *et al.*, 1995; Parent *et al.*, 1995; David *et al.*, 1996). Similarly, in the Snow Lake Allochthon, interpreted peak metamorphic zircon ages range between 1807 ± 7 Ma and 1803 ± 2 Ma (David *et al.*, 1996).

METHODS

In a related study, the structure of the Snow Lake area was determined by detailed structural mapping (see Chapters 2 and 5). In the present study, approximately 200 thin sections of Burntwood and Missi group rocks were examined petrographically in order to examine regional variations in metamorphic grade. Specific targets were variations (1) across the Berry Creek and Snow Lake faults (Fig. 4.4), (2) across the tectonostratigraphic sequence, and (3) along strike of the tectonostratigraphic sequence (between the Snow Lake and McLeod Road fault; Fig. 4.4). Metaturbidite samples from thirteen representative locations (Fig. 4.5) were analysed by electron microprobe to determine mineral compositions for geothermobarometry (Tables 4.1–4.4). In a parallel study of the metamorphism of hydrothermally altered rocks of the Snow Lake assemblage, Menard and Gordon (1997) examined more than 200 additional samples from the Snow Lake area and 10 samples from the Kisseynew gneisses.

Microprobe analysis

The chemical analysis of selected samples was performed on the fully automated JEOL 733 Superprobe at the University of New Brunswick using an acceleration voltage of 15 keV. The maximum counting times were 20 s with a beam current of 50 nA for garnet line traverses, and 40 s at 10 nA for phyllosilicates and plagioclase. Sillimanite was assumed to have an ideal composition. Two detailed compositional profiles were acquired for zoned garnets (Fig. 4.6). Spacing of analyses in the traverses was reduced in steps from 25 μm in the cores of grains to 2 μm at the rims.

Geothermobarometry

Temperatures and pressures (Fig. 4.5) were calculated with the TWQ 1.02 program using thermodynamic data from Berman (1988, 1991), and activity models for garnet (Berman, 1990; Berman and Koziol, 1991), biotite (McMullin *et al.*, 1991), amphibole (Mäder *et al.*, 1994), and plagioclase (Fuhrman and Lindsley, 1988). The results were

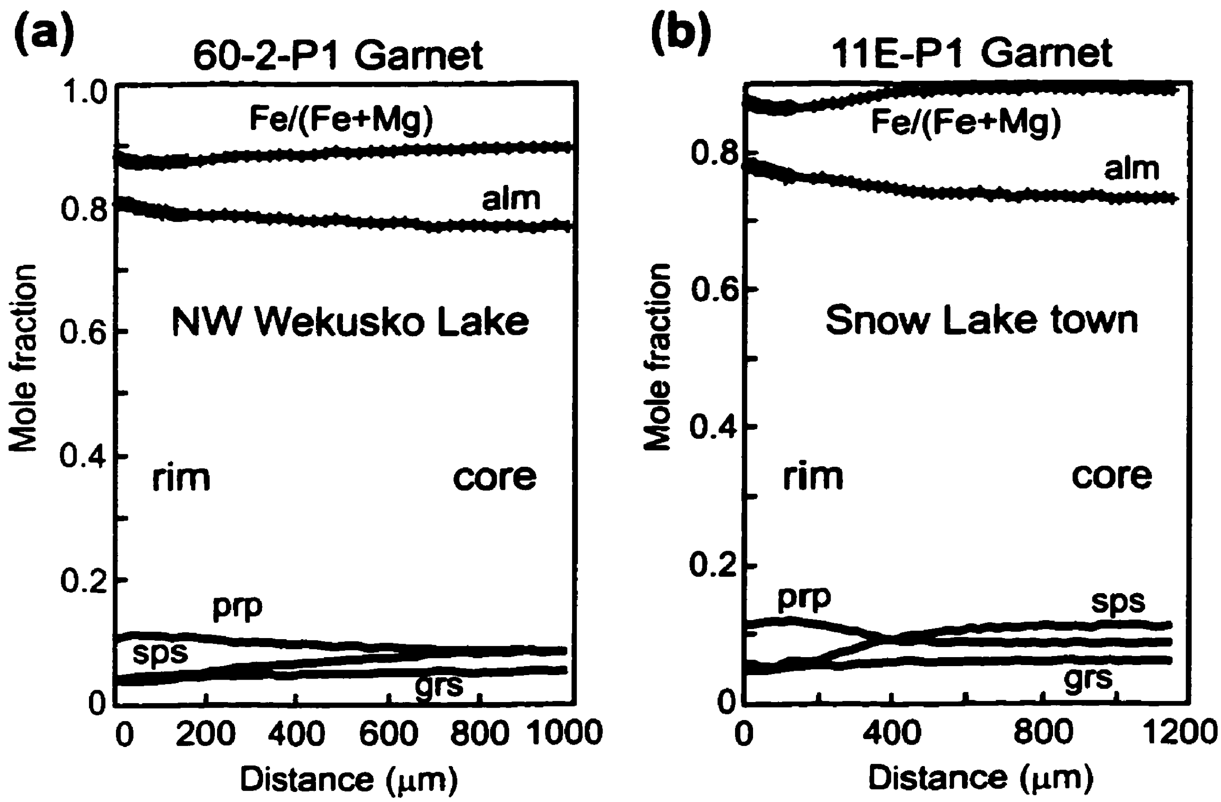

Figure 4.6 Compositional profiles across two grains of garnet in metaturbidite of the Burntwood group. For sample locations, see Figure 4.5.

compared to temperatures and pressures obtained from conventional geothermobarometry (Table 4.5) using the following assemblages: garnet + biotite (Kleemann and Reinhardt, 1994), garnet + biotite + plagioclase + quartz (Hoisch, 1990), and garnet + biotite + muscovite + plagioclase (Hodges and Crowley, 1985; Powell and Holland, 1988; Hoisch, 1990). For compositionally zoned garnets, minimum Fe/(Fe+Mg) values near the garnet rims were used to obtain maximum recoverable temperatures, which likely are underestimates of the peak temperatures (Spear, 1991). For homogenised garnets in high-grade rocks, peak conditions were estimated using core compositions. In all cases, compositions of matrix biotite near, but not in contact with the garnet (both separated by matrix quartz), were used for temperature calculations, together with the assumption of an infinite reservoir of biotite. Only samples without retrograde chlorite were used in order to minimise the effect of retrograde net transfer reactions on the calculated P–T conditions (Spear, 1991, 1993; Spear and Florence, 1992). The construction of metamorphic P–T–t paths from zoned garnets in the metapelites was found to be impossible in the samples studied owing to the lack of either compositionally zoned plagioclase or appropriate inclusions in garnet.

VARIATIONS IN METAMORPHIC GRADE

Chlorite and chlorite+biotite zones

Burntwood group metaturbidtes on the islands near the west side of Wekusko Lake (Figs 4.3 and 4.5) contain the assemblage chlorite ● biotite + quartz + plagioclase + graphite with minor muscovite, ilmenite, rutile, pyrrhotite, tourmaline, magnetite, zircon, and monazite. Chlorite (locally with some muscovite) defines an S_2 slaty cleavage to a crenulation cleavage that crosscuts large (hundreds-of-metres) F_1 folds. Locally, a bedding-parallel S_1 chlorite fabric is preserved. At higher grades, S_2 wraps around biotite porphyroblasts. A distinct garnet+biotite zone is not developed (Froese and Gasparrini, 1975), but garnet appears in and near calc-silicate pods close to the staurolite isograd. These grains of garnet have high Ca and Mn contents and grew at lower temperatures than in typical samples of the Burntwood group (cf. Spear, 1993).

Staurolite+biotite zone

Staurolite-grade metaturbidites occur between Wekusko Lake, Snow Lake, and Squall Lake (Figs 4.3 and 4.5); they contain the assemblage staurolite + biotite + garnet + muscovite + quartz + plagioclase + graphite ± chlorite and accessories as above. Locally, retrograde chlorite partially replaces biotite and rims of garnet grains, and retrograde chlorite and muscovite replace the rims of staurolite grains. Although there is no marker fabric associated with the retrograde chlorite, this replacement occurred most likely during F_3, in agreement with chlorite aligned parallel to a local S_3 in hydrothermally altered rocks of the Snow Lake assemblage of comparable peak metamorphic grade (Menard and Gordon, 1997). The majority of the samples examined from any metamorphic zone, however, lack a pervasive retrograde overprint. Prograde muscovite grew during F_1, defining a bedding-parallel S_1 that was subsequently crenulated and differentiated into an S_2 domainal cleavage during F_2 (Chapter 2; cf. Briggs and Foster, 1992; Connors, 1996). S_2 anastomoses around porphyroblasts of garnet, biotite, and staurolite. Inclusion trails in porphyroblasts of garnet, staurolite, and biotite are straight or preserve open F_2 crenulations of S_1 and thus document early increments of S_2 development (Fig. 4.7). A detailed description of porphyroblast/matrix relationships is given in Chapter 2.

Almandine-rich garnet grains, 1–3 mm in diameter, are compositionally zoned (Fig. 4.6) with Fe/(Fe+Mg), X_{Grs}, and X_{Sps} decreasing from core to rim, and X_{Alm} and X_{Prp} increasing, which may indicate growth during minor heating and loading (Spear *et al.*, 1991). Nevertheless, the magnitude of zoning in garnet is small (Fig. 4.6), indicating that the changes in temperature and pressure during growth were minor. The rims of garnet grains display zoning patterns that suggest minor modification by diffusion during cooling (Fig. 4.6). The lack of significant diffusional garnet homogenisation is in agreement with the modelling by Spear (1988), which predicts that garnets with a radius > 1 mm will not experience significant modification of zoning at a thermal maximum of 585°C (following 65 m.y. of heating).

Porphyroblastic biotite laths up to 2 mm long are aligned with their (001) faces along

Figure 4.7 Orthogonal porphyroblast–matrix relationship between internal S_1 foliation in garnet and external S_2 from the sillimanite zone. Similar relationships are evident in the staurolite zone (Kraus and Williams, 1998) and in the migmatite zone of the central Kisseynew Domain (Menard and Gordon, 1997), indicating that the beginning of garnet growth everywhere predated the development of S_2, and thus F_2 folding (Kraus and Williams, 1998). Sample D238–1–P1. For sample location, see Figure 4.5. Width of field of view: 2.7 mm.

S_2 (Chapter 2). Biotite is compositionally homogeneous. Prograde chlorite is preserved only as inclusions in porphyroblasts, suggesting that chlorite was consumed during growth of the porphyroblasts. Euhedral, poikiloblastic, texturally zoned staurolite grains are up to 14 cm long and contain abundant inclusions of partially corroded garnet, suggesting that garnet was consumed during the staurolite-forming reaction.

Grains of matrix plagioclase are generally small ($\leq$ 0.25 mm), untwinned and virtually unzoned (< 2.5 mol % variation of CaO + Na_2O from core to rim). Compositions vary from An_{20} to An_{36} in typical Burntwood group rocks, and from An_{86} to An_{89} in rare calc-silicate pods and layers. Within an individual thin section, An contents of plagioclase rims vary by only 0.4 to 2.1 mol% An. A second generation of albite-twinned plagioclase occurs in F_2 pressure shadows of staurolite and biotite, and thus postdates growth of the peak metamorphic assemblage.

Sillimanite+biotite and sillimanite+garnet+biotite zones

At metamorphic grades higher than the sillimanite isograd north of Snow Lake (Figs 4.3 and 4.5), metaturbidites of the Burntwood group contain the assemblage biotite + garnet + sillimanite + quartz + plagioclase + graphite ● muscovite ± staurolite and the accessories listed above. In rocks that record peak temperatures of approximately 600°C immediately south of Squall Lake (Fig. 4.5), small volumes of fibrous sillimanite nucleated on plagioclase–plagioclase or plagioclase–quartz grain boundaries. Locally, nodules of fibrolitic sillimanite (Faserkiesel) replaced biotite (cf. Vernon, 1987; Foster, 1991).

Sillimanite fibres that replaced muscovite in the S_2 septa were subsequently kinked by F_3 or F_4, and display recovery features, such as migrated kink-band boundaries and rare growth of new grains parallel to the kink planes, as is common in micas (Etheridge and Hobbs, 1974; Williams *et al.*, 1977). In rocks, in which calculated temperatures exceed 650°C, muscovite and staurolite are not observed in the matrix. Locally, staurolite relics and biotite are armoured by large twinned plagioclase grains, suggesting that the breakdown of staurolite may have involved the formation of plagioclase. Here, an early generation of garnet is texturally identical to the garnet in the staurolite zone (see above), but a second generation of garnet (up to 5 mm in diameter) is texturally zoned with inclusions of quartz, plagioclase, biotite and sillimanite in the core, and fibrolitic sillimanite close to the rim. Both garnet generations are compositionally homogeneous except for strongly retrogressed rims up to 100 mm wide, which yielded calculated temperatures up to 180°C lower than the core. These higher grade rocks contain no staurolite and muscovite but rather a second generation of prismatic sillimanite parallel to S_2.

Spatial distribution of P–T

Calculated temperatures and pressures are shown in Fig. 4.5 and Table 4.5. In the staurolite zone, between the Berry Creek and McLeod Road faults, recorded apparent peak conditions of metamorphism are constant at approximately 540–570°C and 4.1–4.3 kbar, in agreement with 550°C and 5 kbar reported for altered rocks of the Snow Lake assemblage at the Linda and Photo Lake deposits (Fig. 4.5) (Zaleski *et al.*, 1991; Menard and Gordon, 1997).

At the northwestern end of Wekusko Lake, Burntwood group rocks are exposed on both sides of the Berry Creek fault without an apparent discontinuity in metamorphic grade (Fig. 4.5). Calculated temperatures and mineral assemblages in rocks immediately east of the Berry Creek fault indicate progressively lower grades towards the south (Fig. 4.5). There is also no detectable change in metamorphic grade across the Snow Lake fault. Temperature increases to 600°C along strike of the tectonostratigraphic sequence, between Snow Lake and Squall Lake. Along the eastern shore of Squall Lake, temperatures increase to the north along strike up to > 670°C at the north end (Fig. 4.5). Thus, at Squall Lake the isotherms crosscut the F_3 Threehouse synform, in agreement with the regional pattern of isograds (Figs 4.3 and 4.5) (Froese and Gasparrini, 1975; Zaleski and Gordon, 1990). Further north, above the cordierite+garnet isograd, cordierite+garnet+sillimanite assemblages suggest uniform temperatures of 750 ± 50°C throughout the central Kisseynew Domain (Bailes and McRitchie, 1978; Gordon, 1989). The lack of earlier kyanite and the presence of cordierite+garnet indicate that pressures never exceeded 6 kbar (Gordon, 1989; Spear and Cheney, 1989).

As mentioned above, the calculated temperatures for compositionally zoned garnets may be slightly below the peak temperatures. In the staurolite zone, for example, temperatures are constrained by the absence of sillimanite to have been less than 580–590°C (Spear and Cheney, 1989). Thus, the associated calculated pressures may also be erroneously low, because temperatures and pressures are positively correlated in the Snow Lake Allochthon, which experienced heating during loading (Menard and Gordon, 1997; this study). On the other hand, pressures calculated for higher grade rocks that contain compositionally homogenised garnets (T > 650°C) may be slight overestimates, if the calculated temperatures are overestimated, because calculated pressures are temperature dependent (positive slopes of K_{eq} lines). The calculated temperatures in such high-grade rocks depend on correction of the barometers for the non-ideality of (Mg, Fe)–Al^{VI} mixing and (Mg, Fe)–Ti mixing in biotite, which give temperatures up to 100°C lower than those obtained without correction (Spear, 1993). Taking these factors into account, it appears realistic to assume that pressures associated with peak metamorphic temperatures were similar throughout the study area at 5–6 kbar, consistent with pressures determined for the central Kisseynew Domain (Bailes and McRitchie, 1978; Gordon, 1989).

DISCUSSION

Timing of peak metamorphism: evidence of diachronism

Garnet commenced growing in metaturbidite and altered volcanic rocks everywhere in the study area prior to F_2 folding, as shown by identical porphyroblast/matrix relationships (Chapter 2; Menard and Gordon, 1997; this study). The inception of garnet growth was at ~ 500°C, determined from petrogenetic grids (e.g. Spear and Cheney, 1989) and from calculations of P–T–t paths (Menard and Gordon, 1997). Menard and Gordon (1997) report increases in temperature and pressure during garnet growth in samples from the Photo Lake deposit (equivalent to the staurolite zone in the metapelites; Fig. 4.5) of up to 50°C and 1–1.5 kbar to peak conditions during the development of S_2 (Fig. 4.8). Thus, taking into consideration that S_2 predated or coincided with early stages of F_2 folding in strongly anisotropic micaceous rocks (Chapter 2), peak conditions of metamorphism were reached in the staurolite zone early during F_2.

Metamorphism during F_3 in the staurolite zone was a retrograde event at greenschist facies conditions. In contrast, metamorphism during F_3 in the sillimanite zone and above was the peak metamorphic event, as shown by isotherms and isograds that crosscut large F_3 structures such as the Threehouse synform and the File Lake antiform 20 km to the west (Fig. 4.3) (Froese and Gasparrini, 1975; Bailes and McRitchie, 1978; Bailes, 1980a; this study). At File Lake, the staurolite isograd follows bedding in the Burntwood group metaturbidites around most of the F_3 File Lake antiform, whereas the sillimanite and partial melting isograds clearly crosscut the structure (Fig. 4.3) (Bailes and McRitchie, 1978; Bailes, 1980a; see also Connors 1996). Thus, peak metamorphism was diachronous within the Snow Lake Allochthon.

Possible mechanisms for low- to medium-pressure metamorphism

Rocks above staurolite grade had a significantly higher thermal gradient (tighter spacing of isotherms) during peak metamorphism than did rocks at lower metamorphic grades, indicating a thermal anomaly centred in the Kisseynew Domain (Gordon, 1989; Ansdell *et al.*, 1995; Menard and Gordon, 1997). The thermal anomaly started after the

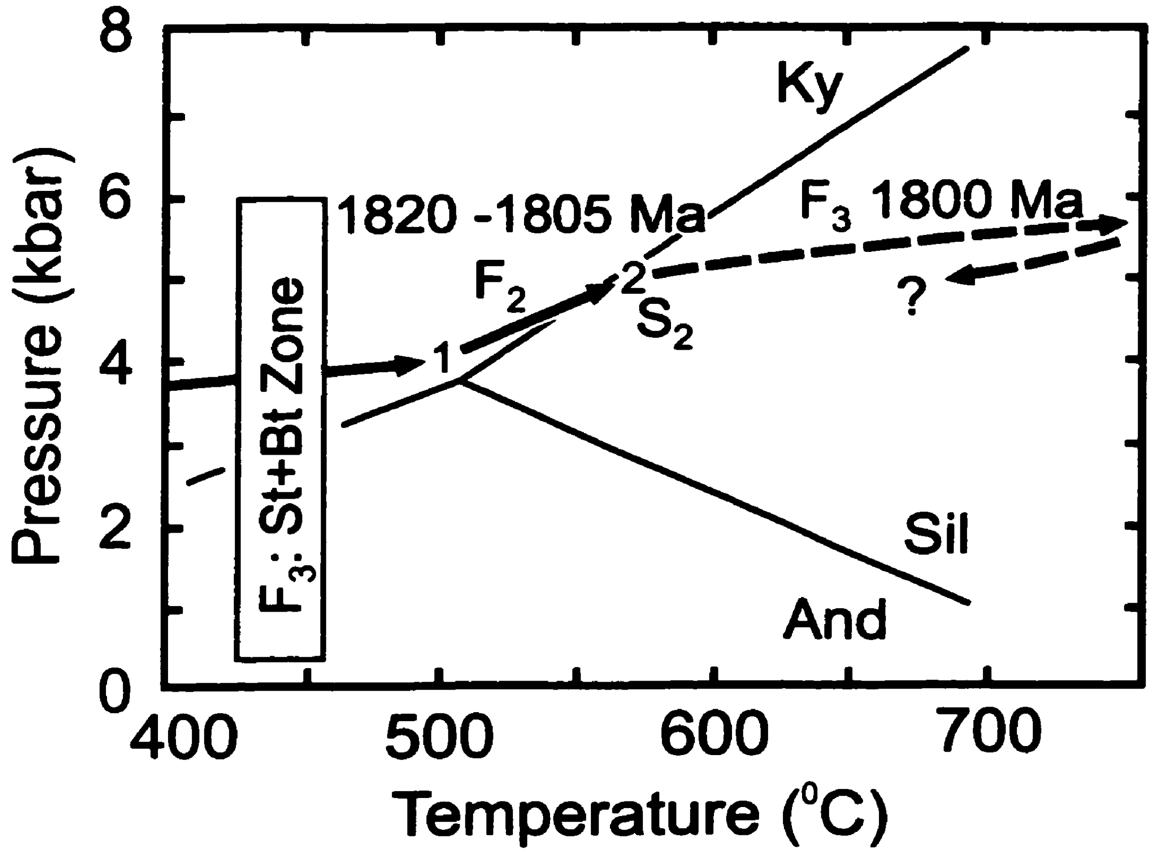

Figure 4.8 Calculated P–T–t paths for the Snow Lake Allochthon and the Kisseynew Domain. Garnet commenced growing at 1; S_2 formed at 2. For further explanation, see text.

development of S_2, as demonstrated by syn-S_2 garnets from Snow Lake and from the Kisseynew Domain, even though the Kisseynew samples subsequently reached much higher temperatures (Fig. 4.8) (Menard and Gordon, 1997).

Several models have been proposed for the cause of the thermal anomaly in the Kisseynew Domain: (1) Radiogenic heat production in the crust was unlikely the sole cause, because it would have required a period of at least 60 m.y. to produce the observed high-temperature metamorphism (Gordon, 1989; Gordon *et al.*, 1993). (2) Conductive response to a high basal heat-flow (England and Richardson, 1977; England and Thompson, 1984) could have resulted in the elevated local thermal gradients during metamorphism (Gordon, 1989; Gordon *et al.*, 1993; Ansdell and Norman, 1995). High basal heat-flow was related by Ansdell and Norman (1995) to the influx of asthenospheric material to the base of the continental lithosphere as a result of crust–mantle delamination (Bird, 1979; Bird and Baumgardner, 1981; Kay and Kay, 1993) or to convective removal of the root of the mantle lithosphere (Platt and England, 1993). (3) Heat advection by the 1.84–1.83 Ga granitoids has been proposed as the cause (Gordon, 1989; Gordon *et al.*, 1993; Ansdell *et al.*, 1995). However, rocks surrounding the 1.84–1.83 Ga Reed and Wekusko Lake plutons (Fig. 4.3) (Gordon *et al.*, 1990; David *et al.*, 1996; R.A. Stern pers. comm., 1996) are of low metamorphic grade (chlorite assemblages), suggesting that the calc-alkaline magmatism contributed little to the overall heat budget. Discussion of these alternatives follows, starting with observable features in the ~ 1.815 Ga granitoids and migmatites of the central Kisseynew Domain.

Third order mechanisms—granitoid emplacement vs* in situ *anatexis?

The widespread migmatites and younger peraluminous granitoids in the central Kisseynew Domain are generally considered to have been generated by *in situ* anatexis and thus as the product rather than the (local) cause of high-temperature metamorphism at moderate pressures (Bailes, 1975; Bailes and McRitichie, 1978; Gordon, 1989; Zwanzig, 1990; Gordon *et al.*, 1990, 1993). In contrast, there is compelling evidence, which is presented below, that heat derived from the ~ 1.815 Ga granitoids caused local anatexis of the metasedimentary country rocks at the presently exposed crustal level. This disparity has important implications for possible crust–mantle interactions (first order mechanism) that may have led to the production of granitic magmas at lower crustal levels (second order mechanism).

The origin of the younger peraluminous granites and the migmatitic paragneisses in the Kisseynew Domain can be constrained by the following lines of evidence: (1) Peraluminous granitic, granodioritic and minor trondhjemitic orthogneisses occupy approximately 40% of the area around Wimapedi Lake immediately north of the Snow Lake gneiss domes (Fig. 4.3) (Bailes, 1975), and up to 75% of the central Kisseynew Domain (Zwanzig, 1990). (2) The granitoids contain xenoblasts of garnet and cordierite, and locally biotite, and up to 15% xenoliths of fertile rocks of the Burntwood group (Bailes, 1975; Bailes and McRitchie, 1978; Gordon, 1989; Zwanzig, 1990). (3) Most of the large granitoids constitute tabular bodies, which are concordant with bedding or are parallel to the axial planes of large folds, but also occur as dykes and stocks (Bailes, 1975; Gordon, 1989;

Zwanzig, 1990; W.D. McRitchie, pers. comm., 1996). (4) The contacts between the granitic rocks and the metasedimentary rocks range from sharp for the larger bodies, to diffuse for the smaller bodies (Bailes, 1975; Gordon, 1989; Zwanzig, 1990). (5) There are no large volumes of noritic restite located at the margins of larger bodies of granitoids. Restite rich in garnet+cordierite+biotite only occurs as small-scale domains associated with ubiquitous small stringers of granitic material (A.H. Bailes, pers. comm., 1996). (6) The Burntwood group paragneisses are compositionally uniform in the Kisseynew Domain and muscovite was not present in the rocks prior to partial melting (Froese and Gasparrini, 1975; Bailes and McRitchie, 1978; Gordon, 1989; W.D. McRitchie, pers. comm., 1996; this study). (7) The peak temperatures recovered from the paragneisses are also uniform at 750 ± 50°C at pressures of 6 kbar or less (Bailes and McRitchie, 1978; Gordon, 1989).

These observations lead to the following implications: (1) The tabular geometries of the granitoids and their field relationships with the metasedimentary country rocks in the Kisseynew Domain imply magma emplacement along zones of primary and structural anisotropy (cf. Collins and Sawyer, 1996). Paragneisses of relatively uniform composition in the entire Kisseynew Domain had uniform solidus temperatures, which cannot account for selective *in situ* generation of stratiform sheets of granitoids with locally sharp contacts to country rock and xenoliths. Local gradational contacts can be explained by anatexis of country rocks, which were already relatively hot at the time of granitoid emplacement (see above), resulting from heat transferred from the granitoids. (2) If the peraluminous granitoids were generated by *in situ* anatexis and remained at the site of generation, there should be large volumes of restite associated with them, which are not observed. Further, magmas created by high melt fractions (> 30–40%) generally have low viscosities and are thus easily extracted to form plutons at higher crustal levels (Wickham, 1987, and references therein). Therefore, the voluminous granitoids exposed in the Kisseynew Domain were probably produced at lower structural levels. (3) The mineral assemblages in the granitoids, in particular the presence of cordierite and the lack of muscovite, implies H_2O-undersaturated conditions during magma generation (Barbarin, 1996). Recent dehydration melting experiments of similar assemblages suggest that the production of large proportions of melt would require temperatures significantly greater than 850°C at 3–15 kbar (Le Breton and Thompson, 1988; Vielzeuf and Holloway, 1988; Patiño Douce and Johnston, 1991; Gardien *et al.*, 1995; Patiño Douce and Beard, 1995). In comparison, more hydrous assemblages started melting at ~750°C, and melt fractions increased from 28 to 60% between 825 and 960°C at 10 kbar (Gardien *et al.*, 1995). Thus, the metamorphic temperatures in the Kisseynew Domain appear too low to account for high melt fractions during "dry" *in situ* anatexis.

The available data can be interpreted as suggesting that intruding granitic magmas of tabular geometry were the local heat source for a regional-scale contact metamorphism, similar to that in northern New England (Lux *et al.*, 1986; De Yoreo *et al.*, 1989b). In contrast to conductive heating, heat advection by intrusions is rapid (e.g. Lux *et al.*, 1986; Barton and Hanson, 1989) and thus commonly produces near-isobaric P–T paths, consistent with the observations of Gordon (1989) and Menard and Gordon (1997). The solidus temperatures of the large volumes of granitic magma in intrusive sheets may have buffered the peak temperatures of metamorphism, resulting in partial melting of the paragneisses at a uniform metamorphic grade, and in the formation of uniform mineral assemblages throughout the Kisseynew Domain (cf. Waters, 1986; De Yoreo *et al.*, 1989b).

Second order mechanisms—implications for lower crustal melting

The peraluminous composition of the ~1.815 Ga granitoids and the abundance of paragneiss xenoliths indicate that the granitoids may have been generated from rocks of the Burntwood group. The site of magma generation was most likely the base of the sedimentary pile, where temperatures exceeded the solidi of the sediments, but not of the mafic rocks of the underlying oceanic crust. One reason that advection of heat and thus high-temperature metamorphism was restricted to the Kisseynew Domain could be that metasediments did not occur at greater depth in the adjacent Amisk collage and Lynn Lake Belt (Fig. 4.1). Consequently, ~1.815 Ga granitic suites are absent in these domains, suggesting that low to medium-grade metamorphism there was triggered mainly by conductive relaxation.

First order mechanisms—possible crust–mantle interactions

The question remains which tectonic process(es) generated a deep-seated heat source that caused melting of metasediments at the base of the Kisseynew Domain. Three possible first order mechanisms are simultaneous crustal thickening and thinning of the mantle lithosphere (Houseman *et al.*, 1981; Loosveld, 1989; Loosveld and Etheridge, 1990), delamination of the lithosphere (Bird, 1979; Bird and Baumgardner, 1981; Kay and Kay, 1993), and convective removal of the base of the thickened lithosphere (Platt and England, 1993), all of which lead to asthenospheric mantle intrusion into, or accretion beneath, the crust (Furlong and Fountain, 1986; Huppert and Sparks, 1988). Such heat addition can be sufficient for dehydration melting of the lower crust to form granitic magma (Huppert and Sparks, 1988; Atherton, 1993). Although the thermal effects of the mechanisms are equivalent, their geological consequences differ (Loosveld and Etheridge, 1990; Platt and England, 1993). Delamination and removal of the root of the lithospheric mantle are typically followed by a short period of extension and uplift (e.g. Bird, 1979; Sacks and Secor, 1990; Nelson, 1992; Kay and Kay, 1993; Platt and England, 1993), for which there is no structural or petrological evidence in the southern Trans-Hudson Orogen. Thickening of the crust and thinning of the lihosphere, commencing during F_1, thus appears to be the most plausible first order mechanism for low- to medium-pressure, high-temperature metamorphism in the Kisseynew Domain.

Duration of the thermal anomaly

In the Wimapedi Lake area of the Kisseynew Domain (Fig. 4.3), the ~1.815 Ga granitoids have been deformed by a minimum of two generations of folds as inferred from Bailes (1975). The earliest fold generation affecting the intrusions constitute south verging, recumbent structures that most likely correlate with the F_2 folds in the Snow Lake Allochthon and the south flank of the Kisseynew Domain at Jungle Lake and Cleunion Lake, approximately 70 km and 90 km west–northwest and west of Snow Lake, respectively (Fig. 4.1). Elsewhere in the central Kisseynew Domain, some bodies of granitic rocks appear as dyke complexes axial planar to south verging (F_2) folds (Zwanzig, 1990). In the high-grade rocks at Squall Lake and File Lake, however, metamorphic isograds crosscut north-northeast trending, open F_3 folds (Fig. 4.3). It thus appears that the granitic magmatism in the Kisseynew Domain outlasted at least F_2, and that temperatures in the Kisseynew Domain and the high-grade rocks of the Snow Lake Allochthon must have remained elevated until after F_3.

Wells (1980) calculated that a thermal anomaly produced by sill-like batholiths lasts as long as 10–20 Ma, if heat transfer is purely by conduction (although heat advection by late-stage fluids would accelerate the relaxation of isotherms; Huppert and Sparks, 1988). In comparison, monazite ages of ~1815 Ma for granitoids in the central Kisseynew Domain (which date the cooling through 725 ± 25°C; Parrish, 1990) are 1806 ± 2 Ma and 1804 ± 2 Ma (Gordon, 1989; Gordon *et al.*, 1990). At Jungle Lake (Fig. 4.1), several phases of syn-F_2 diatexites and leucosomes, interpreted as having formed near the peak of metamorphism, range from 1812 ± 4 Ma to 1789 ± 2 Ma (Parent *et al.*, 1995). Near Cleunion Lake (Fig. 4.1), syn-F_2 gneissic veinlets were dated at 1818 ± 5 Ma, coeval with peak conditions of metamorphsim of greater than 580°C at ~ 5 kbar (Ansdell and Norman, 1995; Norman *et al.*, 1995). Syn-F_3, near-peak metamorphic pegmatites yielded crystallisation ages from 1801 ± 3 Ma to 1799 ± 3 Ma (Norman and Williams, 1993; Ansdell and Norman, 1995). Westward migration of the F_3 deformation, away from the Trans-Hudson–Superior suture zone, could explain why sillimanite-grade conditions were associated with the local F_2 in the

Jungle Lake and Cleunion Lake areas, and with the local F_3 in the Snow Lake–File Lake area, at the same time.

Thus, the duration of high-temperature metamorphism in the Kisseynew Domain may be explained by emplacement of many sheet-like bodies in multiple stages. This scenario can also account for the extent of the thermal effects into the Snow Lake–File Lake area for more than 10 km south of the southernmost exposed granitoid (Lux *et al.*, 1986; De Yoreo *et al.*, 1989a). Such magmatic pulses are compatible with the longevity of a thermal anomaly at the base of the crust caused by thickening of the crust and thinning of the mantle lithosphere owing to convection (Houseman *et al.*, 1981; Loosveld, 1989; Loosveld and Etheridge, 1990). In summary, although the data do not date metamorphism directly, they are consistent with the persistence of near-peak conditions of metamorphsim for 10 m.y. in the Kisseynew Domain and the higher grade rocks of the Snow Lake Allochthon.

SUMMARY AND CONCLUSIONS

Structural mapping, microstructural studies, and geothermobarometry on representative samples suggest that the Snow Lake Allochthon is characterised by syntectonic, diachronous, low- to medium-pressure metamorphism resulting from thermal relaxation after crustal thickening and granitic plutonism in the adjacent Kisseynew Domain. F_1 likely was the major episode of burial, and was followed by thermal relaxation, because the peak metamorphic conditions in the staurolite zone were coeval with early F_2 (Chapter

2). Burial during F_1 was probably rapid (1–5 Ma) as indicated by the youngest detrital zircons in the Burntwood group and ages of granitoids that crosscut F_1 structures (Gordon *et al.*, 1990; Machado and Zwanzig, 1995; David *et al.*, 1996). The ductile style of F_1 structures suggests crustal thickening by thick, internally deformed nappes (thick skinned tectonics). Metamorphic conditions increased within 15–35 m.y. from chlorite grade to staurolite grade, possibly isobarically. During F_2, temperature and pressure increased only slightly suggesting relatively minor crustal thickening after F_1 (Menard and Gordon, 1997). A thermal anomaly developed during or after F_2 which led to high-grade metamorphism in the northern part of the study area and the adjacent Kisseynew Domain. Peak conditions in the high-grade rocks prevailed for some 10 m.y. until after F_3, whereas mineral assemblages in staurolite-grade rocks indicate cooling during F_3.

Few things are harder to put up with than a good example.
Mark Twain

Chapter 5[1]

The structural development of the Snow Lake Allochthon and its role in the evolution of the southeastern Trans-Hudson Orogen in Manitoba, Central Canada

Abstract: The Snow Lake Allochthon is a zone of tectonic interleaving of sedimentary rocks of an inverted marginal basin (Kisseynew Domain) with island arc and oceanic rocks. It is located in the southeastern part of the exposed internal zone of the Trans-Hudson Orogen in Manitoba, Canada, near the external zone (Thompson Belt), that constitutes the local boundary between the Trans-Hudson Orogen and the Archean Superior craton. The Snow Lake Allochthon formed, was deformed, and was metamorphosed up to high grade at low to medium pressure during the Hudsonian orogeny as a result of the collision of Archean cratons ~1.84–1.77 Ga ago. Four generations of folds (F_1–F_4) that formed in at least three distinct kinematic frames over a period of more than 30 m.y. are described. Isoclinal to transposed $F_{1/2}$ structures with a southerly vergence are refolded by large open to tight F_3 folds and, locally, by open to tight F_4 folds. The axes of the $F_{1/2}$ folds are parallel or near-parallel to the axes of F_3 folds, owing to progressive reorientation of the $F_{1/2}$ axes during

---

[1]A modified version of this chapter was accepted for publication by the Canadian Journal of Earth Sciences on 16 November 1998.

southerly tectonic transport, followed by F_3 refolding around the previous linear anisotropy. A tectonic model is presented that reconciles the distinct tectonometamorphic developments in the Snow Lake Allochthon and the adjacent part of the Kisseynew Domain on the one hand, and in the Thompson Belt on the other, during final collision of the Trans-Hudson Orogen with the Superior craton.

INTRODUCTION

The Trans-Hudson Orogen of North America constitutes one of the continental collision zones between Archean fragments, along which the Laurentia–Baltica protocraton was assembled between 2.0 and 1.8 Ga (Fig. 5.1) (e.g. Lewry, 1981; Green *et al.*, 1985; Hoffman, 1988, 1989a; Bickford *et al.*, 1990; Ansdell *et al.*, 1995). In contrast to most contemporaneous suture zones, the internal zone of the Trans-Hudson Orogen preserves large volumes of juvenile Paleoproterozoic crust (Hoffman, 1988; Stern *et al.*, 1995a, b). The external zone of the orogen contains the reworked margins of the bounding Rae–Hearne and Superior cratons including rift facies rocks (Fig. 5.1) (Lewry, 1981; Hoffman, 1988; Bleeker, 1990). The eastern termination of the Snow Lake Allochthon (see Chapter 4) is located less than 30 km west of the external zone of the orogen (Thompson Belt). It formed, was deformed, and was metamorphosed up to high grade at low to medium pressure during the Hudsonian orogeny ~1.84–1.77 Ga ago (e.g. Froese and Gasparrini, 1975; Bailes and McRitchie, 1978; Chapter 4). The allochthon comprises a zone of tectonic interleaving of ~1.9 Ga island arc and oceanic assemblages with 1.86–1.84 Ga metasedimentary rocks of the Kisseynew Domain, a former marginal basin (e.g. Zwanzig, 1990; Stern *et al.*, 1995a; Bailes and Galley, 1996; Connors, 1996; David *et al.*, 1996; Lucas *et al.*, 1996a, 1997; Chapter 4). The Snow Lake Allochthon structurally overlies the 1.92–1.88 Ga Amisk collage of juvenile island arc and oceanic assemblages to the west, structurally underlies migmatitic paragneisses and granitoids of the Kisseynew Domain to the north and east (Figs 5.1 and 5.2), and continues as the Clearwater Domain southward underneath the Phanerozoic

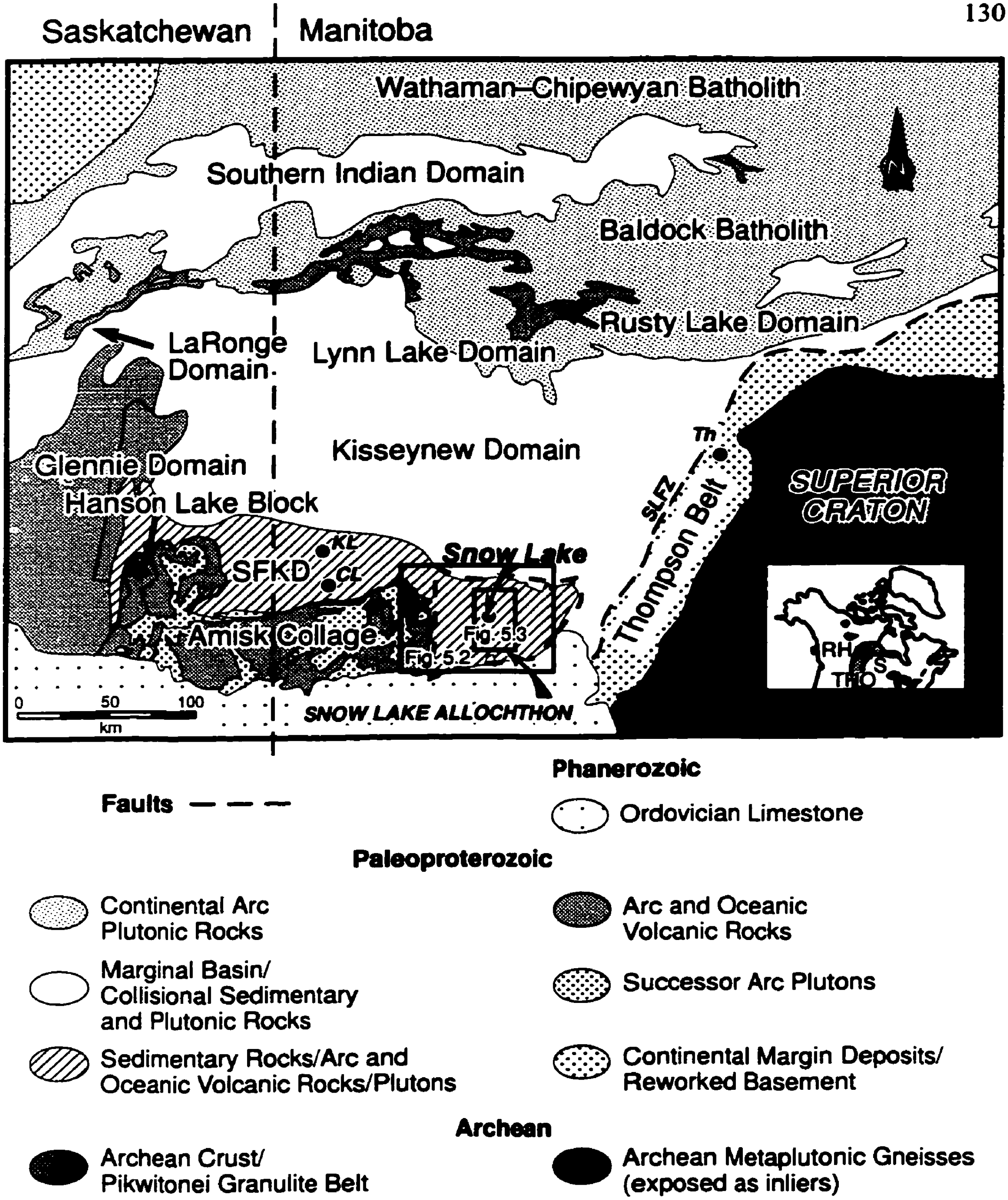

Figure 5.1 Lithotectonic domains of the Trans-Hudson Orogen (see inset map) and location of the Snow Lake Allochthon (within dashed border). After Hoffman (1988). SFKD, southern flank of the Kisseynew Domain; *CL*, Cleunion Lake; *KL*, Kississing Lake; *SLFZ*, Setting Lake fault zone; *Th*, Thompson; SFKD, southern flank of the Kisseyeynew Domain. Inset map: RH, Rae-Hearne craton; S, Superior craton; THO, Trans-Hudson Orogen.

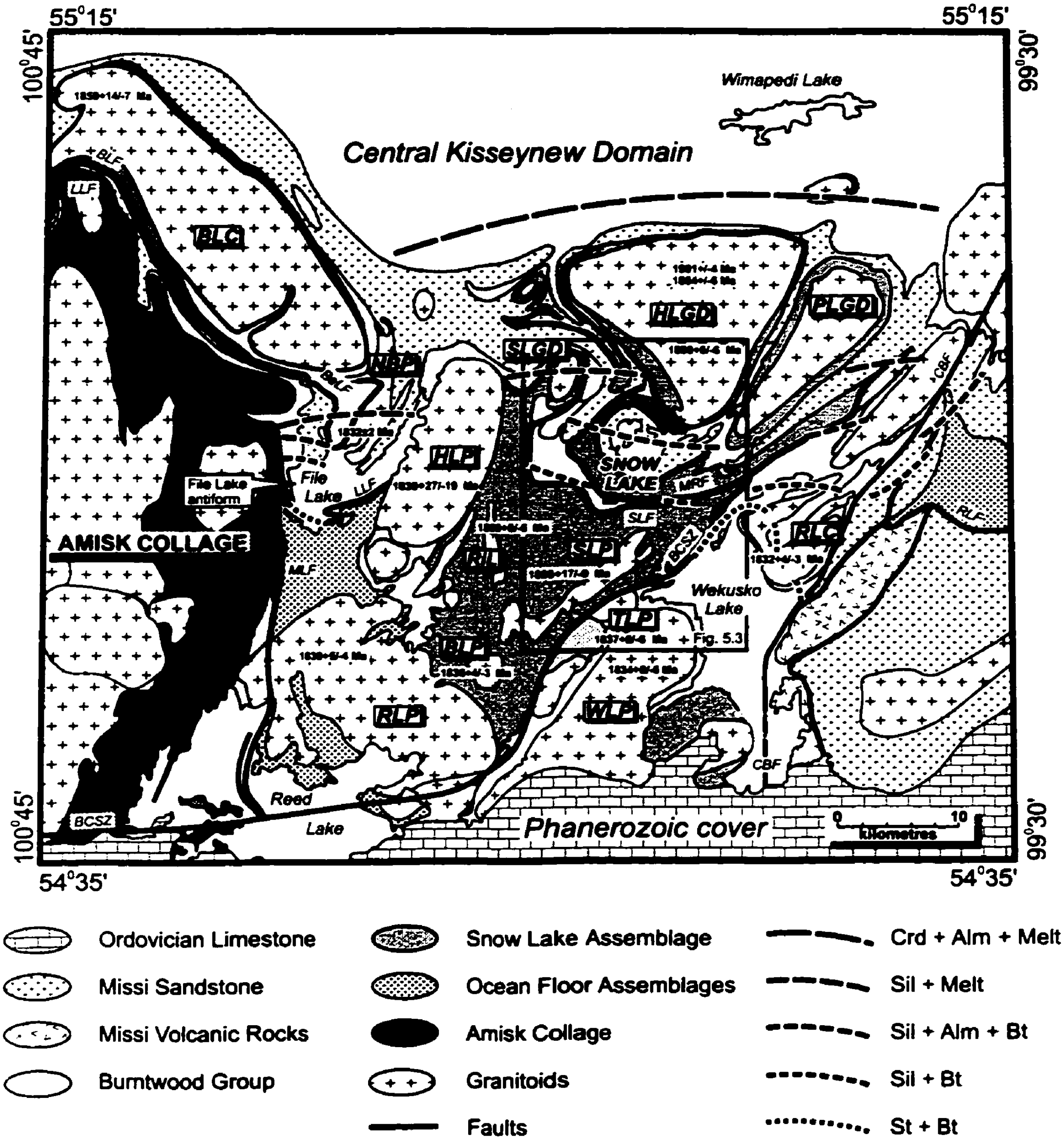

Figure 5.2 Geological map of the Snow Lake–File Lake–Wekusko Lake area, including isograds discussed in Chapter 4. Geochronological data refer to age of emplacement of granitic plutons (from Gordon *et al.*, 1990; Bailes *et al.*, 1991; David *et al.*, 1996). Faults: *BCSZ*, Berry Creek shear zone; *BLF*, Birch Lake fault; *BeLF*, Beltz Lake fault; *CBF*, Crowduck Bay fault; *LLF*, Loonhead Lake fault; *MLF*, Morton Lake fault; *MRF*, McLeod Road fault; *RLF*, Roberts Lake fault; *SLF*, Snow Lake fault. Plutons (P), plutonic complexes (C), and gneiss domes (GD): *BLC*, Batty Lake; *BLP*, Bujarski Lake; *HLGD*, Herblet Lake; *HLP*, Ham Lake; *NBP*, Nelson Bay; *PLGD*, Pulver Lake; *RLC*, Rex Lake; *RLP*, Reed Lake; *RiLP*, Richard Lake; *SLP*, Sneath Lake; *TLP*, Tramping Lake; *WLP*, Wekusko Lake.

cover (Stern *et al.*, 1995a; Connors, 1996; Lucas *et al.*, 1996a; Leclair *et al.*, 1997; Chapter 4). The inverted Kisseynew basin on the one hand and the Snow Lake Allochthon and the juvenile volcanic assemblages on the other are believed to constitute the middle and upper portions of a tectonic pile that overthrust Archean basement (Saskatchewan craton) (Bickford *et al.*, 1990; Ansdell *et al.*, 1995; Lucas *et al.*, 1996a). This basement is now exposed as inliers in the Glennie Domain and in the Hanson Lake Block (Fig. 5.1) (e.g. Ashton *et al.*, 1996, in press; Lucas *et al.*, 1996a; Chiarenzelli *et al.*, 1998;). The Snow Lake Allochthon, according to the interpreted LITHOPROBE seismic lines 2 and 3, is not underlain by Archean crust (Lucas *et al.*, 1993, 1996b; White *et al.*, 1994; Leclair *et al.*, 1997). The relationships between the allochthon and its footwall assemblages, however, cannot be resolved from the seismic reflection data and are thus unknown (e.g. White *et al.*, 1994, fig. 3). In this Chapter, I discuss the tectonometamorphic evolution of the Snow Lake Allochthon in the context of the evolution of the southeastern Trans-Hudson Orogen during final continent-continent collision.

REGIONAL GEOLOGY

Four tectonostratigraphic units are juxtaposed in the Snow Lake Allochthon: (1) Volcano-sedimentary rocks of the Snow Lake (arc) assemblage, (2) ocean floor assemblages, and the younger metasedimentary rock of the (3) Burntwood and (4) Missi groups (Figs 5.2 and 5.3). The Snow Lake assemblage comprises bimodal volcanic and associated

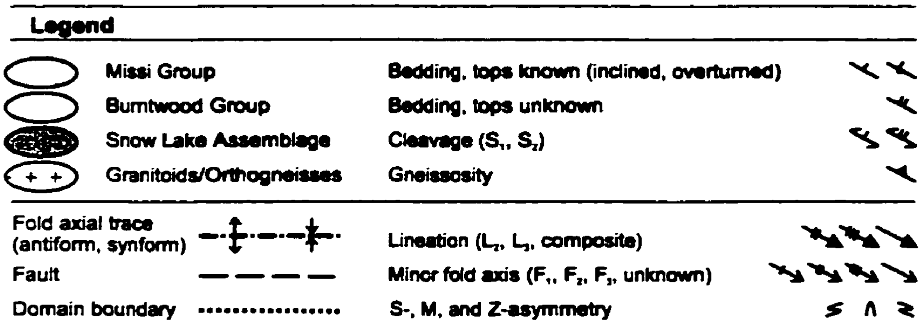

Figure 5.3 Geological map of the Threehouse synform in the Snow Lake area. The letters A–F refer to structural domains. *SL*, town of Snow Lake. ABA, Anderson Bay anticline; ABSZ, Anderson Bay shear zone; BSZ, Bartlett shear zone. For abbreviations of the granitoid plutons see Fig. 5.2. Some of the structural data plotted outside the structural domains are taken from Harrison (1949) and from Froese and Moore (1980).

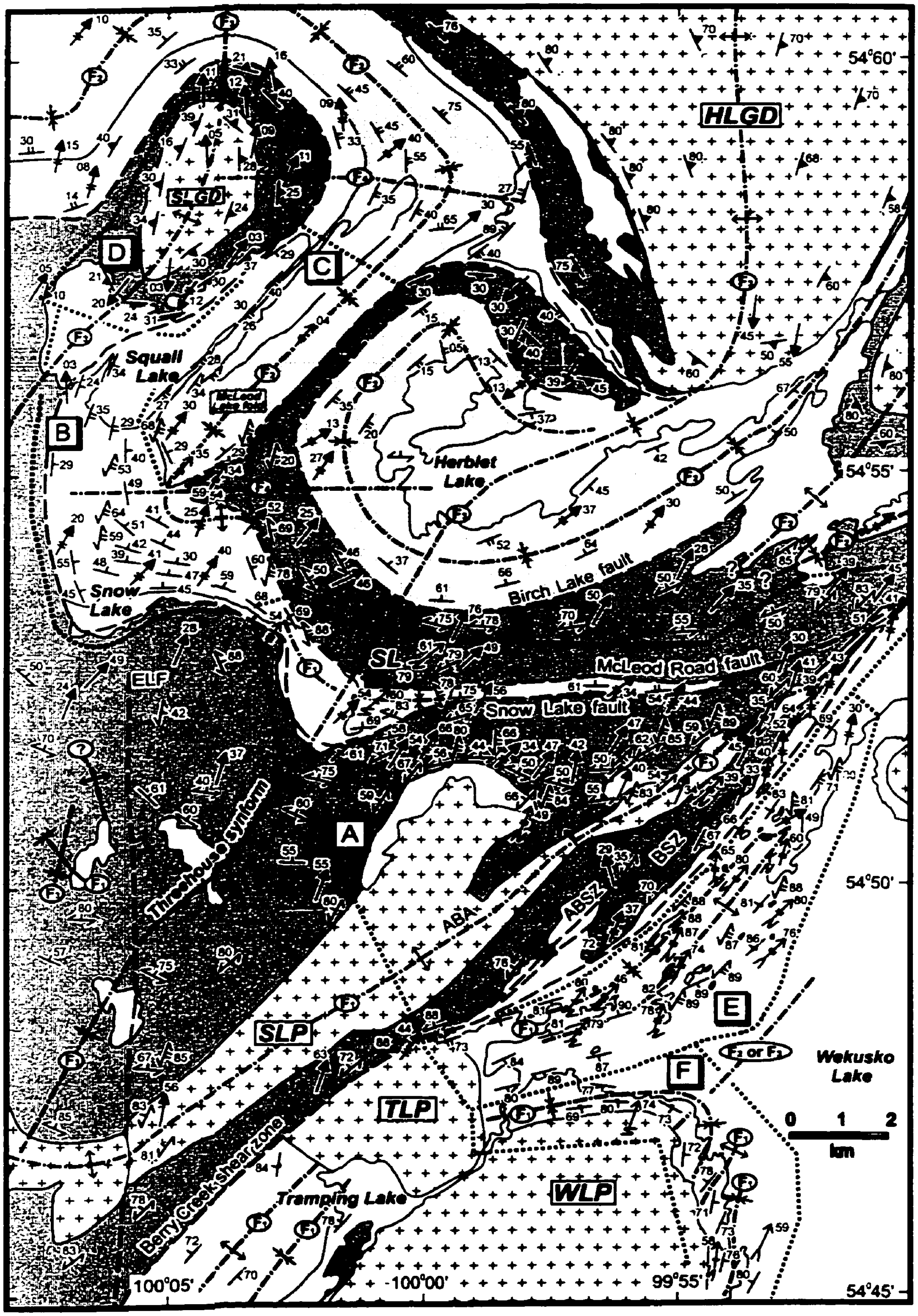
HLGD
SLGD
Squall Lake
McLeod Lake fault
Herblet Lake
Snow Lake
Birch Lake fault
SL
McLeod Road fault
Snow Lake fault
ELF
Threehouse synform
A
B
C
D
E
F
ABA
ABSZ
BSZ
SLP
TLP
WLP
Tramping Lake
Berry Creek shear zone
Wekusko Lake
F₂ or F₃
0 1 2
km
54°60'
54°55'
54°50'
54°45'
100°05'
-100°00'
99°55'

volcaniclastic rocks that host synvolcanic granitoids and gabbros (Figs 5.2 and 5.3) (Galley *et al.*, 1993; Stern *et al.*, 1995a; Bailes and Galley, 1996; David *et al.*, 1996). After metamorphism and polyphase deformation associated with the Hudsonian orogeny, most of the granitoids appear as gneiss domes (Fig. 5.2) (Bailes, 1975). Galley *et al.*, (1993) and Bailes and Galley (1996) established a >6 km thick volcanistratigraphic sequence, which shows upward maturing from primitive arc to evolved arc. This sequence is locally overlain by thin ocean floor basalt. Thicker ocean floor packages are exposed at Reed Lake and east of Wekusko Lake (Fig. 5.2) (Bailes, 1985; Syme *et al.*, 1995). Burntwood and Missi group rocks appear as folded slivers in the arc and ocean floor rocks (Figs 5.2 and 5.3). The Burntwood group comprises uniform, well-bedded greywacke turbidites that can be followed to the north and east, where they occupy the 300 by 150 km Kisseynew Domain (Fig. 5.1). The contemporaneous Missi group contains non-marine, crossbedded, arkosic metasandstones and conglomerates, and forms a rim along the boundary of the Kisseynew Domain (Figs 5.1 and 5.2). Missi-Burntwood contacts are not exposed in the study area (Fig. 5.3). They are, however, most likely transitional (see Syme *et al.*, 1995). Missi-arc assemblage contacts and Burntwood-arc assemblage contacts are, with minor exceptions, tectonic (Fig. 5.2). The tectonostratigraphic sequence is intruded by mafic sills and low angle dykes that contain an S_1 and hence predate F_1 compressional deformation. Voluminous calc-alkaline 1.84–1.83 Ga plutons truncate F_1 structures (Figs 5.2, 5.3 and 5.4a) (Gordon *et al.*, 1990; Bailes, 1992; Connors, 1996; David *et al.*, 1996). Their intrusion ages thus give an upper age limit for F_1. A suite of mafic to felsic volcanic rocks, which is of approximately the same age as the plutons, is exposed east of Wekusko Lake (Fig. 5.2)

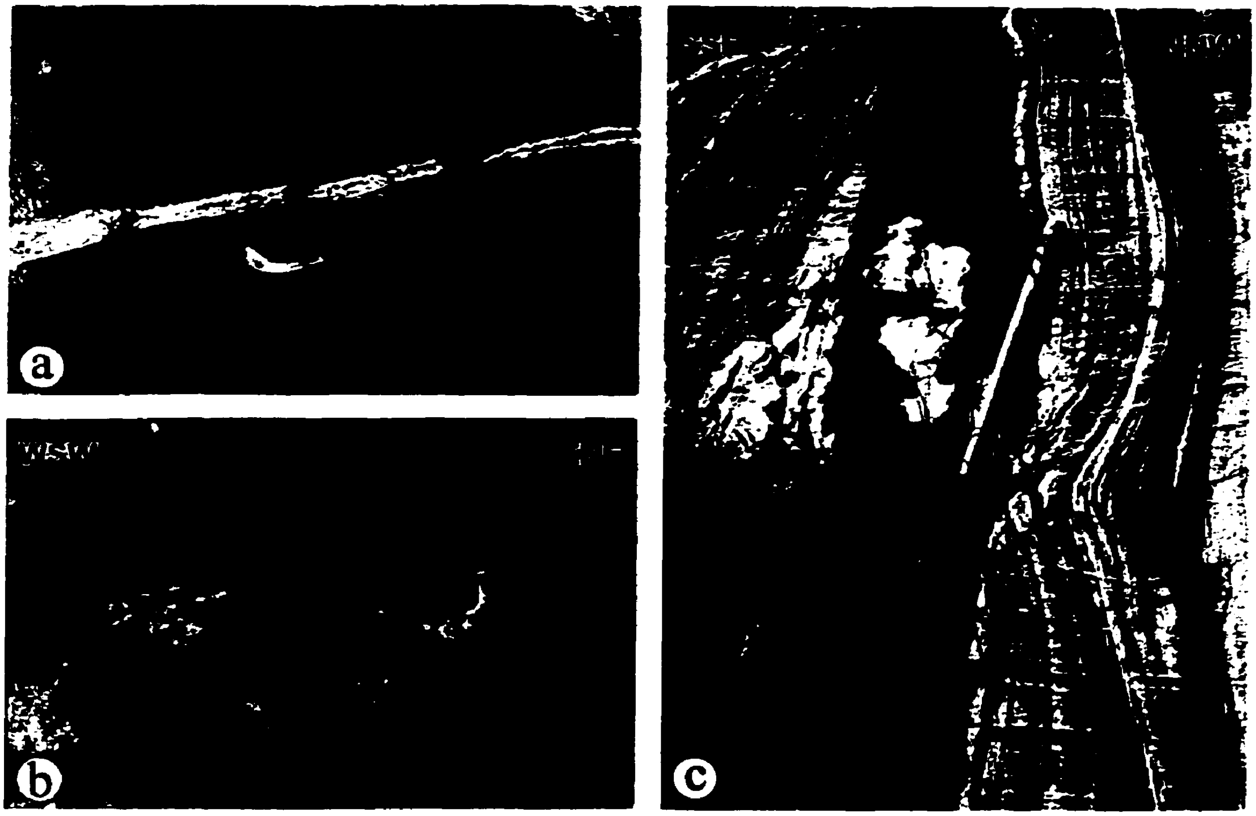

Figure 5.4 (a) F_1 fold crosscut by undeformed, local apophysis of the Wekusko Lake pluton, domain F. (b) and (c) F_1-boudinage in Snow Lake assemblage, domain A. The boudin necks are filled with quartz and felspar. (b) Boudinaged pre-F_1 sill exposed on horizontal surface. the boudin axis is steep. (c) Foliation boudinage exposed on steep surface. The boudin axis is shallow. See text for discussion.

(Gordon *et al.* , 1990; Ansdell, *et al.*, in press). One of the calc-alkaline plutons (Wekusko Lake pluton) is crosscut by east–west-trending posttectonic mafic dykes (Bailes, 1992). Large volumes of late kinematic to postkinematic granitic pegmatite have intruded the higher-grade portions of the Snow Lake Allochthon, the Kisseynew Domain, and its southern flank (Bailes, 1975, 1985; Zwanzig and Schledewitz, 1992; Kraus and Williams, 1994a; Norman *et al.*, 1995; Connors, 1996).

METAMORPHIC ZONES

Froese and Gasparrini (1975) divided the Snow Lake–File Lake area into metamorphic zones that are separated by reaction isograds (Fig. 5.2). These zones were extrapolated east towards the Superior collision zone (Thompson Belt) (Fig. 5.5; see references in Chapter 4). Temperatures at the thermal peak increase to the north in the Snow Lake-File Lake area, and to the north and east on the eastern side of Wekusko Lake, from < 400°C at Wekusko Lake to 750 ± 50°C in the Kisseynew Domain (Fig. 5.5) (e.g. Bailes, 1985; Gordon, 1989; Briggs and Foster, 1992; Leclair *et al.*, 1997; Marshall *et al.*, 1997; Menard and Gordon, 1997; Chapter 4). Metamorphic isotherms and isograds are hence approximately parallel to the Snow Lake Allochthon/Kisseynew Domain boundary (ibid.). The metamorphic field gradient (the P–T conditions along the presently exposed surface) is approximately isobaric; pressures associated with the thermal peak of metamorphism are 4–6 kbar in the Snow Lake–File Lake area and < 4 kbar east of Wekusko Lake (ibid).

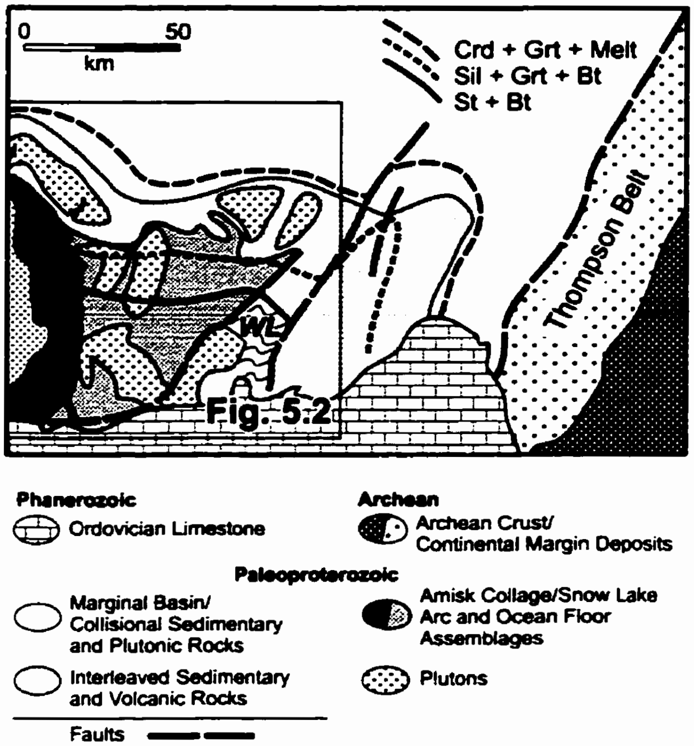

Figure 5.5 Metamorphic isograds of the Snow Lake Allochthon (after Gordon 1989). Mineral abbreviations after Kretz (1983). *WL*, Wekusko Lake.

DEFORMATION HISTORY

Deformation in the study area (Fig. 5.3) resulted in four different generations of folds (F_1–F_4) and associated faults related to at least three distinct kinematic frames. Associated metamorphism occurred in a single, regionally diachronous cycle (Table 5.1). Isoclinal F_1 and F_2 structures verge southerly and are refolded by north-northeast trending open F_3 folds with steep axial planes (Fig. 5.3). Steep east–west-trending F_4 structures are localised in and around the Squall Lake and Herblet Lake gneiss domes north of Snow Lake (Fig. 5.3). Primary layering dips, with exceptions, moderately to steeply northerly and easterly (Fig. 5.3). In large parts of the central Kisseynew Domain and on its southern flank (Fig. 5.1), isoclinal $F_{1/2}$ structures are also southerly verging, but their axial planes are relatively shallow (Zwanzig, 1990; Zwanzig and Schledewitz, 1992; Norman *et al.*, 1995). On the southern flank of the Kisseynew Domain, $F_{1/2}$ structures are steep only in the immediate vicinity of the more rigid Amisk collage footwall (ibid.). Compared with the Snow Lake Allochthon, structures in the Amisk collage are different in style, orientation, and age (Table 5.1) (e.g. Ansdell and Ryan, 1997; Ryan and Williams, in press). Deformation in the Amisk collage was mainly accommodated along steeply dipping shear zones, many of which predate Missi and Burntwood sedimentation (ibid.). A structural correlation between the Amisk collage and the Snow Lake Allochthon was attempted by Ryan and Williams (in press). Individual generations of structures in the Amisk collage and on the southern flank of the Kisseynew Domain were assigned to discrete deformation events based on the different kinematic frames in which these structures developed (Norman *et al.*, 1995; Ryan and Williams, in

Table 5.1. Summary of the tectonometamorphic history of the Snow Lake Allochthon.

Deformation		Structures	Magmatic events	Metamorphism	Age (Ga)	Tectonic setting
		—	Arc volcanism; synvolcanic intrusions (*Sneath Lake tonalite, Herblet Lake and Squall Lake granitoids*)	Synvolcanic fluid alteration (Hydrothermal activity)	1.892–1.886	Subduction of Archean crust
D_1 & D_2		—	Mafic dykes and sills		1.860–1.840	Sedimentation of Burntwood and Missi groups
D_3 (Hudsonian orogeny)	F_1	Isoclinal folds and low-angle shear zones; S_1 parallel to primary layering	Calc-alkaline granitoid suite (e.g. *Wekusko Lake pluton*); Missi volcanic suite	Prograde metamorphism: chl-grade, T < 400°C, P = 4 kbar	1.840–1.830	Overthrusting of K.D. over S.L.A. during N–S convergence; crustal thickening: 12–15 km
D_3 (Hudsonian orogeny)	F_2	Isoclinal curvilinear folds; regional S_2; low-angle shear zones and reactivation of F_1 shear zones		Thermal peak in st-zone and lower: T < 570°C, P = 4–6 kbar	1.820–1.810	Continued N–S convergence. Minor crustal thickening
D_4 (Hudsonian orogeny)	F_3	NNE-trending open to tight folds (*Threehouse synform*); crenulations of S_2		Cooling in st-zone; thermal peak in sil-zone and higher: T = 600–800°C, P = 5–6 kbar	1.810–1.805	E–W shortening: W-directed underthrusting of Superior plate
D_5 (Hudsonian orogeny)	F_4	Local WNW–ESE-trending folds; kink bands	Pegmatites in sil-zone and higher		1.800–1.765	Renewed N–S convergence; Exhumation during orogen-parallel movements
		Brittle features		Blocking temperatures of hbl and bt reached	1.765–1.745	Ongoing exhumation

press). Thus, structures, formed by a progressive strain in a constant kinematic frame, belong to a single deformation event. It is, however, problematic to apply the deformation-event concept to the Snow Lake Allochthon (cf. Connors, 1996), because there F_1 and F_2 structures, although they may have formed in the same kinematic frame, are separated by 15–35 Ma (David *et al.*, 1996). Conversely, overlapping geochronological ages (within error; see below) indicate that F_2, F_3, and possibly F_4 structures formed in successive, continuously changing kinematic frames during a single orogenic cycle rather than in discrete episodes. These changes in kinematic frames are related to the final collision of the internal Trans-Hudson Orogen with the Superior plate (see below). I therefore cautiously designate the structures to deformation events in Table 5.1, however, only for the purpose of correlation with adjacent areas.

F_1–F_4 STRUCTURES AND METAMORPHIC FABRICS

F_1

The Burntwood group rocks contained an S_0-parallel S_1 that was generally destroyed during the formation of an S_2 (Chapter 2). Where locally present, S_1 is defined, depending on metamorphic grade, by chlorite or muscovite aligned parallel to bedding. S_1 is also preserved as straight to curved inclusion trails in porphyroblasts of garnet, staurolite and biotite (see Chapters 2 and 4). An L_1 is only preserved in syn-F_1 bedding-parallel quartz veins; it is defined by stretched quartz aggregates, which plunge approximately parallel to minor fold axes. Three orders of F_1 folds appear in the Burntwood group, with amplitudes of centimetres to metres, tens to hundreds of metres, and kilometres (Fig. 5.3). Small F_1 folds are rare. When several small F_1 folds are exposed in one outcrop, they are variably flattened and have in common that bedding is markedly thicker in the hinge than in the limbs. Many of the small F_1 folds were dismembered by shearing along their limbs and/or axial planes so that a change in younging direction and, commonly, a set of quartz veins tracking the shear planes, are the only evidence of folding. Z- and S-asymmetrical folds and, locally, doubly verging fold pairs (*sensu* Holdsworth and Roberts, 1984) occur on the same limb of larger F_1 structures. All larger folds were also dismembered and hence have not preserved their asymmetry. F_1 features were not identified in the strongly recrystallised Missi group rocks.

In hydrothermally altered volcanic rocks that are now semi-pelitic chloritic schists, S_1 constitutes a fabric parallel to primary layering (where no S_2 is developed) and is defined by aligned chlorite. S_1 is also contained as straight inclusion trails in kyanite, staurolite, garnet, and biotite. These porphyroblasts are, however, not indicative of metamorphic grade (Zaleski *et al.*, 1991). In unaltered volcanic rocks, an S_1 schistosity parallel to primary layering is defined by aligned amphibole in the mafic rocks and by aligned biotite in the felsic rocks. Minor and intermediate F_1 folds are rare in the volcanic rocks and are developed mainly along lithological contacts. Younging criteria and consistently dextral S_0/S_2 and S_1/S_2 asymmetry (see below) suggest that the volcanistratigraphic sequence is possibly repeated between the Snow Lake "fault" and the Berry Creek shear zone across a crustal-scale F_1 anticlinal structure, termed the Anderson Bay anticline (Fig. 5.3) (Walford and Franklin, 1982). The sequence appears to be structurally thinned on the lower limb of this structure near the Berry Creek shear zone. In all rocks, the pre-F_1 mafic dykes/sills and the primary layering are boudinaged in two directions—parallel to and at a high angle to the the moderately to steeply northeasterly plunging lineation (see below)—yielding a chocolate-block pattern (Fig. 5.4b&c). S_1 is deflected around the boudins. S , where present, overprints the boudins.

F_1 shear zones

The Berry Creek shear zone and the Snow Lake–Loonhead Lake (ductile) reverse "fault", both of which juxtapose metasedimentary rocks and volcanic rocks (Figs 5.2, 5.3 and 5.6), were active during F_1. Northeastwards, along the northwestern margin of Wekusko Lake (north of the Tramping Lake pluton; Fig. 5.3), the Berry Creek shear zone becomes part of an anastomosing system, which includes the poorly exposed Anderson Bay and Bartlett shear zones (Figs 5.3 and 5.6). F_1 movement along the Berry Creek shear zone resulted in a less than 100 m wide zone of moderately to steeply northwesterly dipping felsic to mafic tectonites that contain northeasterly plunging stretched clasts (Fig. 5.7a) with aspect ratios of at least 25 : 11.5 : 1. The approximate parallelism of stretched clasts and regional F_1-F_3 fold axes suggests that F_1 transport along the shear zone was toward the southwest, but only if the clasts were not significantly reoriented after F_1. Burntwood group rocks adjacent to the shear zone are relatively weakly strained and young away from it (Fig. 5.3).

The Snow Lake fault constitutes the southern termination of the isoclinally folded

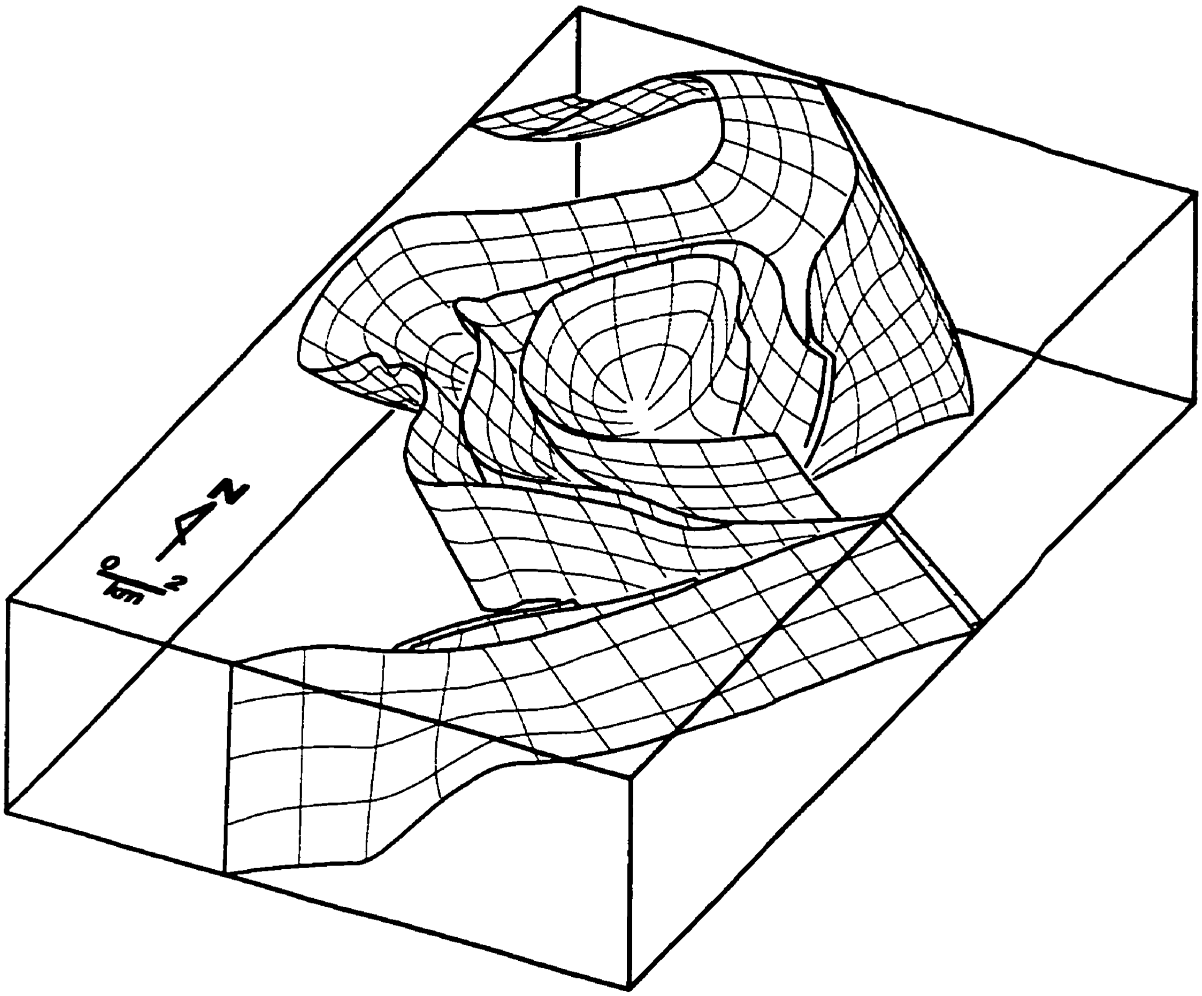

Figure 5.6 Block diagram showing the "fault" and shear-zone surfaces of the Snow Lake area.

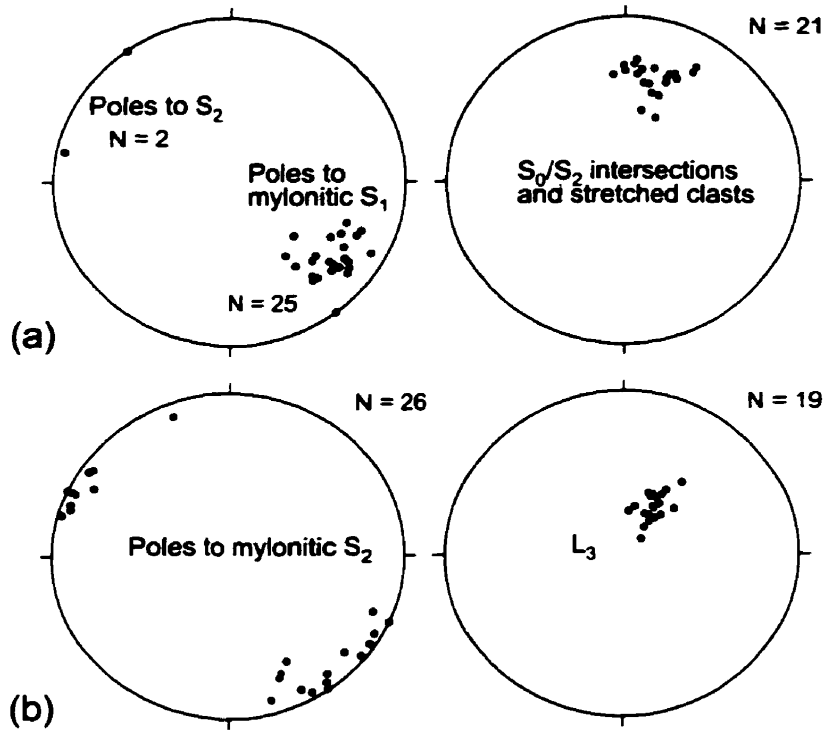

Figure 5.7 Equal-area projections (lower hemisphere, Schmidt net) of structural data for the Berry Creek shear zone (Fig. 5.3). (a) Northwest Wekusko Lake segment. (b) Tramping Lake pluton segment.

Burntwood group sliver at Snow Lake (Figs 5.2, 5.3 and 5.6; see Chapter 2). It extends as the Loonhead Lake fault to the west through the File Lake area where it appears to form the boundary between the Amisk collage and the southern flank of the Kisseynew Domain (Zwanzig and Schledwitz, 1992; Connors, 1996). The Snow Lake fault is cut off in the east by the younger McLeod Road (ductile reverse) "fault". At Snow Lake, the Snow Lake fault is inferred from a local variation in strikes of the rocks in the hanging wall (Burntwood group) relative to the rocks in the adjacent footwall (arc and minor ocean floor rocks), and from abundant quartz–carbonate brecciation. Clasts in metabasalts of the immediate footwall show a high degree of stretching parallel to their northeasterly plunge. The Snow Lake fault is cross-cut by an undeformed, syn- to post-peak metamorphic pegmatite at the southern end of Squall Lake and by the ~1.830 Ga post-F_1 Ham Lake pluton northeast of File Lake (Fig. 5.2) (Connors, 1996; David *et al.*, 1996). South of the town of Snow Lake (Fig. 5.3), the fault cuts off an F_1 syncline in the Burtnwood group at a low angle. The early fault movement is thus constrained to have occurred after the initiation of F_1 folding.

F_2

An S_2 crenulation cleavage or schistosity, which envelops porphyroblasts, is ubiquitous in the metasedimentary rocks and in the hydrothermally altered volcanic rocks (Figs 5.8a–d) (Menard and Gordon, 1997; Chapters 2 and 4). Growth of the porphyroblasts in the Snow Lake Allochthon commenced, independent of final metamorphic grade, in the early stages of F_2 (ibid.). Depending on metamorphic grade, the S_2 septa in the Burntwood

Figure 5.8 (a) Z-asymmetrical F_2 fold with refracted axial-plane S_2 in Burntwood group; domain E. Note the S_2-parallel quartz veins that developed in response to S_2-parallel slip (see Kraus and Williams 1998). Pencil tip on the upper right for scale. (b) L_2 crenulation lineation on S_0 tightened around grains of staurolite; Burntwood group in domain B. (c) S_1 overgrown by kyanite and folded by a Z-asymmetrical F_2; hydrothermally-altered pillow basalt in domain A. An axial-plane S_2 is well developed. (d) Photomicrograph of basal sections of ferroan-pargasitic hornblende porphyroblasts (determined with microprobe) aligned parallel to S_2 in mafic volcanic rock, overprinting the F_1 Berry creek shear zone on northwestern Wekusko Lake. View is down the northeasterly plunge of the hornblende c-axes, which are parallel to the composite $L_{1/2}$ (see Fig. 5.7a). The porphyroblast-matrix relationship suggests that, in analogy to the Burntwood turbidites at Snow Lake town, growth of these porphyroblasts, and thus the local thermal peak of metamorphism, coincided with the development of S_2 (see Chapter 2). Long edge of photomicrograph is 3.7 mm. (e) Gneissosity enveloping garnet in highly-metamorphosed felsic volcanic rock, domain D. (f) Sheath fold in Burntwood group rocks in the McLeod Road fault zone; domain B. View is down the northeast-plunging stretching lineation.

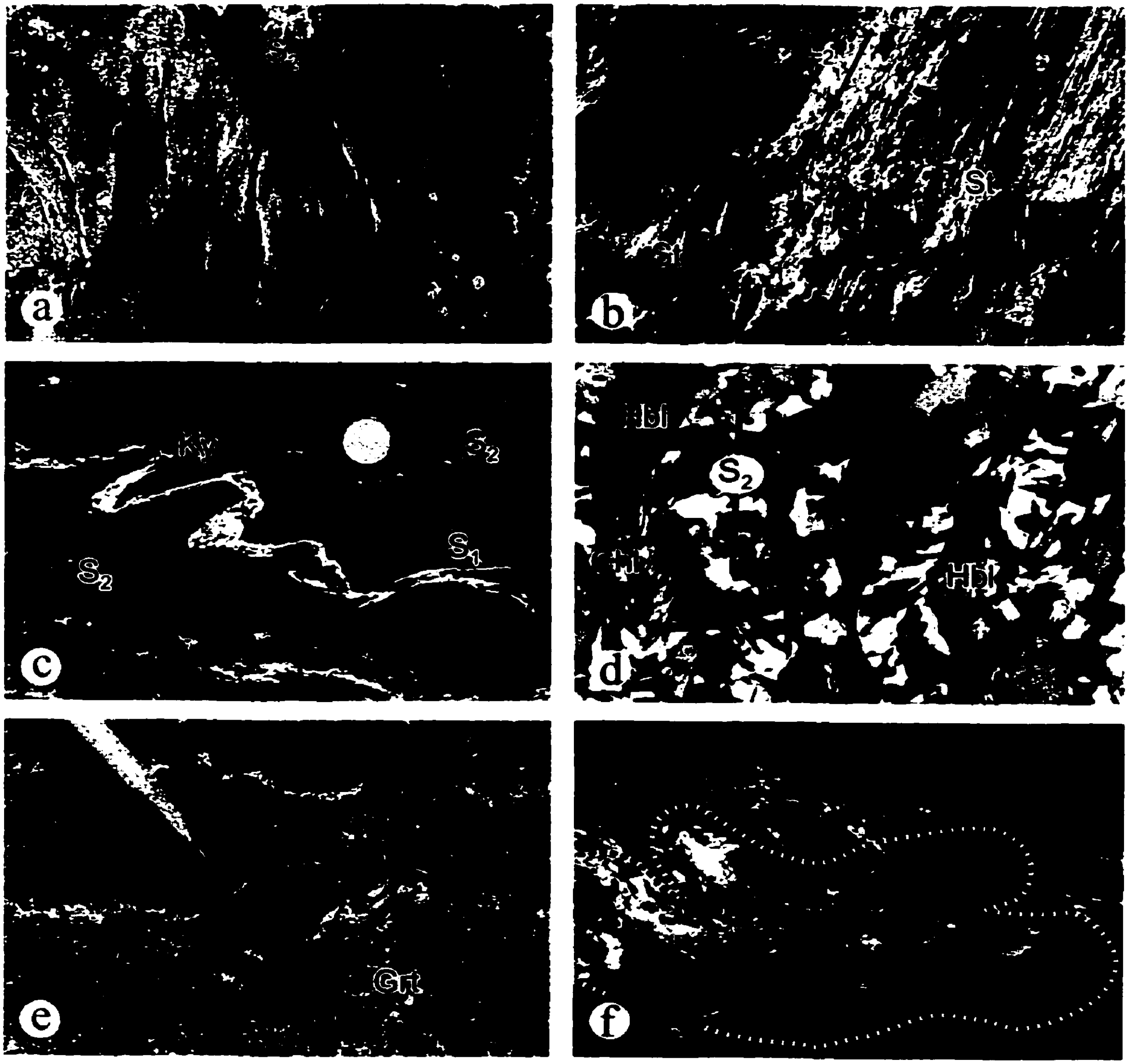
a
b
St
Ky
S_2
S_1
S_2
c
Hbl
S_2
Hbl
d
Grt
e
f

group rocks are defined by muscovite and/or chlorite. Garnet and biotite grains occupy the microlithons, and the biotites are crystallographically and dimensionally aligned parallel to S_2. Many biotite grains are pulled apart, the stretching directions being parallel and at a high angle to the moderately to steeply northeasterly plunging fold axes and S_0/S_2 lineation. Locally, the porphyroblasts have pressure shadows parallel to S_2 at a high angle to the northeasterly plunging F_2 fold axes and S_0/S_2 intersection lineation; these pressure shadows developed early during F_2 folding (Chapter 2). Quartz veins that formed during the subsequent stages of F_2 folding are ubiquitous (Fig. 5.8a). These veins, which are broadly parallel to S_2, locally cut across peak metamorphic staurolite and are crenulated by F_3 (Chapter 2). In Missi group rocks and weakly altered rhyolite, S_2 is defined by dimensionally oriented biotite. In fluid-altered volcanic rocks at Anderson Lake (Fig. 5.3), S_1 is overgrown by kyanite and staurolite porphyroblasts, and both are folded into dm-scale asymmetrical folds, which have an axial-plane domainal S_2 cleavage (Fig. 5.8c). S_2 is, in general, only developed in volcanic rocks that contain phyllosilicates, where the phyllosilicates define the S_2 septa (Fig. 5.8d). In contrast, within the granitic gneiss domes and in the surrounding high-grade rocks, S_2 constitutes a gneissosity that is parallel to lithological contacts and that wraps around garnet grains (Fig. 5.8e). A composite $L_{1/2}$ in all volcanic rocks is defined by stretched quartz aggregates, elongate amygdales and clasts, rods, aligned grains of amphibole, kyanite, staurolite, and disk-shaped garnets (Fig. 5.8d). Where S_2 is present, $L_{1/2}$ is parallel to the S_0/S_2 intersection. Minor F_2 folds are generally rare and are flattened to a lesser degree than F_1 structures; such folds are mainly Z-asymmetrical and have a well-developed axial-plane S_2 (Fig. 5.8a & c). One large F_2 structure, the curvilinear

McLeod Lake fold, has been identified (Fig. 5.3). It is cored by Missi sandstones that young towards the axial plane and appears to be laterally continuous from Snow Lake to File Lake (see Connors, 1996). The significance of this structure is discussed below.

F_2 shear zones

The McLeod Road "fault" and the Birch Lake "fault" are major parallel structures with arcuate traces curved more than 180°, due to F_3 and F_4 refolding (see below) (Figs 5.3 and 5.6). Between Snow Lake and Squall Lake, the moderately northerly to easterly dipping McLeod Road fault cuts up-section across the axial plane of the McLeod Lake fold (Figs 5.3 and 5.9). The McLeod Road fault hence postdates initial stages of F_2 folding. Basalt in the immediate hanging wall is impregnated with synkinematic carbonate in zones 20 cm to several metres wide. The carbonate is strongly foliated and contains transposed minor folds with axes parallel to the stretching lineation, plunging moderately to the northeast (Fig. 5.9). The shear zone fabric in the hanging wall anastomoses around porphyroblasts and lenticular low-strain domains of dm-scale. In the footwall, high strain is concentrated in dm-wide zones containing northeasterly plunging sheath folds, up to 20 m beneath the contact (Fig. 5.8f). Fault-related folds in the hanging wall and footwall overprint peak-metamorphic porphyroblasts. The direction of movement along the McLeod Road fault is thus approximately southwesterly and this direction is roughly preserved after polyphase deformation (see below) and is interpreted as being to the south–southwest. Evidence for the preservation of the transport direction is the approximate parallelism of the local,

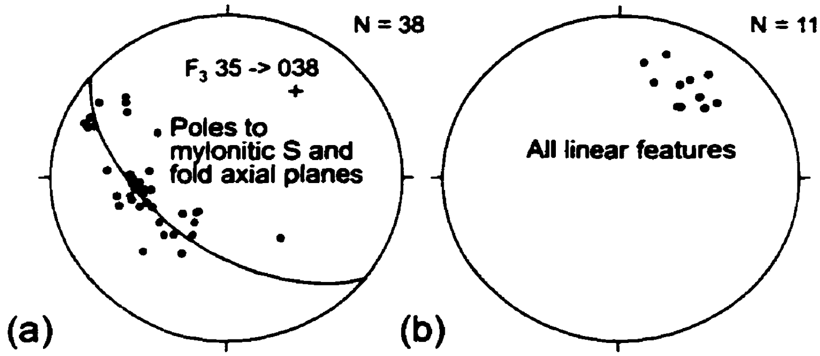

Figure 5.9 Equal-area projections (lower hemisphere, Schmidt net) of structural data for the McLeod Road fault zone in domain B (Fig. 5.3).

northeasterly plunging stretching lineation with the F_1–F_3 linear features in the core of the Threehouse synform at Snow Lake (Fig. 5.9). Thus, the local F_4 overprinting is weak here (see below).

The poorly defined Birch Lake fault defines a >5 m wide zone of ductile deformation, exposed only in the core of the Threehouse synform. Here, the moderately northeast-dipping shear zone foliation contains an amphibole lineation, which plunges down-dip. Volcanic rocks in the footwall dip generally more steeply (65–85°) than rocks in the fault zone and in the hanging wall (40–65°). The relatively shallow dips in the hanging wall extend across Herblet Lake (Fig. 5.3). The Birch Lake fault thus appears, like the McLeod Road fault, to dismember a large F_2 fold, but be folded by the Threehouse synform. Both faults are therefore interpreted as contemporaneous.

The Snow Lake fault and the Berry Creek shear zone were reactivated during F_2. The F_2 manifestation of the Berry Creek shear zone truncates the 1837 +8/-6 Ma (David *et al.*, 1996), post-F_1 Tramping Lake pluton (Figs 5.3 and 5.7b). The transition from undeformed to a subvertical ultramylonitic foliation at the granite margin is only a few centimetres wide. The width of the F_2 deformation zone is indeterminate owing to lack of outcrop, but is in excess of 30 cm. Ultramylonitic portions mainly comprise fine-grained, dynamically recrystallised quartz and feldspar. The quartz, however, is granoblastic due to later static recrystallisation. Shear bands indicate a southerly transport. Subsidiary centimetre- to decimetre-wide steeply dipping ductile shears parallel to the main structure are developed within the otherwise unfoliated pluton. Sericite-rich domains in the subvertical S_2 mylonitic foliation at the pluton margin are crenulated by F_3 and these contain a faint, steep northeasterly plunging L_3 crenulation lineation (Fig. 5.7b). The latest movement along the shear zone system is manifest by pseudotachylyte, which, in one location, cuts across the mylonitic fabric of the Anderson Bay shear zone (Fig. 5.3) and is deflected, indicating a sinistral component of movement.

The northeastern segment of the Berry Creek shear zone (discussed above), on the other hand, was not reactivated during F_2. It is overprinted by the regional S_2 that envelops peak metamorphic porphyroblasts containing S_1, by the L_2 crenulation lineation, by small Z-asymmetrical F_2 folds, and by small symmetrical F_3 folds (Figs 5.7a and 5.8d). L_2 plunges parallel to the clasts stretched during F_1 (Fig. 5.7a). Calculated P-T estimates of ~550°C at 4.1 kbar on both sides of the structure also suggest no major post-peak metamorphic offset (Chapter 4). The local F_2 manifestation of the Berry Creek shear zone appears to run offshore in Wekusko Lake within the Burntwood group metaturbidites, as indicated by linear geoelectrical anomalies (Hudson Bay Mining and Smelting, unpublished data). The segment of the Berry Creek shear zone exposed in the study area is, as a whole, openly folded by F_3, causing its trace to be sinusoidal (Fig. 5.3).

Evidence of F_2 movement along the Snow Lake fault is given by a reversal in S_0/S_2 asymmetry across the structure from sinistral in the northern hanging wall (see Chapter 2) to dextral in the southern footwall. Younging is to the north on both sides of the structure. The dextral S_0/S_2 asymmetry and a corresponding Z-asymmetry of minor F_2 folds remain constant across the inferred F_1 Anderson Bay anticline and in outcrops on Wekusko Lake. This implies that the Snow Lake fault dismembered a major F_2 fold.

F_3 and F_4

F_3 produced polyharmonic folds at all scales throughout the Snow Lake–Reed Lake areas. The largest structure appears to be the Reed Lake fold (Syme *et al.*, 1995), which contains the File Lake antiform and the Threehouse synform (Figs 5.2 and 5.3). These large folds are symmetrical. The Threehouse synform encloses open F_3 folds a few hundreds of metres in scale that are generally discontinuous along their axial planes. Rare minor F_3 folds are open to tight and overprint S_2, trails of peak metamorphic porphyroblasts, and their F_2 pressure shadows (Fig. 5.10a). F_3 crenulations of S_2 are developed locally around the Threehouse synform, where S_2 is at low angles to bedding. These crenulations deform S_2-parallel quartz veins and pressure shadows on staurolite and biotite (see Chapter 2). Pervasive S_3 is only developed in low-grade rocks of the Burntwood group at Reed Lake (Syme *et al.*, 1995).

Approximately east–west-trending F_4 folds overprint F_3 structures, giving rise to dome and basin to mushroom interference structures (Figs 5.2 and 5.3). The variations in the geometry of the interference patterns arise from a regional variation in the orientations of primary layering prior to F_4 folding. F_4 folds occur only locally in approximately north–south-trending domains such as the west limb of the Threehouse synform. Here, no cleavage is associated with the F_4 structures, but Connors (1996) report a local S_4 in F_4 fold hinges north of File Lake. In unfavourably oriented domains, for example on the eastern Threehouse limb, biotites in fluid-altered volcanic rocks, aligned with their (001) faces along a north-northeasterly trending moderate to steep S_2, are kinked. Similarly, conjugate kink

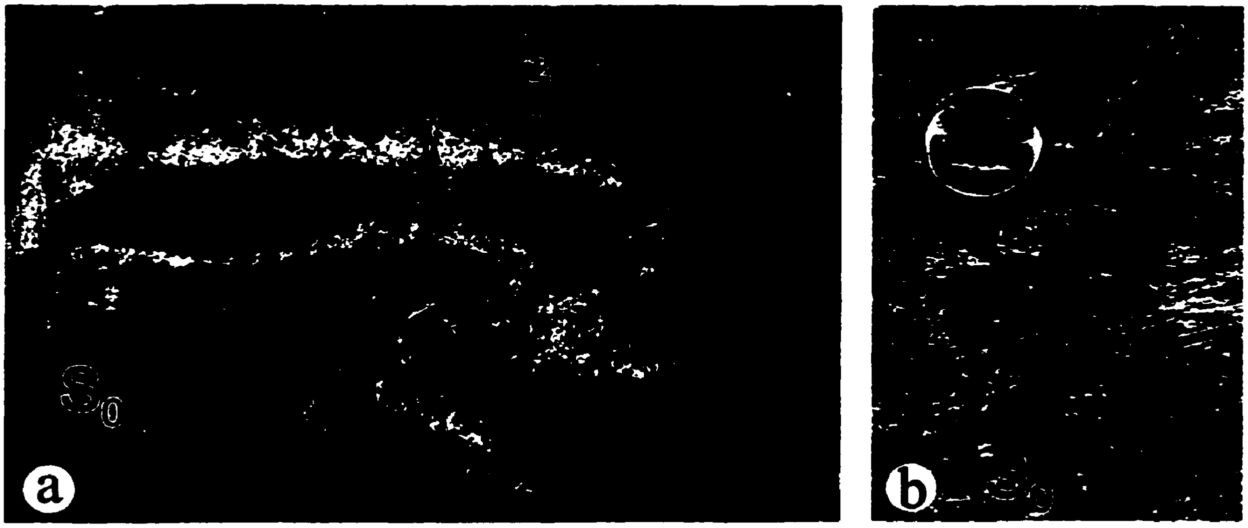

Figure 5.10 Zoned calc-silicate boudin and crosscutting S_2, both overprinted by F_3 fold; Burntwood Group in domain A. Note the opposite asymmetry of S_2 and F_3 with respect to S_0. Pencil in the lower left for scale. (b) F_4 kink band overprinting S_2; Burntwood Group in domain E.

bands in north-northeasterly trending steep S_2 occur on the islands of northwest Wekusko Lake (Fig. 5.10b).

STRUCTURAL DOMAINS

Six structural domains (A–F) are distinguished in the study area based on the orientation of F_1–F_3 structural elements (Fig. 5.3). Domain A (Fig. 5.3) essentially coincides with the staurolite + biotite zone. It is characterised by coaxial F_1–F_3 structures and by coplanar F_1 and F_2 structures (Fig. 5.11). F_1–F_3 fold axes and all other linear features plunge into the northeast quadrant. The poles to the moderately to steeply dipping S_0, S_2, and the axial planes of F_3 crenulations plot on approximately the same great circle. This great-circle girdle dips to the south-southwest and is perpendicular to the local axis of the F_3 Threehouse synform. Similar geometrical relationships apply to large portions of the Kisseynew Domain, where the great-circle girdles are slightly steeper (Bailes, 1975; Zwanzig, 1990). Domain B (Fig. 5.3) is transitional between A and C and contains the axial plane of the F_2 McLeod Lake fold and the McLeod Road fault. Both structures are overprinted by F_3 and F_4. In domain B, all planar elements plot approximately on a great circle that dips to the southwest (Fig. 5.12), less steeply than the girdle in domain A, owing to local F_4 refolding of the axial plane of the F_2 fold about a steep axis. The pole to this girdle is parallel to the local F_2 and F_3 axes and coincides with the southwesterly transport direction along the McLeod Road fault (see above; Fig. 5.9). Domain C (Fig. 5.3) contains a segment of the

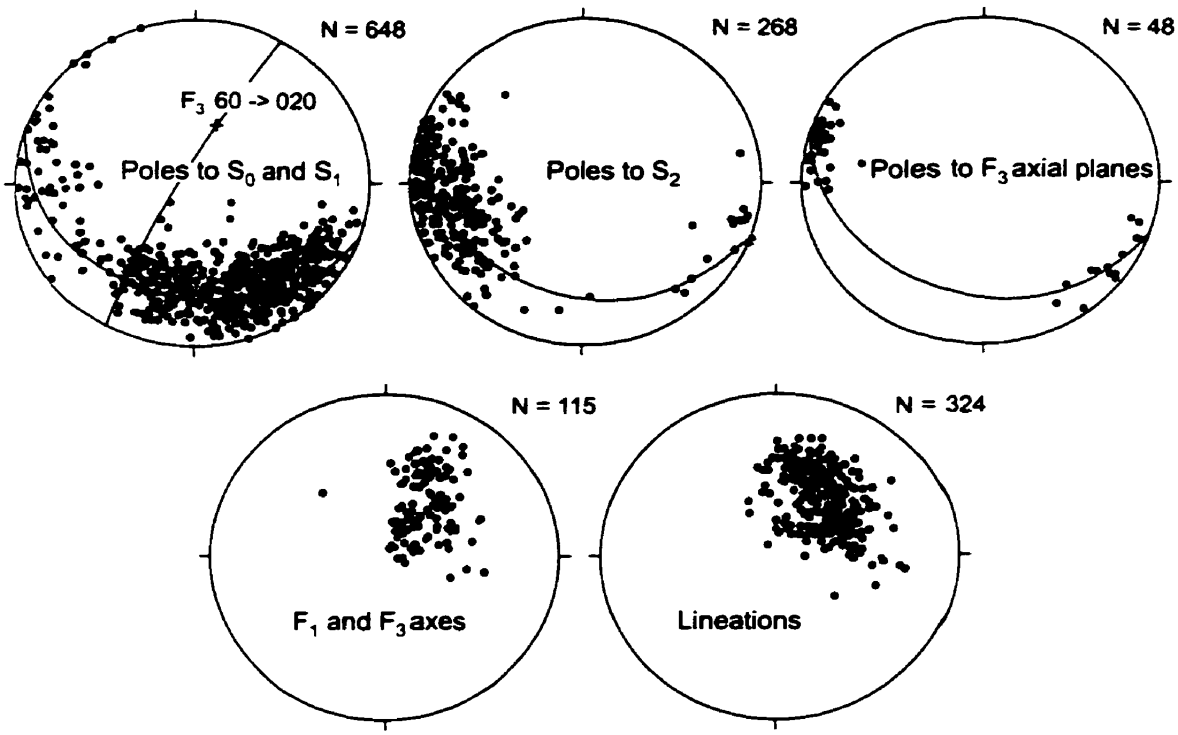

Figure 5.11 (a) Equal-area projections (lower hemisphere, Schmidt net) of structural data for domain A (Fig. 5.3).

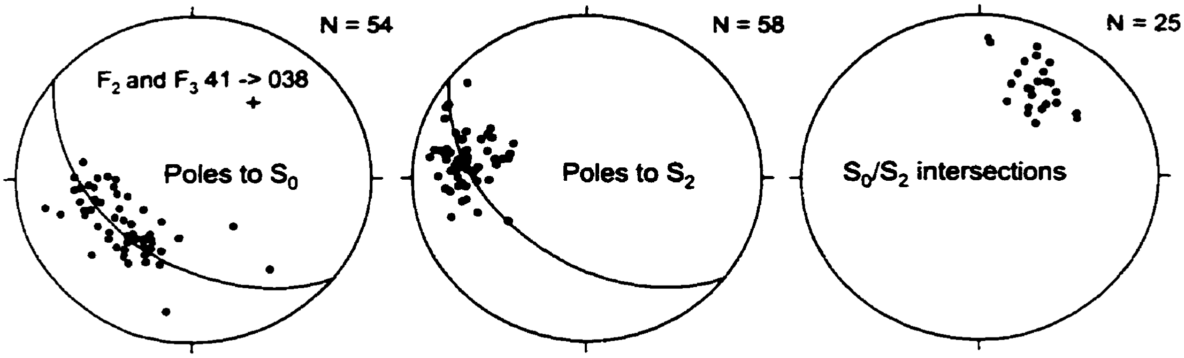

Figure 5.12 Equal-area projections (lower hemisphere, Schmidt net) of structural data for domain B (Fig. 5.3).

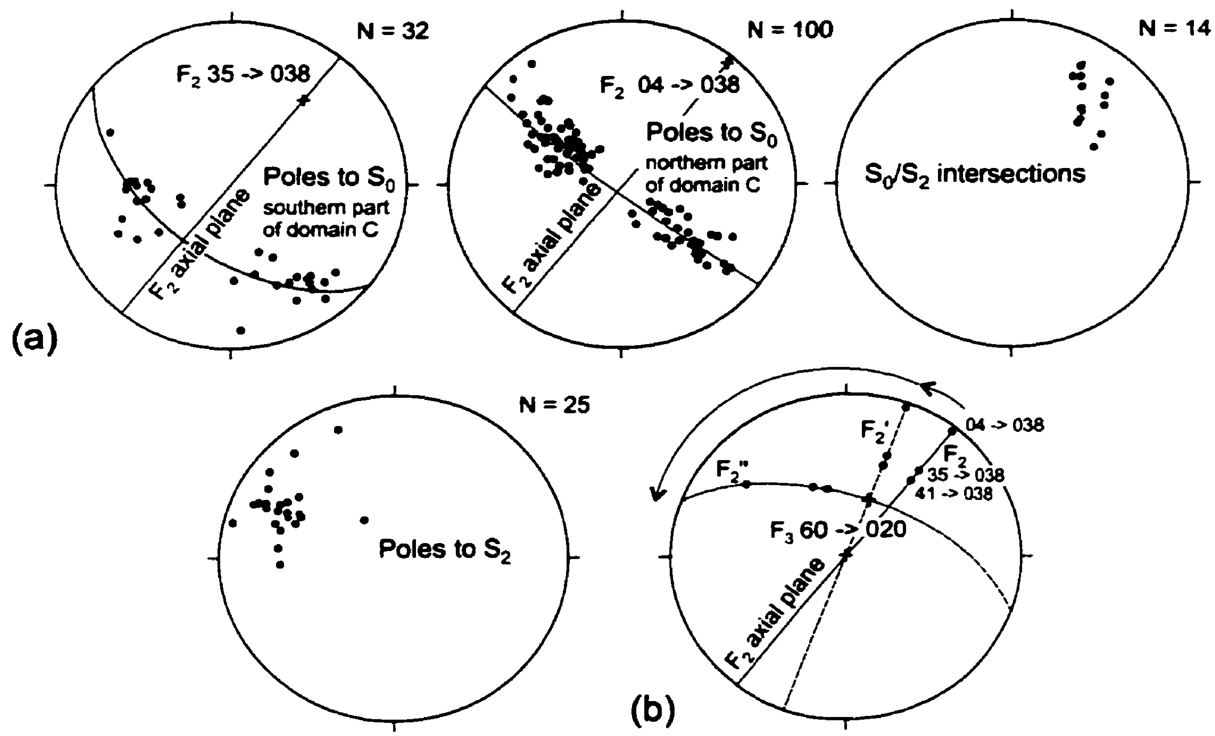

Figure 5.13 (a) Equal-area projections (lower hemisphere, Schmidt net) of structural data for domain C (Fig. 5.3). (b) Schematic unfolding of the McLeod Road fold. The local fold hinge segments for domains B and C (taken from Figs 12 and 13a) plot on a steep northeasterly-trending great circle that coincides with the axial plane of the McLeod Lake fold in domain C. Variation in plunge angles of the individual hinge segments reveals the curvilinear character of the structure. Unfolding procedure: The effects of F_3 and F_4 are removed by rotating the axial plane of the McLeod Lake fold first 18° anticlockwise around a steep F_4 axis into position F_2' (in which the axial plane contains the F_3 Threehouse synform axis), and subsequently 90° anticlockwise around the F_3 Threehouse synform axis into position F_2''.

McLeod Lake fold in Missi group metasandstones that young towards the axial plane (Fig. 5.13). In the hinge area along the Missi-Burntwood boundary, poles to S_0 yield a moderately northeasterly plunging major F_2 axis (southern part of domain C in Fig. 5.13a). The fold hinge is approximately horizontal in the northern part of domain C (Fig. 5.13a). Domain D (Fig. 5.3) hosts the Squall Lake gneiss dome, a culmination within an F_3-F_4 dome and basin interference structure (Fig. 5.14). The gneissosity in granitic orthogneiss dips gently towards the margins of the dome. A shallow mineral lineation appears to track a smoothly curved north-northeast to south-southwest F_3 axis. Domain E (Fig. 5.3) defines a steep belt exposed on islands in northwestern Wekusko Lake (Fig. 5.15). The variations in S_0 trend result from large-scale open F_3 refolding. Linear features are steeper than in domains A and B, but they also plunge into the northeast quadrant. Domain F (Fig. 5.3) comprises steeply dipping Burntwood group rocks around the Wekusko Lake pluton (Fig. 5.16). The pluton occupies the core of a large northeast-closing F_2 or F_3 fold, which overprints a series of refolded F_1 folds. Minor northerly plunging F_1 fold axes are frequent in the southern part of domain F.

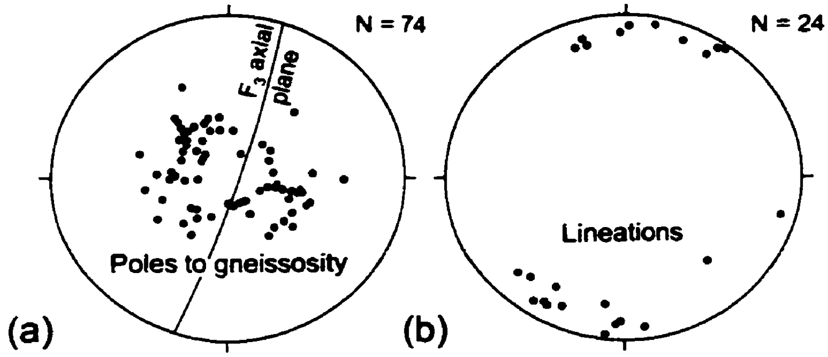

Figure 5.14 Equal-area projections (lower hemisphere, Schmidt net) of structural data for domain D (Fig. 5.3).

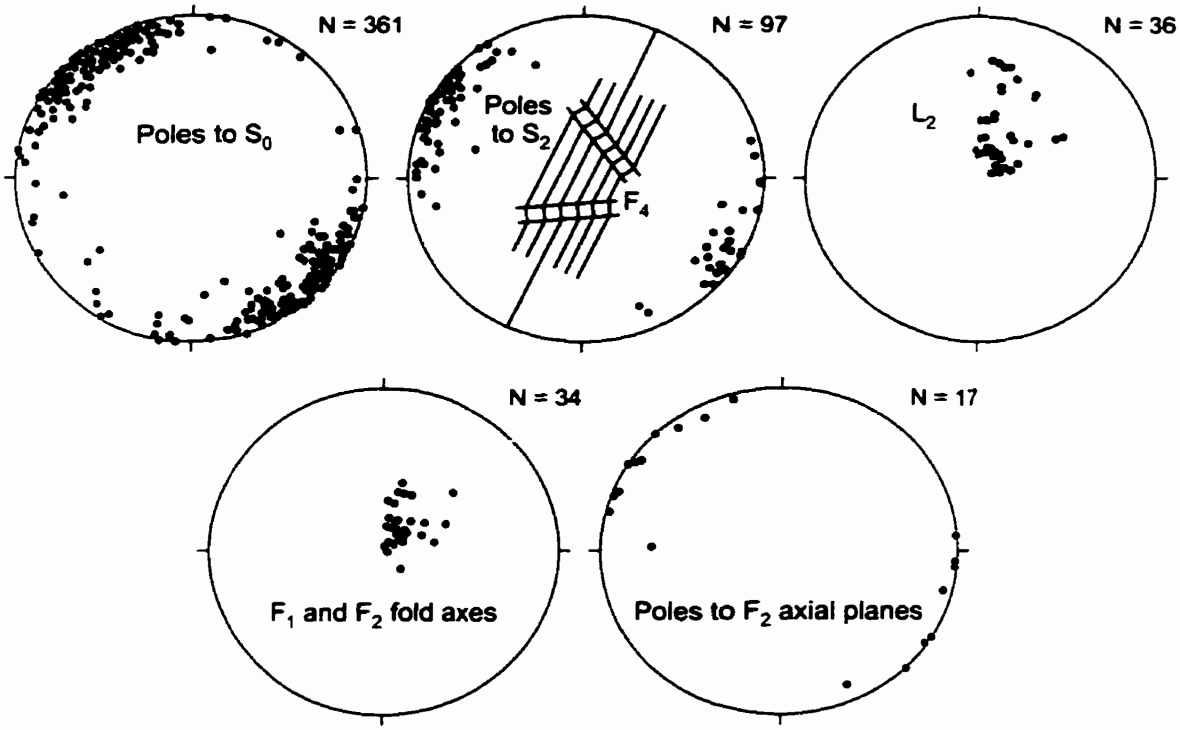

Figure 5.15 Equal-area projections (lower hemisphere, Schmidt net) of structural data for domain E (Fig. 5.3).

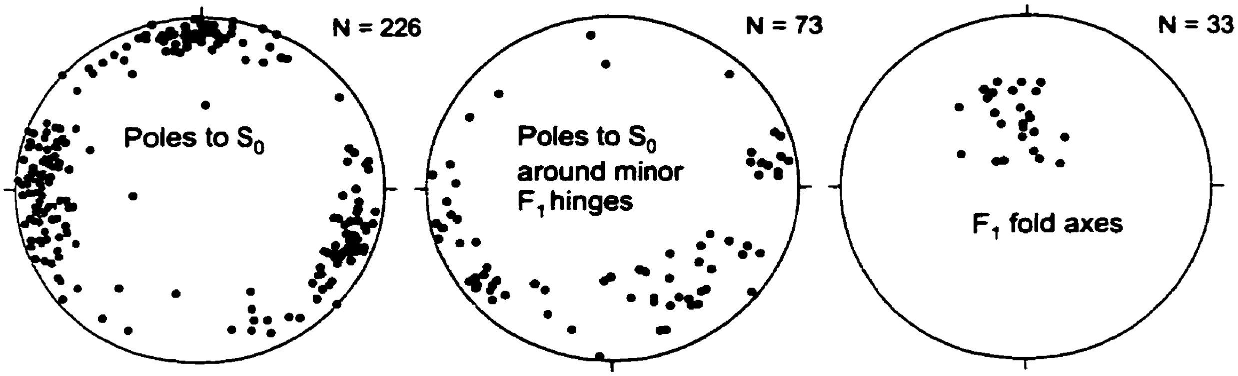

Figure 5.16 Equal-area projections (lower hemisphere, Schmidt net) of structural data for domain F (Fig. 5.3).

DISCUSSION OF DEFORMATION

The McLeod Lake fold—a sheath fold?

Although the hinge of the F_2 McLeod Lake fold is dismembered by the McLeod Road fault in parts of domain B and in domain A (Fig. 5.17), the hypothetical local orientation of the major F_2 axis can be estimated by assuming parallelism of the hinge with the S_0/S_2 lineation. This information is important for the reconstruction of the McLeod Lake fold prior to overprinting. In its present refolded state, the McLeod Lake fold changes its character from a synform in domain C to an antiform in domains B and A (Fig. 5.3), the hinge being curved through ~60°. In the northern part of domain C (Fig. 5.13a), the hinge is subhorizontal and becomes progressively steeper northeasterly plunging in the southern part (Fig. 5.13a) and through domains B and A (Figs 5.11 and 5.12).

In an attempt to reconstruct the original geometry and attitude of the F_2 McLeod Lake fold, I restore its orientation prior to F_3 and F_4 refolding assuming an initial south to southwest vergence, as reported for F_2 structures from the southern flank of the Kisseynew Domain (Fig. 5.1) (Zwanzig and Schledewitz, 1992; Norman *et al.*, 1995; Zwanzig, in press). The unfolding procedure is described in Fig. 5.13b. After unfolding, the F_2 axial plane dips moderately to the north-northeast, and the local hinge segments plunge moderately west-northwest to steeply north-northeast (Fig. 5.13b). Similar orientations of F_2 axial planes and F_2 fold axes in the Cleunion Lake–Kississing Lake area were interpreted as being evidence for a local southerly tectonic transport (Norman *et al.*, 1995). Thus, if there is any validity

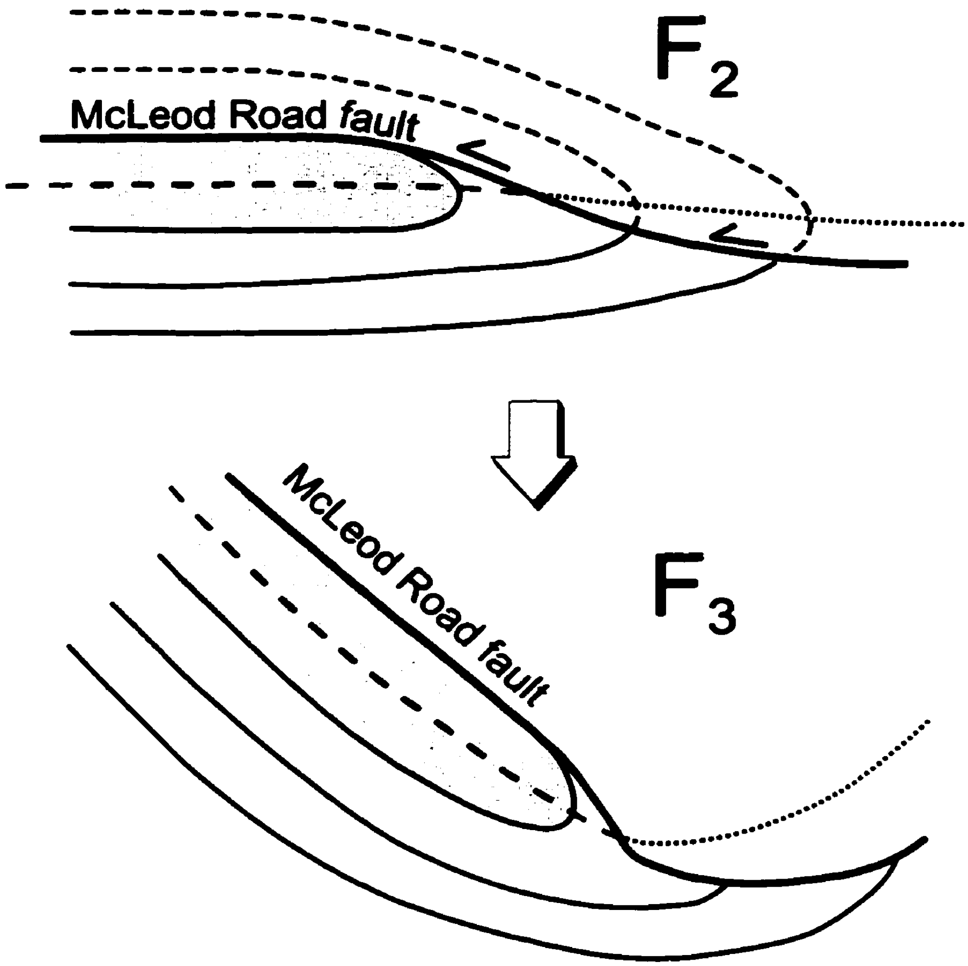

Figure 5.17 Schematic illustration of the sequence of the dismemberment of the regional-scale McLeod Road fold by the McLeod Road fault during F_2. Subsequent refolding during F_3 (and F_4) led to the map-scale pattern in domains B and C (Fig. 5.3). The shaded area refers to the Missi group. See text for discussion.

in this simple unfolding procedure, the McLeod Lake fold was a south to southwest-verging, synformal, curvilinear structure, and possibly a sheath fold. It is similar in geometry and attitude to the large F_2 structures on the southern flank of the Kisseynew Domain (e.g. Zwanzig and Schledewitz, 1992; Zwanzig, in press).

Parallelism of linear features

Except in domains C and D, the axes of the isoclinal F_1 and F_2 folds are broadly parallel to the axes of the open F_3 folds and their azimuth approximately coincides with the inferred southerly tectonic transport. This fold-axis distribution is very similar in large portions of the Kisseynew Domain (Bailes, 1975; Zwanzig, 1990). Coaxiality of earlier tight structures with later open structures has been reported from many orogenic belts (e.g. Knill and Knill, 1958; Bryant and Reed, 1969; Escher and Watterson, 1974; Skjernaa, 1980; Meneilly and Storey, 1986; Norman *et al.*, 1995). In those cases, parallelism of the early fold axes was attributed to progressive rotation of the fold hinges towards the direction of tectonic transport in a constant kinematic frame, associated with high shear strains ($\gamma > \sim 10$) (ibid.). The occurrence of sheath folds is regarded as evidence that this process has operated (Williams and Zwart, 1977). The lack of sheath folds, however, does not exclude this possibility (Williams and Compagnoni, 1983; Mawer and Williams, 1991; Norman *et al.*, 1995). I believe that, in the study area, the near-parallelism of the linear $F_{1/2}$ features and also the chocolate-block boudinage pattern (see above) were achieved by rotation in response to shearing. Boudins that formed by stretching in a direction parallel to the lineation were linear features and were, as straining continued, rotated and further boudinaged in the same way as the fold hinges. F_3 straining, however, was too low to account for the rotation of the axes of the late open folds into parallelism with the axes of the earlier isoclinal folds in a constant kinematic frame, since there is generally a direct relationship between fold tightness and fold axis orientation (Mawer and Williams, 1991). Hence, the isoclinal $F_{1/2}$ and the open F_3 folds must have developed in different kinematic frames. The contrasting vergence and degrees of tightness of $F_{1/2}$ and F_3 structures is good evidence that this was the case. There are three possible ways for the open F_3 folds to have formed, and they all have in common that the orientation of the F_3 axes was controlled by the linear anisotropy developed during the earlier folding (Cobbold and Watkinson, 1981; Watkinson and Cobbold, 1981): (1) The tectonostratigraphic packages were deformed merely by approximately east–west shortening so that the deformation path was coaxial. (2) Flow continued to be southerly directed during F_3, and a component of approximately east–west shortening was superimposed so that the non-coaxial deformation path became constrictional (cf. Meneilly and Storey, 1986). (3) The large F_3 folds simply resulted from draping of the foliation around the previous linear anisotropy and around the large plutons during southerly flow. The third scenario does not involve shortening perpendicular to the axial plane, but it requires that the F_2 and F_3 folds formed simultaneously. I eliminate possibility (3), however, based on the different mineral assemblages and thus the different metamorphic grades associated with F_2 and F_3 (Menard and Gordon, 1997; see Chapter 4). Possibility (2) cannot be ruled out, but it is not likely, as there are no shear sense indicators for southerly flow and no L_3 stretching lineation parallel to the F_3 axes. Further, the tectonostratigraphic packages were already moderately to steeply dipping prior to F_3 (see below), and their attitude therefore inhibited large-scale tectonic transport. The low strains associated with F_3 and the orthorhombic symmetry of the large F_3 folds suggest a bulk coaxial strain path, and thus model (1) is most realistic.

AGES OF DEFORMATION AND METAMORPHISM

U–Pb geochronology of zircon, monazite, and titanite yielded ages of ~1.820–1.805 Ga, which are inferred to date the thermal peak of metamorphism in the southern Trans-Hudson Orogen, including the Thompson Belt (e.g. Gordon, 1989; Gordon *et al.*, 1990; Machado *et al.*, 1990; Ansdell and Norman, 1995, and references therein; Bleeker *et al.*, 1995; David *et al.*, 1996, and references therein). A thermal anomaly, interpreted as the product of prolonged, extensive granitoid intrusion in the Kisseynew Domain was the source of high-grade metamorphism at moderate pressures in the Kisseynew Domain, its southern flank, and the northern and eastern portions of the Snow Lake Allochthon (Bailes, 1975, 1985; Bailes and McRitchie, 1978; Gordon, 1989; Menard and Gordon, 1997; see Chapter 4). The anomaly, which resulted in rapid, possibly isobaric heating from ~550–600°C to ~750–800°C, developed either late-F_2 or post-F_2, and outlasted F_3 (Menard and Gordon, 1997; see Chapter 4). In contrast, rocks metamorphosed not higher than staurolite grade ($T_{max} \leq 580$°C) in the area south of Snow Lake were not affected by the thermal anomaly; these rocks reached metamorphic peak conditions early during F_2 and show evidence of cooling during F_3 (Menard and Gordon, 1997; see Chapters 2 and 4). Titanite in rhyolite from Anderson Lake (T_{max}= ~550°C at 5 kbar) yielded an age of 1812 ± 5 Ma, interpreted as dating the local syn-F_2 peak of metamorphism (Fig. 5.3) (Zaleski *et al.*, 1991; David *et al.*, 1996). Zircon overgrowths in samples from the Herblet Lake gneiss dome (T_{max} = 700–800°C at 5–6 kbar; Menard and Gordon, 1997) yielded interpreted syn-peak metamorphic ages of 1807 ± 7 Ma, 1807 ± 3 Ma, and 1803 ± 2 Ma (David *et al.*, 1996). By comparison, monazite ages interpreted to date the cooling of ~1815 Ma Kisseynew Domain granitoids are 1806 ± 2 Ma and 1804 ± 2 Ma (Gordon, 1989; Gordon *et al.*, 1990). Titanite grains in gneisses from the southern flank of the Kisseynew Domain near Sherridon (T_{max} = 660°C at 5 kbar; Froese and Goetz, 1981) yielded interpreted cooling ages of 1808±2 Ma, 1804±3 Ma and 1805±5 Ma (Fig. 5.1) (Ashton *et al.*, 1992). In summary, the ~1.805 Ga ages date the onset of cooling in the high-grade rocks and thus give a minimum age for F_3.

Late kinematic to postkinematic pegmatites with interpreted crystallisation ages of ~1.805–1.760 Ga are widespread in the high-grade rocks of the southern Trans-Hudson Orogen (e.g. Ashton *et al.*, 1992; Hunt and Zwanzig, 1993; Ansdell and Norman, 1995; Parent *et al.*, 1995; Chiarenzelli *et al.*, 1998). Undated pegmatites north of File Lake were interpreted to be broadly coeval with F_4 (Connors, 1996). The majority of the ages obtained for deformed pegmatites scatter around 1.800–1.790 Ga. Some of the older ages may reflect inheritance of near-peak metamorphic monazites (Parent *et al.*, 1995). Although speculative, it is possible that F_4 followed F_3 within a few million years.

Hornblende and biotite in Missi group rocks from near the eastern shore of Wekusko Lake (Fig. 5.2) yielded minimum cooling ages between 1764 ± 11 Ma and 1747 ± 11 Ma (Marshall *et al.*, 1997), consistent with cooling ages in the Amisk collage (Hunt and

Roddick, 1992, 1993; Fedorowich *et al.*, 1995). It appears that initial cooling during uplift was slow, possibly owing to the intrusion of pegmatites and associated hot fluids. Cooling rates increased rapidly once this activity had ceased.

STRUCTURAL FEATURES BETWEEN WEKUSKO LAKE AND THE SETTING LAKE FAULT ZONE

In the Snow Lake Allochthon east of Wekusko Lake (Fig. 5.5), isoclinal F_1 and F_2 structures verge northwesterly and are coplanar with tight to isoclinal F_3 structures (Connors *et al.*, in press). The F_3 folds are generally tighter than the F_3 folds west of Wekusko Lake (Bailes, 1985; Connors *et al.*, in press). Steep F_3 shear zones (e.g. Crowduck Bay "fault"; Connors *et al.*, in press; Fig. 5.2), some of which may be re-activated $F_{1/2}$ thrusts, trend approximately parallel to the large F_1-F_3 fold hinges and they also parallel the Setting Lake fault zone, which is the boundary between the internal and the external Trans-Hudson Orogen (Fig. 5.1) (Bailes, 1985; Bleeker, 1990a, and references therein; Connors *et al.*, in press). A moderately north-dipping structure (Roberts Lake "fault"; Connors *et al.*, in press; Fig. 5.2) was interpreted as a late, south-verging thrust (Connors *et al.*, in press). In the part of the Kisseynew Domain that is sandwiched between the Snow Lake Allochthon and the Thompson Belt (Fig. 5.1) (hereafter referred to as "southeastern Kisseynew Domain"), the axial planes of large, steep S-asymmetrical (? F_4) folds are overturned in the same way as the axial planes of F_3 folds within the Thompson belt, indicating a component of sinistral shear with respect to the boundary of the Thompson Belt (Bailes, 1985; Bleeker, 1990a).

STRUCTURAL CORRELATION OF THE SNOW LAKE ALLOCHTHON AND THE THOMPSON BELT

The thermal peak of metamorphism in the Thompson Belt of the external Trans-Hudson Orogen outlasted the local F_2 and was broadly coeval with the thermal peak of metamorphism in the internal zone of the orogen (Bleeker, 1990a; Machado *et al.*, 1990; Bleeker and Macek, 1996). Two granites, believed to be associated with the thermal peak of metamorphism, were dated at 1822 ± 3 Ma (zircon) and 1805 ± 2 Ma (monazite), and a paleosome from the Thompson open pit (Fig. 5.1) yielded 1809 ±14 Ma (zircon) (Machado *et al.*, 1990; Bleeker *et al.*, 1995). F_3 folds formed at the inception of widespread pegmatite intrusion and associated retrogressive fluid activity spanning ~1.786–1.765 Ga. The Setting Lake fault zone was active during approximately the same time interval (Lewry, 1981; Green 1985; Bleeker, 1990a; Machado *et al.*, 1990; Machado and David, 1992; Bleeker *et al.*, 1995; Bleeker and Macek, 1996). It thus appears that the F_3 and F_4 structures in the Snow Lake Allochthon were broadly coeval with the F_2 and F_3 structures in the Thompson Belt.

AN EVOLUTIONARY MODEL FOR THE SOUTHEASTERN TRANS-HUDSON OROGEN

The Snow Lake arc assemblage originated as an outboard accretionary complex during continental convergence (Stern *et al.*, 1995a; David *et al.*, 1996). Contamination with Archean crust suggests that the arc was built on continental crust (rifted fragment or subsided margin of the Superior plate?) (Stern *et al.*, 1995a). Alternatively, the arc was built on oceanic crust, providing that magma generation involved melting of continental sediments on the subducting slab. Burntwood group turbidites, derived from the eroding arc and from the Archean continental margins, were deposited at 1.86-1.84 Ga on oceanic crust in the marginal Kisseynew basin (Ansdell *et al.*, 1995; Machado and Zwanzig, 1995; David *et al.*, 1996). Coevally, Missi group sediments were deposited in fluvial-alluvial fans at the basin margin and, locally, on the Amisk collage (Stauffer, 1990; Lucas *et al.*, 1996a). The ~1.84-177 Ga Hudsonian orogeny resulted from the final collision of the Amisk collage, Snow Lake Allochthon, and the Kisseynew basin with the Archean Saskatchewan and Superior cratons (Fig. 5.1) (e.g. Lewry, 1981; Bickford *et al.*, 1990; Bleeker, 1990a; Ansdell *et al.*, 1995; Lucas *et al.*, 1997). During the final closure of the "Manikewan" ocean (see Chapter 1), thick, internally deformed, ductile F_1 nappes derived from the collapsing Kisseynew basin formed a tapering thrust wedge. The sedimentary nappes were emplaced along shallow structures (Snow Lake fault, Berry Creek shear zone) onto and interleaved with arc and ocean floor rocks, causing 12-15 km of crustal thickening (Fig. 5.18a) (see Chapter 4, and references therein). The nappe pile was intruded by calc-alkaline plutons

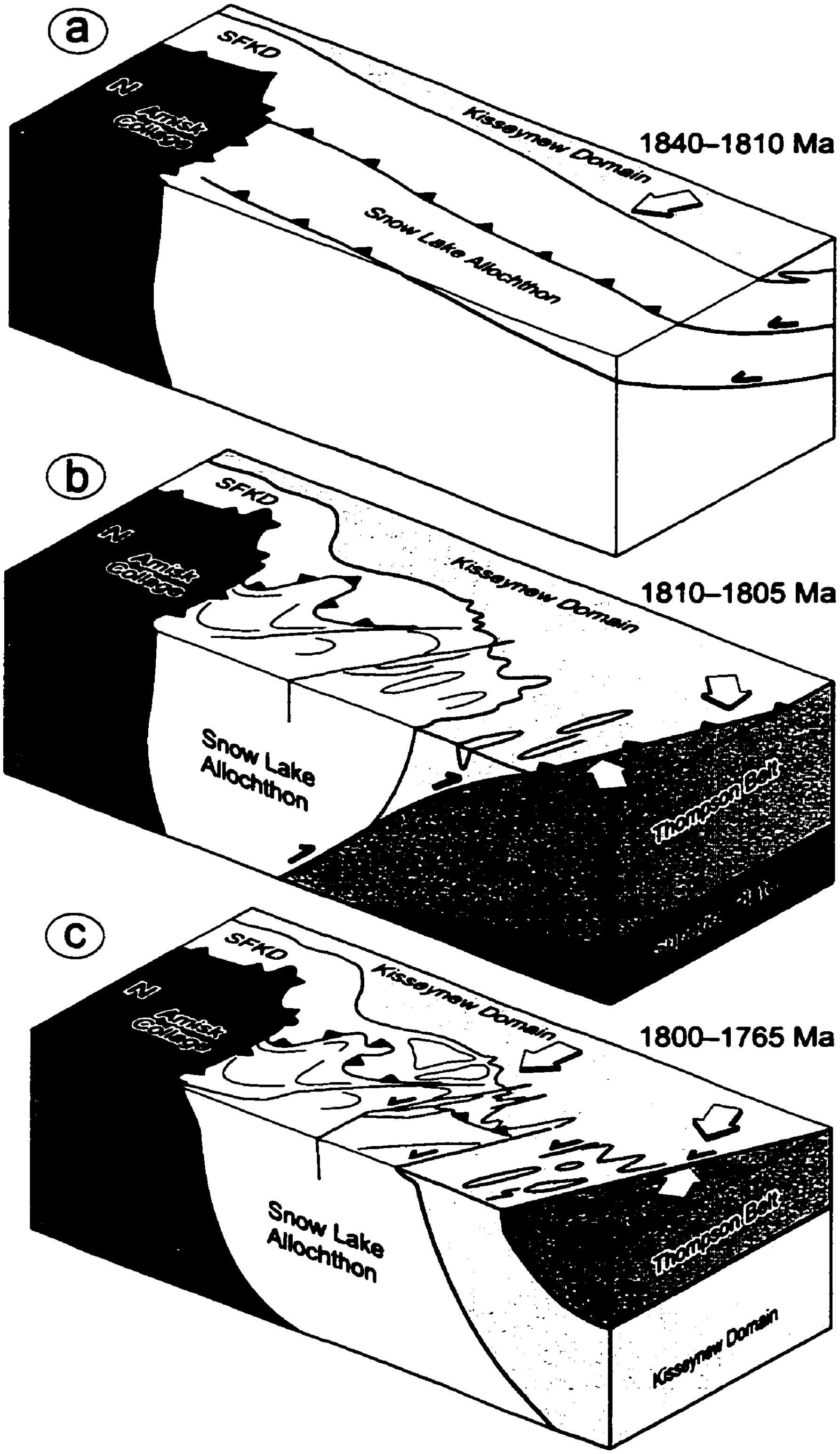

Figure 5.18 Sequence of block diagrams that schematically depicts the tectonic development of the southeastern Trans-Hudson Orogen. See text for explanation. The long edges of blocks are approximately 100 km. SFKD = southern flank of the Kisseynew Domain.

after F_1 (Gordon *et al.*, 1990; David *et al.*, 1996). Both this intrusive activity and coeval arc volcanism have been interpreted as relating to southward subduction of Kisseynew basin oceanic crust (Gordon *et al.*, 1990; Ansdell and Connors, 1995; Ansdell *et al.*, 1995, in press).

Crustal thickening by folding and overthrusting continued during F_2 (Menard and Gordon, 1997; see Chapter 4). The general northeasterly plunge of $F_{1/2}$ linear features suggests southerly $F_{1/2}$ tectonic transport (Fig. 5.18a). I believe that $F_{1/2}$ structures in the allochthon were initially recumbent and were steepened during F_2 by a component of northeast-southwest shortening superimposed on the southwesterly flow. Further steepening was achieved by later F_3 refolding around the previous fold axes. The F_2 shortening may have resulted from both the topographic relief of the footwall assemblages (Connors, 1996) and the inhibition of forward propagation on detachments. For example, the eastern termination of the rigid Amisk collage (footwall to the Morton Lake "fault" zone) may have acted as a steep oblique-lateral ramp (Figs 5.2 and 5.18a). Contemporaneous deformation in the Amisk collage, already characterised by steep anisotropy, was concentrated along steep northerly trending shear zones (Ryan and Williams, in press).

Following the development of the Snow Lake Allochthon during F_1 and F_2, the Superior plate collided with and shallowly underthrust the internal Trans-Hudson Orogen, probably in a sinistral-oblique sense (Fig. 5.18b) (e.g. Lewry, 1981; Green *et al.*, 1985; Bleeker, 1990a). During underthrusting, the allochthon and the southeastern Kisseynew Domain were folded by large amplitude, upright F_3 structures (Fig. 5.18b), which are symmetrical in the Snow Lake–File Lake area. Uplift of the Snow Lake Allochthon may have commenced at that time. Fanning of the steep F_3 axial planes from northeasterly trending at Snow Lake–File Lake to northwesterly trending on the southern flank of the Kisseynew Domain suggests that the F_3 folds formed during broadly east–west shortening (cf. Connors, 1996; Zwanzig, in press). East of Wekusko Lake, $F_{1/2}$ thrusts were steepened and reactivated, and new structures formed (e.g. Crowduck Bay fault; Fig. 5.2). It is, however, uncertain whether the eastward increasing tightness of the large F_3 folds was achieved by F_3 or F_4 strains, or by both. Contemporaneously, in the Thompson Belt, recumbent F_2 folds developed within a nappe pile that translated passive margin sediments easterly onto the Superior plate (Bleeker, 1990a; Bleeker and Macek, 1996).

After a possible vergence reversal and a short-lived period of westward overthrusting of the Superior plate onto the internal Trans-Hudson Orogen, the Thompson Belt, now being uplifted, was transformed into a zone of sinistral transpression during the local F_3 (Fig. 5.18c) (Green *et al.*, 1985; Bleeker, 1990a; White and Lucas, 1994; White *et al.*, 1994; Bleeker and Macek, 1996; Lucas *et al.*, 1996b). Transpression caused steepening of the recumbent earlier structures and the development of west-vergent, near upright, high amplitude, doubly plunging F_3 folds in the Thompson Belt (Bleeker, 1990a; Bleeker and Macek, 1996). At the same time, F_4 folds developed in the Snow Lake Allochthon. The area between Wekusko Lake and the Setting Lake fault zone was likely affected by the transpressional deformation (Connors and Ansdell, 1994a, b; Connors, 1996). Here, the steep F_3 structures were tightened, and further dismembered along a series of reactivated shear zones (e.g. Crowduck Bay fault; Fig. 5.2); F_4 movement along the northeasterly trending, steep structures was possibly sinistral strike slip or oblique slip (Connors *et al.*, in press). Coevally, favourably oriented packages were overthrust in a southerly direction along shallowly northerly dipping structures (e.g. Roberts Lake fault; Fig. 5.2). In the Snow Lake–File Lake area, in contrast, the $F_{1/2}$ kinematic frame was approximately restored during F_4. There, only favourably oriented northerly trending domains in highly metamorphosed rocks north of Snow Lake were deformed by large F_4 folds. These rocks were still relatively hot and thus more susceptible to straining than the colder, more rigid rocks to the south. The temperature gradient between the high-grade and the low-grade rocks was maintained during this stage of cooling, possibly owing to syn-F_4 and younger pegmatites, and to associated retrogressive fluids that affected all high-grade domains of the southern Trans-Hudson Orogen (e.g. Bleeker, 1990a; Connors, 1996; Chiarenzelli *et al.*, 1998). The generally steep attitude of the tectonostratigraphic packages inhibited further southward-directed thrusting in the Snow Lake Allochthon.

If the world should blow itself up, the last audible voice would be that of an expert saying it can't be done.
Peter Ustinov

Chapter 6

Conclusions

INTRODUCTION

The Snow Lake Allochthon, a domain in the internal part of the southeastern Trans-Hudson Orogen, was investigated in a combined structural and metamorphic study. The study has focussed on the delineation of the tectonometamorphic history of the allochthon. The findings were extrapolated to adjacent areas in order to improve the understanding of the larger scale tectonometamorphic developments and thus the role of the allochthon in the evolution of the orogen. Two complementary thematic studies focussed on porphyroblast–matrix relationships in the context of folding and the development of cleavage. In this Chapter, the conclusions of the various topics studied are summarised, and, where appropriate, problems arising from these studies are discussed.

STRUCTURE

Two generations of structures were recognised in the study area by previous workers—tight to isoclinal F_1 folds and open F_2 folds (Threehouse synform), the latter were believed to be associated with an axial-plane cleavage, S_2. This fabric is regionally pervasive and can be also found in the adjacent Amisk collage (S_4 of Ryan and Williams, in press). S_2 is thus a marker usable for the spatial correlation of the structural and metamorphic development in most of the NATMAP study area. Superficially, S_2 appears to be axially planar to F_3 folds. It is shown, however, that: (1) S_2 is axial planar to a second generation of tight to isoclinal folds (e.g. the F_2 McLeod Lake fold) that predate the Threehouse synform (F_3 in this thesis); (2) S_2 has the wrong asymmetry on the eastern limb of the Threehouse synform to be genetically related to this structure; (3) S_2 changes vergence on the east limb of the Threehouse synform across the Snow Lake fault; (4) S_2 is crenulated by F_3 where favourably oriented. A fourth generation of structures (F_4) is limited to favourably oriented domains that are located mainly north of the study area.

These four generations of folds formed in at least three distinct kinematic frames over a minimum period of 30 m.y.. The axes of the $F_{1/2}$ folds are parallel or near-parallel to the axes of the open F_3 folds, owing to progressive reorientation of the $F_{1/2}$ axes during emplacement of thick, internally deformed nappes, followed by F_3 refolding around the previous linear anisotropy.

F_1 strains were generally very high, as indicated by the tight cluster of fold axes (Figs 5.11–5.15), the strain in clasts, and the transposition of F_1 folds. Evidence of these high strains on a grain scale has been, however, obliterated by metamorphism and subsequent deformation. This hindered, in particular, the reconstruction of the early histories of the long-lived shear zones. $F_{1/2}$ folds and thrusts were likely recumbent and horizontal and may have formed in a constant kinematic frame. The large F_2 McLeod Lake fold has a strongly curved hinge, similar to the large F_2 folds on the southern flank of the Kisseynew Domain (e.g. Sherridon structure of Zwanzig and Schledewitz, 1992). Relatively steep F_3 folds developed in a different kinematic frame that reflects the terminal collision of the Trans-Hudson Orogen with the Archean Superior plate. Coevally, the Paleoproterozoic continental margin sequence was thrust on top of the Superior plate. The thermal peak of metamorphism in the high-grade portions of the Snow Lake Allochthon, in the adjacent part of the Kisseynew Domain, and in the Thompson Belt outlasted the development of the F_3 folds in the allochthon. F_4 folds in the Snow Lake Allochthon coincided with transpressional deformation in the Thompson Belt during incipient uplift and cooling of the orogen.

Cleavage–porphyroblasts–large-scale folding relationships

The development and overprinting of S_2 during F_2 and F_3 was established in Burntwood group rocks of the staurolite zone. Several lines of evidence suggest that S_2 initiated as crenulations early during F_2 folding and coincided with the growth of the peak metamorphic mineral assemblage. Initiation of cleavage appears to coincide generally with the early stages of folding in strongly anisotropic, micaceous, pelitic rocks. It is further shown that development of new cleavage from crenulation of the previous generation of cleavage depends on the orientation of the older cleavage. If the older cleavage was refracted, the new cleavage may thus not be pervasive, and two generations of cleavage may be present in adjacent beds (e.g. Henderson, 1997). It is interesting to note that the F_3 crenulations in the study area did not develop into a new cleavage, although fluids were abundant. In contrast, the lower grade rocks at Reed Lake contain a well-developed S_3 (Syme *et al.*, 1995). In general, the most spectacular differentiated cleavages occur in low-grade rocks (e.g. Williams, 1972; Weber, 1981). A discrete S_3 did not develop in the study area, because the intragranular strain in the micas and possibly also the bulk strain were low. A new domainal fabric that develops from an older domainal fabric is expected to comprise generally wider spaced domains than the older fabric (e.g. Hoeppener, 1956; Williams, 1972), because the wavelength of the crenulations is controlled by the thickness of the microlithons of the old fabric and by the porphyroblasts sited in these microlithons. If the grain size of the mica grains that define the septa of the older fabric did not increase much by recrystallisation, as in this case, the grain-scale strains around any new crenulation are accommodated by a low degree of bending of each grain compared to the sharp kinking of the mica grains during the formation of the older, narrower spaced fabric. The dislocation density and thus the stored strain energy in any mica grain in an F_3 crenulation is therefore expected to be low, so that these grains were not susceptible to dissolution and neocrystallisation/recrystallisation, which are important processes in the formation of a differentiated fabric.

Rotation of porphyroblasts with respect to the geographical reference frame

A solution to the contentious question, whether metamorphic porphyroblasts rotate (or not) with respect to the geographical reference frame during folding, was presented. The cleavage–porphyroblast–fold relationships of the Burntwood group rocks are useful for my argument in that, despite strong cleavage refraction, the inclusion trails in biotite and garnet porphyroblasts remained at a high angle to the enveloping S_2 throughout F_2 and F_3 folding. Therefore, although these porphyroblast–matrix relationships are in agreement with the strain field diagram of Bell (which he regarded as evidence for general porphyroblast non-rotation with respect to the geographical reference frame), the porphyroblasts have rotated relative to each other. Hence, some of the porphyroblasts, if not most, have rotated with respect to the geographical reference frame. These relationships uncover a logical problem in the porphyroblast non-rotation discussion that arises from the inconsistent use of reference frames; that is, the characterisation of the local deformation path does not rely on the geographical reference frame.

METAMORPHISM

The study area had been divided previously into Barrovian metamorphic zones distinguished by discontinuous metamorphic reactions that produce characteristic index minerals such as staurolite and sillimanite (Froese and Gasparrini, 1975; Bailes and McRitchie, 1980; Froese and Moore, 1980). The reactions had been inferred for the pelitic rocks, and the reaction isograds were extrapolated through the arc rocks (ibid.). Such an extrapolation is, however, problematic, because the pelitic and the volcanic rocks have distinct chemical compositions. Hence, the different rock types contain different mineral assemblages, and they are therefore characterised by distinct metamorphic reactions. As a result, an isograd, which is based on the first appearance of a certain (index) mineral produced by a certain metamorphic reaction, cannot be extrapolated through rocks, in which this reaction did not occur. Further, an index mineral, such as garnet, commences growing at temperatures as low as 450°C in a rock that contains sufficient Ca and Mn (e.g. in a rhyolite) and therefore at a lower temperature compared to garnet in a pelite (e.g. Spear, 1993). In other words, isograds based on the first occurrence of an index mineral do not coincide with the isotherms in an area that hosts a wide compositional variety of rock. Isograds are therefore of limited use for describing variations in metamorphic grade in such areas.

Geothermobarometry, which, in pelitic rocks (e.g. Burntwood group), does not depend on compositional homogeneity, was employed to determine the spatial variation in pressure and temperature in the study area, to calculate metamorphic P–T–t paths, and to decipher the relative timing of deformation and metamorphism in the higher grade rocks, where the porphyroblast–matrix relationships are less clear than in the lower grade rocks. It is suggested that the Snow Lake Allochthon is characterised by a syntectonic, diachronous, low- to medium-pressure metamorphism resulting from thermal relaxation after crustal thickening and from granitic plutonism in the adjacent Kisseynew Domain. F_1 was likely associated with the major episode of burial, and was followed by thermal relaxation, because the peak metamorphic conditions in the staurolite zone were coeval with early F_2. Burial during F_1 was probably rapid (1–5 Ma) as indicated by the youngest detrital zircons in the Burntwood group and ages of granitoids that crosscut F_1 structures (Gordon *et al.*, 1990; Machado and Zwanzig, 1995; David *et al.*, 1996). The ductile style of F_1 structures suggests crustal thickening by development and stacking of thick, internally deformed nappes (thick-skinned tectonics). Metamorphic conditions increased within 15–35 m.y. from chlorite grade to staurolite grade, possibly isobarically. During F_2, temperature and pressure increased only slightly, suggesting relatively minor crustal thickening after F_1. A thermal anomaly developed during or after F_2 which led to high-grade metamorphism in the northern part of the study area and the adjacent Kisseynew Domain. High-temperature conditions in the high-grade rocks prevailed for some 10 m.y. until after F_3, whereas mineral assemblages in staurolite-grade rocks indicate cooling during F_3.

The high-grade rocks in the Snow Lake Allochthon and in the Kisseynew Domain share the characteristics of many low- to medium-pressure, high-temperature terrains that formed in response to anomalously high thermal gradients caused by the intrusion of magma rather than by increased heating as the result of increased burial: (1) They record approximately the same pressures as the adjacent medium-grade rocks; (2) peak conditions are near the sillimanite–kyanite transition within the sillimanite stability field; and (3) there are no extensional features during cooling (cf. Bohlen, 1987). The general lack of late extension in the Manitoba–Saskatchewan segment of the Trans-Hudson Orogen (Hajnal *et al.*, 1996) suggests that erosion was the major exhumation mechanism (England and Thompson, 1984).

The prograde parts of the P–T–t paths calculated for the high-grade portions of the Snow Lake Allochthon and for the Kisseynew Domain (Fig. 4.8) show characteristics of an anticlockwise loop (T_{max} coincides with P_{max}) typical for low- to medium-pressure terrains (e.g. Sandiford and Powell, 1991), in contrast to the classic clockwise loops of overthrust terrains, where P_{max} is reached long before T_{max}, owing to thermal equilibration by relaxation of isotherms after thrusting (e.g. England and Thompson, 1984). Although mineral reaction textures, which are diagnostic of the retrograde history, in particular pressure-sensitive ones, are absent in the study area, the structural developments on the retrograde path and thermal calculations for the Kisseynew Domain (Gordon, 1989) suggest that cooling was associated with at least some decompression. The total P–T–t paths therefore approach a clockwise curve (Gordon, 1989; Chapter 4). In the high-grade-rocks, the P–T–t paths are a function of the timing and the duration of granitoid intrusion relative to deformation.

Cooling of the southeastern Trans-Hudson Orogen was relatively slow (more than 50 m.y.) and may have been, to some extent, slowed by pegmatites and associated hot fluids. This late activity may reflect slow cooling of the underaccreted and/or intruded mantle-derived magmas, and it may have resulted from of the long-lived thermal effect of the crustal thickening/concomitant thinning of the mantle lithosphere.

The metamorphic study also reveals a well-known, but frequently overseen, problem inherent in geobarometry in general—the dependence of the calculated pressures on the calculated temperatures (both are positively correlated in the geobarometers). In high-grade rocks, where temperatures are commonly overestimated owing to the biotite model used, the calculated pressures are also overestimated. This may result in apparent variations of the calculated pressures in areas characterised by a steep temperature gradient along the exposed surface. The solution to this problem would be a truly temperature-independent barometer (horizontal slope of the K_{eq} line).

Discussion—Archean basement underneath the Kisseynew Domain?

High-grade Archean basement gneisses appear as structural windows in the Hanson Lake Block and in the Glennie Domain, as mentioned in Chapter 1. These windows were interpreted as being culminations of the Saskatchewan craton, an Archean continental fragment which, according to interpreted LITHOPROBE seismic lines 3, 5, 9, and 10 (see Fig. 1.1. for location), is believed to underlie much of the internal Trans-Hudson Orogen, possibly including the Kisseynew Domain (e.g. Lewry *et al.*, 1990, 1994; Lucas *et al.*, 1993, 1994; Ansdell *et al.*, 1995; Chiarenzelli *et al.*, 1998). The Amisk collage, the southern flank of the Kisseynew Domain in Manitoba, and the Snow Lake Allochthon, are interpreted not to be underlain by Archean crust according to the interpreted LITHOPROBE seismic lines 2, 3 and 7 (Lucas *et al.*, 1993, 1994; White *et al.*, 1994; Leclair *et al.*, 1997). The basement is believed to have been overridden by the juvenile domains and by the Kisseynew Domain at 1.84–1.81 Ga, prior to (or, less likely coeval with) the thermal peak of metamorphism (e.g. Bickford *et al.*, 1990; Lewry *et al.*, 1990; Ansdell *et al.*, 1995; Lucas *et al.*, 1996a).

The new metamorphic data allow a statement concerning the possible presence of Archean basement underneath the Kisseynew Domain in the absence of seismic reflection data. High-grade Archean gneisses are generally refractory and depleted in radioactive heat-producing elements (U, Th, K, and Rb) (Tarney, 1976; Tarney *et al.*, 1982; Windley and Tarney, 1986; J. Tarney, pers. comm. 1997). Thus, Archean basement gneisses, if they were granulites, would likely not have contributed to the crustal heat budget; on the contrary, they may have dampened metamorphism by acting as insulators, hence preventing the upward conduction of heat generated at the base of the crust. Therefore, if basement underthrusting predated F_2, it would be hard to explain, how the rocks of the Kisseynew Domain experienced a stage of medium-grade metamorphism by conductive relaxation prior to the high-grade metamorphism, and the 1.84–1.83 Ga granitoid suite in the Kisseynew Domain would be expected to contain xenoliths of Archean rocks. But, even if the underthrusting coincided with F_2, the insulating effect of the Archean basement rocks may have prevented anatexis at the base of the sedimentary nappe pile overlying the Archean rocks in response to the proposed crust–mantle interactions as described in Chapter 4. Only if the Archean rocks had been wedged into the Kisseynew Domain rocks, could anatexis have occurred in sedimentary rocks underneath the Archean slice. If this were the case, the ~ 1.815 Ga granite suite in the Kisseynew Domain, which is thought to be responsible for triggering the high-temperature metamorphism at the presently exposed crustal level, would be expected to contain xenoliths of Archean rocks. Xenoliths are abundant in both granitoid suites, but they are exclusively sedimentary. The extent of the buried Archean basement may therefore be limited to the Glennie Domain, the Hanson Lake Block, and the southern flank of the Kisseynew Domain in Saskatchewan, with a possible continuation to the south. This hypothesis, however, needs further testing using Nd isotopes.

REFERENCES

Aerden, D.G.A.M. (1994) Kinematics of orogenic collapse in the Variscan Pyrenees deduced from microstructures in porphyroblastic rocks from the Lys-Caillaouas massif. *Tectonophysics* **238**, 139–160.

Aerden, D.G.A.M. (1995) Porphyroblast non-rotation during crustal extension in the Variscan Lys-Caillaouas Massif, Pyrenees. *Journal of Structural Geology* **17**, 709–725.

Aggarwal, P.K. and Nesbitt, B.E. (1987) Pressure and temperature conditions of metamorphism in the vicinity of three massive sulfide deposits, Flin Flon – Snow Lake belt, Manitoba. *Canadian Journal of Earth Sciences* **24**, 2305–2315.

Alcock, F.J. (1920) The Reed–Wekusko Map-Area. *Geological Survey of Canada Memoir* 119.

Ansdell, K.M. (1993) U–Pb zircon constraints on the timing and provenance of fluvial sedimentary rocks in the Flin Flon and Athapapuskow basins, Flin Flon Domain, Trans-Hudson Orogen, Manitoba and Saskatchewan. In *Radiogenic Age and Isotopic Studies: Report 7, Geological Survey of Canada Paper* 93-2, pp. 49–57.

Ansdell, K.M. and Bleeker, W. (1997) The margin of the Superior craton: neodymium isotope constraints on the evolution of the Thompson Nickel Belt. *Geological Association of Canada, Program with Abstracts* 22, A–4.

Ansdell, K.M. and Connors, K.A. (1995) Geochemistry of mafic volcanic rocks, east Wekusko Lake, Manitoba. *Lithoprobe Trans-Hudson Orogen Transect Report* **48**, 198–205.

Ansdell, K.M., Connors, K.A., Stern, R. and Lucas, S.B. Coeval sedimentation, magmatism, and fold-thrust belt development in the Trans-Hudson Orogen: Geochronological evidence from the Wekusko Lake area, Manitoba. *Canadian Journal of Earth Sciences*, in press.

Ansdell, K.M., Lucas, S.B., Connors, K.A. and Stern, R.S. (1995) Kisseynew metasedimentary gneiss belt, Trans-Hudson Orogen (Canada). Back-arc origin and collisional inversion. *Geology* **23**, 1039–1043.

Ansdell, K.M. and Norman, A.R. (1995) U–Pb geochronology and tectonic development of the southern flank of the Kisseynew domain, Trans-Hudson Orogen, Canada. *Precambrian Research* **72**, 147–167.

Ansdell, K.M. and Ryan, J.J. (1997) Timing of early deformation within the long-lived Elbow Lake shear zone, Trans-Hudson Orogen, Manitoba. In *Radiogenic Age and Isotopic Studies: Report 10, Geological Survey of Canada, Current Research* 1997–F, pp. 79–88.

Armstrong, J.E. (1941) Wekusko, Manitoba. *Geological Survey of Canada Map* 665A, with descriptive notes.

Ashton, K.E., Heaman, L.M., Lewry, J.F., Hartlaub, R.P. and Shi, R. Age and origin of the Jan Lake Complex: a glimpse at the buried Archean craton of the Trans-Hudson Orogen. *Canadian Journal of Earth Sciences*, in press.

Ashton, K.E., Hunt, P.A. and Froese, E. (1992) Age constraints on the evolution of the Flin Flon volcanic belt, Saskatchewan and Manitoba. In *Radiogenic Age and Isotopic Studies: Report 5, Geological Survey of Canada Paper* 91–2, pp. 55–69.

Ashton, K.E. and Lewry, J. (1996) Geological history of the northern Hanson Lake Block and age relationships between the Pelican décollement zone and Sturgeon–Weir shear zone. *Lithoprobe Trans-Hudson Orogen Transect Report* **55**, 73–81.

Ashton, K.E., Wilcox, K.H., Wheatley, K.J., Paul, D. and de Tombe, J. (1987) The boundary zone between the Flin Flon Domain, Kisseynew gneisses and Hanson Lake block, northern Saskatchewan. In *Summary of Investigations* 1987, *Saskatchewan Geological Survey, Saskatchewan Energy and Mines, Miscellaneous Report*, pp. 109–111.

Aspler, L.B. and Chiarenzelli, J.R. (1997) Initiation of ca. 2.45–2.1 Ga intracratonic basin sedimentation of the Hurwitz Group, Keewatin Hinterland, Northwest Territories, Canada. *Precambrian Research* **81**, 265–298.

Aspler, L.B. and Chiarenzelli, J.R. (1998) Two Archean supercontinents? Evidence from the Paleozoic. *Sedimentary Geology* **120**, 75–104.

Atherton, M.P. (1993) Granite magmatism. *Journal of the Geological Society of London* **150**, 1009–1023.

Bailes, A.H. (1975) Geology of the Guay–Wimapedi lakes area. *Manitoba, Department of Mines, Resources and Environmental Management, Mineral Resources Division, Geological Services Branch, Publication* 75–2.

Bailes, A.H. (1980a) Geology of the File Lake area. *Manitoba Mineral Resources Division, Geological Report* 78–1.

Bailes, A.H. (1980b) Origin of Early Proterozoic volcaniclastic turbidites, south margin of the Kisseynew sedimentary gneiss belt, File Lake, Manitoba. *Precambrian Research* **12**, 197–225.

Bailes, A.H. (1985) Geology of the Saw Lake area. *Manitoba Energy and Mines, Geological Report* GR83–2.

Bailes, A.H. (1992) Wekusko Lake (North) project (NTS 63J/13SW). In *Manitoba Department of Energy and Mines, Minerals Division, Report of Activities*, pp. 56–64.

Bailes, A.H. and Galley, A.G. (1994) Geology of the Anderson–Stall volcanic-hosted massive sulfide area, Snow Lake, Manitoba. *Geological Survey of Canada Open File* 2772, map with descriptive notes.

Bailes, A.H. and Galley, A.G. (1996) Setting of Paleoproterozoic volcanic-hosted massive metal sulphide deposits, Snow Lake Manitoba. In *EXTECH I: A multidisciplinary approach to massive sulphide research in the Rusty Lake–Snow Lake greenstone belts, Manitoba*, ed. G.F. Bonham-Carter and G.E.M. Hall, Vol 426, pp. 105–138. *Geological Survey of Canada Bulletin*.

Bailes, A.H., Hunt, P.A. and Gordon, T.M. (1991) U–Pb dating of possible synvolcanic plutons in the Flin Flon belt at Snow Lake, Manitoba. In *Radiogenic Age and Isotopic Studies: Report 4, Geological Survey of Canada Paper* 90–2, pp. 35–43.

Bailes, A.H. and McRitchie, W.D. (1978) The transition from low to high grade metamorphism in the Kisseynew sedimentary gneiss belt, Manitoba. In *Metamorphism in the Canadian Shield*, ed. J.A. Fraser and W.W. Heywood. *Geological Survey of Canada Paper* 78–10, pp.155–178.

Bailey, E.B. (1923) The metamorphism of the South-West Highlands. *Geological Magazine* **60**, 317–331.

Baldwin, D.A., Syme, E.C., Zwanzig, H.V., Gordon, T.M., Hunt, P.A. and Stevens, R.D. (1987) U–Pb zircon ages from the Lynn Lake and Rusty Lake metavolcanic belts, Manitoba: two ages of Proterozoic magmatism. *Canadian Journal of Earth Sciences* **24**, 1053–1063.

Baragar, W.R.A. and Scoates, R.F.J. (1981) The Circum-Superior belt: a Proterozoic plate margin? In *Precambrian Plate Tectonics*, ed. A. Kröner, pp. 297–330. Elsevier, Amsterdam.

Barbarin, B. (1996) Genesis of the two main types of peraluminous granitoids. *Geology* **24**, 295–298.

Barrow, G. (1912) On the geology of lower Deeside and the southern highland border. *Proceedings of the Geological Association* **23**, 268–284.

Barton, M.D. and Hanson, R.B. (1989) Magmatism and the development of low-pressure metamorphic belts: Implications from the western United States and thermal modeling. *Geological Society of America Bulletin* **101**, 1051–1065.

Bell, T.H. (1981) Foliation development—the contribution, geometry and significance of progressive, bulk, inhomogeneous shortening. *Tectonophysics* **75**, 273–296.

Bell, T.H. (1985) Deformation partitioning and porphyroblast rotation in metamorphic rocks: a radical reinterpretation. *Journal of Metamorphic Geology* **3**, 109–118.

Bell, T.H. (1986) Foliation development and refraction in metamorphic rocks: reactivation of earlier foliations and decrenulation due to shifting patterns of deformation partitioning. *Journal of Metamorphic Geology* **4**, 421–444.

Bell, T.H. and Forde, A. (1995) On the significance of foliation patterns preserved around folds by mineral growth. *Tectonophysics* **246**, 171–181.

Bell, T.H., Forde, A. and Hayward, N. (1992a) Do smoothly curved, spiral-shaped inclusion trails signify porphyroblast rotation? *Geology* **20**, 59–62.

Bell, T.H., Forde, A. and Hayward, N. (1992b) Reply on 'Do smoothly curved, spiral-shaped inclusion trails signify porphyroblast rotation?'. *Geology* **20**, 1055–1056.

Bell, T.H., Forde, A and Wang, J. (1995) A new indicator of movement direction during orogenesis: measurement technique and application to the Alps. *Terra Nova* **7**, 500–508.

Bell, T.H., Hickey, K.A. and Wang, J. (1997) Spiral and staircase trail axes within garnet and staurolite porphyroblasts from schists of the Bolton Syncline, Connecticut: timing of porphyroblast growth and the effects of fold development. *Journal of Metamorphic Geology* **15**, 467–478.

Bell, T.H. and Johnson, S.E. (1989) Porphyroblast inclusion trails: the key to orogenesis. *Journal of Metamorphic Geology* **7**, 279–310.

Bell, T.H. and Johnson, S.E. (1990) Rotation of relatively large rigid objects during ductile deformation: well established fact or intuitive prejudice? *Australian Journal of Earth Sciences* **37**, 441–446.

Bell, T.H. and Johnson, S.E. (1992) Shear sense: a new approach that resolves conflicts between criteria in metamorphic rocks. *Journal of Metamorphic Geology* **10**, 99–124.

Bell, T.H., Johnson, S.E., Davis, B., Forde, A., Hayward, N. and Wilkins, C. (1992c) Porphyroblast inclusion-trail orientation data: eppure non son girate! *Journal of Metamorphic Geology* **10**, 295–307.

Bell, T.H. and Rubenach, M.J. (1983) Sequential porphyroblast growth and crenulation cleavage development during progressive deformation. *Tectonophysics* **92**, 171–194.

Bell, T.H., Rubenach, M.J. and Fleming, P.D. (1986) Porphyroblast nucleation, growth and dissolution in regional metamorphic rocks as a function of deformation partitioning during foliation development. *Journal of Metamorphic Geology* **4**, 37–67.

Berman, R.G. (1988) Internally-consistent thermodynamic data for minerals in the system Na_2O–K_2O–CaO–MgO–FeO–Fe_2O_3–Al_2O_3–SiO_2–TiO_2–H_2O–CO_2. *Journal of Petrology* **29**, 445–552.

Berman, R.G. (1990) Mixing properties of Ca–Mg–Fe–Mn garnets. *American Mineralogist* **75**, 328–344.

Berman, R.G. (1991) Thermobarometry using multi-equilibrium calculations: a new technique, with petrological applications. *Canadian Mineralogist* **29**, 833–855.

Berman, R.G. and Koziol, A.M. (1991) Ternary excess properties of grossular–pyrope–almandine garnets and their influence in geothermobarometry. *American Mineralogist* **76**, 1223–1231.

Bickford, M.E., Lewry, J.F., van Schmus, W.R. and Chiarenzelli, J.R. (1990) Proterozoic collisional tectonism in the Trans-Hudson Orogen. *Geology* **18**, 14–18.

Biot, M.A. (1964) Theory of internal buckling of a confined multilayered structure. *Geological Society of America Bulletin* **75**, 563–568.

Bird, P. (1979) Continental delamination and the Colorado Plateau. *Journal of Geophysical Research* **84**, 7561–571.

Bird, P. and Baumgardner, J. (1981) Steady propagation of delamination events. *Journal of Geophysical Research* **86**, 4891–4903.

Bleeker, W. (1990a) New structural–metamorphic constraints on Early Proterozoic oblique collision along the Thompson Nickel Belt, Manitoba, Canada. In *The Early Proterozoic Trans-Hudson Orogen of North America*, ed. J.F. Lewry and M.R. Stauffer, Vol. 37, pp. 57–73. *Geological Association of Canada Special Paper*.

Bleeker, W. (1990b) Evolution of the Thompson Nickel Belt and its Nickel Deposits, Manitoba. Unpublished Ph.D. Thesis, University of New Brunswick, Fredericton.

Bleeker, W. and Macek, J. (1996) Evolution of the Thompson Nickel belt, Manitoba: setting of Ni–Cu deposits in the western part of the circum Superior boundary zone. *Geological Association of Canada* Field Trip A1.

Bleeker, W., Nägerl, P. and Machado, N. (1995) The Thompson Nickel Belt, Manitoba: some new U–Pb ages. *Geological Association of Canada, Program with Abstracts* 20, A–8.

Bohlen, S.R. (1987) Pressure–temperature–time paths and a tectonic model for the evolution of granulites. *Journal of Geology* **95**, 617–632.

Briggs, W. and Foster, C.T. (1992) Pressure–temperature conditions of Early Proterozoic metamorphism during the Trans-Hudson Orogen as determined from rocks straddling the Flin Flon – Kisseynew boundary at Niblock and File lakes, Manitoba. *Canadian Journal of Earth Sciences* **29**, 2497–2507.

Bristol, C.C. (1974) Sphalerite geobarometry of some metamorphosed orebodies in the Flin Flon and Snow Lake districts, Manitoba. *Canadian Mineralogist* **12**, 308–315.

Bristol, C.C. and Froese, E. (1989) Highly metamorphosed altered rocks associated with the Osbourne Lake volcanogenic sulfide deposit, Snow Lake area, Manitoba. *Canadian Mineralogist* **27**, 593–600.

Brooks, C. and Theyer, P. (1981) Rb/Sr geochronology in the Thompson Nickel Belt, Manitoba: implications for Aphebian crustal development and metallogenesis. *Canadian Journal of Earth Sciences* **18**, 932– 943.

Bruce, E.L. (1917) Schist Lake and Wekusko Lake area, northern Manitoba. In *Geological Survey of Canada Summary Report* 1916, pp. 159–169.

Bruce, E.L. (1918) Amisk–Athapapuskow Lake district. *Geological Survey of Canada Memoir* 105.

Bryant, B. and Reed, J.C. (1969) Significance of lineation and minor folds near major thrust folds in the southern Appalachians and the British and Norwegian Caledonides. *Geological Magazine* **106**, 412–429.

Bryndzia, L.T. and Scott, S.D. (1987) Application of chlorite–sulfide–oxide equilibria to metamorphosed massive sulfide ores, Snow Lake area, Manitoba. *Economic Geology*

83, 963–979.

Carmichael, D.M. (1969) On the mechanism of prograde metamorphic reactions in quartz-bearing pelitic rocks. *Contributions to Mineralogy and Petrology* **20**, 244–267.

Carmichael, D.M. (1970) Intersecting isograds in the Whetstone Lake area, Ontario. *Journal of Petrology* **11**, 147–181.

Chandler, F.W. and Parrish, R.R. (1989) Age of the Richmond Gulf Group and implications for rifting in the Trans-Hudson Orogen, Canada. *Precambrian Research* **18**, 932–943.

Chauvel, C., Arndt, N.T., Kielinzcuk, S. and Thom, A. (1987) Formation of Canadian 1.9 Ga continental crust I: Nd isotopic data. *Canadian Journal of Earth Sciences* **24**, 396–406.

Chiarenzelli, J.R., Aspler, L.B. and Villeneuve, M. (1996) Characterization, origin, and Paleoproterozoic history of the Saskatchewan craton and possible implications for Trans-Hudson Orogen. *Lithoprobe Trans-Hudson Orogen Transect Report* **55**, 26–38.

Chiarenzelli, J.R., Aspler, L.B., Villeneuve, M. and Lewry, J.F. (1998) Early Proterozoic evolution of the Saskatchewan craton and its allochthonous cover, Trans-Hudson Orogen. *Journal of Geology* **106**, 247–267.

Chiarenzelli, J.R. and Lewry, J.F. (1988) The Nistowiak gneisses: evidence of a collisional suture in the Trans-Hudson Orogen, northern Saskatchewan. *Geological Association of Canada, Program with Abstracts* 13, A–20.

Cobbold, P.R. and Watkinson, A.J. (1981) Bending anisotropy: a mechanical constraint on the orientation of fold axes in an anisotropic medium. *Tectonophysics* **72**, T1–T10.

Collins, W.J. and Sawyer, E.W. (1996) Pervasive granitoid magma transfer through the lower–middle crust during non-coaxial compressional deformation. *Journal of Metamorphic Geology* **14**, 565–579.

Connors, K.A. (1996) Unraveling the boundary between turbidites of the Kisseynew belt and volcano-plutonic rocks of the Flin Flon belt, Trans-Hudson Orogen, Canada. *Canadian Journal of Earth Sciences* **33**, 811–829.

Connors, K.A. and Ansdell K.M. (1994a) Revision of stratigraphy and structural history in the east Wekusko Lake area, eastern Trans Hudson Orogen. In *Manitoba Energy and Mines, Minerals Division, Report of Activities*, pp. 104–107.

Connors, K.A. and Ansdell K.M. (1994b) Timing and significance of thrust faulting along the boundary between the Flin Flon and Kisseynew domains, eastern Trans-Hudson Orogen. *Lithoprobe Trans-Hudson Orogen Transect Report* **38**, 112–122.

Connors, K.A., Ansdell, K.M. and Lucas, S.B. Coeval sedimentation, magmatism, and fold-thrust belt development in the Trans-Hudson Orogen: Propagation into an active continental arc setting, Wekusko Lake, Manitoba. *Canadian Journal of Earth Sciences*, in press.

Cowie, J.W. and Basset, M.G. (compilers) (1989) 1989 Global stratigraphic chart. *Episodes* **12**, no.2, supplement.

Cowie, J.W., Ziegler, W. and Remane, J. (1989) Stratigraphic commission accelerates progress 1984–1989. *Episodes* **12**, 73–83.

Dallmeyer, R.D., Kean, B.F., Odom, A.L. and Jayasinghe, N.R. (1983) Age and contact-metamorphic effects of the Overflow Pond Granulite: an undeformed pluton in the Dunnage Zone of the Newfoundland Appalachians. *Canadian Journal of Earth Sciences* **20**, 1639–1645.

David, J., Bailes, A.H. and Machado, N. (1996) Evolution of the Snow Lake portion of the Paleoproterozoic Flin Flon and Kisseynew belts, Trans Hudson Orogen, Manitoba, Canada. *Precambrian Research* **80**, 107–124.

Dewey, J.F. and Burke, K.B.S. (1973) Tibetan, Variscan and Precambrian basement reactivation: products of continental collision. *Journal of Geology* **81**, 683–692.

De Yoreo, J.J., Lux, D.R. and Guidotti, C.V. (1991) Thermal modelling of low-pressure/high-temperature metamorphic belts. *Tectonophysics* **188**, 209–238.

De Yoreo, J.J., Lux, D.R., Guidotti, C.V., Decker, E.R. and Osberg, P.H. (1989a) The Acadian thermal history of western Maine. *Journal of Metamorphic Geology* **7**, 169–190.

De Yoreo, J.J., Lux, D.R., Guidotti, C.V., Decker, E.R. and Osberg, P.H. (1989b) The role of crustal anatexis and magma migration in the thermal evolution of regions of thickened continental crust. In *Evolution of metamorphic belts*, ed. J.S. Daly, R.A. Cliff and B.W.D. Yardley, pp. 187–202. *Geological Society of London Special Publication* 43.

Donath, F.A. and Parker, R.B. (1964) Folds and folding. *Geological Society of America Bulletin* **75**, 45–62.

Dunsmore, D.J. and Symons, D.T.A. (1990) Paleomagnetism of the Lynn Lake gabbros in the Trans-Hudson Orogen and closure of the Superior and Slave cratons. In *The Early Proterozoic Trans-Hudson Orogen of North America*, ed. J.F. Lewry and M.R. Stauffer, Vol. 37, pp. 215–228. *Geological Association of Canada Special Paper.*

Elliott, C.G. (1995) The Tabbernor fault and Proterozoic and Phanerozoic movements in Saskatchewan and Manitoba. *Lithoprobe Trans-Hudson Orogen Transect Report* **48**, 148–155.

Elliott, C.G. (1996a) Phanerozoic deformation in the "stable craton", Manitoba, Canada. *Geology* **24**, 909–912.

Elliott, C.G. (1996b) The Tabbernor fault in four dimensions. *Lithoprobe Trans-Hudson Orogen Transect Report* **55**, 5–9.

England, P.C. and Richardson, S.W. (1977) The influence of erosion upon the mineral facies of rocks from different metamorphic environments. *Journal of the Geological Society of London* **134**, 201–213.

England, P.C. and Thompson, A.B. (1984) Pressure–temperature–time paths of regional metamorphism I. Heat transfer during the evolution of regions of thickened continental crust. *Journal of Petrology* **25**, 894–928.

Escher, A.J. and Watterson, J. (1974) Stretching fabrics, folds and crustal shortening. *Tectonophysics* **22**, 223–231.

Etheridge, M.A. and Hobbs, B.E. (1974) Chemical and deformational controls on recrystallisation of mica. *Contributions to Mineralogy and Petrology* **43**, 111–124.

Fedorowich, J.S., Kerrich, R. and Stauffer, M.R. (1995) Geodynamic evolution and thermal history of the central Flin Flon domain, Trans-Hudson Orogen: Constraints from structural development, $^{40}Ar/^{39}Ar$, and stable isotope geothermometry. *Tectonics* **14**, 472–503.

Ferguson, C.C. and Harte, B. (1975) Textural patterns at porphyroblast margins and their use in determining the time relations of deformation and crystallisation. *Geological Magazine* **112**, 467–480.

Foster, C.T. Jr. (1991) The role of biotite as a catalyst in reaction mechanisms that form sillimanite. *Canadian Mineralogist* **29**, 943–963.

Friend, C.R.L., Kinny, P.D., Rogers, G., Strachan, R.A. and Paterson, B.A. (1997) U–Pb zircon geochronologicai evidence for Neoproterozoic events in the Glennfinnan

Group (Moine Supergroup): the formation of the Ardgour granitic gneiss, north-west Scotland. *Contributions to Mineralogy and Petrology* **128**, 101–113.

Froese, E. and Gasparrini, E. (1975) Metamorphic zones in the Snow Lake area, Manitoba. *Canadian Mineralogist* **13**, 162–167.

Froese, E. and Goetz, P.A. (1981) Geology of the Sherridon Group in the vicinity of Sherridon, Manitoba. *Geological Survey of Canada Paper* 80–21.

Froese, E. and Moore, J.M. (1980) Metamorphism in the Snow Lake area, Manitoba. *Geological Survey of Canada Paper* 78–27.

Fuhrman, M.L. and Lindsley, D.H. (1988) Ternary-feldspar modeling and thermometry. *American Mineralogist* **73**, 201–215.

Fumerton, S.L., Stauffer, M.R. and Lewry, J.F. (1984) The Wathaman batholith: Largest known Precambrian pluton. *Canadian Journal of Earth Sciences* **21**, 1082–1092.

Furlong, K.P. and Fountain, D.M. (1986) Continental crustal underplating: thermal considerations and seismic-petrologic consequences. *Journal of Geophysical Research* **91**, 8285–8294.

Fyson, W.K. (1975) Fabrics and deformation of Archean metasedimentary rocks, Ross Lake – Gordon Lake area, Slave Province, Northwest Territories. *Canadian Journal of Earth Sciences* **12**, 765–776.

Fyson, W.K. (1980) Fold fabrics and emplacement of an Archean granitoid pluton, Cleft Lake, Northwest Territories. *Canadian Journal of Earth Sciences* **17**, 325–332.

Fyson, W.K. (1982) Complex evolution of folds and cleavages in Archean rocks, Yellowknife, N.W.T. *Canadian Journal of Earth Sciences* **19**, 878–893.

Fyson, W.K. (1984) Basement-controlled structural fronts forming an apparent major refold pattern in the Yellowknife domain, Slave Province. *Canadian Journal of Earth Sciences* **21**, 822–828.

Fyson, W.K. and Helmstaedt, H. (1988) Structural patterns and tectonic evolution of supracrustal domains in the Archean Slave Province, Canada. *Canadian Journal of Earth Sciences* **25**, 30–315.

Galley, A.G., Ames. D.E. and Franklin, J.M. (1988) Geological setting of gold mineralization, Snow Lake, Manitoba. *Geological Survey of Canada Open File* 1700, map with descriptive notes.

Galley, A.G., Bailes, A.H. and Kitzler, G. (1993) Geological setting and hydrothermal evolution of the Chisel Lake and North Chisel Zn–Pb–Cu–Ag–Au massive sulfide deposits, Snow Lake, Manitoba. *Exploration and Mining Geology* **2**, 271–295.

Gardien, V., Thompson, A.B., Grujic, D. and Ulmer, P. (1995) Experimental melting of biotite + plagioclase + quartz ± muscovite assemblages and implications for crustal melting. *Journal of Geophysical Research* **100**, 15581–15591.

Gibb, R.A. (1975) Collision Tectonics in the Canadian shield. *Earth and Planetary Science Letters* **27**, 378–382.

Gibb, R.A. (1983) Model for suturing of Superior and Churchill plates: An example for double indentation tectonics. *Geology* **11**, 413–417.

Gibb, R.A. and Walcott, R.I. (1971) A Precambrian suture in the Canadian shield. *Earth and Planetary Science Letters* **10**, 417–422.

Gibson, R.L. (1992) Sequential, syndeformational porphyroblast growth during Hercynian low-pressure/high temperature metamorphism in the Canigou massif, Pyrenees. *Journal of Metamorphic Geology* **10**, 637–650.

Glen, R.A. (1979) Evidence for cyclic reactions between andalusite, 'sericite' and sillimanite, Mount Franks area, Willyama Complex, N.S.W. *Tectonophysics* **58**, 97–112.

Gordon, T.M. (1981) Metamorphism in the Crowduck Bay area, Manitoba. In *Current Research, Part A, Geological Survey of Canada Paper* 81–1A, pp. 315–316.

Gordon, T.M. (1989) Thermal evolution of the Kisseynew sedimentary gneiss belt, Manitoba: metamorphism at an early Proterozoic accretionary margin. In *Evolution of metamorphic belts*, ed. J.S. Daly, R.A. Cliff and B.W.D. Yardley, pp. 233–244. *Geological Society of London Special Publication* 43.

Gordon, T.M., Aranovich, Y. and Fed'kin, V.V. (1993) Mineral assemblage and thermobarometric constraints on the temperature–depth history of the Kisseynew and Flin Flon belts, Manitoba. *Lithoprobe Trans-Hudson Orogen Transect Report* **34**, 131–138.

Gordon, T.M., Aranovich, L.Y. and Fed'kin, V.V. (1994a) Exploratory data in thermobarometry: An example from the Kisseynew sedimentary gneiss belt, Manitoba, Canada. *American Mineralogist* **79**, 973–982.

Gordon, T.M. and Gall, Q. (1982) Metamorphism in the Crowduck Bay area, Manitoba. In

Current Research, Part A, Geological Survey of Canada Paper 82–1A, pp. 197–201.

Gordon, T.M., Hunt. P.A., Bailes, A.H. and Syme, E.C. (1990) U–Pb ages of the Flin Flon and Kisseynew domains, Manitoba: chronology of crust formation at an Early Proterozoic accretionary margin. In *The Early Proterozoic Trans-Hudson Orogen of North America*, ed. J.F. Lewry and M.R. Stauffer, Vol. 37, pp. 177–199. *Geological Association of Canada Special Paper.*

Gordon, T.M., Jungwirth, T.L. and Plint, H.E. (1994b) Metamorphic studies in the Reindeer zone in Manitoba. *Lithoprobe Trans-Hudson Orogen Transect Report* **38**, 196–204.

Gower, C.F. (1985) Correlations between the Grenville Province and the Sveconorwegian orogenic belt—Implications for Proterozoic evolution of the southern margin of the Canadian and Baltic shields. In *The deep Proterozoic crust in the North American Provinces*, ed. A.C. Tobi and J.L.R. Touret, pp. 247–257. Dordrecht, Netherlands, Reidel.

Green, A.G., Cumming G. L. and Cedarwell, D. (1979) Extension of the Superior–Churchill boundary zone into southern Canada. *Canadian Journal of Earth Sciences* **16**, 1691–1701.

Green, A.G., Hajnal, Z. and Weber, W. (1985) An evolutionary model for the western Churchill Province and western margin of the Superior Province in Canada and the north-central United States. *Tectonophysics* **116**, 281–322.

Hajnal, Z., Lucas, S., White, D., Lewry, J.F., Bezdan, S. and Stauffer, M.R. (1996) Seismic reflection images of high-angle faults and linked detachments in the Trans-Hudson Orogen. *Tectonics* **15**, 427–439.

Halden, N.M., Clark, G.S., Corkery, M.T., Lenton, P.G. and Schledewitz, D.C.P. (1990) Trace-element and Rb–Sr isotopic constraints on the origin of the Chipewyan, Thorsteinson, and Baldock batholiths, Churchill Province, Manitoba. In *The Early Proterozoic Trans-Hudson Orogen of North America*, ed. J.F. Lewry and M.R. Stauffer, Vol. 37, pp. 201–214. *Geological Association of Canada Special Paper.*

Harley, S.L. (1989) The origins of granulites: a metamorphic perspective. *Geological Magazine* **126**, 215–247.

Harrison, J.M. (1949) Geology and mineral deposits of File–Tramping lakes area, Manitoba. *Geological Survey of Canada Memoir* 250.

Harrison, J.M. (1951) Precambrian correlation and nomenclature, and problems of the Kisseynew gneisses, in Manitoba. *Geological Survey of Canada Bulletin* 20.

Hayward, N. (1990) Determination of early fold axis orientations within multiply deformed rocks using porphyroblasts. *Tectonophysics* **179**, 353–369.

Hayward, N. (1992) Microstructural analysis of the classical spiral garnet porphyroblasts of south-east Vermont: evidence for non-rotation. *Journal of Metamorphic Geology* **10**, 567–587.

Heaman, L.M. (1997) Global mafic magmatism at 2.45 Ga: Remnants of an ancient large igneous province? *Geology* **25**, 299–302.

Heaman, L.M. and Corkery, T. (1996) U–Pb geochronology of the Split Lake block, Manitoba: preliminary results. *Lithoprobe Trans-Hudson Orogen Transect Report* **55**, 60–68.

Heaman, L.M., Machado, N., Krogh, T. and Weber, W. (1986) Precise U–Pb zircon ages for the Molson dyke swarm and the Fox River sill: implications for Early Proterozoic crustal evolution in NE Manitoba, Canada. *Contributions to Mineralogy and Petrology* **94**, 82–89.

Henderson, J.R. (1997) Development of a chevron cleavage pattern and porphyroblast rotation in graded metaturbidites, Slave structural province, Northwest Territories, Canada. *Journal of Structural Geology* **19**, 653–661.

Henderson, J.R., Wright, T.O. and Henderson, M.N. (1986) A history of cleavage and folding: an example from the Goldenville Formation, Nova Scotia. *Geological Society of America Bulletin* **97**, 1354–1366.

Hobbs, B.E., Means, W.D. and Williams, P.F. (1976) *An Outline of Structural Geology*. Wiley, New York.

Hodges, K.V. and Crowley, P.D. (1985) Error estimation and empirical geothermobarometry for pelitic systems. *American Mineralogist* **70**, 702–709.

Hoffman, P.F. (1981) Autopsy of Athapuscow Aulacogen: a failed arm affected by three collisions. In *Proterozoic basins of Canada*, ed. F.H.A. Campbell. *Geological Survey of Canada Paper* 81–10, pp. 97–101.

Hoffman, P.F. (1985) Is the Cape Smith belt (northern Quebec) a klippe? *Canadian Journal of Earth Sciences* **22**, 1361–1369.

Hoffman, P.F. (1988) United plates of America, the birth of a craton: Early Proterozoic assembly and growth of Laurentia. *Annual Reviews of Earth and Planetary Sciences* **16**, 543–603.

Hoffman, P.F. (1989a) Speculations on Laurentia's first gigayear (2.0–1.0 Ga). *Geology* **17**, 135–138.

Hoffman, P.F. (1989b) Precambrian Geology and the tectonic history of North America. In *The Geology of North America – An overview*, ed. A.W. Bally and A.R. Palmer, Vol. A, pp. 447–512. *Geological Society of America.*

Hoffman, P.F. (1990) Subdivision of the Churchill Province and Extent of the Trans-Hudson Orogen. In *The Early Proterozoic Trans-Hudson Orogen of North America*, ed. J.F. Lewry and M.R. Stauffer, Vol. 37, pp. 15–39. *Geological Association of Canada Special Paper.*

Hoisch, T.D. (1990) Empirical calibration of six geobarometers for the mineral assemblage quartz + muscovite + biotite + plagioclase + garnet. *Contributions to Mineralogy and Petrology* **104**, 225–234.

Holdsworth, R.E. and Roberts, A.M. 1984. Early curvilinear fold structures in the Moine of the Glen Garry region, Inverness-shire. *Journal of the Geological Society of London* **141**, 327–338.

Holland, H.D., Feakes, C.R. and Zbinden, E.A. (1989) The Flin Flon paleosol and the composition of the atmosphere at 1.8 BYBP. *American Journal of Science* **289**, 362–389.

Hoeppener, R. (1956) Zum Problem der Bruchbildung, Schieferung und Faltung. *Geologische Rundschau* **45**, 247–283.

Houseman, G.A., McKenzie, D.P. and Molnar, P. (1981) Convective instability of a thickened boundary layer and its relevance for the thermal evolution of continental convergence belt. *Journal of Geophysical Research* **86**, 6115–6132.

Hunt, P.A. and Roddick, J.C. (1992) A compilation of K–Ar ages, Report 22. In *Radiogenic Age and Isotopic Studies: Report 6, Geological Survey of Canada Paper* 92–2, pp. 179–226.

Hunt, P.A. and Roddick, J.C. (1993) A compilation of K–Ar and ^{40}Ar–^{39}Ar ages, Report 23. In *Radiogenic Age and Isotopic Studies: Report 7, Geological Survey of Canada Paper* 93–2, pp. 127–157.

Hunt, P.A. and Zwanzig, H.V. (1993) U–Pb ages of intrusion, metamorphism and deformation in the Batty Lake area, Kisseynew gneiss belt, Manitoba. In *Manitoba Energy and Mines, Minerals Division, Report of Activities*, pp. 34–37.

Huppert, H.E. and Sparks, S.J. (1988) The generation of granitic magmas by intrusion of basalt into continental crust. *Journal of Petrology* **29**, 599–624.

Hutcheon, I. (1978) Calculation of metamorphic pressure using the sphalerite–phyrrotite equilibrium. *American Mineralogist* **63**, 87–95.

Hutcheon, I. (1979) Sulfide–oxide–silicate equilibria; Snow Lake, Manitoba. *American Journal of Science* **279**, 643–665.

Jackson, A.N.R. (1983) Volcanism and genesis of Cu–Zn mineralization at Cook Lake, Snow Lake greenstone belt, Manitoba. Unpublished Ph.D. Thesis, University of Western Ontario, London.

Jamieson, R.A. and Vernon, R.H. (1987) Timing of porphyroblast growth in the Fleur de Lys Supergroup, Newfoundland. *Journal of Metamorphic Geology* **5**, 273–288.

Jefferey, G.B. (1922) The motion of ellipsoidal particles immersed in a viscous fluid. *Royal Society of London Proceedings Series A* **102**, 161–177.

Johnson, S.E. (1990) Lack of porphyroblast rotation in the Otago schists, New Zealand: implications for crenulation cleavage development, folding and deformation partitioning. *Journal of Metamorphic Geology* **8**, 13–30.

Johnson, S.E. and Vernon, R.H. (1995) Inferring the timing of porphyroblast growth in the absence of continuity between inclusion trails and matrix foliations: can it be reliably done? *Journal of Structural Geology* **17**, 1203–1206.

Kay, R.W. and Kay, S.M. (1993) Delamination and delamination magmatism. *Tectonophysics* **219**, 177–189.

Kienow, S. (1942) Grundzüge einer Theorie der Faltungs- und Schieferungsvorgänge. *Fortschritte der Geologie und Paläontologie* **14**, 1–129.

Klasner, J.S. and King, E.R. (1990) A model for the tectonic evolution of the Trans-Hudson Orogen in North and South Dakota. In *The Early Proterozoic Trans-Hudson Orogen of North America*, ed. J.F. Lewry and M.R. Stauffer, Vol. 37, pp. 271–285. *Geological Association of Canada Special Paper*.

Kleemann, U. and Reinhardt, J. (1994) Garnet–biotite thermometry revisited: The effect of AL^{VI} and Ti in biotite. *European Journal of Mineralogy* **6**, 925–941.

Knill, J.L. and Knill, D.C. (1958) Some discordant fold structures from the Dalradian of Craignish, Argyll, and Rosguill, Co. Donegal. *Geological Magazine* **95**, 497–510.

Knipe, R.J. (1981) The interaction of deformation and metamorphism in slate. *Tectonophysics* **78**, 249–272.

Knipe, R.J. and White, S.H. (1977) Microstructural variation of an axial plane cleavage around a fold – a high voltage electron microscope study. *Tectonophysics* **39**, 355–380.

Kornik, L.J. and MacLaren, A.S. (1966) Aeromagnetic study of the Churchill–Superior boundary in northern Manitoba. *Canadian Journal of Earth Sciences* **3**, 547–557.

Kraus, J. and Menard, T. (1995) Metamorphism of the File Lake Formation, Snow Lake: Preliminary results. In *Manitoba Energy and Mines, Minerals Division, Report of Activities*, pp. 160–163.

Kraus, J. and Menard, T. (1996) Low-medium pressure, low to high temperatures metamorphism during shortening of thinned crust: Transition Flin Flon-Kisseynew Belts, Snow Lake segment, Manitoba. *Geological Association of Canada, Program with Abstracts* **21**, A–52.

Kraus, J., Menard, T., Gordon, T.M. and Williams, P.F. (1996) Low- to high-temperature, low- to medium-pressure metamorphism during compressional deformation, Kisseynew sedimentary gneiss belt, internal Trans-Hudson Orogen, Canada. *Tectonics Studies Group Meeting, Program with Abstracts.*

Kraus, J. and Williams, P.F. (1993a) Tectonometamorphic development of the eastern segment of the Flin Flon–Snow Lake greenstone belt, Trans-Hudson Orogen, Manitoba. *Geological Association of Canada, Program with Abstracts* **18**, A–54.

Kraus, J. and Williams, P.F. (1993b) Structural studies in the eastern segment of the Flin Flon-Snow Lake greenstone belt, Trans-Hudson Orogen, Snow Lake, Manitoba. *Canadian Tectonics Group Annual Meeting, Program with Abstracts.*

Kraus, J. and Williams, P.F. (1993c) Structural studies along the northern margin of the Flin Flon –Snow Lake greenstone belt, Snow Lake. In *Manitoba Energy and Mines, Minerals Division, Report of Activities*, pp. 117–118.

Kraus, J. and Williams P.F. (1994a) Structure of the Squall Lake area, Flin Flon-Snow Lake domain-Kisseynew boundary, Trans-Hudson Orogen, Snow Lake, Manitoba. *Canadian Tectonics Group Annual Meeting, Program with Abstracts.*

Kraus, J. and Williams, P.F. (1994b) Structure of the Squall Lake area, Snow Lake (NTS 63K/16). In *Manitoba Energy and Mines, Minerals Division, Report of Activities*, pp. 189–193.

Kraus, J. and Williams, P.F. (1994c) Cleavage development and the timing of metamorphism in the File Lake Formation across the Threehouse synform, Snow Lake, Manitoba: A new paradigm. *Lithoprobe Trans-Hudson Orogen Transect Report* **38**, 230–237.

Kraus, J. and Williams, P.F. (1995a) History of a single foliation during the Hudsonian orogeny, Kisseynew belt, Snow Lake, Manitoba. *Geological Association of Canada, Program with Abstracts* **20**, A–54.

Kraus, J. and Williams, P.F. (1995b) Porphyroblast–matrix relationships and a simple answer to porphyroblast rotation from Snow Lake, Manitoba. *Canadian Tectonics Group Annual Meeting, Program with Abstracts.*

Kraus, J. and Williams, P.F. (1995c) The tectonometamorphic history of the Snow Lake area, Manitoba, revisited. *Lithoprobe Trans-Hudson Orogen Transect Report* **48**, 206–212.

Kretz, R. (1983) Symbols for rock-forming minerals. *American Mineralogist* **68**, 277–279.

Le Breton, N. and Thompson, A.B. (1988) Fluid-absent (dehydration) melting of biotite in metapelites in the early stages of crustal anatexis. *Contributions to Mineralogy and Petrology* **99**, 226–237.

Leclair, A.D., Lucas, S.B., Broome, H.J., Viljoen, D.W. and Weber, W. (1997) Regional mapping of Precambrian basement beneath Phanerozoic cover in southeastern Trans-Hudson Orogen, Manitoba and Saskatchewan. *Canadian Journal of Earth Sciences* **34**, 618–634.

Lewry, J.F. (1981) Lower Proterozoic arc—Microcontinent collisional tectonics in the western Churchill province. *Nature* **294**, 69–72.

Lewry, J.F. and Collerson, K.D. (1990) The Trans-Hudson Orogen: extent, subdivision, and problems. In *The Early Proterozoic Trans-Hudson Orogen of North America*, ed. J.F. Lewry and M.R. Stauffer, Vol. 37, pp. 1–14. *Geological Association of Canada Special Paper*.

Lewry, J.F., Hajnal, Z., Green, A., Lucas, S.B., White, D., Stauffer, M.R., Ashton, K.E., Weber, W. and Clowes, R. (1994) Structure of a Paleoproterozoic continent–continent collision zone: a LITHOPROBE seismic reflection profile across the Trans-Hudson Orogen, Canada. *Tectonophysics* **232**, 161–178.

Lewry, J.F., Lucas, S.B., Stern, R.A. and Ansdell, K.M. (1996) Tectonic assembly and orogenic closure in the Trans-Hudson Orogen. *Geological Association of Canada, Program with Abstracts* 21, A–56.

Lewry, J.F., MacDonald, R., Livesey, C., Meyer, R., Van Schmus, R. and Bickford, M.E. (1987) U–Pb geochronology of accreted terranes in the Trans-Hudson Orogen. In *Geochemistry and mineralization of Proterozoic volcanic suites*, ed. T.C. Pharaoh, R.D. Beckinsdale and D. Rickard, pp. 147–166. *Geological Society of London Special Publication* 33.

Lewry, J.F. and Sibbald, T.I.I. (1977) Variaton in lithology and tectonometamorphic relationships in the Precambrian basement of northern Saskatchewan. *Canadian Journal of Earth Sciences* **14**, 1453–1467.

Lewry, J.F. and Stauffer, M.R. (editors) (1990) The Early Proterozoic Trans-Hudson Orogen of North America. *Geological Association of Canada Special Paper* 37.

Lewry, J.F., Stauffer, M.R. and Fumerton, S.L. (1981) A Cordilleran-type batholithic belt in the Churchill Province in northern Saskatchewan. *Precambrian Research* **14**, 277–313.

Lewry, J.F., Thomas. D.J., MacDonald, R. and Chiarenzelli, J.R. (1990) Structural relations in accreted terranes of the Trans-Hudson Orogen, Saskatchewan: Telescoping in a collisional regime? In *The Early Proterozoic Trans-Hudson Orogen of North America*, ed. J.F. Lewry and M.R. Stauffer, Vol. 37, pp. 75–94. *Geological Association of Canada Special Paper*.

Lister, G.S. (1993) Do smoothly curved, spiral-shaped inclusion trails signify porphyroblast rotation?: comment. *Geology* **21**, 479–480.

Lister, G.S. and Williams, P.F. (1983) The partitioning of deformation in flowing rock masses. *Tectonophysics* **92**, 1–33.

Loosveld, R.J.H. (1989) The synchronism of crustal thickening and low–pressure facies metamorphism in the Mount Isa Inlier, Australia 2. Fast convective thinning of mantle lithosphere during crustal thickening. *Tectonophysics* **165**, 191–218.

Loosveld, R.J.H. and Etheridge, M.A. (1990) A model for low-pressure facies metamorphism during crustal thickening. *Journal of Metamorphic Geology* **8**, 257–267.

Lucas, S.B. (1989) Structural evolution of the Cape Smith Thrust Belt and the role of out-of-sequence faulting in the thickening of mountain belts. *Tectonics* **8**, 655–676.

Lucas, S.B. (1990) Relations between thrust belt evolution, grain scale deformation and metamorphic processes: Cape Smith Belt, northern Quebec. *Tectonophysics* **178**, 151–182.

Lucas, S.B., Green, A., Hajnal, Z., White, D., Lewry, J.F., Ashton, K.E., Weber, W. And Clowes, R. (1993) Deep seismic profile across a Proterozoic collision zone: surprises at depth. *Nature* **363**, 339–342.

Lucas, S.B., Stern, R.A., Syme, E.C., Reilly, B.A. and Thomas, D.J. (1996a) Intraoceanic tectonics and the development of continental crust: 1.92-1.84 Ga evolution of the Flin Flon Belt, Canada. *Geological Society of America Bulletin* **108**, 602–629.

Lucas, S.B., Stern, R.A., Froese, E., Syme, E.C., Zwanzig, H.V., Bailes, A.H., Ashton, K.E., Maxeiner, R.O., Ansdell, K.M., Lewry, J.F., Ryan, J.J. and Kraus, J. (1997) Tectonics and terminology of the southeastern Reindeer Zone, Trans-Hudson Orogen (Manitoba and Saskatchewan). *Geological Association of Canada, Program with Abstracts* **22**, A–93.

Lucas, S.B. and St-Onge, M.R. (1992) Terrane accretion in the internal zone of the Ungava orogen, northern Quebec. Part 2: Structural and metamorphic history. *Canadian Journal of Earth Sciences* **29**, 765–782.

Lucas, S.B., White, D.J., Bleeker, W., Hajnal, Z., Lewry, J.F., and Weber, W. (1996b) Crustal structure of the Superior boundary zone (Thompson Belt) from new Lithoprobe seismic reflection data. *Lithoprobe Trans-Hudson Orogen Transect Report* **55**, 82–94.

Lucas, S.B., White, D., Hajnal, Z., Lewry, J., Green, A., Clowes, R., Zwanzig, H.V., Ashton, K.E., Schledewitz, D., Stauffer, M.R., Norman, A.R., Williams, P.F. and Spence, G. (1994) Three-dimensional collisional structure of the Trans-Hudson Orogen. *Tectonophysics* **232**, 161–178.

Lux, D.R., De Yoreo, J.J., Guidotti, C.V. and Decker, E.R. (1986) Role of plutonism in low-pressure metamorphic belt formation. *Nature* **323**, 794–797.

Machado, N. and David, J. (1992) U–Pb geochronology of the Reindeer–Superior transition zone and of the Snow Lake area: preliminary results. *Lithoprobe Trans-Hudson Orogen Transect Report* **26**, 26–43.

Machado, N., David, J., Scott, D.J., Lamothe, D., Philippe, S., and Gariépy, C. (1993) U–Pb geochronology on the Western Cape Smith Belt, Canada: New insights on the age of initial rifting and arc magmatism. *Precambrian Research* **63**, 211–224.

Machado, N., Heaman, L., Krogh, T.E. and Weber, W. (1987) U–Pb geochronology program: Thompson Belt, northern Superior Province. In *Manitoba Energy and Mines, Minerals Division, Report of Activities*, pp. 145–150.

Machado, N., Krogh, T.E. and Weber, W. (1990) U–Pb geochronology of basement gneisses in the Thompson Belt (Manitoba): evidence for pre-Kenoran and Pikwitonei-type crust and early Proterozoic basement reactivation in the western margin of the Archean Superior Province. *Canadian Journal of Earth Sciences* **27**, 794–802.

Machado, N. and Zwanzig, H.V. (1995) U–Pb geochronology of the Kisseynew Domain in Manitoba: Provenance ages for metasediments and timing of magmatism. *Lithoprobe Trans-Hudson Orogen Transect Report* **48**, 133–134.

Machado, N., Zwanzig, H.V. and Parent, M. (1996) U–Pb geochronology of the Kisseynew Domain, Manitoba: Provenance ages for metasediments and timing of magmatism, metamorphism and deformation. *Geological Association of Canada, Program with Abstracts* 21, A–61.

Mäder, U.K., Percival, J.A. and Berman, R.G. (1994) Thermobarometry of garnet-clinopyroxene-hornblende granulites from the Kapuskasing structural zone. *Canadian Journal of Earth Sciences* **31**, 1134–1145.

Mancktelow, N.S. (1994) On volume change and mass transport during the development of crenulation cleavage. *Journal of Structural Geology* **16**, 1217–1231.

Mancktelow, N.S. and Visser, P. (1993) The rotation of garnet porphyroblasts around a single fold, Lukmanier Pass, Central Alps: Reply. *Journal of Structural Geology* **15**, 1369–1372.

Mandler, H.A.F. and Clowes, R.M. (1997) Evidence for extensive tabular intrusions in the Precambrian shield of western Canada: A 160-km-long sequence of bright reflectors. *Geology* **25**, 271–275.

March, A. (1932) Mathematische Theorie der Regelung nach der Korngestalt bei affiner Deformation. *Zeitschrift für Kristallographie, Kristallgeometrie und Kristallphysik* **81**, 285–297.

Marlow, P.C. and Etheridge, M.A. (1977) Development of a layered crenulation cleavage in mica-schists of the Kanmantoo Group near Macclesfield, South Australia. *Geological Society of America Bulletin* **88**, 873–882.

Marshall, D., Connors, K.A. and Ansdell, K.M. (1997) Thermochronology of hornblende and biotite from the Wekusko Lake area, Flin Flon Domain, Trans-Hudson Orogen, Manitoba. In *Radiogenic Age and Isotopic Studies: Report 8, Geological Survey of Canada, Current Research* 1994–F, pp. 87–96.

Mawer, C.K. and Williams, P.F. (1991) Progressive folding and foliation development in a sheared, coticule-bearing phyllite. *Journal of Structural Geology* **13**, 539–555.

McKenzie, D.P. (1978) Some remarks on the development of sedimentary basins. *Earth and Planetary Science Letters* **40**, 25–32.

McMullin, D.W.A., Berman, R.G. and Greenwood, H.J. (1991) Calibration of the SGAM thermobarometer for pelitic rocks using data from phase equilibrium experiments and natural assemblages. *Canadian Mineralogist* **29**, 889–908.

Means, W.D. (1994) Rotational quantities in homogeneous flow and the development of small-scale structure. *Journal of Structural Geology* **16**, 437–445.

Menard, T. and Gordon, T.M. (1995) Syntectonic alteration of VMS deposits, Snow Lake, Manitoba. In *Manitoba Energy and Mines, Minerals Division, Report of Activities*, pp. 164–167.

Menard, T. and Gordon, T.M. (1997) Metamorphic P–T paths from the eastern Flin Flon Belt and Kisseynew Domain, Snow Lake, Manitoba. In *Tectonometamorphic Studies in the Canadian Shield (part I)*, ed. R.G. Berman and R.M. Easton. *Canadian Mineralogist* **35**, 1093–1115.

Menard, T. and Spear, F.S. (1993) Metamorphism of calcic pelitic schists, Stafford Dome, Vermont: compositional zoning and reaction history. *Journal of Petrology* **34**, 977–1005.

Meneilly, A.W. and Storey, B.C. (1986) Ductile thrusting within a subduction complex on Signy island, South Orkney islands. *Journal of Structural Geology* **8**, 457–472.

Meyer, M.T., Bickford, M.E. and Lewry, J.F. (1992) The Wathaman batholith: an Early Proterozoic continental arc in the Trans-Hudson orogenic belt, Canada. *Geological Society of America Bulletin* **104**, 1073–1085.

Moore, J.M. and Froese, E. (1972) Geological setting of the Snow Lake area. In *Report of Activities, Part B, Geological Survey of Canada Paper* 72–B, pp. 78–81.

Morton, R.L. and Franklin, J.M. (1987) Two-fold classification of Archean volcano-associated massive sulphide deposits. *Economic Geology* **82**, 1057–1063.

Mukhopadhyay, M. and Gibb, R.A. (1981) Gravity anomalies and deep structure of eastern Hudson Bay. *Tectonophysics* **72**, 43–60.

Nelson, K.D. (1992) Are crustal thickness variations in old mountain belts like the Appalachians a consequence of lithospheric delamination? *Geology* **20**, 498–502.

Nelson, K.D., Baird, D.J., Walters, J.J., Hauck, M., Brown, L.D., Oliver, J.E., Ahern, J.L., Hajnal, Z., Jones, A.G. and Sloss, L.L. (1993) Trans-Hudson Orogen in Montana and North Dakota: New COCORP deep-profiling results. *Geology* **21**, 447–450.

Nickelsen, R.P. (1979) Sequence of structural stages of the Alleghany Orogeny, at the Bear Valley Strip Mine, Shamokin, Pennsylvania. *American Journal of Science* **279**, 225–271.

Norman, A.R. and Williams, P.F. (1993) The corundum conundrum: lower crustal anatexis in the Kisseynew gneiss belt at 1830 Ma. In *New perspectives on the Flin Flon–Snow Lake–Hanson Lake belt from the NATMAP Shield Margin Project. Special Meeting of the Flin Flon–Creighton CIM Branch,* Extended abstracts volume, pp. 34–45.

Norman, A.R., Williams, P.F. and Ansdell, K.M. (1995) Early Proterozoic deformation along the southern margin along the southern margin of the Kisseynew gneiss belt, Trans-Hudson Orogen: a 30 million year progressive deformation cycle. *Canadian Journal of Earth Sciences* **32**, 875–894.

Parent, M., Machado, N and Zwanzig, H.V. (1995) Timing of metamorphism and deformation in the Jungle Lake area, southern Kisseynew belt, Manitoba: evidence from U–Pb geochronology of monazite and zircon. *Lithoprobe Trans-Hudson Orogen Transect Report* **48**, 131–132.

Park, A.F. (1991) Continental growth by accretion: A tectonostratigraphic terrane analysis of the evolution of the western and central Baltic Shield, 2.50 to 1.75 Ga. *Geological Society of America Bulletin* **103**, 522–537.

Parrish, R.R. (1989) U–Pb geochronology of the Cape Smith belt and Sugluk block, northern Quebec. *Geoscience Canada* **16**, 126–130.

Parrish, R.R. (1990) U–Pb dating of monazite and its application to geological problems. *Canadian Journal of Earth Sciences* **27**, 1431–1450.

Passchier, C.W. (1987) Efficient use of the velocity gradients tensor in flow modelling. *Tectonophysics* **136**, 159–163.

Passchier, C.W. and Trouw, R.A.J. (1996) *Microtectonics*. Springer Verlag.

Passchier, C.W., Trouw, R.A.J., Zwart, H.J. and Vissers, R.L.M. (1992) Porphyroblast rotation: eppur si muove? *Journal of Metamorphic Geology* **10**, 283–294.

Patiño Douce, A.E. and Beard, J.S. (1995) Dehydration melting of biotite gneiss and quartz amphibolite from 3–15 kbar. *Journal of Petrology* **36**, 707–738.

Patiño Douce, A.E. and Johnston, A.D. (1991) Phase equilibria and melt productivity in the pelitic system: implications for the origin of peraluminous granitoids and aluminous granulites. *Contributions to Mineralogy and Petrology* **107**, 202–218.

Perkins, D. (1991) Metamorphism of the Kisseynew gneisses and related rocks of the Reindeer zone, Trans-Hudson Orogen, northern Saskatchewan. *Canadian Journal of Earth Sciemces* **28**, 1664–1676.

Phillips, E.R. and Key, R.M. (1992) Porphyroblast–fabric relationships: an example from the Appin Group in the Glen Roy area. *Scottish Journal of Geology* **28**, 89–101.

Platt, J.P. and England, P.C. (1993) Convective removal of lithosphere beneath mountain belts: thermal and mechanical consequences. *American Journal of Science* **293**, 307–336.

Powell, R. and Holland, T.J.B. (1988) An internally consistent dataset with uncertainties and correlations: 3. Applications to geobarometry, worked examples and a computer program. *Journal of Metamorphic Geology* **6**, 173–204.

Ramberg, H. (1963) Evolution of drag folds. *Geological Magazine* **100**, 97–106.

Ramberg, H. (1964) Selective buckling of composite layers with contrasted rheological properties, a theory for simultaneous formation of several orders of folds. *Tectonophysics* **1**, 307–341.

Ramsay, J.G. (1962) The geometry and mechanics of formation of "similar" type folds. *Journal of Geology* **70**, 309–327.

Reinhardt, J. (1992) Low-pressure, high-temperature metamorphism in a compressional tectonic setting: Mary Kathleen Fold Belt, northeastern Australia. *Geological Magazine* **129**, 41–57.

Reinhardt, J. and Rubenach, M.J. (1989) Temperature–time relationships across metamorphic zones: evidence from porphyroblast–matrix relationships in progressively deformed metapelites. *Tectonophysics* **158**, 141–161.

Rickard, M.J. (1961) A note on cleavages in crenulated rocks. *Geological Magazine* **98**, 324–332.

Ricketts, B.D. and Donaldson, J.A. (1981) Sedimentary history of the Belcher Group of Hudson Bay. In *Proterozoic Basins of Canada*, ed. F.H.A. Campbell. *Geological Survey of Canada Paper* 81–10, pp. 235–254.

Rosenfeld, J.L. (1970) Rotated garnets in metamorphic rocks. *Geological Society of America Special Paper* 129.

Russell, G.A. (1957) Structural Studies of the Snow Lake–Herb Lake area, Herb Lake Mining Division, Manitoba. *Manitoba Mines Branch Publication* 55–3.

Ryan, J.J. and Williams, P.F. (1995) The Elbow Lake area: a long lived deformation corridor. *Lithoprobe Trans-Hudson Orogen Transect Report* **48**, 156–161.

Ryan, J.J. and Williams, P.F. (1996a) Pre-Missi deformation in the Central Flin Flon Belt; The steepening of strata and crustal thickening. *Lithoprobe Trans-Hudson Orogen Transect Report* **55**, 50–59.

Ryan, J.J. and Williams, P.F. (1996b) The structural anatomy of the central Flin Flon Belt, northern Manitoba. In *Current Research, Part C, Geologial Survey of Canada, Paper* 1996–C, pp. 105–116.

Ryan, J.J. and Williams, P.F. Structural evolution of the Eastern Amisk collage, southeastern Trans-Hudson Orogen. *Canadian Journal of Earth Sciences*, in press.

Sacks, P.E. and Secor, D.T. (1990) Delamination in collisional orogens. *Geology* **18**, 999–1002.

Sander, B. (1930) *Gefügekunde der Gesteine.* Julius Springer, Wien.

Sandiford, M. and Powell, R. (1991) Some remarks on high-temperature—low-pressure metamorphism in convergent orogens. *Journal of Metamorphic Geology* **9**, 333–340.

Scoates, R.F.J. (1981) The volcanic rocks of the Fox River belt, northeastern Manitoba. *Manitoba Energy and Mines, Minerals Division, Geological Report* GR81–1.

Scott, D.J. and St-Onge, M.R. (1995) Contraints on Pb-closure temperature in titanite based on rocks from the Ungava orogen, Canada: Implications for U–Pb gechronology and P-T-t path determinations. *Geology* **23**, 1123–1126.

Scott, S.D. (1976) Application of the sphalerite geobarometer to regionally metamorphosed terranes. *American Mineralogist* **61**, 661–670.

Sharpton, V.L., Grieve, R.A.F., Thomas M.D. and Halpenny, J.F. (1987) Horizontal gravity gradient: an aid to the definition of crustal structure in North America. *Geophysical Research Letters* **14**, 808–811.

Skirrow, R.G. (1987) Silification in a lower semiconformable alteration zone near the Chisel Lake Zn–Cu massive sulphide deposit, Manitoba. Unpublished M.Sc. Thesis, Carleton University, Ottawa.

Skjernjaa, L. (1980) Rotation and deformation of randomly oriented planar and linear structures in progressive simple shear. *Journal of Structural Geology*, **2**, 101–109.

Schmidt, W. (1932) *Tektonik und Verformungslehre*. Gebrüder Bornträger, Berlin.

Schoneveld, C. (1977) A study of some typical inclusion patterns in strongly paracrystalline-rotated garnets. *Tectonophysics* **39**, 453–471.

Schoneveld, C. (1979) The geometry and significance of inclusion patterns in syntectonic porphyroblasts. Unpublished PhD thesis, University of Leiden.

Sitter, L.U. de (1956) *Structural Geology*. McGraw-Hill, New York.

Spear, F.S. (1988). Metamorphic fractional crystallisation and internal metasomatism by diffusional homogenization of zoned garnets. *Contributions to Mineralogy and Petrology* **99**, 507–517.

Spear, F.S. (1991) On the interpretation of peak metamorphic temperatures in light of garnet diffusion during cooling. *Journal of Metamorphic Geology* **9**, 379–388.

Spear, F.S. (1993) Metamorphic phase equilibria and pressure–temperature–time paths. *Mineralogical Society of America Monograph* 1.

Spear, F.S. and Cheney, J.T. (1989) A petrogenetic grid for pelitic schists in the system SiO_2–Al_2O_3–FeO–MgO–K_2O–H_2O. *Contributions to Mineralogy and Petrology* **101**, 149–167.

Spear, F.S. and Florence, F.P. (1992) Thermobarometry in granulites: pitfalls and new approaches. *Precambrian Research* **55**, 209–241.

Spear, F.S., Kohn, M.J., Florence, F.P. and Menard, T. (1991) A model for garnet and plagioclase growth in pelitic schists: implications for thermobarometry and P–T path determinations. *Journal of Metamorphic Geology* **8**, 683–696.

Spry, A. (1969) *Metamorphic Textures*. Pergammon Press, Oxford.

Stauffer, M.R. (1981) Lower Proterozoic arc–Microcontinent collisional tectonics in the western Churchill province. *Nature* **294**, 69–72.

Stauffer, M.R. (1984) Manikewan: an Early Proterozoic ocean in central Canada, its igneous history and orogenic closure. *Precambrian Research* **25**, 257–281.

Stauffer, M.R. (1990) The Missi Formation: an Aphebian mollasse deposit in the Reindeer Lake Zone the Trans-Hudson Orogen, Canada. In *The Early Proterozoic Trans-Hudson Orogen of North America*, ed. J.F. Lewry and M.R. Stauffer, Vol. 37, pp. 121–141. *Geological Association of Canada Special Paper*.

Stauffer, M.R. and Lewry, J.F. (1993) Regional setting of the Needle Falls Shear Zone, Trans-Hudson Orogen. *Canadian Journal of Earth Sciences* **30**, 1338–1354.

Steinhardt, C.K. (1989) Lack of porphyroblast rotation in noncoaxially deformed schists from Petrel Cove, South Australia, and its implications. *Tectonophysics* **158**, 127–140.

Stern, R.A., Syme, E.C., Bailes, A.H. and Lucas, S.B. (1995a) Paleoproterozoic (1.90–1.86 Ga) arc volcanism in the Flin Flon Belt, Trans-Hudson Orogen, Canada. *Contributions to Mineralogy and Petrology* **119**, 117–141.

Stern, R.A., Syme, E.C. and Lucas, S.B. (1995b) Geochemistry of 1.9 Ga MORB- and OIB-like basalts from the Amisk collage, Flin Flon Belt, Canada: Evidence for an intra-oceanic origin. *Geochimica et Cosmochimica Acta* **59**, 3131–3154.

Stewart, L.K. (1997) Experimental investigation of the effects of fluid heterogeneity upon the motion of rigid ellipsoidal inclusions during bulk inhomogeneous shortening. *Journal of Structural Geology* **19**, 1231–1243.

Stockwell, C.H. (1937) Gold Deposits of the Herb Lake area, northern Manitiba. *Geological Survey of Canada Memoir* 208.

Stockwell, C.H. (1961) Structural provinces, orogenies, and time classification of rocks of the Canadian Precambrian Shield. In *Age determinations by the Geological Survey of Canada*, ed. J.A. Lowden. *Geological Survey of Canada Paper* 61–17, pp. 108–118.

St-Onge, M.R. and Lucas, S.B. (1991) Evolution of regional metamorphism in the Cape

Smith Thrust belt (northern Quebec, Canada): interaction of tectonic and thermal processes. *Journal of Metamorphic Geology* **9**, 515–534.

St-Onge, M.R. and Lucas, S.B. (1993) Geology of the eastern Cape Smith Belt. Parts of the Kangiosujuaq, Cratére du Nouveau-Quebec, and Lacs Nuvilik map areas, Quebec. *Geological Survey of Canada Memoir* 438.

St-Onge, M.R. and Lucas, S.B. (1995) Large-scale fluid infiltration, metasomatism and re-equilibration of Archean basement granulites during Paleoproterozoic thrust belt construction, Ungava orogen, Canada. *Journal of Metamorphic Geology* **13**, 509–535.

St-Onge, M.R., Lucas, S.B. and Parrish, R.R. (1992) Terrane accretion in the internal zone of the Ungava orogen, northern Quebec. Part 1: Tectonostratigraphic assemblages and their tectonic implications. *Canadian Journal of Earth Sciences* **29**, 765–782.

Syme, E.C. (1990) Stratigraphy and geochemistry of the Lynn Lake and Flin Flon volcanic belts, Manitoba. In *The Early Proterozoic Trans-Hudson Orogen of North America*, ed. J.F. Lewry and M.R. Stauffer, Vol. 37, pp. 143–161. *Geological Association of Canada Special Paper.*

Syme, E.C. and Bailes, A.H. (1993) Stratigraphic and tectonic setting of volcanigenic massive sulfide deposits, Flin Flon, Manitoba. *Economic Geology* **88**, 566–589.

Syme, E.C., Bailes, A.H. and Lucas, S.B. (1995) Geology of the Reed Lake area (parts of 63/K9 and 63/K10). In *Manitoba Energy and Mines, Minerals Division, Report of Activities*, pp. 42–60.

Symons, D.T.A. (1991) Paleomagnetism of the Proterozoic Wathaman batholith and the suturing of the Trans-Hudson Orogen in Saskatchewan. *Canadian Journal of Earth Sciences* **28**, 1931–1938.

Symons, D.T.A. (1994) Geotectonics of the Peter Lake domain in the Proterozoic Trans-Hudson orogenic belt of Saskatchewan, Canada, from Paleomagnetism. *Precambrian Research* **69**, 11–24.

Symons, D.T.A., Gala, M. and Palmer, H.C. (1995) Fitting paleomagnetic data to a plate tectonic model for the Trans-Hudson Orogen with a focus on the Hanson Lake Block. *Lithoprobe Trans-Hudson Orogen Transect Report* **48**, 66–77.

Symons, D.T.A., Lewchuk, M.T., Harris, M.J., Gala, M. and Palmer, H.C. (1996) Paleomagnetic studies in the Trans-Hudson Orogen. *Lithoprobe Trans-Hudson Orogen Transect Report* **55**, 69–72.

Tarney, J. (1976) Geochemistry of Archaean high-grade gneisses, with implications as to the origin and evolution of the Precambrian crust. In *The Early History of the Earth*, ed. B.F. Windley, Wiley-Interscience, London, pp. 405–418.

Tarney, J., Weaver, B.L. and Windley, B.F. (1982) Geological and geochemical evolution of the Archaean continental crust. *Revista Brasileira de Geosciências* **12**, 53–59.

Thom, A., Arndt, N. and Chauvel, C. (1987) Volcanic arcs and granitoid rocks in the Reindeer Lake zone, Saskatchewan. *Geological Association of Canada, Program with Abstracts* 12, A–95.

Thom, A., Arndt, N., Chauvel, C. and Stauffer, M.R. (1990) Flin Flon and western La Ronge belts, Saskatchewan: Products of Proterozoic subduction-related volcanism. In *The Early Proterozoic Trans-Hudson Orogen of North America*, ed. J.F. Lewry and M.R. Stauffer, Vol. 37, pp. 163–176. *Geological Association of Canada Special Paper*.

Thompson, A.B. (1981) The pressure–temperature (P,T) plane viewed by geophysicists and petrologists. *Terra Cognita* **1**, 11–20.

Thomas, M.D., Sharpton, V.L. and Grieve, R.A.F. (1987) Gravity patterns and the Precambrian structure in the North American central plains. *Geology* **15**, 489–492.

Thompson, P.H. (1989) Moderate overthickening of thinned sialic crust and the origin of granitic magmatism and regional metamorphism in low-P – high-T terranes. *Geology* **17**, 520–523.

Tobisch, O.T., Fleuty, M.J., Merth, S.S., Mukhopadhyay, D. and Ramsay, J.G. (1970) Deformational and metamorphic history of the Moinian and Lewisian rock between Strathconon and Glenaffric. *Scottish Journal of Geology* **6**, 243–265.

Tobisch, O.T. and Paterson, S.R. (1988) Analysis and interpretation of composite foliations in areas of progressive deformation. *Journal of Structural Geology* **10**, 745–754.

Todt, W., Chauvel, C., Arndt, N. and Hoffman, A.W. (1984) Pb isotopic composition and age of Proterozoic komatiites and related rocks from Canada. *EOS, Transactions of the American Geophysical Union* 65, pp. 1129.

Trembath, G.D. (1986) The compositional variation of staurolite in the area of Anderson Lake Mine, Snow Lake, Manitoba. Unpublished M.Sc. Thesis, University of Manitoba, Winnipeg.

Turner, F.J. and Weiss, L.E. (1963) *Structural analysis of metamorphic tectonites*. McGraw-Hill, New York.

Van Schmus, W.R., Bickford, M.E., Lewry, J.F. and MacDonald, R. (1987) U–Pb geochronology of the Trans-Hudson Orogen in northern Saskatchewan, Canada. *Canadian Journal of Earth Sciences* **24**, 407–427.

Vernon, R.H. (1977) Relationships between microstructures and metamorphic assemblages. *Tectonophysics* **39**, 439–452.

Vernon, R.H. (1978) Porphyroblast–matrix microstructural relationships in deformed metamorphic rocks. *Geologische Rundschau* **67**, 288–305.

Vernon, R.H. (1987) Growth and concentration of fibrous sillimanite related to heterogeneous deformation in K-feldspar-sillimanite metapelites. *Journal of Metamorphic Geology* **5** 51–68.

Vernon, R.H. (1988) Microstructural evidence of rotation and non-rotation of mica porphyroblasts. *Journal of Metamorphic Geology* **6**, 595–601.

Vernon, R.H. (1989) Porphyroblast–matrix microstructural relationships: recent approaches and problems. In *Evolution of metamorphic belts*, ed. J.S. Daly, R.A. Cliff and B.W.D. Yardley, pp. 83–112. *Geological Society of London Special Publication* 43.

Vielzeuf, D. and Holloway, J.R. (1988) Experimental determination of the fluid-absent melting relations in the pelitic system. Consequences for crustal differentiation. *Contributions to Mineralogy and Petrology* **98**, 257–276.

Visser, P. and Mancktelow, N.S. (1992) The rotation of garnet porphyroblasts around a single fold, Lukmanier Pass, Central Alps. *Journal of Structural Geology* **14**, 1193–1202.

Voll, G. (1960) New work on petrofabrics. *Liverpool Manchester Geological Journal* **2**, 503–567.

Walford, P.C. and Franklin, J.M. (1982) The Anderson Lake mine, Snow Lake, Manitoba. In *Precambrian Sulphide Deposits, H.S. Robinson Memorial Volume*, ed. R.W. Hutchinson, C.D. Spence and J.M. Franklin, Vol 25, pp. 481–521. *Geological Association of Canada, Special Paper*.

Wallis, S. (1992) Comment on "Do smoothly curved, spiral-shaped inclusion trails signify porphyroblast rotation?" *Geology* **20**, 1054–1055.

Warren, R.G. and Ellis, D.J. (1996) Mantle underplating, granite tectonics, and metamorphic P–T–t paths. *Geology* **24**, 663–666.

Waters, D.J. (1986) Metamorphic history of sapphirine-bearing and related magnesian gneisses from Namaqualand, South Africa. *Journal of Petrology* **27**, 541–565.

Watkinson, A.J. and Cobbold, P.R. (1981) Axial directions of folds in rocks with linear/planar fabrics. *Journal of Structural Geology* **3**, 211–217.

Watters, B.R. and Pearce, J. (1987) Metavolcanic rocks of the La Ronge Domain in the Churchill Province, Saskatchewan: Geochemical evidence for a volcanic arc origin. In *Geochemistry and mineralization of Proterozoic volcanic suites*, ed. T.C. Pharaoh, R.D. Beckinsdale and D. Rickard, pp. 167–182. *Geological Society of London Special Publications* 33.

Watters, B.R., Dostal, J., Slimmon, W.L. and Thomas, D.J. (1994) Geochemistry, petrogenesis and tectonic setting of Early Proterozoic volcanic rocks of the Flin Flon Domain, Saskatchewan (Canada): oceanic back-arc volcanism. *Neues Jahrbuch für Mineralogie Monatshefte* **9**, 416–432.

Weber, K. (1976) Gefügeuntersuchungen an transversalgeschieferten Gesteinen aus dem östlichen Rheinischen Schiefergebirge (Ein Beitrag zur Genese der transversalen Schieferung). *Geologisches Jahrbuch Reihe D* **15**, 1–99.

Weber, K. (1981) Kinematic and metamorphic aspects of cleavage formation in very low-grade metamorphic slates. *Tectonophysics* **78**, 291–306.

Weber, W. (1990) The Churchill–Superior Boundary Zone, Southeast Margin of the Trans-Hudson Orogen: A Review. In *The Early Proterozoic Trans-Hudson Orogen of North America*, ed. J.F. Lewry and M.R. Stauffer, Vol. 37, pp. 41–55. *Geological Association of Canada Special Paper.*

Weber, W. and Scoates, R.F.J. (1978) Archean and Proterozoic metamorphism in the northwestern Superior Province and along the Churchill–Superior boundary. In *Metamorphism in the Canadian Shield*, ed. J.A. Fraser and W.W. Heywood. *Geological Survey of Canada Paper* 78–10, pp. 5–16.

Wells, P.R.A. (1980) Thermal models for the magmatic accretion and subsequent metamorphism of continental crust. *Earth and Planetary Science Letters* **46**, 253–265.

White, D.J. and Lucas, S.B. (1994) A closer look at the Superior boundary zone. *Lithoprobe Trans-Hudson Orogen Transect Report* **38**, 35–41.

White, D.J., Lucas, S.B., Hajnal, Z., Green, A.G., Lewry, J.F., Weber, W., Bailes, A.H., Syme, E.C. and Ashton, K.E. (1994) Paleo-Proterozoic thick-skinned tectonics:

Lithoprobe seismic reflection results from the eastern Trans-Hudson Orogen. *Canadian Journal of Earth Sciences* **31**, 458–469.

White, D.J., Lucas, S.B., Hajnal, Z., Zwanzig, H. and Lewry, J.F. (1996) Seismic reflection images across the Kisseynew Domain northern boundary. *Lithoprobe Trans-Hudson Orogen Transect Report* **55**, 95–98.

Wickham, S.M. (1987) The segregation and emplacement of granitic magmas. *Journal of the Geological Society of London* **144**, 281–297.

Wickham, S.M. and Oxburgh, R.E. (1985) Continental rifts as a setting for regional metamorphism. *Nature* **318**, 330–333.

Wickham, S.M. and Oxburgh, R.E. (1987) Low pressure regional metamorphism in the Pyrenees and its implications for the thermal evolution of rifted continental crust. *Royal Society of London Philosophical Transactions, Series A*, **321**, 219–243.

Williams, M.L. (1994) Sigmoidal inclusion trails, punctuated fabric development, and interactions between metamorphism and deformation. *Journal of Metamorphic Geology* **12**, 1–21.

Williams, P.F. (1972) Development of metamorphic layering and cleavage in low-grade metamorphic rocks at Bermagui, Australia. *American Journal of Science* **272**, 1–47.

Williams, P.F. (1977) Foliation: a review and discussion. *Tectonophysics* **39**, 305–328.

Williams, P.F. (1979) The development of asymmetrical folds in a cross-laminated siltstone. *Journal of Structural Geology* **1**, 19–30.

Williams, P.F. (1985) Multiply deformed terrains-problems of correlation. *Journal of Structural Geology* **7**, 269–280.

Wiiiams, P. F. (1990) Differentiated layering in metamorphic rocks. *Earth Science Reviews* **29**, 267–281.

Williams, P.F and Compagnoni, R. (1983) Deformation and metamorphism in the Bard area of the Sesia Lanzo Zone, Western Alps, during subduction and uplift. *Journal of Metamorphic Geology* **1**, 117–140.

Williams, P.F., Means, W.D. and Hobbs, B.E. (1977) Development of axial-plane slaty cleavage and schistosity in experimental and natural materials. *Tectonophysics* **42**, 139–158.

Williams, P.F. and Schoneveld, C. (1981) Garnet rotation and the development of axial plane crenulation cleavage. *Tectonophysics* **78**, 307–334.

Williams, P.F. and Zwart, H.J. (1977) A model for the development of the Seve-Koeli Caledonian nappe complex. In *Energetics of Geological Processes*, ed. S.K. Saxena and S. Battacharji, pp.169–187, Springer Verlag.

Windley, B.F. and Tarney, J. (1986) The structural evolution of the lower crust of orogenic belts, present and past. In *The Nature of the lower Continental Crust*, ed. J.B. Dawson, D.A. Carlswell, D.A. Hall and K.H. Wedepohl, pp. 221–230. *Geological Society of London Special Publication* 24.

Wright, T.O. and Henderson, J.R. (1992) Volume loss during cleavage formation in the Meguma Group, Nova Scotia, Canada. *Journal of Structural Geology* **14**, 281–290.

Wyborn, L.A.I., Page, R.W. and McCulloch, M.T. (1988) Petrology, geochronology and isotope geochemistry of the post-1820 Ma granites of the Mount Isa Inlier: Mechanisms for the generation of Proterozoic anorogenic granites. *Precambrian Research* **40/41**, 509–541.

Zaleski, E. (1989) Metamorphism, structure and petrogenesis of the Linda massive sulphide deposit, Snow Lake, Manitoba, Canada. Unpublished Ph.D. Thesis, University of Manitoba, Winnipeg.

Zaleski, E. and Gordon, T.M. (1990) Metamorphic/structural reinterpretation of the Snow Lake region, Manitoba. *Lithoprobe Trans-Hudson Orogen Transect Report* **12**, 22.

Zaleski, E., Froese E. and Gordon, T.M. (1991) Metamorphic petrology of Fe–Zn–Mg–Al alteration at the Linda volcanogenic massive sulfide deposit, Snow Lake, Manitoba. *Canadian Mineralogist* **29**, 995–1017.

Zhai, Y. and Halls, H.C. (1994) Multiple episodes of dike emplacement along the northwestern margin of the Superior Province, Manitoba. *Journal of Geophysical Research* **99**, 21717–21732.

Zwanzig, H.V. (1990) Kisseynew Gneiss Belt in Manitoba: stratigraphy, structure and tectonic evolution. In *The Early Proterozoic Trans-Hudson Orogen of North America*, ed. J.F. Lewry and M.R. Stauffer, Vol. 37, pp. 95–120. *Geological Association of Canada Special Paper*.

Zwanzig, H.V. Evolution of the southern Kisseynew Belt, Manitoba: 1.9 Ga juvenile crust to 1.8 Ga collisional orogen. *Canadian Journal of Earth Sciences*, in press.

Zwanzig, H.V. and Schledewitz, D.C.P. (1992) Geology of the Kississing–Batty lakes area. *Manitoba Energy and Mines Geological Services Open File* OF92–2.

Zwart, H.J. (1960) The chronological succession of folding and metamorphism in the Central Pyrenees. *Geologische Rundschau* **50**, 203–218.

Zwart, H.J. (1962) On the determination of polymetamorphic mineral associations, and its application to the Bosost area (Central Pyrenees). *Geologische Rundschau* **52**, 38–65.

Zwart, H.J. (1967) The Duality of Orogenic Belts. *Geologie en Mijnbouw* **46**, 283–309.

Zwart, H.J. (1969) Metamorphic facies series in the European orogenic belts and their bearing on the causes of orogeny. *Geological Association of Canada. Special Paper* 5, pp. 7–16.

APPENDIX A: Mineral compositions used for P–T calculations

TABLE 4.1. GARNET COMPOSITIONS USED FOR P-T CALCULATIONS (WT %)

Sample	432 -P	425 -P1	420C -P3	60-2 -P1	CKOR3 -P2	93-40 -P10	XX5 -P1-B	SL53 -A-P1	D58 -P1	D156 -P1	D238 -1-P1	D238 -FK1	AN5 -1-2P
SiO_2	38.07	37.76	37.49	37.25	37.95	37.69	35.86	38.79	38.31	38.66	38.63	38.52	38.25
TiO_2	0.05	0.11	0.04	n.d.	0.02	0.08	0.09	n.d.	n.d.	0.04	n.d.	n.d.	0.04
Al_2O_3	21.35	20.97	21.19	21.43	21.28	21.29	21.00	21.78	21.45	21.57	21.79	21.56	21.55
MgO	1.76	1.19	2.44	2.86	3.08	3.16	2.76	4.40	2.98	3.95	4.62	4.66	4.40
FeO	32.03	24.95	37.84	35.33	35.85	32.76	37.97	33.40	37.97	36.78	35.13	34.10	35.02
MnO	3.83	8.80	0.72	2.16	1.99	2.63	0.21	0.62	0.46	0.87	0.69	1.22	1.49
CaO	4.64	7.40	1.76	1.52	1.66	2.35	1.30	3.61	1.69	1.48	2.13	1.34	1.46
Total	101.73	101.18	101.48	100.55	101.83	99.96	99.19	102.60	102.86	103.35	102.99	101.40	102.21

n.d. = not detected

TABLE 4.2. BIOTITE COMPOSITIONS USED FOR P-T CALCULATIONS (WT %)

Sample	432 -P	425 -P1	420C -P3	60-2 -P1	CKOR3 -P2	93-40 -P10	XX5 -P1-B	SL53 -A-P1	D58 -P1	D156 -P1	D238 -1-P1	D238 -FK1	AN5 -1-2P
SiO_2	35.52	35.36	35.31	35.65	35.29	35.10	34.50	37.05	35.56	35.75	36.41	34.87	35.44
TiO_2	1.81	1.83	1.53	1.92	1.51	1.98	2.02	1.48	1.39	1.48	1.93	1.86	1.77
Al_2O_3	18.07	17.91	19.20	19.18	19.64	19.12	19.61	16.85	19.25	19.63	18.47	19.22	19.55
Cr_2O_3	0.03	0.06	0.01	0.07	n.d.	0.04	0.09	0.01	0.05	n.d.	0.08	0.08	0.02
MgO	8.91	9.44	9.15	10.03	10.33	10.50	9.16	13.26	9.85	10.96	11.28	10.38	10.43
FeO	20.99	21.14	20.45	19.10	18.88	18.75	20.81	16.94	19.35	18.51	18.31	19.91	19.03
MnO	0.06	0.17	0.01	0.01	0.01	0.10	n.d.	n.d.	n.d.	n.d.	n.d.	0.05	n.d.
K_2O	9.18	9.12	8.90	8.79	8.71	8.15	7.81	8.56	8.74	8.63	8.24	8.16	8.54
CaO	0.05	0.07	0.03	n.d	0.01	0.03	0.07	n.d.	0.03	n.d	0.03	n.d.	n.d.
Na_2O	0.10	0.02	0.28	0.34	0.20	0.31	n.d.	0.01	0.29	0.25	0.31	0.14	0.20
Total	94.72	95.12	94.87	95.09	94.58	94.08	94.07	94.16	94.51	95.21	95.06	94.67	94.98

n.d. = not detected

TABLE 4.3. MUSCOVITE COMPOSITIONS USED FOR P-T CALCULATIONS (WT %)

Sample	420C -P3	60-2 -P1	CKOR3 -P2	93-40 -P10	XX5 -P1-B	SL53-A -A-P1	D58 -P1	D156 -P1
SiO_2	47.93	48.41	44.23	44.78	44.75	47.88	44.87	45.70
TiO_2	0.21	0.18	0.54	0.57	0.26	n.d.	0.41	0.30
Al_2O_3	33.92	33.97	34.90	35.18	36.27	35.18	36.25	36.90
Cr_2O_3	n.d.	0.01	n.d.	0.01	n.d.	n.d.	n.d	n.d.
MgO	0.34	0.46	1.01	0.74	0.41	0.69	0.51	0.35
FeO	0.65	0.86	2.65	1.30	0.67	0.83	1.01	0.84
MnO	n.d.	n.d.	n.d.	n.d.	n.d.	n.d.	n.d.	n.d.
CaO	0.35	n.d.	n.d.	0.03	n.d.	n.d.	n.d.	n.d.
Na_2O	2.79	1.39	1.06	1.22	1.54	0.47	1.31	1.77
K_2O	7.78	8.30	8.68	9.10	7.68	9.96	9.06	8.63
Total	93.97	93.58	93.07	92.93	91.58	95.01	93.42	94.49

n.d. = below detection limit

TABLE 4.4. PLAGIOCLASE COMPOSITIONS USED FOR P-T CALCULATIONS (WT %)

Sample	420C -P3	60-2 -P1	CKOR3 -P2	93-40 -P10	XX5 -P1-B	SL53 -A-P1	D58 -P1	D156 -P1	D238 -1-P1	D238 -FK1	AN5 -1-2P
SiO_2	62.42	61.89	62.52	60.20	62.33	46.00	61.80	62.82	59.82	62.34	63.26
Al_2O_3	24.60	24.35	24.83	25.98	23.18	35.52	24.36	24.10	26.41	24.30	25.00
FeO	n.d.	0.02	0.02	0.19	0.12	0.04	0.23	0.08	n.d.	0.20	n.d.
CaO	5.48	5.35	5.71	6.96	4.89	18.29	5.64	5.05	7.69	5.32	5.58
Na_2O	8.76	8.74	8.88	8.07	8.84	1.35	7.72	9.29	7.56	9.01	8.86
K_2O	0.07	0.23	0.17	0.08	0.07	0.05	0.07	0.08	0.22	0.07	0.11
Total	101.33	100.58	102.13	101.48	99.43	101.25	99.82	101.42	101.70	101.24	102.81

n.d. = below detection limit

APPENDIX B: Mineral assemblages and calculated P–T estimates

TABLE 4.5. MINERAL ASSEMBLAGES AND CALCULATED P–T ESTIMATES

			P (kbar)*						T (°C)**	
Sample	Assemblage	TWQ P-	1-Mg	2-Fe	2-Mg	2-Fe	3	4	K & R	TWQ
432-P2	Grt+Pl+Bt+Chl+Qtz								540–550	540–550
425-1	Grt+Pl+Bt+Qtz								505–515	500–510
420C-P3	St+Grt+Pl+Bt+Ms+Qtz	4.1—540	4.2	4.2	4.0	4.1	4.5	4.4	545–555	
60-2-P1	St+Grt+Pl+Bt+Ms+Qtz	4.1—550	4.1	4.1	4.1	4.2	4.6	4.5	550–560	
CKOR3-P2	St+Grt+Pl+Bt+Ms+Qtz	4.5—560	4.4	4.5	4.4	4.4	4.7	4.6	555–565	
93-40-P10	Sil+St+Grt+Pl+Bt+Ms+Qt	5.6—600	5.8	5.8	5.6	5.6	5.7	5.9	585–595	
XX5B-P1-B	St+Gr+Pl+Bt+Ms+Qtz	4.3—570	4.7	4.7	4.5	4.6	4.8	4.6	565–575	
SL53-A-P1	St+Grt+Pl+Hbl+Bt+Ms+Q	6.0—600	6.1	6.1	6.1	6.1	4.4	4.9	595–605	
D58-P1	St+Grt+Pl+Bt+Ms+Qtz	4.5—560	4.4	4.6	4.5	4.8	4.9	4.9	555–565	
D156-P1	St+Grt+Pl+Bt+Ms+Qtz	5.6—605	4.8	4.6	5.0	4.6	5.4	4.7	590–600	
D238-1-P1	Grt+Pl+Bt+Qtz		6.3†	6.4†					645–655	660–670
D238-FK1	Sil+Grt+Pl+Bt+Qtz	7.0—740	7.5	7.1					705–715	
AN5-1-2P	Sil+St+Grt+Pl+Bt+Qtz	6.0—680	6.4	6.3					655–660	

Methods: (1-Mg) Hoisch (1990), Mg end member (R1), (1-Fe) Fe end member (R2); (2-Mg) Hoisch (1990), Mg end member (R5), (2-Fe) Fe end member (R6); (3) Powell & Holland (1988); (4) Hodges & Crowley (1985); (K&R) Kleemann & Reinhardt (1994); (TWQ) TWQ version 1.02 (Berman 1991).

Notes: *P calculated at T from TWQ ** T calculated at 4 and 6 kbar † at 670°C